Algae-based Biomass for the Production of Fuels and Chemicals

Final Report

Alberta Innovates (ABI-14-004) & Emissions Reduction Alberta (B0150002)

Submitted by

Adetoyese Oyedun, Mayank Kumar, Stan Pankratz, Edson Nogueira Jr., and Amit Kumar

Department of Mechanical Engineering, University of Alberta, Edmonton, Canada

February, 2019

Funding Partners

- Alberta Innovates (Bio Division), Agreement number: ABI-14-004
- Emissions Reduction Alberta (ERA) [earlier known as Climate Change and Emissions Management Corporation (CCEMC)]: CCEMC CRDPJ 452968 Kumar & B0150002
- Natural Sciences and Engineering Research Council of Canada (NSERC), Agreement number: NSERC CRDPJ 452968
- Symbiotic EnviroTek Inc.: MULTI SEI/AI-BIO CRD 452968 Kum

This work is funded by Alberta Innovates (Bio Division), Emissions Reduction Alberta (ERA) (earlier known as the Climate Change and Emissions Management Corporation [CCEMC]), the Natural Sciences and Engineering Research Council of Canada (NSERC), and Symbiotic EnviroTek Inc. through the NSERC Collaborative Research and Development program. This progress report does not necessarily reflect the views or policies of the funding partners. All conclusions are those of the authors and are not endorsed by either the financial sponsors of this work nor the many people who offered comments and suggestions.

Acknowledgements

The authors are grateful to Alberta Innovates (Bio Division) (AI), Emissions Reduction Alberta (ERA) (formerly the Climate Change and Emissions Management Corporation [CCEMC]), the Natural Sciences and Engineering Research Council of Canada (NSERC), and Symbiotic EnviroTek Inc. for the financial support to carry out this project.

The authors would like to thank the steering committee for their constant input and feedback during the first year of the project. The steering committee includes:

Art Deane (Symbiotic EnviroTek Inc.)
Christine Murray (AI)
Laurie Vaughan-Evans (ERA)
Steve Price (AI)
Susan Wood-Bohm (ERA)

The authors are also thankful to many others in the several provincial and federal agencies and the engineering community who have provided valuable inputs in the research work. The authors also thank Astrid Blodgett for editing this report.

All conclusions, recommendations, and opinions are solely the authors' and are not endorsed by either the financial sponsors of this work nor the many people offered comments and suggestions.

Executive Summary

Fuels and chemicals produced from biomass are gaining considerable interest as they have a low greenhouse gas (GHG) footprint over the life cycle. This research project is aimed at assessing algae-based hydrogen and diluent production. Algae have higher biomass production rates than most agricultural and forest-based biomass. Hydrogen is required to upgrade bitumen, and demand for hydrogen is expected to increase significantly in the future. Currently most of this hydrogen is produced from natural gas. Bitumen is mixed with diluent for pipeline transport, and demand for bitumen is also expected to increase. If hydrogen and diluents are produced from algal biomass, the GHG footprint of the oil sands can be significantly reduced. This research develops data-intensive techno-economic models to assess the use of algal biomass for the production of diluents and hydrogen in terms of cost. An energy and emission assessment of the different algae conversion pathways over the life cycle is also performed. The net energy ratio for different conversion pathways is developed; this will help in understanding the amount of energy required to produce a unit of energy through different conversion pathways. A range of algal production and harvesting systems is assessed. The results of this project will help the energy industry understand the cost of algal biomass-based hydrogen and diluent production. This project aims to train highly qualified personnel (HQPs) in the area of energy modeling and bioenergy who could play a significant role in the quickly developing bioenergy sector in Canada. The key results are summarized briefly in the following paragraphs.

A new data-intensive analytical model that predicts algae biomass production (growth and cultivation) known as SATOPR (SATellite Open Pond Raceway) has been developed. The key parameters in developing the SATOPR model are media temperature and solar light intensity. Given the global reach of satellites, using the model results to predict open pond raceway (OPR) system performance both in Canada and the rest of the world makes the model both unique and beneficial for comparative analyses of OPR system performance. We also demonstrate here how the model provides additional supportive analytic capabilities useful in techno-economic analyses (TEAs) and life cycle assessments (LCAs) of various pathways of algae utilization.

The techno-economic analysis for the cost of producing algae-biomass in Canada shows that the minimum biomass selling price (MBSP) for a tonne of algae biomass from OPR and photobioreactor (PBR) cultivation systems in Fort Saskatchewan, AB, is 1,288 and 550 $/tonne, respectively. The analysis also shows that in Canada a PBR cultivation system has the potential to produce algae biomass at a significantly lower MBSP than an OPR system at the same location. In fact, it is projected that the PBR MBSP could rival that of OPR systems located in even the most favorable climatic locations. Environmental and operating parameters have been identified and show potential for continuing to improve MBSP and are recommended for further study.

Two thermochemical pathways for conversion of algae to diluent were studied. The hydrothermal liquefaction (HTL) is a process in which a slurry of algae with water is converted to bio-oil and other products under high pressure and temperature. The results show that the cost of diluent production from HTL is 1.60 $/L for a plant capacity of 2000 tonnes day^{-1}. All costs in this study are in US dollars ($) except otherwise stated for Canadian dollars (C$).

The fixed capital investment at this capacity is 503 M$. Pyrolysis is another process which produces bio-oil was studied. This process includes heating of dried algae (less than 10% moisture content) in absence of air. The cost of diluent production from pyrolysis is 1.69 $/L for a plant capacity of 2000 tonnes day^{-1}, while the fixed capital investment at this capacity for pyrolysis is lower than that of HTL (around 385 M$). The sensitivity analysis shows that diluent cost is highly sensitive to diluent yield, algal biomass cost, and the internal rate of return (IRR). The plant capacity versus price profile shows that the optimum capacity can exceed 6000 tonnes day^{-1} of algal biomass; however, algal biomass availability at this capacity is a challenge. Therefore, the price of diluent at this capacity (i.e., 6000 tonnes day^{-1}) is 1.55 $/kg and 1.63 $/kg, respectively, for HTL and the pyrolysis process and is illustrated in Figures E1 and E2. On a commercial scale, the size of the plant will be lower than this to reduce the risk.

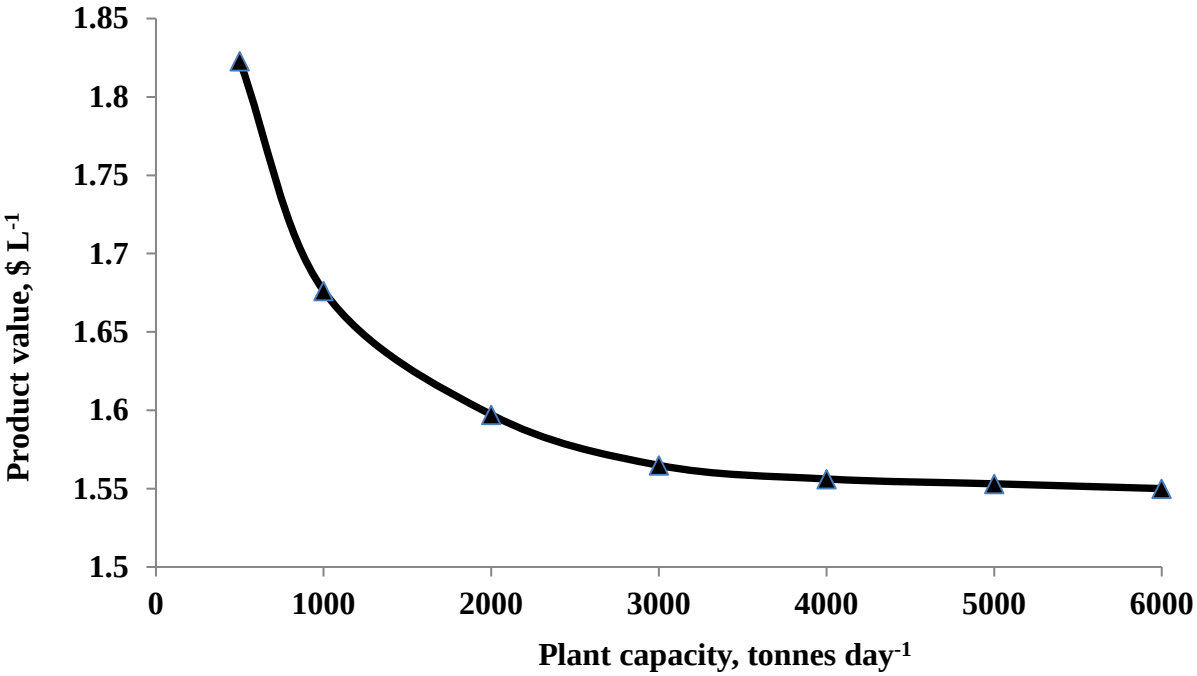

Figure E1: Product value of diluent production from hydrothermal liquefaction at different plant capacities

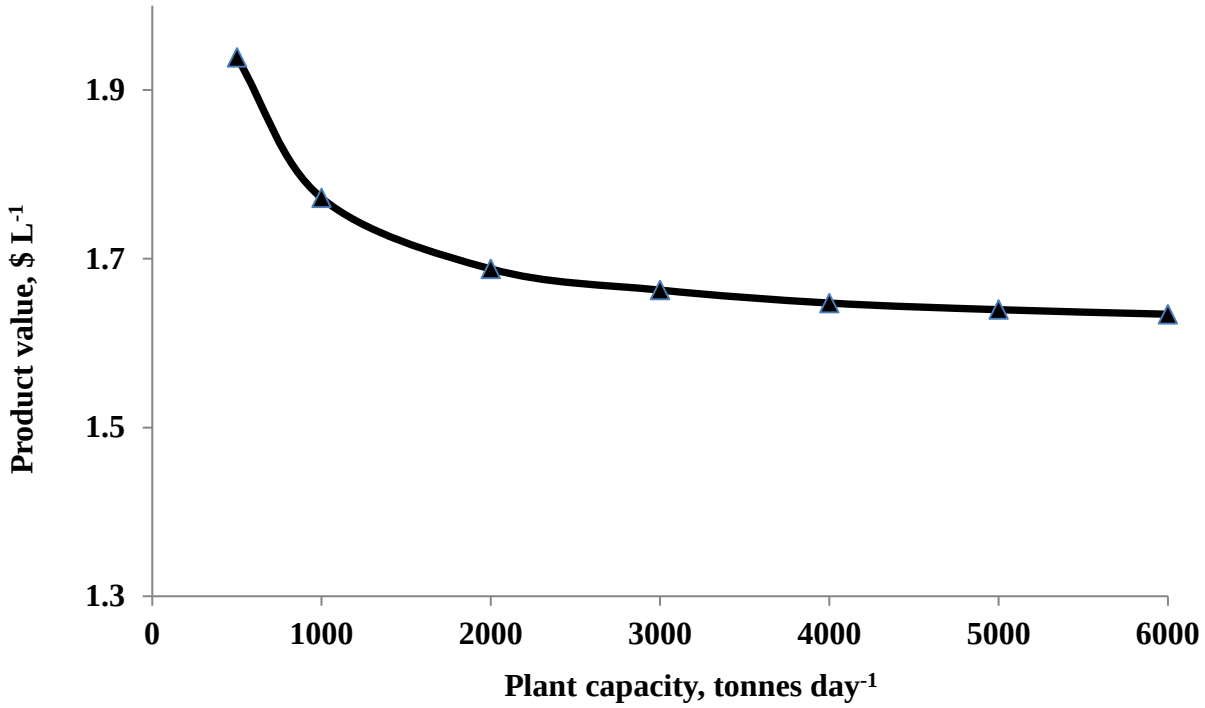

Figure E2: Product value of diluent production from pyrolysis at different plant capacities

The HTL study also focused on the understanding the impact of different parameters on using microalgae as a feedstock to produce diluents for bitumen transport. The cost of diluent obtained from crude oil distillation is 0.7 $/L. Producing diluent through current technological platforms is not competitive with the diluents from the conventional sources. Hence, a robust system with a special focus on reducing algal costs is needed and increasing product yield would offer significant benefits. The sensitivity analysis showed that diluent yield and internal rate of return have the highest influence on the cost of diluent. The energy from biochar, a by-product of pyrolysis process, is sufficient for algal biomass drying and heat supply to the pyrolysis reactor. The use of biochar as an energy source in the system results in a cost of 1.67 $/L. The variation of plant capacity with diluent product value for the above two thermochemical pathways is shown in Figure E3. The impact of using industrial CO_2 (where the CO_2 producer pays the algae conversion plant to avoid the payment of carbon levy) is assessed. The impact on the product value of diluent is further assessed (see Figure E4). For HTL and pyrolysis, the product value of diluent falls to 1.06 $/L and 1.16 $/L, respectively, when CO_2 cost is increased to 40 $/tonne. It is apparent that microalgae-based diluents are technologically feasible; however, costs need to be lowered to make diluent cost competitive in the market. The modeling and cost results provide useful insights into the development of large-scale commercial thermochemical technology.

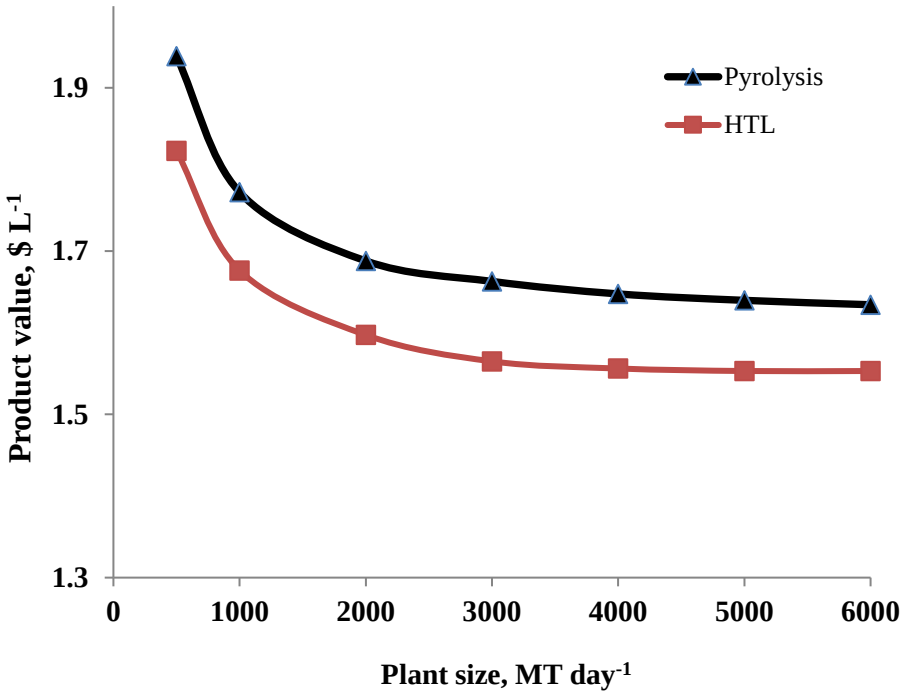

Figure E3: Plant capacity profile showing changes in product value with differing plant sizes for (a) hydrothermal liquefaction and (b) pyrolysis

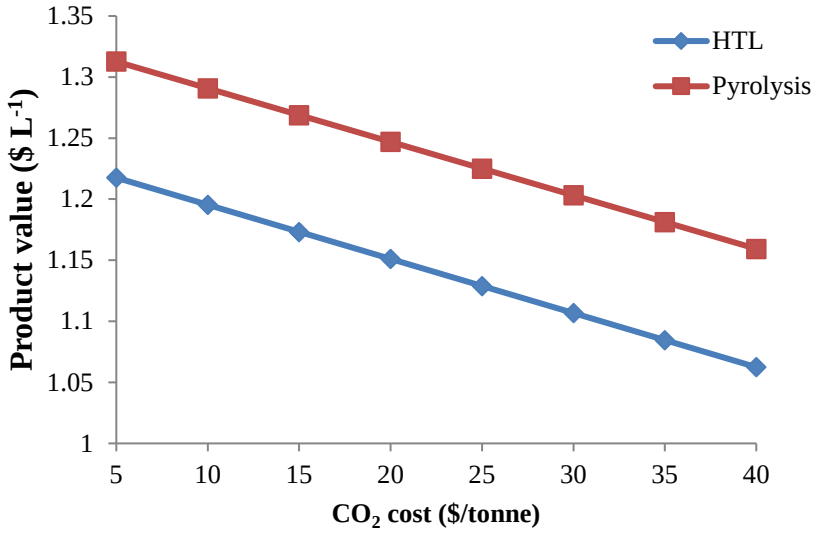

Figure E4: Effect of the cost of industrial CO_2 on the product value of diluent

Another product of interest to the oil sands industry is hydrogen, a potential energy source. Canadian oil sands operations process bitumen into synthetic crude oil, which requires upgrading. Most of the hydrogen for upgrading is produced with natural gas and this leads to significant greenhouse gas (GHG) emissions. Hence, other methods of hydrogen production from technologies such as supercritical water gasification (SCWG) and thermal gasification needs to be

evaluated. This study explored the application of SCWG to produce H_2 from algal biomass. The simulation featured the hydrothermal gasification of algal biomass to produce syngas, syngas cleaning, and the conversion of syngas into H_2. The reactor model results were validated with results from the literature. A parametric study of the effects of key operating parameters on syngas yield through HTG was performed. Higher temperatures improved H_2 yield and decreased CH_4 yield, as shown in Figure E5. Lower pressures increased H_2 yield, and increasing feed content reduced H_2 yield. With an algal biomass plant capacity of 500 tonnes/day, 52 tonnes/day of H_2 was obtained. Similarly, a process model for the thermal gasification pathway was studied to produce hydrogen.

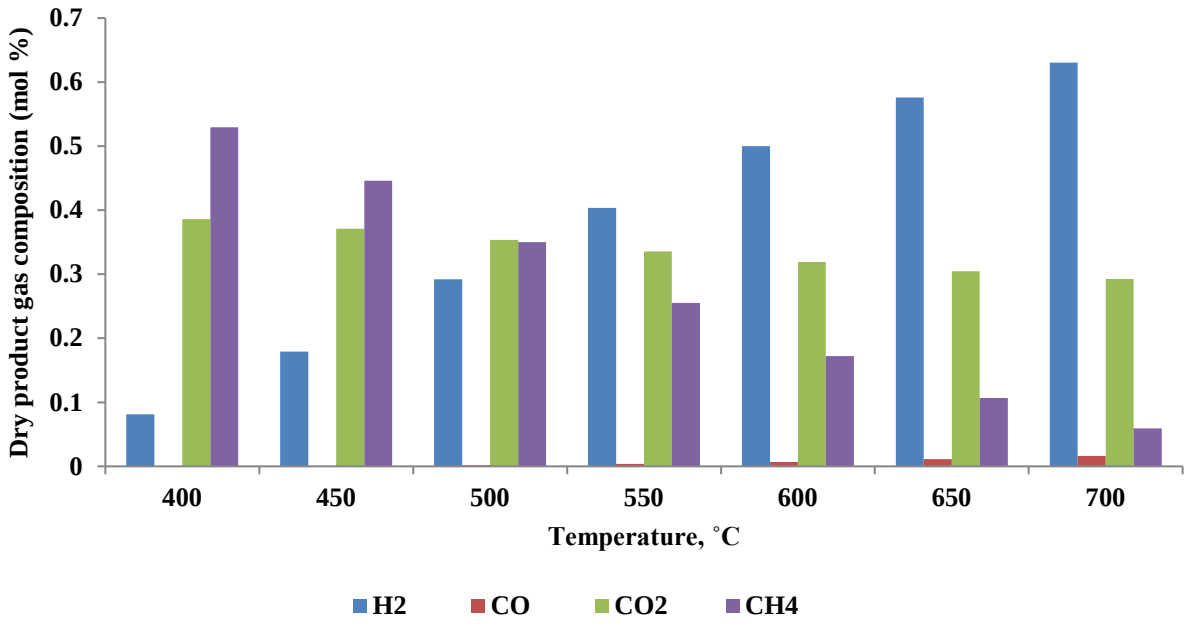

Figure E5: Effect of temperature on dry product gas composition during hydrothermal gasification

A techno-economic assessment of hydrothermal gasification and thermal gasification showed that 2000 dry tonnes/day plant required a fixed capital investment of 277.7 M $ and 196.62 M $ with hydrogen product values of 4.59 ± 0.10 $/kg and 5.66 ± 0.10 $/kg, respectively. In Western Canada, most hydrogen is obtained from natural gas with a cost of 0.78 $/kg. A thermochemical plant using 2000 dry tonnes/day algae as a feedstock is not economical. However, algae's carbon neutrality and its ability to take up CO_2 make it highly attractive. The sensitivity analysis indicated that algae feedstock cost is the most sensitive parameter in the economics of the process, highlighting the importance of algal biomass availability. Figure E6 shows the effect of the plant size on the product value of hydrogen for both thermochemical processes. Supercritical water gasification holds tremendous potential because of its ability to handle wet biomass, thereby avoiding the cost-intensive drying step. The effect of using industrial CO_2 (where the CO_2 producer pays to the algae conversion plant to avoid the payment of carbon levy) on the product value of hydrogen is assessed and shown in Figure E7. For supercritical water gasification plant and thermal gasification, the product value of hydrogen drops to 2.60 $/kg and 3.65 $/kg, respectively, when

payment for CO_2 use is increased to 40 $/tonne. The economic analysis suggests that the feasibility of the technology depends heavily on the cost of algal biomass and the yield obtained.

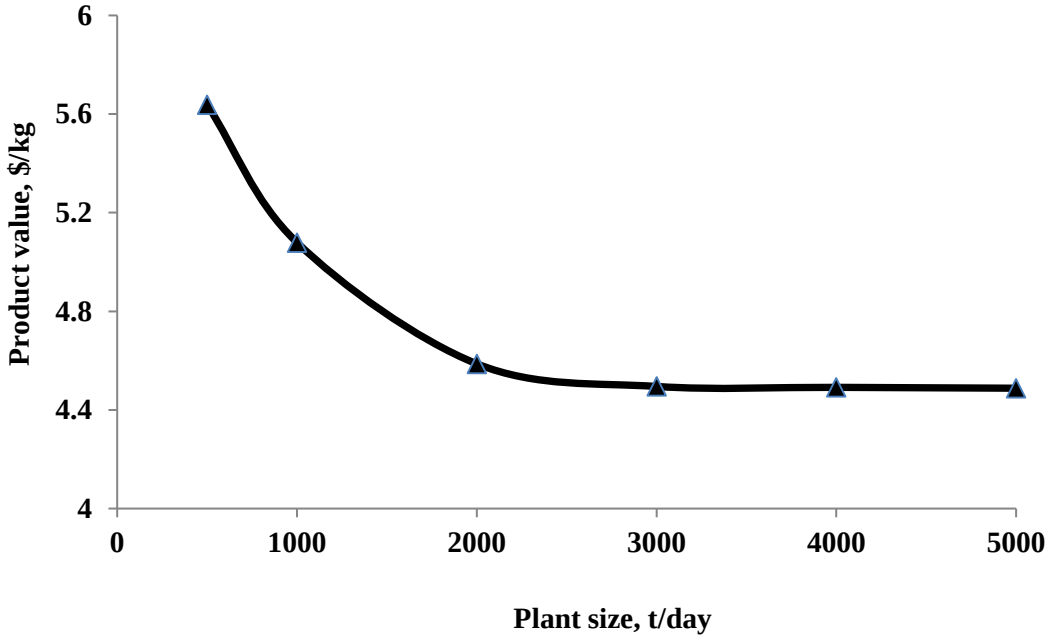

(a)

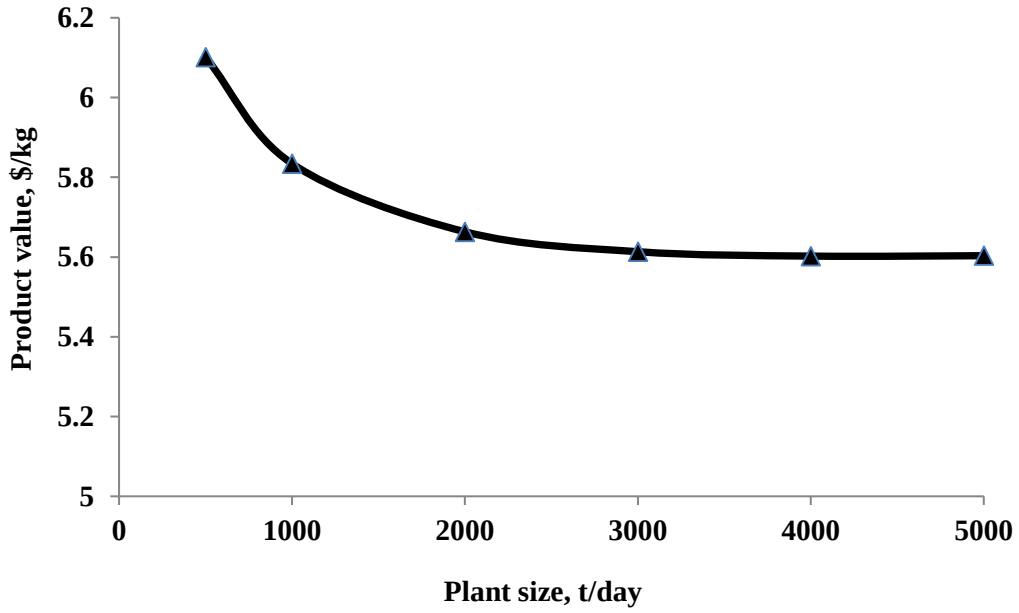

(b)

Figure E6: Effect of plant scale factor on product value of hydrogen for (a) supercritical water gasification (b) thermal gasification

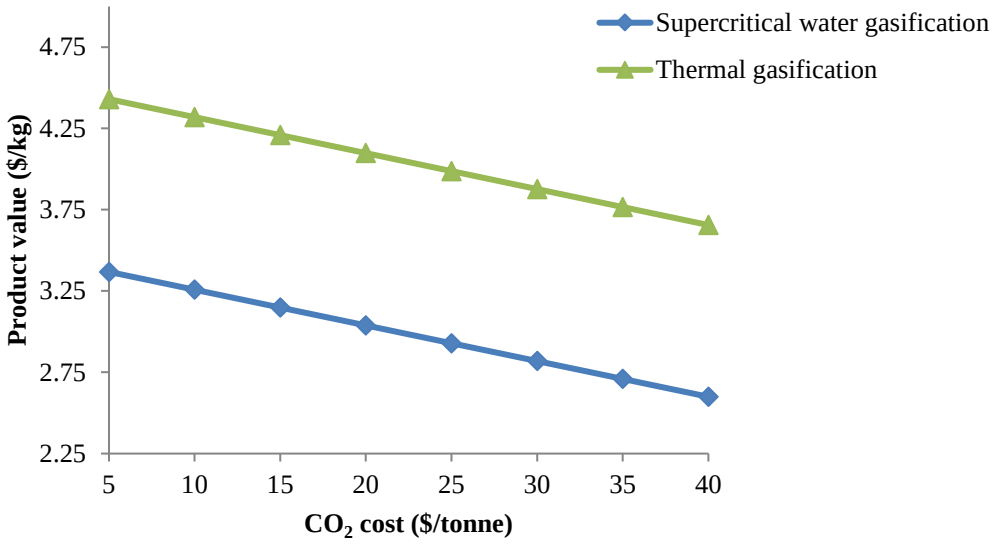

Figure E7: Effect of the cost of industrial CO_2 on the product value of hydrogen

Four thermochemical technology platforms – hydrothermal liquefaction and pyrolysis for diluent production, and supercritical water gasification and thermal gasification for hydrogen production – were studied. Industrial-scale (2000 tonnes/day) dry biomass processing was modeled on a system level based on these conversion techniques. The GHG emissions for four pathways arise from the conversion process only. An HTL pathway contributes GHG emissions of 29.6 $gCO_{2\text{-}eq}$/MJ based on inputs from the process modeling developed for the HTL pathway in this study, as shown in Figure E8. The production of diluent from HTL has advantages with respect to the use of high moisture containing microalgae; drying is not needed, and thus energy and corresponding GHG emissions pertaining to microalgae drying are eliminated. As shown in Figure E8, an algae-based pyrolysis pathway in this study has GHG emissions of 81.1 $gCO_{2\text{-}eq}$/MJ of diluent based on inputs from process modeling developed for the pyrolysis pathway in this study. Microalgae conversion incorporates two main processes in pyrolysis, microalgae drying and natural gas heating in the pyrolysis reactor; both are energy intensive and have direct environmental impacts.

As shown in Figure E9, hydrogen production in the supercritical water gasification (SCWG) pathway emits GHGs of 28.5 $gCO_{2\text{-}eq}$/MJ of hydrogen based on inputs from the process modeling developed for the supercritical water gasification pathway, whereas the algae-based thermal gasification pathway contributes GHG emissions of 173.8 $gCO_{2\text{-}eq}$/MJ of hydrogen based on inputs from the process modeling developed for the thermal gasification pathway. The GHG emission results showed that HTL performed better than pyrolysis for diluent production, while HTG had better environmental metrics than thermal gasification for hydrogen production from biomass.

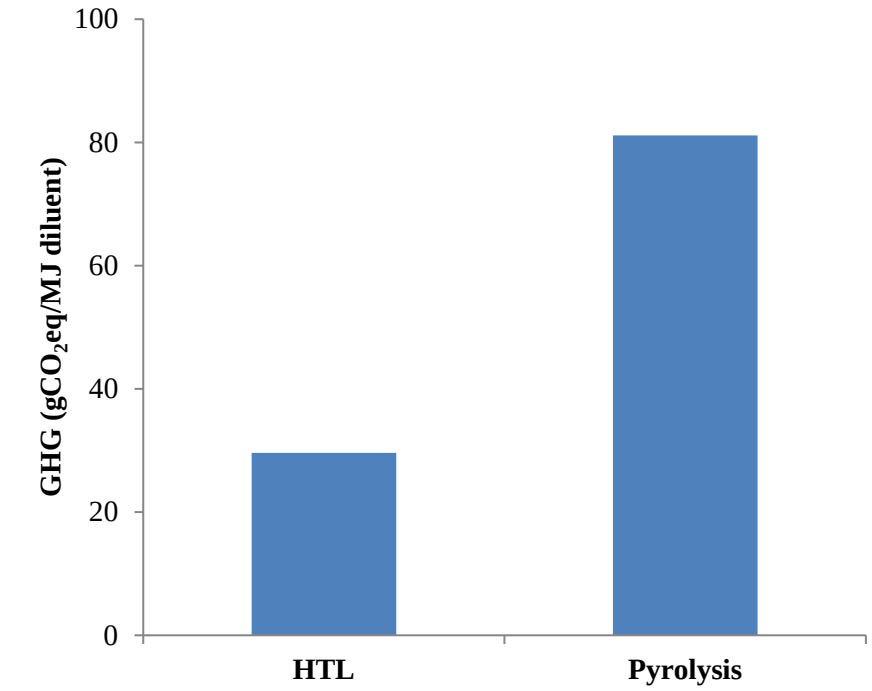

Figure E8: Breakdown of GHG emissions for HTL and pyrolysis for diluent production

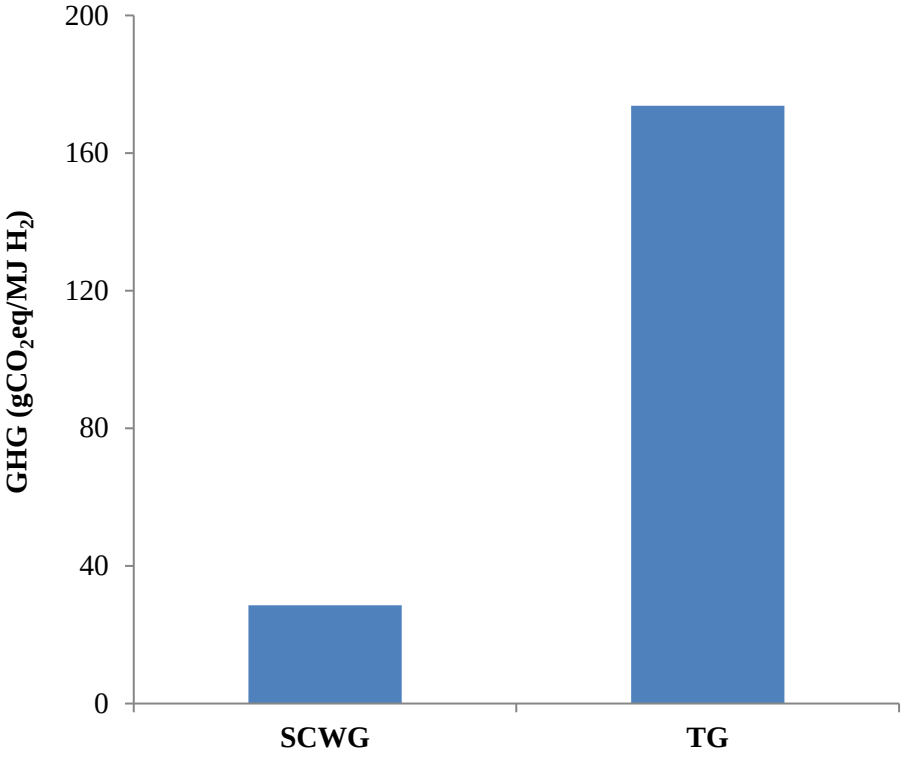

Figure E9: Breakdown of GHG emissions for SCWG and TG for hydrogen production

The results for the life cycle water footprint show that there is high fresh water requirement for algae production and it is necessary to recycle harvested water or use alternative water sources. To produce 1 kg of algae through ponds, 1564 L of water is required. When photo bioreactors (PBRs) are used, only 372 L water is required; however, the energy requirements for PBRs are about 30 times higher than for ponds. From a final product perspective, the gasification of algae biomass pathway was the thermochemical conversion method that required the most water per MJ produced (mainly due to its low hydrogen yield), followed by pyrolysis and HTL. HTG, on the other hand, has the lowest water footprint, mainly because the large amount of electricity generated as part of the process compensates for the electricity used by the system. The performance for all pathways can be improved through recycling channels. Supercritical water gasification offers the better performance in terms of GHG emissions in the production of hydrogen compared thermal gasification (92.1-138.3 g $CO_{2\text{-}eq}$/MJ). With respect to GHG emissions for diluent production, there are environmental benefits associated with HTL processing, which avoids energy and consequently GHG emissions associated with drying the biomass feedstock in pyrolysis (10.2-45.65 g $CO_{2\text{-}eq}$/MJ). These results will prove useful in making better informed investment decisions related to these processes.

This project resulted in training of 6 highly qualified personnel (HQP) including 2 PhD students, 1 MSc student, 2 undergraduate students and 1 postdoctoral fellow. The project results were disseminated through different medium. These include: 11 publications in peer-reviewed journals; and, 12 presentations at various international and national conferences and workshops.

Table of Contents

List of Tables

List of Figures

1 Introduction

The overall objective of this research is to develop data-intensive techno-economic process models to estimate the production cost of fuels and chemicals from algal biomass sources through a range of conversion pathways at various production plant sizes. The detailed models consider the unit operations involved in the production process over the life cycle from production to use and determine the optimumplant size, that is, the size at which cost would be lowest. The factors that have the greatest influence on the production costs of the fuels and chemicals are assessed through sensitivity analysis. The environmental assessment of diluent and hydrogen production is done through a life cycle assessment considering all direct and indirect energy use and emissions. Overall, the scope of the project includes the life cycle assessment of diluent and hydrogen starting from algae biomass cultivation to the distribution of fuels and chemicals to users, taking into account all the input and output flows of energy and emissions occurring throughout the life cycle. The specific objectives of the research include:

- The development of unit operations for diluent and hydrogen production from algal biomass feedstock;
- The development and collection of cost and technology characteristics data of each unit operation;
- The development of energy and mass balance models for each unit operation for diluent and hydrogen production pathways;
- The development of unit operation boundaries for the life cycle assessment of diluent production;
- The development of models to estimate full life cycle costs by applying appropriate discount factors to a life cycle cash flow forecast, once credible cost factors are identified;
- The development of unit operation boundaries for the life cycle assessment of hydrogen production;
- The development and collection of data on life cycle energy output-input ratios and GHG emissions of various operations for diluent production;
- The development and collection of data on life cycle energy output-input ratios and GHG emissions of various operations for hydrogen production;
- The comparative assessment of diluent and hydrogen production for their integration with fossil fuel-based diesel production for the Canadian oil and gas industry;
- The development of scale factors for different equipment;
- The development of life cycle GHG emissions and net energy ratios for diluent production;
- The development of cost versus capacity profiles;
- The development of life cycle GHG emissions and net energy ratios for hydrogen production;
- The development of optimum diluent and hydrogen production plant sizes; and
- The assessment of the impacts of input parameters on various unit operations involved in techno-economic and life cycle assessments of diluent and hydrogen production through detailed sensitivity analysis.

Hydrocarbons such as naphtha, also referred as a diluent, can be used to lower the viscosity of bitumen and thereby ease its transportation in pipelines [1]. Typically, the most common diluent, natural gas condensate, is used to transport heavy hydrocarbons through pipelines. Diluent is used

to meet pipeline viscosity and density specifications and thus the supply of natural gas may not keep pace with demand in the long term [1]. Heavy hydrocarbons need to flow through pipelines with low amounts of diluting agents.

The Western Canadian Sedimentary Basin in Alberta holds the world's largest natural bitumen reservoir. The oil sands are used to produce bitumen, which is modified to make petroleum products. Currently, Alberta's fossil fuel industry (mainly petroleum refining and upgrading) accounts for 17% of the province's greenhouse gas (GHG) emissions; this industry is the second largest emitter after the power generation sector (55%). The bitumen extracted from the oil sands needs to be upgraded to synthetic crude oil. To upgrade each barrel of bitumen, 3-5 kg of hydrogen is required [2]; hence the hydrogen requirement for Alberta's bitumen upgrading industry is enormous. Natural gas and coal are the primary sources of the hydrogen produced. Since these fossil fuels have a large carbon footprint, the production of hydrogen is solely responsible for 28% of the total GHG emissions from the oil sands industry in Alberta [2]. The demand for hydrogen for bitumen upgrading is expected to increase, and with it, GHGs; therefore, it is necessary to find ways to mitigate overall GHG emissions from the oil sands industry. One solution is to replace fossil fuel-based hydrogen with hydrogen produced from renewable biomass sources. This study assesses biohydrogen production pathways for their possible application in a bitumen upgrading plant. In addition to its use in bitumen upgrading, biohydrogen can be used in the transportation sector and in the food, petrochemical, and manufacturing industries. Producing diluents and hydrogen from biomass feedstock is strongly favored since biomass has the potential to reduce the environmental footprints of fossil fuel use [3-5]. Algae-based biomass has emerged at the forefront of biofuel research due to algae's high productivity and ability to grow on marginal lands [6, 7].

The focus of this report is to highlight the various technological and cost characteristics of the unit operations involved in diluent and hydrogen production from algae biomass through the development of data-intensive techno-economic models. The models and cost curves are used to assess changes in diluent and hydrogen production costs from algal biomass as the plant size changes as well as the economic optimum size of diluent and hydrogen production plants based on algal biomass. The effect of input parameters on various unit operations in the overall techno-economic and life cycle assessments of diluent and hydrogen production is studied through detailed sensitivity analysis. Finally, life cycle energy output-input ratios and GHG emissions for both the diluent and the hydrogen production pathways based on algal biomass are developed.

2 Review of Algae Production Platforms for Canada's Northern Climate

2.1 Introduction

Over the past relatively short period, there has been renewed interest in growing and cultivating microalgae for commercial purposes. These single cell plants are extraordinary in their capacity to more than double biomass within a single day [8]. Research shows the plant's ability to synthesize a host of highly valued compounds, including bio-oils for energy [9-17], hydrogen and isoprene production [18], food, livestock and fish feed [19, 20], and coveted health and nutrition ingredients [21-25], while simultaneously improving water [26-28] and air quality [29-33]. It is for this reason that algae are seen to hold enormous potential for meeting a number of our world's pressing challenges.

There are more than 40,000 species of algae [33, 34], each with a unique composition and grown in micro-environments suitable for their existence. Considerable research has been conducted to isolate strains of algae with high growth yields and high lipid content [35]. Both qualities are important to building a business case for a sustainable renewable energy industry.

For commercial purposes, natural environmental growth conditions are weighed against artificial environments that can be tightly controlled and generally lead to much higher yields [33]. When considering artificial environments, emphasis shifts from working only with indigenous algae strains found in particular geographic locations to cultivating strains that offer the greatest yield potential for desired products and potential bi-products.

In Canada's challenging northern climate, unless there is a specific environmental burden that can be improved through the cultivation of algae in situ, i.e., oil sand tailing ponds, control of algae blooms (or blue-green algae, also known as cyanobacteria, which can negatively affect habitats), it is generally necessary to create artificial environments to achieve meaningful commercial yields of algae biomass.

Each strain will have a unique composition and makeup and will likewise require a tightly controlled growing environment to optimize yield. Photobioreactors are constructed to tightly monitor and control all aspects of the growth conditions including lighting, nutrients, temperature, pH, media composition, etc., and ensure optimal growth of a specific algae strain. The challenge in photobioreactor construction is to minimize capital and operating costs to the point where the cost of the biomass produced for industry is less than other competing renewable inputs to biofuel production [33] and/or other valued production endpoints.

An overarching goal of a series of studies by this research group is to develop a model that allows researchers to benchmark technology, evaluate performance and compare different technologies and processes to identify those technologies and processes that will support an economically viable and sustainable algae biomass industry.

2.2 Microalgae review

Generally, when considering microalgae for economic and commercial uses, it is important to first identify algae strains naturally growing in a region of interest, document the composition of the media and environmental conditions in which they naturally grow, characterize the composition

of the algae, and select those species that already demonstrate a natural capacity to synthesize compounds of interest.

By way of example, a recent study on the cultivation of *Nannochloropsis sp. F&M-M24* under altered media nitrogen availability demonstrates how cultivation conditions may alter the elemental composition of the produced microalgae biomass [36] (see Table 1).

Table 1: Sample microalgae composition [36]

Parameter	NS	ND	Units
Ash	10.9	14.3	% w/w_{db}
C	52.1	53.9	% w/w_{db}
H	7.2	7.5	% w/w_{db}
N	7.8	3.8	% w/w_{db}
S	0.7	0.6	% w/w_{db}
O	21.3	19.6	% w/w_{db}
Total Lipid	23	45	% w/w_{db}
Heating Value (High)	25.8	25.5	MJ/kg_{db}
Heating Value (Low)	24.3	23.9	MJ/kg_{db}

NS = Nitrogen surplus
ND = Nitrogen deprived
db = Dry basis

Mostafa [37] reviewed metabolites as well as phytochemical and biologically active compounds including fatty acids, sterols, carotenoid pigments, and antioxidants along with anti-cancer, anti-microbial, anti-viral, nematicidal, and molluscicidal activity. Microalgae can also be used for feed, fertilizer, CO_2 sequestration, wastewater treatment, biofuel production, and phytoremediation for heavy metals.

There is also an ongoing investigative task to determine ways to augment the growth media and environment to optimize both algae growth and the expression of the compounds of interest. Sustainable commercial viability is determined by the balance of capital and input costs versus revenues gained from saleable output products and avoided operating costs (i.e., GHG penalties). There are more exciting possibilities with the investigation of enhanced genetically modified organisms (GMOs) [38]. Acién et al., Norsker et al., and Chen et al. emphasize the importance of achieving biomass production yields that will support economic and commercial viability [39-41]. Abdelaziz et al. and Slade et al. point to the importance of reaching a net positive energy balance for all processes leading to commercial products [42, 43].

Industry is looking for economically sustainable and scalable algae production platforms that will deliver algae biomass at costs that are lower than existing competing inputs. Recent publications provide a useful background on this topic [44-47]. It is the purpose of this research paper to determine the current ability of the algae industry to deliver algae biomass in Canada's northern climate by:

- Reviewing cultivation technologies involving artificial environments that are currently being developed and are deployable in Canada;
- Identifying a range of cultivation technologies with the potential for Canada; and
- Identifying gaps in knowledge on algae cultivation in Canada.

2.3 Algae cultivation techniques

The algae cultivation method used significantly influences growth characteristics, yield, and composition [48]. Algae growth generally depends on sufficient light and a carbon source for photosynthesis, but, depending on the environmental conditions, algae may assume a different metabolism approach [49]. The cultivation methods include phototrophic, mixotrophic, heterotrophic, and photoheterotrophic [50, 51]. Chen et al. summarized biomass productivity, lipid content, and productivity for different algae species under various cultivation methods [41]. Their review shows that the phototrophic approach is the most common, although biomass and lipid productivities were relatively low compared with the heterotrophic method when the same algae species were considered. The work by Liang et al. [52] showed that phototrophic cultivation provided higher cellular lipid content (38% for *Chlorella vulgaris*) but much lower lipid productivity compared with algae growth under heterotrophic conditions. Different algae strains can grow using different cultivation techniques. For example, while *Chlorella vulgaris*, *Arthrospira (Spirulina) platensis*, and *Haematococcus pluvialis* grow under phototrophic, heterotrophic, and mixotrophic conditions, strains such as *Selenastrum capricornutum* and *Scenedesmus acutus* grow favorably under phototrophic, heterotrophic, and photoheterotrophic conditions.

Bacterial contamination and infestation by predatory microorganisms, i.e., rotiphers, are a major concern in algae cultivation, and addressing is challenging given the high levels of organic substrates in the algae that support predator rapid growth. An infestation can rapidly destroy the culture. Great care is generally taken to ensure that the culture is anexic and is maintained in that way [53]. Given the challenges associated with maintaining anexic cultures, there has been a shift, especially over the past five years, toward exploring the benefits of maintaining a biodiverse polyculture [54]. Different cultivation methods are discussed briefly below.

2.3.1 Phototrophic cultivation method

The phototrophic algae cultivation method involves the consumption of light and CO_2 as a source of energy and inorganic carbon [50]. The phototrophic, also known as photoautotrophic, culture method converts light into chemical energy via photosynthetic reactions [41, 48, 49]. This method of culturing algae is the most commonly used cultivation condition for algae growth and generally results in media with low cell density at relatively low cost. The method provides scalability with relative ease, although the low cell density leads to higher costs to concentrate the media [41]. The benefit of phototrophic cultivation is the potential use of CO_2 from flue gases emitted from power plants and heavy industries for its biological fixation [41, 50].

2.3.2 Heterotrophic cultivation method

The heterotrophic cultivation method uses only organic compounds as sources of carbon and energy and therefore eliminates the requirement for light [48]. This method generally results in higher biomass concentration (cell densities of 50-100 g of dry biomass/L) and lipid productivity than autotrophic cultivation (cell densities of 30 g of dry biomass/L) [53]. Examples of organic carbon sources that can be assimilated by algae for growth include glucose, fructose, sucrose, galactose, acetate, glycerol, and mannose [52]. The cultivation method can be scaled up as a conventional fermenter, but there are issues associated with scaling up, such as contamination and competition with other microorganisms, the limited number of microalgae species that may be

grown heterotrophically, inhibition from excess organic substrate, the inability to produce light-induced metabolites, and high energy and substrate costs [41, 53].

2.3.3 Mixotrophic cultivation method

This method uses light as the main energy source to perform photosynthesis, although CO_2 and organic compounds are equally essential. In this cultivation method, algae can be cultured phototrophically or heterotrophically depending on the concentration of light intensity and available organic compounds [41, 48, 50]. The carbon sources for this method are both organic and inorganic with medium cell density. The reactor scale-up for the mixotrophic cultivation method is a closed photobioreactor; drawbacks include high equipment cost, high substrate cost, and contamination [41, 53]. Experiments using this approach to cultivate algae have shown maximal growth rates for certain algae species along with higher lipid, starch, and protein productivity than under photoautotrophic regimes, as well as lower production costs [55].

2.3.4 Photoheterotrophic cultivation method

In this cultivation approach, light is required to use the organic compounds as carbon source. Photoheteroterophic cultivation is also known as photoorganitrophy, photoassimilation, and photometabolism [49]. This approach is similar to the mixotrophic cultivation method except for the energy source required for growth and the metabolism reaction [48]. Similar to the mixotrophic method, high equipment and substrate costs and contamination are issues with the reactor scale-up. Medium cell density is also common with this cultivation approach. In any case, it is rarely used for algae growth or biodiesel production [41].

2.4 Algae cultivation in Canada

Commercial algae cultivation to date has largely taken place in geographic regions where sunlight energy of is prevalent, temperatures are moderate, and there are ready sources of water and low-cost nutrients. The most prevalent commercial-scale algae cultivation operations use raceway open ponds systems. These are relatively “low tech” and considered the most cost-effective, from an initial capital outlay perspective, and thus offer good potential for a viable and economically sustainable operation. However, the system has significant drawbacks and vulnerabilities.

From a geographic climatic perspective, open pond raceway systems are not ideal for a Canadian context. They can only operate for four to six months annually and thus are not economically viable. Although conventional advocacy of OPR systems persists, there are no known research attempts to experimentally quantify or model these systems in Canada.

To bridge the climatic challenge, several alternative, controlled environmental algae growth technologies have been developed. These include photobioreactor (PBR) systems for cultivating algae under phototrophic/autotrophic conditions, flat plate and membrane systems, plastic/glass tube systems, and fermenters that take advantage of algae’s unique capability to grow in heterotrophic conditions in the absence of light and rely on carbon sources other than sunlight for the energy used in growth. Other algae cultivation systems use both autotrophic and heterotrophic conditions (mixotrophic) to achieve growth objectives.

There have been several commercial attempts to cultivate algae at economically sustainable production levels. Most have failed and have thus been withdrawn from active commercial/research and development activities. Companies formerly involved include SFN Biosystems Inc. (Calgary), International Energy Inc. (Vancouver), Centurion BioFuels Corp. (Hamilton) (recently renamed Algaeneers Inc. and looking to convert glycerin to n-butanol), and Algae Fuel Systems (Saskatoon).

The National Resources Canada – National Research Council of Canada (NRC) sets a context for algae technology development in Canada. The NRC Institute for Marine Biosciences in Halifax has a history spanning more than 50 years of cultivating algae. Before 2010, the Government of Canada [56] put together a multi-party research and development (R&D) program, linking Agriculture and Agri-Food Canada (AAFC) with National Resources Canada – National Research Council of Canada (NRC) to set in place the National Bioproducts Program (NBP) to address Canadian priorities for sustainable energy, the environment, and rural revitalization. This research program was expected to bring together stakeholders and expertise from government, academia, and industry to tackle this large-scale multi-dimensional project.

The NBP identified microalgae biomass as holding the greatest potential to meet the stated objectives and set out to develop and support Canadian industries focused on the production of renewable fuels from microalgae biomass for electrical generation, land transportation, and aerospace applications. The NBP's goals were to achieve biomass production capability that would be cost effective and competitive with other conventional energy sources, provide a positive impact on the environment and sustainable energy, and contribute to the economic vitality of the Canadian energy sector [49].

To achieve the desired outcomes, several significant barriers needed to be overcome. One major barrier was the identification of algae strains that demonstrate the best potential for producing biofuels. Efficient and scalable cultivation technologies for Canadian climatic conditions would need to be developed. Then, cost-effective industrial-scale processing technologies compatible with end-use applications required development.

With that context, NRC came up with four sub-projects. The first screened algae species for biofuel applications. The second supported commercial-scale photobioreactor cultivation technologies aimed at concentrating solar energy for algae production, heat, and power. The third focused on the development and evaluation of processing and conversion technologies. The main steps leading from the production of algae to its conversion to biofuel were mapped out. Current solutions and process limitations were identified along with areas where research was required for cost-effective solutions to meet the overarching objectives. The fourth and final project evaluated the algae-derived fuels and lubricants for the aerospace industry [56].

Today, the NBP links Canada and the US under the collaborative Clean Energy Dialogue, a partnership that includes the US-DOE, the National Renewable Energy Laboratory (NREL), Sandia National Laboratories (SNL), and the Pacific Northwest National Laboratory (PNNL).

While progress continues to be made on all four projects outlined above, considerable work remains. Of interest related to the NBP is the development of the NRC's "Brite-Box" algae cultivation photobioreactor (PBR), discussed below.

2.5 Algae cultivation technologies suitable for the Canadian climate

The following section introduces nine scalable PBR algae cultivation technologies with potential application to Canadian northern climates. Table 2 provides relevant patent information [57-77] on PBR technologies used by the companies discussed in this study.

Table 2: List of patents on PBR technologies

Company Name	Patent Number	Date	Patents/Comments	Ref.
Algae Aqua Culture Technology	WO2014015184	1/23/2014	Biorefinery system, components therefor, methods of use, and products derived therefrom	[75]
	WO2014018785	3/20/2014	Biorefinery control system, components therefor, methods of use	[76]
	WO2012100093	10/26/2012	Biorefinery system, components therefor, methods of use and products derived therefrom	[77]
AlgaBloom Technologies	20140315290	10/22/2012	Low-cost photobioreactor	[73]
Industrial Plankton	WO2014006551A	1/9/2014	Photobioreactor for liquid cultures	[74]
National Research Council of Canada	CA 2394518A1	1/23/2003	Photobioreactor	[57]
Pond Biofuels, Inc.	20140199639	7/17/2014	Process for managing photobioreactor exhaust	[67]
	20140186931	7/3/2014	Process for operating several photobioreactors	[72]
	20140113275	4/24/2014	Recovering off-gas from photobioreactors	[68]
	20130316439	11/28/2013	Biomass production	[71]
	20130183744	7/18/2013	Producing biomass using pressurized exhaust gas	[66]
	20120276633	11/1/2012	Supplying treated exhaust gases for effecting growth of phototrophic biomass	[64]

Company Name	Patent Number	Date	Patents/Comments	Ref.
	20120202281	8/9/2012	Light energy supply for the photobioreactor system	[65]
	20120156669	6/21/2012	Biomass production	[70]
	20110283618	11/24/2011	Supplying bioreactor gaseous effluent to the combustion process	[59]
	20110287405	11/24/2011	Biomass production	[69]
	20110287507	11/24/2011	Process for growing biomass by modulating supply of gas to the reaction zone	(60]
	20110287522	11/24/2011	Producing biomass using pressurized exhaust gas	[61]
	20110287523	11/24/2011	Recovering makeup water during biomass production	[62]
	20110287525	11/24/2011	Diluting exhaust gas being supplied to the bioreactor	[63]
Symbiotic EnviroTek Inc.	WO2011050472A1	5/5/2011	Apparatus, method, and system for algae growth	[58]

2.6 Open pond raceways (OPR) and algae raceway integrated design (ARID)

Open pond raceways (OPRs) are currently the most cost-effective means of cultivating algae. A good example of this technology can be found at the University of Arizona. Although not currently considered viable or sustainable for Canada, no known research has attempted to quantify the extent to which this technology could be employed. Its two greatest barriers are temperature and access to ambient light during winter.

Open pond raceways require large water surface areas to allow for light penetration, especially as the algae culture density increases. For this reason these ponds are generally less than a half meter deep. The large surface area enables higher use of solar photons, the energy that allows the microalgae plants to grow but during colder periods contributes to the rapid cooling of the ponds, thereby limiting metabolic activity associated with algae growth.

Given the many energy-intensive industrial processes used in the province of Alberta, there may be an opportunity to harvest the associated low-grade heat and thus maintain favorable pond temperatures and increase productivity.

To counteract the fluctuating temperatures associated with OPRs, an algae raceway integrated design (ARID) was developed and continues to undergo testing, with early results showing good promise. With this approach, the ponds are drained at night into a deeper holding area. In the morning, after the sun has heated the greater pond area, media are recirculated into the cultivation ponds. The deep pond retains the heat from the day to a great extent, resulting in a more favorable cultivation temperature. More research specific to the Canadian context is warranted.

2.6.1 Algae Aqua-Culture Technology (2010), MT

The Algae Aqua-Culture Technology (AACT) PBR for algae cultivation is designed for challenging climatic conditions and is part of a fully integrated production bio-cluster or closed-loop biorefinery platform. The system includes photobioreactors for algae cultivation, anaerobic bioreactors that digest the algae using benign digestive bacteria, and an Organic Carbon Engine (OCE) that generates syngas from waste wood from a neighboring lumber mill to produce bio-oil and biocarbon (biochar).

The 465 m^2 facility run by a staff of 4 can convert 6 tonnes of waste wood to 2 tonnes of soil amendment daily, generate 2.1 GJ/hr heat, and create up to 250 kW of continuous power. The associated CO_2 and nitrous oxide fuel algae growth. The patented automated computer control system, ANT (Autonomous Networked Technology), keeps all of the operation components in balance and adapting to environmental changes [78].

Algae produced in a serial batch process with daily harvesting go into to the biodigester to produce methane used in the OCE. The nutrient-rich digestate is combined with biochar to produce a dry saleable fertilizer. The approximate 370 m^2 of algae ponds represents some 50 m^3 of growth media and use carbon dioxide from the pyrolysis of the waste wood residue from the adjoining lumber mill [79, 80]. The system, an integrated biorefinery, can have a five-year payback in isolated

regions where energy prices are high. Research continues on the extraction of other high-value products from algae biomass.

2.6.2 Algae Tec Limited. (2007), Australia

Algae Tec Limited (ASX:AEB) has developed the proprietary McConchie-Stroud algae cultivation system. This publicly traded company has conducted hundreds of its own research trials from laboratory scale to bench-top and pilot tests, as well as detailed engineering evaluations of a commercial-scale plant operation. The company, reporting revenues of $4.5 million AUD in 2014 [81], claims significant advances in product yield, productivity, and CO_2 sequestration, as well as reduced capital cost savings. It is commencing a joint commercial-scale algae plant project in India consisting of a high-yield modular PBR and harvesting system. An industrial-scale plant is also underway near Sydney to convert CO_2 from the Macquarie coal-fired power plant into valuable bio-oil. The facility is targeted to produce 50 million L (50,000 T) of algal oil per year. Oil production was scheduled for the end of 2014.

2.6.3 AlgaBloom Technologies (2009), BC

The focus of AlgaBloom Technologies is to develop large-scale microalgae farming solutions. The company has developed a suite of PBRs from the land-based "AlgaBioReactor" to the roof-based "AlgaRoof," the "AlgaBag," a large-scale bioreactor bag with an integrated sparging and agitation system, and the "AlgaBox," a compact multi-level bioreactor. The modular multi-layer matrix design, consisting of both thin-film and suspended components, enables control over both environmental and nutritional factors. 400 m^2 of growth media surface area is achieved within a 30 m^2 footprint.

AlgaBloom is also developing associated oil extraction, harvesting, and monitoring capabilities. One of the strains of algae considered is *Synechococcus PCC 7002*.

The company has established a commercial partnership with Qponics Limited based in Australia on an omega-3 oil production project.

2.6.4 AlgaeCan Biotech Ltd. (2009), BC

AlgaeCan Biotech Ltd. is currently financing a demonstration plant with PBRs of a scalable commercial biorefinery that includes both the cultivation and subsequent processing of the algae through to saleable products. An initial key market with the production of astaxanthin from *Haematococcus pluvailis* is the primary focus of research activities, along with reducing energy inputs. Key production achievements include:

- Attaining >3% yield (wt) of dried algae biomass (open pond producers only achieve 1.5%);
- Establishing the following key optimization parameters:
  - Light frequency, intensity, saturation, low energy
  - Consistent, non-shearing low energy flow
  - Dependable, simple, low-cost sterilization
  - Monitoring and control capability of 5 crucial bioreactor factors

- Nutrient formulation to ensure cost-effective yields specific to their algae strain

❖ Establishing production protocols to efficiently transition the algae from the vegetative growth phase through the induction of astaxanthin production and the extraction of this product into an oleoresin without the use of solvents; and
❖ Production of 4 mg softgels using a toll processor technology.

The work of the company has progressed from lab-scale trials to bench-top and 1000 L and 7,000 L PBRs. The company is currently building a 14,000 L PBR.

2.6.5 Hy-Tek Bio LLC (2008), MD

Hy-Tek Bio has developed a PBR based on cylindrical PVC bags (a mylar-like material with carbon fiber and Kevlar structural support) that provide a growth media column approximately 1 m diameter and 6-7 m high and a total growth volume of 6.8 m^3. The system is housed in a protective building environment that helps control environmental temperatures. The PBR includes system monitoring and control capability. Hy-Tek's technology takes down stack gas emissions from industrial processes, with algae absorbing not only CO_2 but also the other potent greenhouse gases like SO_x and NO_x. Carbon credits as well as offsets from not having to use other costly gas scrubbers and their associated maintenance are anticipated. The company is achieving algae culture densities that support relatively high production yields.

Together with the University of Maryland, the company has isolated a proprietary *HTB-1* strain of algae that shows the greatest promise for the company's commercial objectives. The algae has a 42-47% lipid content and is able to survive environments with 100% CO_2. The algae can also withstand high variability in pH from acidic to basic and temperature swings from 15^0C-43^0C. In natural conditions, algae double their mass in 22 hr. In research trials, they can double within 12 hr.

Significant research headway has been made on the monitoring and control of nutrients and lighting to optimize algae growth. Lighting regimes have reduced energy use to 10% of traditional LED lighting systems.

The cost of the 6.8 $m^3$30 kg tank is approximately 25% of the cost of a similar volume stainless-steel tank. The development plan is to construct a commercial-scale tank that holds 18m^3 of growth media. Other key data include:

❖ Flue gas: 100 scfm/PBR @ 11.8%CO_2 and 130 ppm NO_x
❖ Flue gas temperature: 425^0C stack T and 27^0C PBR T
❖ Nutrient requirement: 375L proprietary nutrient/PBR/day based on waste chicken manure
❖ 5% water loss due to photosynthesis
❖ Power: 180W lighting/PBR and 1.5kW air injection
❖ Gas injection/media mixing via micro-bubble full-floor sparging system
❖ Algae: HTB1
❖ Culture density: 3-5 g/L
❖ Production: 23-34 kg/day or 3.4-5 g/L/day
❖ O_2 production: 8.5 cfm 90% O_2

- Harvesting: 10% of media harvested when optical density reaches upper threshold
- Dewatering: use bacterial aggregation agent. Removed water is filtered and replenished with nutrients, then returned to PBR
- Drying/packaging: remaining slurry spray dried and vacuum packaged for shipping
- Cycle repeated every 1.5 hr
- Automated control system

2.6.6 Industrial Plankton Inc. (2011), BC

Industrial Plankton is a recent algae cultivation technology developed in Victoria, BC. The technology is a fully automated PBR with monitoring and control capability that enables significant production yields. Industrial Plankton has recorded algae densities up to 210 million cells/ml (*Nanochloropsis),* 25 million cells/ml (*Isochrysis),* 18 million cells/ml (*Thalassiosira weissflogii*), 20 million cells/ml (*Skeletonema costatum*), and 4.5 million cells/ml (*Tetraselmis).* To date the company has developed a 100 L research-scale and 500, 1,000 and 1,250 L automated PBR systems complete with sterilization. Air and water are micro-filtered and there is a UV sterilization cycle. The control system includes scale-up density, nutrient addition, light levels, harvest density, etc., complete with data logging for analytical research. Scaling up from 20 L to 1,000 L takes 7-10 days depending on the algae species. Harvesting takes place automatically and removed media is replaced with fresh water and nutrients. PBRs use LED lighting systems. The 75 L unit uses an average of 900 W and the 1,000 L unit uses an average of 1,600 W. Several of this company's PBRs have been installed commercially.

2.6.7 National Research Council of Canada (NRC), NS

The Brite-Box is proprietary technology owned by the NRC [82] and developed at 250, 500, and 1,000 L. Each unit is comprised of a cooling loop, fluorescent lights, and a pH probe coupled to CO_2 solenoid for sparging this gas into the growth media for pH control. A 50,000 L cultivation pilot plant is planned.

Data published in 2010 showed *Chaetoceros mulleri* and *Isochrysis galbana* cultivated at 20 ^{0}C in seawater reached 0.6 gm/L/D over a 21-day trial cycle [83, 84]. The Brite-Box has been used to conduct algae cultivation studies on many algae strains [85].

From data collected by cultivating algae using this technology, valuable information has been accumulated to benchmark current state-of-the-art systems. From the R&D activities, the NRC has documented algae biomass yield data and extracted several unique algae strains. The information has also been used to evaluate the potential to scale up cultivation processes and determine carbon/energy balances for the biomass-to-fuel conversions. This empirical data has also been valuable for developing meaningful life cycle analyses (LCAs) and conducting techno-economic (TE) assessments.

The Brite-Box PBR was developed in collaboration with Carbon2Algae Solutions and Menova Energy Inc. and the biomass production capability in conjunction with Ocean Nutrition Canada.

The NRC collaborates with industrial/commercial partners including several of the companies mentioned below to conduct research that advances scientific knowledge and related technology development to support the evolution of the algae industry in Canada.

2.6.8 Pond Biofuels (2007), ON

Pond Biofuels came into existence in May 2007 and since its inception has filed 17 patents related to algae cultivation technology processes including factors related to scalability, handling of input and output gases, and recycling processed water [86].

This Canadian company, working with St. Mary's Cement and using pulsed red LED lighting systems, has successfully scaled up their PBR technology to two 12.5 m^3 tanks (2013). The lighting system can to inject more than 1 kW of light energy per m^3 of growth media. The company claims to grow between 4 and 6 generations of algae daily [87].

Pond Biofuels is Canada's largest and most publicized algae biomass company. They were recently awarded a $19 million demonstration plant in cooperation with the Government of Canada and Canadian Natural Resources Ltd. (CNRL) [88].

Their re-developed PBR system is based on injecting high-intensity light into large (10,000 L) plastic vessels with monitor and control capability using CO_2 from industry. Energy and CO_2 are provided by a natural gas-fired 4 MW generation system in Bonnyville, Alberta. Nutrients, including N, P, and trace elements, are obtained from chemical processes.

2.6.9 Symbiotic EnviroTek Inc. (2008) AB

Symbiotic EnviroTek Inc. was established in 2008 with the primary goal to develop a commercial scale photobioreactor (PBR) that would cost-effectively cultivate algae for commercial purposes in adverse (Canadian) climatic conditions. The first test PBR fabricated by the company holds 106,000 L. Testing in 2010 and 2011 demonstrated that algae could be successfully grown at this scale. The company's initial focus was on developing mechanical technology, including all supporting systems (i.e., proprietary controllable, submersible LED lighting, mixing the algae media, appropriate aeration for efficient CO_2 infusion, and nutrient mixing and delivery). Symbiotic has expanded its research to include the entire spectrum of technologies and capabilities to take strains of algae, customize their associated growth parameters, and adjust the associated monitoring and control capabilities to effectively optimize the growth of several different algae strains.

In 2012 and 2013, R&D activities included developing protocols for specific algae strains by using agricultural waste nutrient sources and testing specific light frequencies to optimize yields and minimize energy/cost of inputs. The company anticipated it would demonstrate sustained growth at levels above 4 gm/L/d in 2015.

Symbiotic's system was designed to be scalable for deployment and integration/co-location at existing waste industrial/agricultural waste streams at source to minimize the GHG footprint associated with an overall bio-cluster operation. An envisioned bio-field consisting of 64 modules

each having 106 m^3 of growth media situated on 2 acres is estimated to use over 45 tonnes of CO_2 daily and produce 25 tonnes of algae biomass.

2.7 Technology assessment

Given the limited information on the technologies in the public domain, it is difficult to predict a technology best suited for the Canadian context. Table 3 provides comparative data for the technologies discussed here. From an economic perspective, success is achieved in part by minimizing the total costs of several key factors including the aggregation of a suite of related technologies that comprise the algae biomass production platform. Decisions are made for capital, down-time, operating, nutrient, media (including water), and maintenance costs. Economic success is also coupled directly to species selected for cultivation and to optimized biomass yields in both quantity and composition. However, without reliable and accurate algae production platform data, we cannot make a meaningful economic comparison and assessment.

Table 3: Algae cultivation technologies suitable for Canada's northern climate

Technology Supplier	Type	Size	Process	Associated Processes	CO_2 source	N_2O	Output Products	Algae Species	Density Achieved	Energy Required
Generic ATP3 Demonstration	OPR	125 m^3			air		research facility			
ASCATI ATP3 Demonstration	ARID	30 m^3			air		research facility			
Algae Aqua-Culture Technology (2009), MT	EPR	370 m^2	coupled serial batch with waste wood pyrolysis	AD, pyrolysis	Pyrolysis	Pyrolysis	6 tonnes/d wood waste to 2 tonnes/d soil amendment fertilizer with biochar, biofuels			
Algae Tec Limited (2007), Australia	PBR				atmosphere, stack gases		ethanol, biodiesel, jet fuel, EPA/DHA nutraceuticals			
AlgaBloom Technologies (2009)	PBR	400 m^2					food, omega 3	spirulina/synechococcus		
AlgaeCan Biotech Ltd (2009)	PBR	7.5 m^3	batch multi-phase approach				astaxanthin	haematococcus pluvialis	30 g/L	

Technology Supplier	Type	Size	Process	Associated Processes	CO_2 source	N_2O	Output Products	Algae Species	Density Achieved	Energy Required
Hy-Tek Bio LLC (2008)	PBR	6.8 m^3	batch/continuous flow	HTL, enzyme conversion to biodiesel	natural gas engine exhaust	exhaust, chicken manure	methane, biodiesel, jet fuel	HTB1	3-5 g/L	1.68 kW
Industrial Plankton (2010)	PBR	1.25 m^3	batch/continuous flow				algae biomass	Nannochloropsis	210 m cells/ml, 2.5 g/L	1.6 kW
National Research Council	PBR	1 m^3	batch/continuous flow	HTL			research facility, algae biomass, biodiesel	Isochrysis	0.6 g/L/d	
Pond Biofuels Inc. (2007)	PBR	10 m^3	batch/continuous flow	HTL	natural gas engine exhaust, cement production gas emissions	chemical processes	algae biomass, bio-fuels			
Symbiotic EnviroTek Inc (2008)	PBR	103 m^3	batch/continuous flow	HTL	bottled gas	waste streams	algae biomass, bio-fuels			

EPR – Enclosed Pond Raceway, OPR – Open Pond Raceway, ARID – Algae Raceway Integrated Design, PBR – Photobioreactor

2.8 Factors affecting the economic viability of photobioreactors

All of the PBR designs are unique, with each company choosing to focus on specific aspects of their PBR design that they believe to be most crucial. PBR design optimization studies generate reference data useful for adjusting design parameters for enhanced yield outcomes [89].

The National Research Council, colleges and universities, and independent commercial laboratories continue to isolate algae strains that show high concentrations of desired compounds of commercial interest. A few noteworthy strains include *Chlorella protothecoides* and *Scenedesmus obliquus* (51% lipid concentration) [41, 90] for biofuel production and *Haematecoccus pluvialis* for astaxanthin production [91, 92].

Chlorella protothecoides has been demonstrated to grow at densities of up to 17 g/L in heterotrophic conditions and 0.87 g/L in autotrophic conditions under 12:12 hour light:dark cycles [93]. For *Scenedesmus sp.*, recent growth trials achieved 1.3 g/L dry biomass at a density of 1.5 million cells/L and a growth rate of 0.62 div/day under 12:12 hour light:dark cycles [94].

Haematococcus pluvialis, known to synthesize high-value astaxanthin, has been documented (2003) to grow at a rate of 0.7 div/day and 0.228-258 mg/L at cell densities of 200-250 thousand cells/ml [91]. A more recent study achieved astaxanthin accumulation of 18.21 g/m^3 (3.63% by dry weight), reaching a growth rate of 0.52 div/day with a cell density of 330,000 cells/ml and an estimated production cost of $1000/kg astaxanthin [95]. A 2009 study demonstrated the complexity of interactions in the algae growth platform based on the effects of light and pH [92].

A 2011 conceptual model comparing commercial-scale (100 ha plant) open pond raceways, tubular PBRs, and flat panel PBRs estimated (based on current exchange rates) costs of $6.96, $5.85, and $8.38, respectively, per kg of dewatered algae biomass. When optimized for location, irradiation, zero costs for CO_2 and nutrients, these costs dropped to $1.80, $0.98, and $0.96 per kg [40]. A recent review of bio-oil production from fifteen algae research reports results in a range of cost estimates from $0.82-$10.93 /L of oil produced [45].

In 2008, over $350 million was invested in algae projects [96]. In 2009, Exxon Mobil Corp planned to invest some $700 million, anticipating the development of algae fuels within 10 years. In 2013, however, after spending $120 million, the company determined that the project was unsuccessful in achieving commercial viability and that it would likely take at least another 15 years to reach its objective [97]. Industry reports continue to point to the significant challenges to be overcome for algae cultivation to achieve commercial viability [17, 42]. In the US alone, more than $1 billion has been invested in the algae industry [98]. These investment figures provide useful reference points when assessing the technologies introduced above with consideration to their respective economic viability. However, little information on their operational performance is available in the public domain.

The production of algae requires the monitoring and control of many variables. Different algae strains have different growth rates, and the composition of the resulting biomass varies significantly and in turn determines the value of the saleable product. Each company is focused on different product outputs. In some cases, a single relatively low-value, high-volume market is targeted (i.e., biofuels). In other cases, high-value nutraceuticals are the focus (i.e., astaxanthin).

Although each company has a primary output product, in every case consideration is given to a biorefinery approach to derive economic benefits from one hundred percent of output products to create a favorable economic output [99]. Each company has independent approaches to sourcing CO_2 and infusion, light sources, wavelengths, light-dark cycles, and intensity regimes. Sourcing lower cost nutrients and more energy efficient dewatering processes will help improve profitability.

The algae biorefinery concept is relatively new and first appeared in technical journals in 2008 (based on a Scopus search). Of 310 published articles on the subject at the end of 2016, 241 were released between 2013 and 2016. Because of the complexity of multiple pathways, including technologies and processes from cultivation to oil upgrading, there is a body of analytical research and simulation modelling that compares biorefinery pathways and provides recommendations for large-scale algae biofuel production. A recent study explores a process "superstructure" of carbon capture for wet biomass use. In the study, four technology alternatives are considered for off-gas purification, algae cultivation, harvesting, dewatering, lipid extraction, remnant treatment, and biogas and algal oil use [99, 100].

The impact of environmental parameters like light intensity, wavelengths, and photoperiods are not included in many studies. Yet, lighting regime and photoperiod are considered key factors related to algae growth rates and biomass production [101, 102]. A recent study focused on light using *Scenedesmus obliquus* achieved cell concentrations of up to 114 million cells/ml, a growth rate of 0.86, and a density of 3.3 gm/L [103] under a specific pulsed fluorescent lighting regime.

Another area requiring further research is the correlation between cell weight and algae biomass composition to parameters like temperature, dissolved oxygen, dissolved carbon dioxide, electrical conductivity, specific nutrient concentrations, pH, and light intensity. The findings to this point appear inconclusive [103].

Successful commercialization of algae technology platforms will depend on adherence to regimented operational protocols controlling the multiple parameters involved ongoing research and development activities that further optimize production (see Table 4).

Table 4: Factors affecting algae biomass production

Climate
Solar irradiance
Capital costs
Nutrient source and cost
Algae species/composition
Energy costs
Operating costs
Colocation with symbiotic industry partners
Ability to control production factors
Optimization of biomass yield
SCADA/Automation
Active research and development – access to highly qualified multi-disciplinary scientific community
Integration of advanced production platform technologies i.e., dewatering, extraction of active ingredients, processing, etc.
Analytic data modeling

2.9 Delivery costs of algae biomass in Canada

For the algae industry globally to become a meaningful and potentially dominant economic force, the costs of cultivating, harvesting, and processing algal biomass must be significantly lower than current market prices for products extracted from biomass.

To date, relatively few life cycle assessments [43, 104] or techno-economic analyses of the inclusion of technologies and processes from algae cultivation to the production of valued products have been conducted. There is also skepticism among some authors about whether there is less environmental impact in producing products from algal biomass than from conventional feedstocks and petroleum resources. Research is required to provide better information. From a sustainability perspective, research must also include water use as part of an environmental impact analysis.

How algae cultivation platforms are operated and integrated with other industries will have significant impacts not only on commercial but also on environmental outcomes. For example, algae cultivation could be co-located with municipal wastewater treatment facilities, landfill operations, agricultural effluent streams (i.e., feedlots; breweries; sugar beet, corn, and potato processors), conventional energy extraction/refineries, co-generation facilities, etc. Association with such operations could result in favorable symbiotic commercial and environmental outcomes (see Table 4). With existing algae cultivation systems, there are challenges with access to accurate costing information. This challenge is made more difficult given that the process of algae cultivation leading to the delivery of dry biomass to industry generally involves many steps.

Given that this is an emerging industry requiring significant resources, the developers of algae-related technologies generally focus on single steps in the overall production platform. Technology coupling throughout the platform will provide a complete and integrated solution. There are few integrated algae production platforms in Canada and even fewer that provide plausible scalability for industrial purposes. What may work as a prototype may not work meaningfully at a larger scale.

For some companies, algae biomass production has been focused on delivering high-value compounds rather than simply generating biomass. Operation and production data are confidential. Because of the high value of the end product, meaningful revenues can be achieved even with very modest amounts of biomass produced. Costs for the production of biomass for astaxanthin, which may have a street value of $2,500/kg [105], although important, are less a consideration than producing a million tonnes of biomass for the extraction of algal oil for biofuels (i.e., biodiesel at $1/L[kg]).

From a production perspective, comparative costing is meaningful. Palm oil, viewed to yield the lowest cost bio-oil, has a reference production cost of $603/tonne ($0.61/L). To be competitive, algae biomass (with 30% lipid content) through to oil extraction should cost $164/tonne or less. If the reference is soybean, which in the US is the main source for biofuel production, with a commodity price of $623/tonne (based on 20% lipid content), then algae biomass through to extracted oil should cost $169/tonne or less. Where the reference is crude oil priced at $118/barrel, the same algae biomass should cost $204/tonne or less [104]. See Table 5 for a summary of equivalent required pricing for algae to compete with other feedstocks.

Table 5: Comparative and competitive algae production pricing [104]

Feedstocks	Production Cost ($/tonne)	Algae Required Equivalent ($/tonne)
Palm oil	603	164
Soybean oil	623	169
Crude oil	752	204

Current cost estimates for algae biomass as a feedstock for electricity generation are $233/tonne for open algae systems and $17,292/tonne for closed environmentally controlled production platforms for health foods. For high-value products, production costs increase to $30,704/tonne in open systems and $40,895/tonne in closed systems. Reported production costs vary tremendously from $3,118 to $19,486/tonne for open systems based on raceway ponds and $3,774 to $94,430/tonne for closed systems. Interestingly, 100 tonne/yr algae biomass operations had production costs of $4,930/tonne for open systems and $3,828/tonne for closed systems [104]. Furthermore, for algae production platforms, economies of scale do not appear to work well when going from 50 ha to 500 ha to a 5,000 ha production facility since very little cost reduction appears possible [104]. See Table 6 for a summary of production cost variability in OPR and PBR technologies found in the literature.

Table 6: Cost to produce algae biomass

Technology	For Biofuels ($/tonne)	For High-Value Products ($/tonne)	Literature Variability in Pricing ($/tonne)		100 T/yr capacity ($/tonne)
			Minimum	Maximum	
OPR	233	30,704	3,118	19,486	4,830
PBR	17,292	40,895	3,774	94,430	3,828

In the context of Canada, given the relatively short growing season, open systems have not been considered a viable commercial option and therefore only closed systems need be considered. For many algae production platforms, a large negative gap remains between actual production costs and pricing for commercial products derived from the biomass. To bridge this gap, several companies that were initially focused on a single, large, and subsidized biofuel commodity market shifted their primary focus to high-value by-products with residual oils going to biofuel production. This shift leads to operational changes including a potential shift in algae strains used, cultivation practices including nutritional and environmental factors, and the addition of production steps that enhance the expression of desired compounds.

Other opportunities for overcoming the costing challenge include research to lower energy input, incorporating existing “waste” streams that can offset fertilizer costs and potentially provide an add-back value from the deferral waste disposal transportation and landfill costs, the uptake of amines to significantly reduce operating costs in these industrial applications, as well as the potential for CO_2 mitigation credits.

Research may provide techno-economic data on processes leading to biomass at a laboratory scale but these may have little relevance to commercial scale costing. Other research has used powerful software modeling capabilities (i.e., ASPEN), but results are scrutinized and questioned because of the great assumptions and parameters that need to be considered. Like challenges related to economies of scale, these modelling tools may have value for thoroughly understood commercial operations currently found in industry but may prove inadequate for the meaningful evaluation of processes related to the operation of an algae production platform. The algae industry is evolving and involves complex micro-biological, physical, botanical, marine, biochemical, and environmental interactions with thousands of strains. Moreover, cultivating, harvesting, and processing these single cell organisms introduce other technological challenges.

There have been many attempts to increase algae biomass yield and reduce costs. There is ample opportunity to discover other new and innovative approaches that will undoubtedly lead to breakthroughs in cost-effective algae production strategies.

Vocal commercial, environmental, and political interest groups that ask daunting questions related to energy and carbon balances distract the research initiatives. Environmentalists and politicians are looking for meaningful solutions to climate change and reducing airborne greenhouse gas (GHG) emissions. It is well understood that algae, one of the world's fastest growing plants, can more than double their mass in a single 24-hour period. Every tonne of biomass created will take down 1.8 tonnes of CO_2 [8, 106]. Hence, significantly scaling up algae biomass production to offset GHG emissions is more than plausible. The "fly in the ointment" is: what do you plan to do with the biomass? Turning biomass to biochar is seen to be a great CO_2 mitigation strategy that locks up carbon in one of its most stable forms. Any positive net difference between GHGs produced and GHGs sequestered in the cultivation and processing of algae would qualify for carbon credits. However, this would ignore economic considerations. Furthermore, to be awarded carbon credits, a quantitative life cycle assessment that meets the International Standards Organization (ISO) guidelines must be conducted to validate results. Currently, there are concerns that the LCA results may be misleading because rarely are parameters in an LCA calculation identical [43].

With respect to the production of biofuel from algae, environmental interest groups ask similar probing questions: What is the net energy ratio? Is more energy produced through algae cultivation than consumed through associated processes? How do these compare to using conventional non-renewable energy resources? There are concerns that in many cases more input energy is required than produced through the algae cultivation process. The same logic would hold true for CO_2 emissions.

2.10 Strategies and opportunities for sustainable algae cultivation in Canada

Algae companies have recently shifted focus to producing high-value biomass-derived products since it shows the greatest promise of economic sustainability and can be done without government subsidies. Having determined a primary product, these companies selected algae strains known to synthesize meaningful amounts of the desired compound. Research has followed to optimize axenic algae growth by carefully conducting multiple tests to determine a combination of best lab-scale nutritional and environmental conditions and processes. Once an optimized regime has been documented, stringent protocols are established. Rigorous data logs are maintained for analysis and become part of a company's intellectual property. Based on favorable yield results, an

economic model for scaling the production platform to the next stage is constructed [9]. This is essential for attracting investment funding to build the platform to each successively larger scale [107].

Scalability poses a further challenge [108]. Shifting from a laboratory setting to increasingly larger demonstration and production platforms requires a multi-disciplinary design team to ensure that axenic conditions are maintained and that the multi-variant conditions associated with growth through each production phase can be controlled, thus eliminating adverse operating effects. Controlling these conditions is necessary for a flourishing, closed growth environment (PBRs) but not possible to achieve in open cultivation systems.

As noted in this paper, there are companies and research institutions conducting primary research related to algae cultivation. Some entities compare algae composition data and others are focused on optimizing growth parameters for specific strains of algae. Yet others focus on technologies that will support the algae cultivation platform. Because of the challenges associated with each step in an algae cultivation platform, each research group focusses narrowly on a specific aspect. It is therefore prudent for research teams to find collaborative strategies for integrating and coupling strains, cultivation regimes, and associated technologies with other research groups to find more cost-effective and efficient technologies and processes to apply to their own work. These collaborations would lead to meaningful production volumes and thus early incomes of high-value products. Using a business model to supply a specific product will help ease commercial transactions.

Once a successful and profitable algae business is established, there is opportunity to consider complimenting business revenues with other sources of value derived from the residual components of algae biomass, including biofuels and carbon credits. When we understand the mechanics and processes of algae cultivation in a specific, profitable niche, doors will open to cost-effective production of algae feedstock for commodities like biofuels and to carbon credits.

Scientific engineering advances may be incorporated to enhance yields of specific products including biofuels [109]. Photosynthetic research may provide important clues to maximizing yield by taking advantage of maximal irradiance [110-112]. In general, algae growth has been associated with C3 photosynthesis. More recent studies suggest that C4 photosynthesis may also take place and have implications for improving growth yields [113].

We recommend that governments set in place integrated algae cultivation and biomass production/processing platforms like or in association with ATP3 (Algae Testbed Public Private Partnership) that lead to commercial products and establishing production benchmarks. In facilities like AzCATI (the Arizona Center for Algae Technology and Innovation), innovators and companies integrate specific technologies and test systems against existing benchmarks. When new technologies prove more efficient and effective, they will set new production standards and thereby improve efficiency.

2.11 Conclusions

Much of the impetus for the recent renewed interest in algae biomass is related to the acknowledgement that algae biomass has the potential to address pressing global challenges, i.e., it may help reduce atmospheric CO_2 and reliance on conventional fossil fuels and provide a good

source for food and cleaner water. Climate change is and will continue to affect the entire global community. Access to energy is fundamental to maintaining a productive and healthy economy. Given that energy is a commodity, cost will always be a factor, and therefore the cheapest products are favored. Government incentives in the form of subsidies for renewable energy are important in signaling to industry that change is required and promoting the adoption of alternative energy forms.

In the case of algae biomass, past government subsidies created a frenzy of commercial activity through legislation demanding that increasing percentages of petroleum fuels be from renewable sources. Over the past 20 years, over a billion dollars has been spent attempting to cultivate algae biomass that would deliver a more cost-effective feedstock from which to produce renewable fuels. Although significant investments have been made, the singular focus to deliver cheap biofuels has been an elusive objective. The recent shift to cultivate algae for high-value products to established markets and/or develop a bio-refining model to deliver multiple algae-based products is a more pragmatic approach to launch the algae industry sustainably and economically.

Future government incentives should factor in not only the development and delivery of cheap biofuel feedstocks but also the capability to mitigate GHG emissions. In order to both facilitate more rapid commercialization and to track the progress within the industry, metrics need to be established. Any government subsidies should be tied to the release of key operating and production data for both progress tracking and collaborative research purposes. Given the multi-disciplinary complexities associated with algae production platforms, access to quality data is imperative for overcoming multiple challenges still associated with algae cultivation. Open access to research data sets would enable advancement of the overall algae knowledge base for the benefit of the greater community and accelerate the transition into commercial viability for the entire industry. This would facilitate more effective technology evaluation and enable better commercial decisions to be made.

For the Canadian context, the reviewed algae cultivation technologies show tangible progress toward delivering cost-effective algae biomass for downstream bio-refining applications. In order to achieve this outcome along with the national objective of GHG mitigation, further research needs to demonstrate improved crop yields with sustained and consistent growth; more efficient dewatering, processing, extraction, and refining capability; cost-effective scalability of related technologies; and reduced energy inputs in the algae production platform.

3 A Review on the Current Status of Various Hydrothermal Technologies on Biomass Feedstock

3.1 Introduction

Increasing energy demands related to increasing population, rapid industrialization, and stringent environmental regulations call for alternative routes of energy production, as conventional energy derived from fossil fuels cause severe environmental harm through the release of greenhouse gas emissions. Moreover, the imbalance in supply and demand makes it inevitable that substitutes for conventional energy sources are needed [114]. Biomass refers to biological matter or waste obtained from living organisms that has solar energy stored in it. It is deemed to be a potential energy source [115, 116] and is considered to be inexpensive, clean, and environmentally friendly. Biomass wastes include plants or plant-based wastes, municipal wastes, industrial wastes, animal wastes, and household wastes. Due to its renewability and sustainability, biomass waste could become a viable alternative source of energy and, moreover, is expected to provide 25% of the world's energy demand [117]. Biomass with high moisture content is not economical to process by conventional technologies, as a significant amount of energy goes into the drying process. Hydrothermal processing is efficient as it eliminates the costly drying step, thereby making it attractive. The energy required for drying exceeds that used for hydrothermal processing at supercritical conditions for biomass with a moisture content of 30% or greater [118].

Hydrothermal processing is a thermochemical process that involves thermal disintegration of biomass in hot compressed water, wherein a series of complex reactions causes changes in the water's physical properties (i.e., its density, solubility, and dielectric constant) [119]. The process converts biomass into a solid (biochar), a liquid (bio-oil or biocrude), or a gas (e.g., hydrogen, methane). The process also leads to by-products that can be used for power generation and the recovery of useful nutrients [120]. The desired products are obtained by manipulating variables such as temperature, pressure, catalyst, and time [121]. Of late, hydrothermal processing technologies have been the subject of major research for a range of biomass types including agricultural wastes and algae [122, 123]. There are many challenges facing the commercialization of these technologies, including expensive and complex reactors [124] that require high capacity water handling equipment [122]. Overall poor understanding of mass balance further make it difficult to accurately measure product yields during the hydrothermal run [125]. The hydrothermal processes (carbonization, liquefaction, and gasification) illustrated in Figure 1 are based on data from Kruse et al. and Toor et al. [126, 127]. Thermochemical processing technologies have been used since 1788 to convert biomass to biocrude [128]. They are gaining widespread interest as a means of catering to energy demands and tackling growing environmental concerns related to increasing global warming and decreasing fossil fuel reserves.

Hydrothermal processing can produce energy-dense fuels and valuable chemicals. The process allows efficient heat integration and thus takes into account the energy penalty due to water valorization from hydrothermal media [129]. Hydrothermal processing such as liquefaction and gasification produces an aqueous phase. The residual carbon of the aqueous phase can be used to produce biogas through anaerobic digestion. The gas thus produced can be used for heat and to generate electricity through a combined heat and power generation system and, therefore, the hydrothermal process coupled with anaerobic digestion allows a useful use of energy, thereby reducing energy requirements in the process [130, 131]. With that said, the use of organics in the

aqueous phase is a way to reduce the operating costs of the hydrothermal technology, as using organics helps reduce wastewater treatment costs. In the case of algal feedstocks, the aqueous phase has biogenic carbon, phosphorous, nitrogen, and micronutrients that can be recycled for algal cultivation purposes. In addition, high-value chemicals such as ethanol, acetone, and acetic acid can be obtained through extraction and catalytic processes [132]. A pinch analysis can be used to optimize the process by identifying intensive heat streams, i.e., heat can be recovered and used in the process to make HT more economical [133, 134]. Considerable improvements in homogeneous and heterogeneous catalysts, including metallic catalysts, have led to major advancements in hydrothermal processing technologies [135].

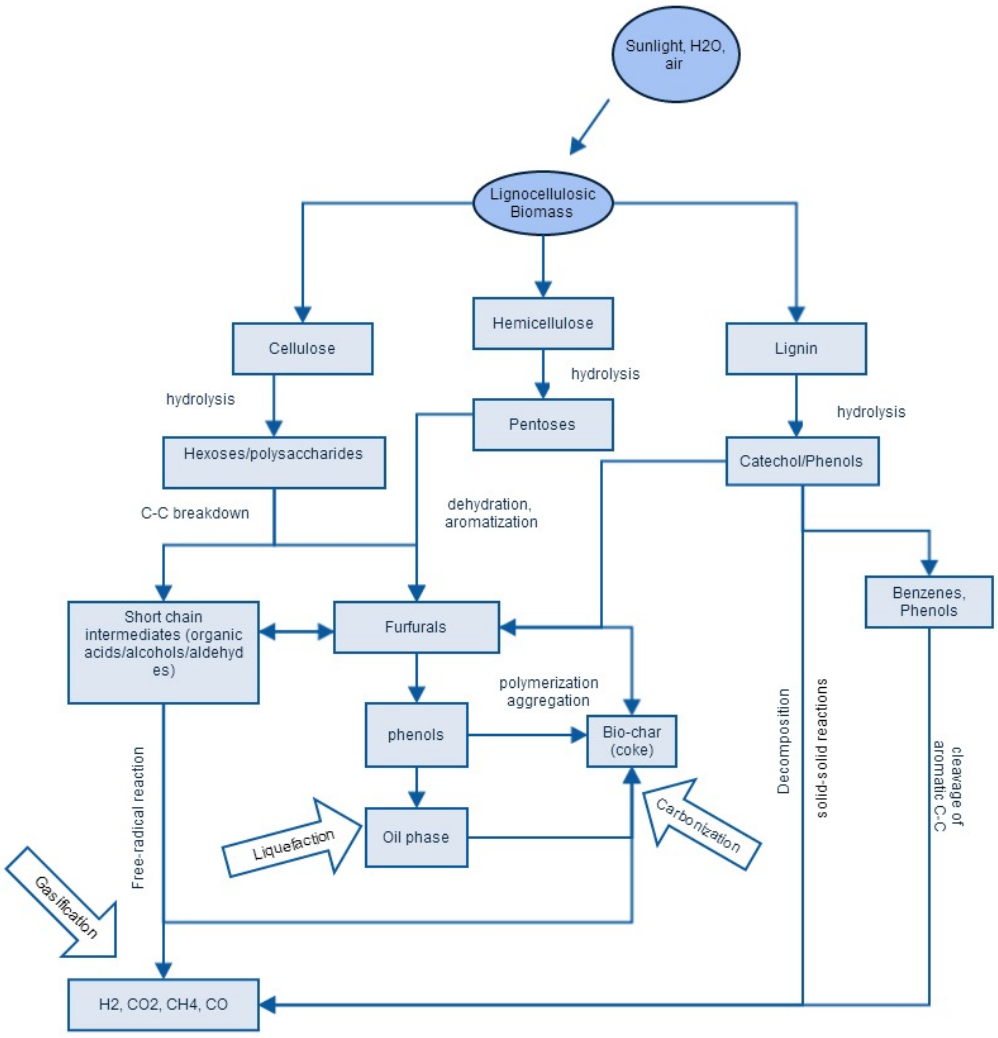

Figure 1: Schematic of a hydrothermal processing technology

Hydrothermal processing operates in one of two states: subcritical and supercritical. The states are defined with respect to the critical point of water (T_c = 373 °C, p_c = 22.1 MPa). The hydrothermal process commences with the dispersion of the water-soluble part of biomass into water at 100 °C followed by subsequent hydrolysis above 150 °C, causing the disintegration of the cellulosic and hemicellulosic fractions of biomass into its monomeric chains. Then, slurry forms at 200 °C under

1 MPa and proceeds towards either liquefaction or gasification depending on the desired product [121]. The first study on supercritical water gasification was published in 1985 by Modell [136], who used maple wood sawdust as a feedstock. Research efforts have been underway in this promising field for a long time, and hydrothermal technology research has had a sudden upsurge in publications that show the technology's potential for biomass conversion. However, existing knowledge is disconnected, and this review aims at collecting and analyzing the existing experimental studies on hydrothermal technologies. It is challenging to establish the research findings due to the variations that arise from different types of feedstock and reaction environments. Hydrothermal technology processes, along with process parameters needs, need to be understood. Hence, the overall objective of this section is to conduct a review of the hydrothermal processing of biomass feedstocks. The specific objectives are:

- To review and summarize hydrothermal liquefaction processes and discuss operating parameters that have a major impact on the processes;
- To review and detail the experimental studies on the catalytic hydrothermal liquefaction process of different biomass feedstocks;
- To review and analyze the reaction mechanisms of the hydrothermal gasification process and study the operating parameters;
- To review and illustrate the experimental studies on the catalytic hydrothermal gasification process of different biomass feedstocks;
- To study and provide a brief account of experimental studies on the hydrothermal carbonization of biomass feedstock; and
- To identify the gaps in knowledge and economic bottlenecks relevant to the large-scale commercialization of hydrothermal technologies.

3.2 History of hydrothermal processing

There is great potential in continuous process hydrothermal technology for large-scale commercial conversion of wet biomass to energy-rich fuels and chemicals [137, 138]. When biomass is subjected to hydrothermal conditions, water molecules cause the degradation of the larger molecules in biomass into smaller fragments. During the 1970s and 1980s, early research efforts on hydrothermal processing were undertaken at the Pittsburgh Energy Research Center; there, the technology was based on the process of lignite coal liquefaction [139]. Then it was discovered by researchers at the Lawrence Berkeley Laboratory [140] and Biomass Liquefaction in Albany [141]. The processes developed at the Pittsburgh Research Center and the Lawrence Berkeley Laboratory varied with respect to pre-treatment methods and post-conversion processes; the former used drying and grinding whereas the latter used acid hydrolysis [142]. In the Netherlands, Shell developed a hydrothermal upgrading unit for biomass liquefaction [143]. NextFuels in Asia is in the process of developing a commercial hydrothermal liquefaction facility based on a daily production scale of 1000 barrels of oil from palm oil wastes [144]. A Danish company developed CatLiq, which processes sewage sludge including algae and manure [145]. All of these initiatives led to the formation of companies like Steeper Energy, which, in collaboration with Aalborg University, is developing a commercial technology [146]. Changing World Technologies was being known to be developing a commercial HTL plant to convert turkey waste to oil through thermal de-polymerization [147]. Unfortunately, Changing World Technologies suffered from bankruptcy and was purchased by Ridgeline Energy Services in Canada [148, 149]. Early investigations into hydrothermal liquefaction were carried out at the University of Toronto

(Canada), the University of Arizona (USA), and the Royal Institute of Technology (Sweden) [139]. This research focused mainly on terrestrial biomass feedstock and later on algal feedstocks. The interest in HTL-based technologies remains a key driver for the production of fuels and chemicals towards an HTL bio-refinery concept.

The concept of hydrothermal gasification was initially proposed by Modell's group in a report published by the Massachusetts Institute of Technology (USA) [150]. Modell and coworkers performed supercritical water decomposition of glucose and then applied this novel technology to test hazardous organic wastes in supercritical water. They also studied oxidation in supercritical water, referred to as supercritical water oxidation (SCWO), to gain an understanding of the technology [151]. Following Modell's research, the Pacific Northwest National Laboratory (USA) developed a technology featuring the application of metal catalysts at low temperatures (400 ˚C) [152, 153]. Later, a research group at the University of Hawaii developed a technology based on high temperatures (600 ˚C) using a carbonaceous catalyst [154, 155]. This led teams of scientists and researchers from other research centers and universities such as the Karlsruhe Research Center [156], Hiroshima University [157], the University of Michigan [158], the University of Leeds [159] and elsewhere to contribute to research efforts.

The concept of hydrothermal carbonization, initially suggested by Friedrich Bergius as early as 1913, simulated a natural coalification technique [160]. The process later became known as the hydrothermal degradation of organics for the production of fuels and chemicals [161, 162]. The burgeoning number of publications in hydrothermal processing technology shows the interest world-wide in research in this area.

3.3 Biomass: a possible future energy source

Biomass, an abundant source of renewable energy, is often composed of organic substances derived from carbon, hydrogen, and oxygen. The substances are categorized based on a range of sources such as trees, algae, grass, urban wastes, agricultural wastes, forestry wastes, domestic wastes, municipal wastes, and industrial wastes [163-165]. Biomass makes up 10-14% of world-wide energy demand [166]. It is usually a heterogeneous mixture of organic substances together with a small amount of inorganic substances. On a dry basis, biomass has typically 30-40% oxygen, 30-60% carbon, and 5-6% hydrogen, depending on ash content. Other inorganic elements include nitrogen, chlorine, and sulphur, which together make up < 1% of the biomass. Broadly, biomass is composed of cellulose, hemicellulose, lignin, and extractives including proteins, ash, and pectin [167, 168]. The carbohydrate portion of the biomass is the cellulose and the hemicellulose, and the non-carbohydrate portion is made up of lignin [114]. Cellulose, $(C_6H_{10}O_5)_n$, is an abundant natural polymer formed by β-1,4 glycosidic linkage of D-glucopyranose units that are held together by strong intra- and intermolecular hydrogen bonds [169]. Cellulose, being crystalline, is insoluble in water and resistant to enzymatic attack. However, it rapidly decomposes and dissolves under subcritical and supercritical conditions of water. Hemicellulose, a hetero-polysaccharide, is an amorphous polymer formed by the branching of a straight chain skeleton of xylan and gulucomannan [170]. It is composed of monomers of D-glucopyranose, D-mannopyranose, D-galactopyranose, D-xylopyranose, and L-arabinofuranose [171] and constitutes 20-40% of biomass. It is linked to cellulose and lignin via hydrogen and covalent bonding, respectively. It is less crystalline because of its non-uniformity and the presence of side groups. It is easily hydrolyzed by an acid or a base at temperatures above 180 °C [161]. The third component, lignin,

is an aromatic compound of *p*-hydroxyphenylpropanoid units in which hydroxyl and methoxy bonds are linked through ether bonds [118]. Lignin is composed of basic building blocks of molecules such as trans *p*-coumaryl alcohol, coniferyl alcohol, and sinapyl alcohol [161]. It is hydrophobic and resistant to biological degradation. It has a higher heating value than cellulose and hemicellulose [172]. Extractives in biomass are made up of other heterogeneous materials including inorganic and organic compounds, proteins, fatty acids, phenols, resins, and terpenes [171, 173]. Extractives make up < 2% of the dry matter and accounts for its color, odor, and durability [170, 171] and can be extracted by various polar or non-polar solvents [170]. Biomass is widely used as a source of fuel, energy, and chemicals [115]. The selection of biomass for a particular energy conversion technology depends on the nature and composition of the biomass [115].

3.4 Water: a boon for hydrothermal processing

Water is regarded as an environmentally innocuous medium for most organic reactions. It exists in three phases: solid, liquid, and gas. Below water's critical point, the vapor pressure curve separating the liquid and vapor phase ends at the critical point (T_c = 373 °C, p_c = 22.1 MPa). Beyond the critical point, the properties of water can be changed without any phase transition. The supercritical state (SC) refers to the zone of high temperature and pressure at the critical point at which water acts as both a reactant and a catalyst. At this condition, properties such as the ionic product, density, viscosity, and dielectric constant of water show quick variations. Supercritical water (SCW) is an excellent solvent for most homogeneous organic reactions owing to high miscibility and the absence of any phase boundaries. It acts as a "nonpolar" solvent and has a dipole moment of 1.85 D. The dipole moment is a measure of the ability of the solvent to form dipoles. Water in the supercritical state is able to react with different compounds. As shown in Figure 2, the dielectric constant, a gauge of hydrogen bond effectiveness, is 80 at normal temperature and pressure and reduces substantially to 5 at the critical point, which is typical of a non-polar solvent [149]. This is usually due to the reduction in ordered hydrogen bonds per molecule of water with the increase in temperature. As a result, the affinity of water towards hydrophilic molecules increases [174]. This change in the dielectric constant of water makes water a suitable medium for solvating organic molecules, which causes reactions to occur in a single phase, leading to higher reaction rates due to improved nucleophilic substitutions and eliminations [175], and subsequent hydrolysis reactions [176]. However, the phase transition of water to its organic form causes the precipitation of salts due to its decreased solubility, which often results in clogging issues. The organic reactions that take place in acidic/alkaline pH occur in a neutral condition in sub-critical water [177]. Similarly, water viscosity tends to decrease with an increase in temperature, leading to a higher diffusion coefficient and mass transfer.

The ionic product of water (K_w) initially increases from 10^{-14} mol^2 L^{-2} at 25 °C to ~ 10^{-11} mol^2 L^{-2} at 300 °C, beyond which it drops sharply below 10^{-20} mol^2 L^{-2} at the supercritical point [178, 179]. The initial increase in K_w proliferates [H^+] and [OH^-]. This promotes heterolytic cleavage of aromatics and catalyzes acid/base reactions [180]. Delocalization of p-electrons, owing to the substitution of hydroxyl groups, causes instability and benzene ring cleavage [181]. The further decline in K_w is attributed to the decrease in density that leads to accelerated free radical reactions [182].

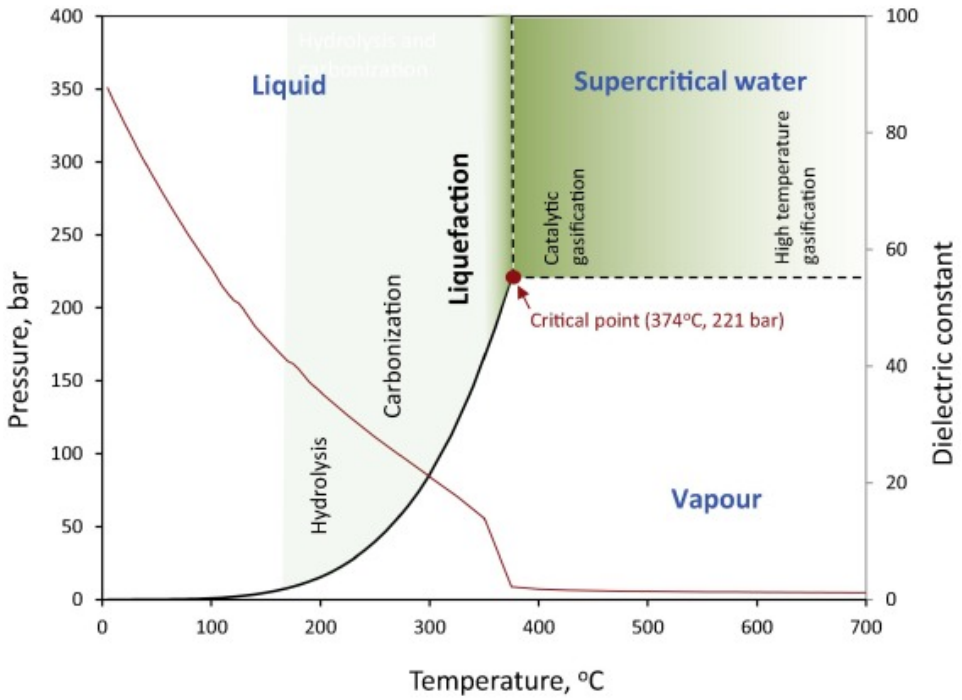

Figure 2: Phase diagram of water (pressure-temperature) and static dielectric constant at 200 bar (Adapted from Tran et al. [149])

The role of water in hydrothermal processing cannot be underestimated. At high temperature, free-radical mechanism proceeds via two phases. The first phase is an induction period wherein a radical pool is generated. The second phase involves free radicals reactions. Both phases depend on process variables [181]. Low water density supports the free radical reaction; however, high water density dictates the ionic reaction mechanism [182]. Hydrolysis releases catalytic acid or alkali from water and salt [183, 184]. The protons released at high temperature and pressure generate alkyl and C–N radicals and cause ring opening of heterocyclic compounds [185]. Water at a supercritical state shows the intermediate behavior of a liquid and a gas. The physico-chemical properties of water with respect to temperature, summarized in Table 7, are obtained from Tekin et al. and Onwudili and Williams [166, 186].

Table 7: Properties of water under different temperature regimes

Parameters	**Normal water**	**Sub-critical water**	**Super-critical water**
Temperature (°C)	25	250	400
Pressure (MPa)	0.1	5	25
Density (g/cm^3)	0.997	0.80	0.17
Viscosity (m Pa s)	0.89	0.11	0.03
Dielectric constant	78.5	27.1	5.9
Heat capacity (KJ/kg/K)	4.22	4.86	13
pK_{su}	14.0	11.2	19.4
Thermal conductivity (mW/m/K)	608	620	160

3.5 Effects of hydrothermal processing on biomass

Many studies focus on simple model compounds rather than real biomass to circumvent problems associated with the heterogeneity and complexity of biomass. Glucose and xylose used as a model for cellulose and hemicellulose, respectively, while phenol is used to model lignin, as cellulose, hemicellulose and lignin are the main constituents of lignocellulose fractions. A few studies have used methanol in models for alcohol and others have used 5-hydroxymethylfurfural (5-HMF), an intermediate for glucose gasification. Cellulose is the main component in lignocellulosic biomass fractions and mostly yields glucose [187]. The hemicellulosic fraction is made up of five-membered carbons such as xylose and arabinose and six-membered sugar units like glucose, mannose, and galactose, which may be substituted with phenolics, uronics, and acetyl groups [188]. Hemicellulose easily undergoes hydrolysis into oligosaccharides, monosaccharides, and other products like furfural, hydroxymethylfurfural, and acetic acid via hydrothermal processing [189]. Similarly, xylan, a building block of hemicellulose, can be broken into xylose oligosaccharides and intermediates that can be used as prebiotics, making them a highly valuable nutritive [190-193]. The xylose oligosaccharides do not act as a direct source of nutrients for microorganisms and thus require further breakdown into simple monosaccharides, by a chemical or enzymatic approach, to be used as a medium for the production of xylitol [194-196], a reduced precursor of xylose.

Hydrothermal processing has also been used for the production of lactic acid [197] and xylanases [198]. Improvements in the recovery and purification of xylose oligosaccharides through hydrothermal processing have been achieved by using active carbons [199] and ultra or nano filtration membranes [200] and reactor configurations [201-203]. As discussed above, lignin and other heterogenic polymers of phenolics are made up of p-coumaryl, coniferyl, and sinapyl alcohols with the aromatic groups p-hydroxyphenyl, guaiacyl and syringyl [204, 205]. Hydrothermal processing is supposed to re-localize lignin on the surface of biomass, thereby improving the accessibility of enzymes for hydrolysis [206-208]. Lignin components are usually depolymerized through a series of reactions involving degradation and re-localization, the degree of which depends on process conditions [209, 210]. The mechanism of lignin breakdown involves the fast cleavage of lignin-carbohydrate bonds into low molecular weight and highly reactive lignin fragments that undergo gradual re-condensation and re-polymerization in the presence of organic acids [209, 211]. The release of soluble lignin is quantitatively determined at an ultraviolet (UV) absorbance of either 205 or 280 nm, due to its aromaticity [212, 213]. Phenolics, by-products of lignin degradation, are natural antioxidants and food additives [214, 215]. Guaiacol (G) units of lignin are known to produce vanillin, vanillic acid, dihydroconiferyl alcohol, and guaiacol [216]; syringaldehyde, syringic acid and sinapaldehyde are usually obtained from syringyl (S) units of lignin [217].

3.6 Hydrothermal liquefaction

Hydrothermal liquefaction (HTL) involves the thermochemical conversion of a broad range of biomass types in the presence of hot compressed water at subcritical conditions into a liquid product known as bio-oil [127, 218-237]. HTL requires an operating temperature of 300-350 °C at 5-20 MPa for 5-60 min, wherein water is in the liquid phase [238]. The process begins with solvolysis of biomass in micellar forms, the disintegration of biomass fractions (cellulose, hemicellulose, and lignin), and thermal depolymerization into smaller fragments [239, 240]. HTL,

which mimics the processing of fossil fuels buried deep inside the earth, occurs in minutes or hours [241]. HTL produces oil with low oxygen content as opposed to other processes like fast pyrolysis. HTL proves to be very energy efficient as it entails temperatures lower than those reached during pyrolysis [242, 243].

The process is driven by a complex set of reactions and transformations in subcritical water. The process mechanism involves the hydrolysis of biopolymers into water-soluble oligomers followed by the breakup of intra- and intermolecular hydrogen bonds into simple monomers like glucose and other products such as acetaldehyde, acetic acid, and furfural compounds [242]. Hemicellulose is easily susceptible to hydrolysis around 180 °C [161]. Xylose, a component of hemicellulose, may exist either in pyranose, furanose, or open chain form. The furfural is believed to form a pyranose ring structure while formic acid and glyceraldehyde form an open structure [242]. Lignin decomposes to phenolics in hydrothermal media [244]. During the hydrothermal run, the oxygen content of the organics decreases from about 40% to 10-15% [245]. Oxygen is removed in the form of a gas such as CO_2, CO, CH_4, and H_2. Along with gases, an aqueous fraction of water and other small organics are formed. The products from liquefaction processes have fewer process conditions and the resulting products can be safely stored and transported [246]. Srokol and coworkers observed that the acid-catalyzed reactions result in a 5-hydroxymethylfurfural via dehydration while base-catalyzed reactions produce glyeraldehyde, which could further break down into lactic acid, formic acid, acetic acid, etc.

Figure 3 (A) depicts plausible pathways of bio-oil via hydrothermal liquefaction from polysaccharides [247]. Polysaccharides are made of pentoses and hexoses bound together by glycosidic bonds [248]. The degradation products of polysaccharides are comprised of low molecular weight compounds such as phenols, ketones, aldehydes and acids, of which cyclic ketones constitute nearly 50% [247]. During hydrothermal liquefaction, polysaccharides undergo hydrolysis into monosaccharides, which further undergoes isomerization, cyclization and dehydration to produce phenols or cyclic ketones. Carbohydrates are known to form aromatics through ring opening and subsequent reactions involving cyclization and condensation [249]. The plausible decomposition of proteins into bio-oil are summarized in Figure 3 (B) [247]. The nitrogen-containing compounds are the major ones and consist of pyrroles, pyrazines, and amines. Proteins undergoes hydrolysis into amino acids which then either proceeds decarboxylation to produce carbonic acid and amines or deamination reaction into ammonia and organic acids [129]. The resulting molecules results in pyrazine, pyrrole, indoles, and aromatic amides molecules via cyclization and condensation [250].

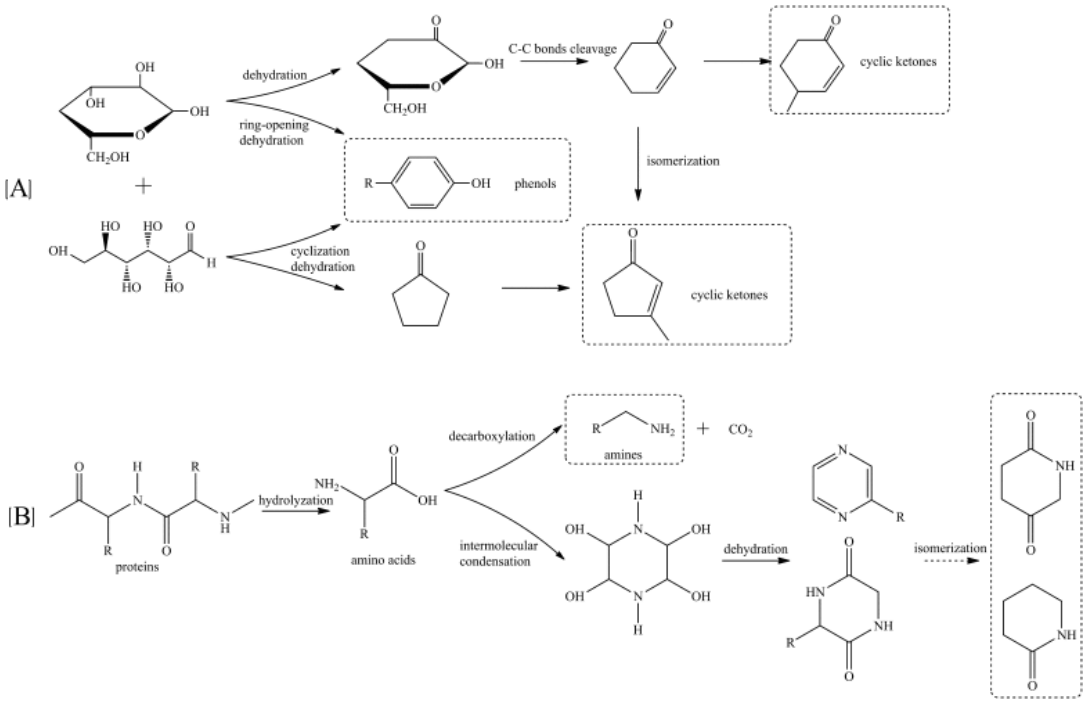

Figure 3: Plausible pathways of formation of bio-oils via hydrothermal liquefaction of biomass (Adapted from Yang et al. [247])

As shown in Figure 4, the formation of polycyclic nitrogenous compounds involves Maillard reactions between reducing sugars and amino acids, obtained from carbohydrate and protein hydrolysis, respectively [251]. The formation of Melanoidin-like polymers in Maillard reactions occurs at a low temperature of 260 °C, which does not favor the formation of bio-oil [231, 251]. With an increase in temperature, the Melanoidin-like polymers decompose and turn into monocyclic compounds like pyrazines and pyrroles, thereby improving bio-oil yield [251].

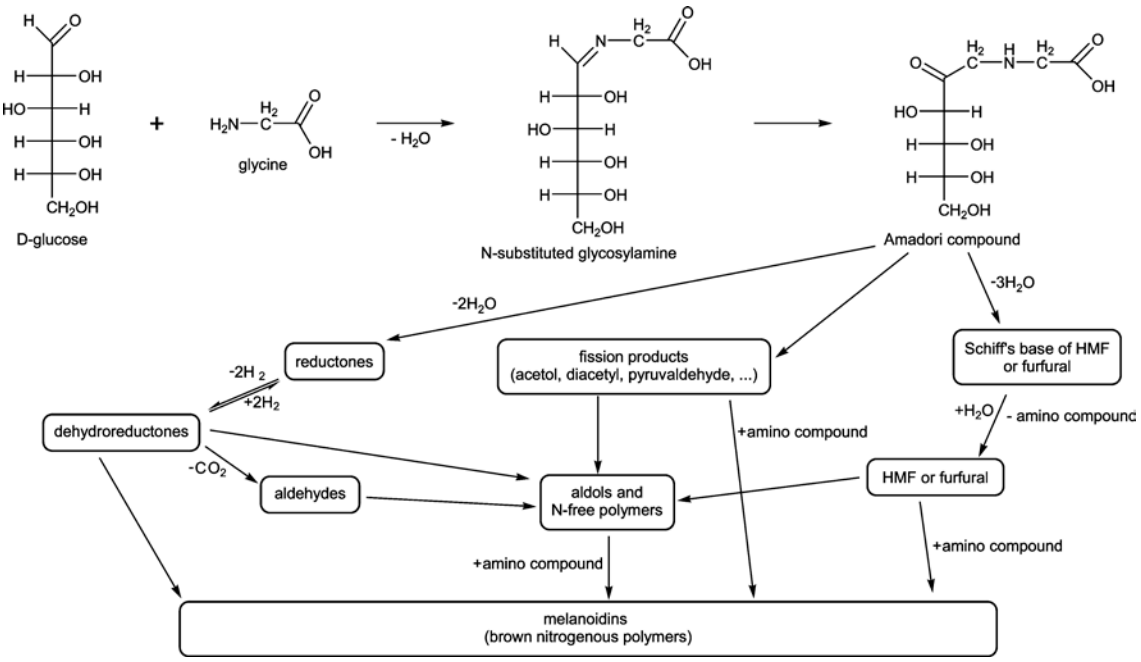

Figure 4: Schematic of Maillard reaction network (Adapted from Peterson et al. [251])

Conditions such as temperature [134, 252-266], pressure [267-270], particle size [271], and reaction times [134, 272-284] influence the conversion of biomass into bio-oil. Temperature improves fragmentation and lignocellulosic fraction cleavage and has a considerable effect on product yield. It is imperative to overcome the energy barrier and use sufficient activation energy for biomass breakup to achieve higher concentrations of free radicals. Biomass liquefaction is usually endothermic at low temperatures and becomes exothermic at high temperatures [285]. As a result, bio-oil yield increases with temperature and reaches a point where a further rise in temperature suppresses liquefaction. Reduced bio-oil yield could also be due to the dominating secondary decomposition and Boudouard gas reactions [286] along with the recombination effects of high concentrations of free radicals into char. At moderately low temperatures (< 275 °C), bio-oil yield also shows a decline due to the partial breakdown of biomass components. Thus, it is believed that an intermediate temperature range of 300-350 °C will likely result in a higher bio-oil yield [287-289].

Pressure is another crucial factor in the hydrothermal liquefaction process as it helps maintain water in the liquid state and thus incur savings by avoiding the high energy costs of a two-phase system [143]. An increase in pressure results in the effective penetration and extraction of biomass. However, pressure becomes insignificant and has little impact on liquid oil near or at supercritical water liquefaction reaction conditions [268, 269, 290]. It should to be noted that a further elevation of pressure under supercritical conditions results in higher local solvent density, which prevents C-C bond fragmentation. Residence time affects product composition and hydrothermal liquefaction conversion efficiency [274, 291]. As degradation under supercritical conditions occurs rapidly, it is often desirable to have short residence times [292]. This is because the dominating secondary and tertiary reactions in a temperature reaction medium form liquids or gases from heavy intermediates and thus decreases bio-oil yield [285]. So, bio-oil attains maximum yield, after which it declines with further increases in residence times [293].

The nature of biomass feedstock affects bio-oil yield due to differing biomass compositions. Hemicellulose and cellulose increase bio-oil yield while lignin goes into the residue fraction [294] because hemicellulose, being amorphous, is easily susceptible to degradation, and cellulose, with a relatively intermediate degree of polymerization, also tends to degrade; however, lignin's decomposition is limited by its high degree of polymerization and complex interlinkage [242].

The biomass type also affects the nature of the bio-oil. Loosely packed biomass liquefaction results in bio-oil with high oxygen and moisture content that is undesirable as it lowers the quality and HHV of the fuel [285]. The small particle size improves accessibility and penetration of heat, thereby improving conversion rate and bio-oil efficiency. As grinding to the smallest possible size may increase costs, it is better to have a standard particle size of 4-10 mm for the hydrothermal run [285]. A summary of the factors influencing the hydrothermal liquefaction of biomass is presented in Table 8.

Table 8: Summary of factors influencing the hydrothermal liquefaction of biomass

Factors	Biomass type	Reaction conditions	Remarks	Ref.
Temperature	Jack pine powder	200-350 °C	25% increase in oil yield with 150 °C increase in temperature	[252]
	Microalgae	180-300 ˚C	Temperatures lower than 275 ˚C promote lipid extraction. Temperatures above 275 ˚C facilitate the degradation of protein and carbohydrates in biomass, which increases oil yield.	[256]
	Palm biomass	330-390 ˚C	A temperature of 390 ˚C yields maximum bio-oil due to the increase in the rate of decomposition via the radical mechanism.	[258]
	Algal cultures	260-320 ˚C	The highest biocrude yield was obtained at 300 ˚C. An increase in temperature caused the biocrude to decompose into char/gas.	[259]
	Microalgae	250-400 ˚C	The maximum bio-oil yield of 51.22 wt% was obtained at 400 ˚C, the temperature considered to be optimum for bio-oil production.	[260]
	Algae	330-370 ˚C	The maximum bio-oil yield was obtained at 360 ˚C. Increasing the temperature	[264]

Factors	Biomass type	Reaction conditions	Remarks	Ref.
			had a positive influence on higher heating value.	
	Cornstalks	240-350 ˚C	Temperatures from 260 ˚C-320 ˚C had no significant effect on bio-oil yield; however, the solid yield fell with an increase in temperature.	[265]
	Rice straw	280-320 ˚C	Up to 300 ˚C, there was no significant change in the bio-oil product distribution. However, beyond 320 ˚C, bio-oil yield fell.	[266]
	Sawdust	180- 280 °C	Oil yield increased with temperature.	[253]
	Swine manure	260-340 °C	Increasing temperature from 260 to 340 °C increased the amount of bio-oil by 9.3%.	[254]
	Wood stalks	250 -290 ˚C	The bio-oil yield increased from 44.5% to 50.4% with an increase in temperature in ethanol solvent.	[257]
	Microalgae	250-350 ˚C	Conversion efficiency increased with temperature in this order: lipids > proteins > carbohydrates.	[261]
	Oilmill wastewater	240-300 ˚C	Bio-oil yield improved from 28.25 wt% to 58.09 wt% with an increase in temperature while the solid yield fell from 43.87 wt% to 17.18 wt%. The optimal temperature was 280 ˚C.	[134]
	Algae	180-330 ˚C	Nannochloropsis sp. attained the highest bio-oil yield of 47.5%. Increasing the temperature improved biocrude yield.	[262]
	Crude glycerol and aspen wood	380-420 ˚C	Biocrude and char yields, as well as biocrude composition, were not affected by temperature changes.	[263]

Factors	Biomass type	Reaction conditions	Remarks	Ref.
	Algae	180-300 ˚C	Increasing the temperature improved biocrude oil yield. Biocrude yield increased from 11% at 250 ˚C to 16.98% at 300 ˚C, suggesting that the increase in biocrude yield occurred not only from lipids, but also from other non-lipid components such as proteins and carbohydrates. The improvement in biocrude oil is attributed to hydrolysis and repolymerization.	[255]
Particle size	Grass perennials	350 °C	Particle size has no effect on liquid oil yield.	[271]
Pressure	Coal	370-490 °C; up to 12.2 MPa	An increase in pressure resulted in high liquid yield due to improved solvent power and diffusivity.	[267]
	Glucose	300-400 °C, 25-40 MPa	Rate constant for glucose degradation was lowered by a rise in pressure, which could likely be due to the reduction in the epimerization rate to fructose.	[268]
	Fruit bunch, palm, kernel shell	330-390 ˚C, 25-35 MPa	The increase in pressure caused an increase in solvent density and solubility. However, the increase in pressure also caused a caging effect. At 390 ˚C, the increase of pressure from 25 to 35 MPa reduced bio-oil yields.	[270]
Residence time	Sawdust	180-280 °C	In temperatures from 250 to 280 °C, longer reaction times reduced oil yield due to secondary reactions; however, oil yield increased	[272]

Factors	Biomass type	Reaction conditions	Remarks	Ref.
			at a low temperature (180 °C).	
	Poplar wood	350 °C	Poplar suppressed the bio-oil yield except for very high biomass-to-water ratios	[273]
	Sawdust	150-450 °C	The conversion and yield of gaseous products are the same but the yield of bio-oil increases with an increase in reaction time.	[274]
	Kenaf	300 ˚C	The liquefaction time of 60 min resulted in an oil yield of 77.2%.	[275]
	Willow	400 ˚C, 32 MPa, 0-20 min	A longer reaction time negatively influenced the biocrude yield while solid residues and gas yield increased, signifying that re-polymerization and gasification are favored at longer residence times.	[276]
	Oil mill wastewater	240-300 ˚C, 15-45 min	Increasing residence time promoted bio-oil yield, in this case, an increase from 55.76 wt% at 15 min to 58.09 wt% after 30 min. With a further increase in time, gas and solid residue yield increased. This could be attributed to competing depolymerization and hydrolysis reactions.	[134]
	Fermented corn stalks	250-400 ˚C 15-105 min	Bio-oil yield increased until 30 min, after which it fell, indicating that a longer residence time caused depolymerization and cracking of bio-oil.	[277]
	Microalgae	100-400 ˚C, 10 s-60 min	Solid product yields fell with longer reaction times. However, longer residence times (t > 40 min) at higher	[278]

Factors	Biomass type	Reaction conditions	Remarks	Ref.
			temperatures (300 ˚C) reduced biocrude yield.	
	Spent coffee grounds	5-30 min	The highest biocrude yield (31.63%) was reached after 10 min, after which yield fell. The bio-oil decomposed with time.	[279]
	Algae	350 ˚C, 10-60 min	A longer reaction time reduced the yield of water-soluble biocrude and increased the yield of water-insoluble biocrude. However, total biocrude yield was not affected by residence time.	[280]
	Microalgae	350 ˚C; 1.4-5.8 min	Higher biocrude yields were obtained at lower residence times, and greater energy recovery was possible at a residence time of 5.8 min.	[281]
	Algae	220-400 ˚C, 10-60 min	Initially, biocrude yield increased (39.54% at 50 min), but after 50 min. it decreased.	[282]
	Swine carcasses	150-250 ˚C; 20-120 min	The yield of bio-oil improved from 45.5 wt% (20 min) to 58.2 wt% (60 min). The longer reaction time (60-120 min) lowered the yield due to prevailing reactions involving secondary cracking.	[283]
	Microalgae and lignocellulosics	300 ˚C, 20-90 min	Biocrude yield increased with an increase in reaction time up to 60 min, after which it decreased. The decrease is attributed to the repolymerization and recondensation of biocrude.	[284]

3.6.1 Catalytic hydrothermal liquefaction

3.6.1.1 Homogeneous catalysts

The use of catalysts in hydrothermal liquefaction processes is intended to improve process efficiency by reducing char and tar formation. Two types of catalysts, homogeneous and heterogeneous, are reported in the literature and are summarized here.

Homogeneous catalysts, as shown in Table 9, comprise alkali salts such as Na_2CO_3, K_2CO_3 and $KHCO_3$ [253, 255, 295-316]. Alkali salts reduce char/tar formation and improve product yield by accelerating the water–gas shift reaction. They are economical to use for hydrothermal technologies. The working mechanism involves the formation of esters through the decarboxylation reaction between the hydroxyl groups in biomass and the formate ions in alkali carbonates. Ester formation is followed by a series of reactions, i.e., dehydration, deoxygenation, decarboxylation, and the dehydrogenation of micellar-like fragments into smaller ones. This is followed by a cycle of rearrangements through cyclization, polymerization, and condensation [317]. Karagöz et al. [318] suggested that potassium salts are more catalytically active than other salts (K_2CO_3 > KOH > Na_2CO_3 > NaOH). Along with these salts, other catalysts in the form of acids and gases have been used [319]. With homogeneous catalysts, there are some advantages: decreased solids production, increased biocrude yield, and improved biocrude properties. Moreover, the incorporation of alkali salts in the hydrothermal media elevates pH, thereby decreasing dehydration reactions, which usually lead to unstable unsaturated molecules [320]. With NaOH, less char is produced [311]. This is because the OH^- neutralizes the molecules causing polymerization in char formation. The polymerization reaction between the hydroxyl groups at the residue surface and the carboxylic groups in the aqueous stream produces ester bonds, which form char. Hence, NaOH cannot cause polymerization, due to the neutralization of carboxylic acids. As a result, NaOH's participation is restricted in condensation reactions [289]. A recent publication discussed the use of catalysts such as colemanite and borax for the hydrothermal processing of biomass [321]. According to the study, a borax catalyst is effective to 300 ˚C, and colemanite is much more effective than borax.

Table 9: Homogeneous catalysts used for the hydrothermal liquefaction of model compounds and biomass

Model compounds/ Real biomass	Operating parameters	Reactor/ device/ tubing	Catalysts (with/ without support)	Key findings/remarks/observations	Ref.
Algae	300 ˚C	Bench-scale micro-reactor	KOH	Biocrude yield increased from 16.98% (without catalyst) to 22.67% with KOH after 30 min at 10% solid loading. The incorporation of the catalyst improved the extraction of carbohydrates.	[255]

Model compounds/ Real biomass	Operating parameters	Reactor/ device/ tubing	Catalysts (with/ without support)	Key findings/remarks/observations	Ref.
Kraft lignin	280-350 ˚C	Batch	K_2CO_3	The catalyst increased the yield of liquid products and reduced char formation. The catalyst improved the yield of monomeric aromatics.	[305]
Wood	280 ˚C	Batch	K_2CO_3, KOH, Na_2CO_3, NaOH	With K_2CO_3, the highest bio-oil yield of 34.9 wt% with the lowest solid residue yield of 6.8 wt% was obtained. The order of reactivity based on liquid yield was: K_2CO_3 > KOH > Na_2CO_3 > NaOH	[306]
Sorghum	300 ˚C	Tubular	KOH, K_2CO_3	With K_2CO_3, biocrude had a HHV of 33.1 MJ/kg, and the highest biocrude yield was 61.8%.	[307]
Pinewood sawdust	300 ˚C	Autoclave	K_2CO_3	The use of K_2CO_3 doubled the bio-oil yield. The maximum bio-oil yield (30.8 wt%) and the minimum solid yield (28.9 wt%) were obtained with ethanol solvent. The use of water as solvent reduced the bio-oil yield as a fraction of bio-oil was found in the aqueous phase.	[308]
Microalga		Batch	Na_2CO_3	Na_2CO_3 increased biocrude yield to 51.6% from around 29.2% without a catalyst. The catalyst also led to the lowest energy consumption ratio during the hydrothermal run.	[309]
Birchwood sawdust	300 ˚C	Bench top	KOH, K_2CO_3	Biocrude oil yield with KOH more than doubled (~ 40 wt%) that under non-catalytic reaction. Also, solid residue decreased from ~ 33 to 12 wt%.	[310]
Blackcurrant pomace	290-335 ˚C	Batch	NaOH	The catalyst increased bio-oil yield and reduced char formation.	[311]
Bamboo chopsticks	290-380 ˚C	Autoclave	K_2CO_3	At 290 ˚C, yield reached 21.2 wt% compared to 3.8 wt% in a non-catalytic run. In addition, the heating value increased to	[312]

Model compounds/ Real biomass	Operating parameters	Reactor/ device/ tubing	Catalysts (with/ without support)	Key findings/remarks/observations	Ref.
				31.6 MJ kg^{-1}, showing the effectiveness of the catalyst.	
Rice straw	220-300 ˚C	Autoclave	Na_2CO_3	The catalyst improved hydrolysis of cellulose and hemicellulose in the presence of glycerol. Na_2CO_3 promoted alcohol formation. Bio-oil yield was 50.31 wt% under optimum conditions of 260 ˚C.	[313]
Dried distiller grain with solubles	350 ˚C	Bomb type	K_2CO_3	The catalyst, together with the recycled HTL aqueous phase, increased the yield compared to non-catalytic HTL; however, the water content in the biocrude also increased.	[314]
Sewage sludge	400-500 ˚C	Batch	K_2CO_3, Na_2CO_3	Catalysts decreased the yield of biocrude at 50 wt% of dried sludge.	[315]
Algae	250-350 ˚C		Na_2CO_3	The catalyst improved the biocrude yield for high-carbohydrate biomass at higher temperatures (300-350 ˚C), while high-protein biomass yielded more bio-oil at a lower temperature (250 ˚C).	[316]
Wood	280 °C	Autoclave	K_2CO_3	The absence of water yielded liquid products equivalent to a biomass/water ratio of 6.1 M. K_2CO_3 showed the maximum biomass conversion along with considerable drop in solid residue (by 4%).	[253]
Corn stalk	410 °C, 25 MPa	Fixed-bed	Na_2CO_3	The catalyst had a positive effect at relatively higher temperatures. Yield conversions increased to 95 wt% (dry basis); 77% liquid product yield was reported at 25 MPa.	[298]
Pinewood sawdust	300 °C, ~ 7.93 MPa	Autoclave	K_2CO_3	K_2CO_3 doubled bio-oil yield. Maximum bio-oil was attained (30.8 wt%) and the minimum solid residue yield (28.9 wt%)	[299]

Model compounds/ Real biomass	Operating parameters	Reactor/ device/ tubing	Catalysts (with/ without support)	Key findings/remarks/observations	Ref.
				when ethanol was used as a solvent.	
Oil palm shell	210-330 °C	Autoclave	K_2CO_3, Na_2CO_3, NaOH	Similar results were obtained with 10% K_2CO_3 and 10% Na_2CO_3 while 10% NaOH had maximum solid conversion (84%) and liquid product (53.4%). 10% NaOH also reduced the gaseous product yield.	[295]
Barley straw	300 °C	Autoclave	K_2CO_3	K_2CO_3 produced more phenolic compounds and less carboxylic acid. Further analysis of solid residue confirmed improved decarboxylation of barley straw liquefaction with K_2CO_3. Carbon and energy recovery doubled with the catalyst. High biocrude yield (34.85 wt%) was achieved with K_2CO_3.	[304]
Barley straw	280-400 °C	Batch	K_2CO_3	A lower temperature favored the formation of biocrude. High biomass conversion (> 87 wt%) was observed. The biocrude yields were in the range of 20.35-35.24 wt%. Optimal HTL conditions were 300 °C. HHVs of biocrude increased with temperature, ranging from 26.75 to 35.48 MJ/kg. Biocrude consisted of carboxylic acid, phenolics, ketones, and aldehydes.	[303]
Cellulose	200-350 °C, 3 MPa	Autoclave	Na_2CO_3	Alkali catalyst inhibited the formation of char from oil and caused stabilization of oil.	[296]
Polysaccharides	200 °C	Bomb-type batch	CO_2	The glucose yield increased by 49.3%. The production of 5-HMF, a secondary decomposition product of hexoses, dropped more in CO_2-	[319]

Model compounds/ Real biomass	Operating parameters	Reactor/ device/ tubing	Catalysts (with/ without support)	Key findings/remarks/observations	Ref.
				enriched water than in aqueous HCl.	

3.6.1.2 Heterogeneous catalysts

As discussed, homogenous catalysts such as NaOH, Na_2CO_3, and KOH have been widely used for the catalytic HTL of biomass. Homogenous catalyst recovery is expensive due to the cost-intensive separation process and is also energy intensive. Although heterogeneous catalysts are used mostly in hydrothermal gasification, a few reports have discussed the hydrothermal liquefaction of lignocellulosic biomass to improve biocrude quality, as shown in Table 10. Some gasification is needed to remove oxygen; however, prolonging it could reduce bio-oil yield.

Heterogeneous catalysts include platinum, nickel, and palladium. As these metals are rare, there has been shift of focus to metallic oxides, i.e., zirconium dioxide (ZrO_2) [271, 322-324]. Apart from these catalysts, studies on catalytic hydrothermal liquefaction have used alkali catalysts, which improve bio-oil yield. Other known metal oxide catalysts include MnO, MgO, NiO, ZnO, CeO_2, La_2O_3, etc. [325-327]. Nanocatalysts involving use of Ni have been tested as they have the potential to improve bio-oil yield at low temperatures, which could help in the commercialization of HTL [328]. Reductive noble metal catalysts such as Pt and Ru are expensive; therefore, an attempt has been made to use a CuZnAl catalyst, which has the potential to covert furfural into cyclopentanone via hydrogenation and hydrogenolysis [329]. Moreover, the activity of such catalysts can be modified by varying Cu or Zn oxide and allows recycling through reactivation in a H_2 gas environment. Zeolite has been cited as a catalyst for the hydrothermal liquefaction of biomass [307].

The transition metal improves the quality of bio-oil [330]. However, in order to avoid the deactivation of catalysts during a hydrothermal run, catalysts showing high hydrothermal stability are important. Keeping in mind industrial applications, carbonaceous materials such as carbon nanotubes (CNTs) using activated carbon as a support for metallic catalysts are suitable because they can provide a large surface area and recycle noble metals [331, 332].

The use of carbon nanotube-supported transition metals for the catalytic HTL of biomass into bio-oil has also been studied [333]. Apart from catalysts, studies have considered co-solvents, which scavenge unsaturated molecules that form through dehydration and that may otherwise be re-polymerized. The most commonly used organic solvents are methanol, butanol, phenol, acetone, and propylene glycol [334-338]. Another study on the use of transition metal chlorides ($ZnCl_2$, $CuCl_2$, and $NiCl_2$) for subcritical hydrothermal liquefaction has also been performed [339].

Table 10: Heterogeneous catalysts used for the hydrothermal liquefaction of model compounds or biomass

Model compounds/ Real biomass	Operating conditions	Reactor/device/ tubing	Catalysts (with/without support)	Key findings/remarks/ observations	Ref.
Dunaliella tertiolecta	320 ˚C	Autoclave	Co/CNTs	95.78% conversion was achieved along with a bio-oil yield of 40.25 wt%. The catalyst produced bio-oil with low O/C ratios.	[333]
Sorghum	300-350 ˚C	Tubular	Ni_2P, Ni/Si-Al, zeolite	Ni/Si-Al performed better than all catalysts tested. The resulting biocrude yield was 45% at 300 ˚C.	[307]
Fruit bunch	390 ˚C	Inconel batch	CaO, MgO, MnO, ZnO, NiO, SnO, CeO_2, Al_2O_3	Catalysts, namely CaO, La_2O_3, MnO, and CeO_2, yielded highest bio-oil yield (about 1.40 times without catalyst).	[325]
Rice husk	300 ˚C	Micro-reactor	La_2O_3, Dy_2O_3	La_2O_3 produced the highest biocrude yield of 32.5 wt% at a water/rice husk mass ratio of 5. The highest HHV (31.78 MJ/kg) of biocrude was also obtained. The catalyst reduced the amount of phenols and acids and promoted hydrocarbon formation.	[326]

Model compounds/	Model compounds/	Model compounds/	Model compounds/	Model compounds/	Model compounds/
Bagasse	200-330 ˚C	Autoclave	$MgMnO_2$	At optimized conditions (250 ˚C for 15 min), the catalyst liquefied 93.7% biomass. The catalyst showed good recyclability. The increased OH concentration due to thermal hydrolysis of the catalyst improved biomass liquefaction.	[327]
Coconut shell	240-330 ˚C	Batch	$ZnCl_2$, $CuCl_2$, and $NiCl_2$	The highest yield of 13.9 wt% of bio-oil was reported. The catalytic effect of the transition metal on cellulose decomposition was observed.	[339]
Microalgae	210-250 ˚C; 20 MPa	Batch	Ni/SiO_2	The catalyst improved the yield of bio-oil. The highest bio-oil yield of 30 wt% was reached at 250 ˚C.	[328]
Grassland perennials	300-450 °C	Parr high-pressure vessel	SO_4^{2-}/ZrO_2–Al_2O_3, solid alkali CaO–ZrO_2	At a heating rate of 140 °C/min, a liquid yield of 82.1% was reported for 1 min at 374 °C. Particle size and catalysts had little influence on liquid yield. The liquefaction process with a fast heating rate shored more potential.	[271]
Stearic acid	400 °C, 25 MPa	bomb type	ZrO_2, CeO_2, Y_2O_3	Catalysts enhanced decarboxylation of C_{17}-acid into CO_2 and C_{16} alkene.	[324]

Distillers grains	350 °C, 25 MPa	Stop-flow	ZrO_2	No major effect of either catalyst or reactor wall was observed on bio-oil yield or quality. ZrO_2 acted as a poor catalyst for HTL.	[322]
Waste	330 °C, 25 MPa	Continuous (loop)	ZrO_2, K_2CO_3	A high calorific value bio-oil was obtained. A BET surface area (32.7 m^2/g) of ZrO_2 was used	[323]

3.7 Hydrothermal gasification

Hydrothermal gasification is a process that involves a reaction temperature above 350 °C in the absence of oxidants and produces a flue gas rich in either H_2 or CH_4, depending on reaction conditions [340]. HTG is done in either batch or continuous mode. The batch process offers the advantage of carrying out experiments at different concentrations and catalysts, while the continuous system allows for studies of reaction kinetics. Hydrothermal gasification has three main types: aqueous phase refining, catalytic gasification in a near-critical state, and supercritical water gasification. Aqueous phase refining occurs at low concentrations at ~ 215-265 °C to produce H_2 and CO_2 in the presence of a heterogeneous catalyst [341, 342]. The process is not desired unless hydrogen is used in situ for the hydrogenation of biomass [343]. Catalytic gasification of biomass in a near-critical state occurs at 350-400 °C and produces CH_4 and CO_2 in the presence of a heterogeneous catalyst wherein CO undergoes hydrogenation to CH_4 [344-347]. This process was first performed in a batch reactor at Battelle Memorial Institute [348, 349] and later realized in a bench-scale continuous system [350]. Supercritical water gasification (SCWG) uses water at a supercritical state in the range of 600-700 °C to generate mainly H_2 and CO_2 with/without a catalyst. SCWG is preferred for biomass with a moisture content above 30% [351]. Even biomass with a moisture content as high as 90% (w/w) can be gasified. SCWG uses high energy to raise the temperature of water to 600 °C, and the energy content in the product can be easily recovered by passing it through a heat exchanger. Heat exchangers operate at high pressures, which makes heat recovery possible [352]. Moreover, reactors at supercritical conditions operate at high pressure and do not require gas pressurization afterwards and thus the compressed medium allows gasification to occur with minimal heat loss [353-355]. The further dissolution of reaction intermediates in the reaction medium minimizes coke and tar formation [352]. When process conditions and the nature of the catalyst are varied, the desired products are obtained [354, 356]. Hydrothermal gasification has significant advantages over traditional processes. The traditional method produces low-quality syngas with impurities such as char/tar that lead to clogging issues. This low-quality syngas needs to be purified, which increases costs [357, 358].

The products from hydrothermal gasification include CO_2, H_2, CO, and CH_4, with small amounts of C_2H_4 and C_2H_6. Figure 5 depicts the simplified process flow for the conversion of biomass to gaseous products via aqueous intermediate compounds under hydrothermal conditions [359]. At

low temperatures, cellulose undergoes hydrolysis into glucose, which is isomerized into mannose and fructose [360]. At subcritical temperatures, the saccharides thus generated undergo dehydration into furans and furfural compounds [361]. However, above critical temperature and pressure, saccharides undergo hydration through free radical reaction to produce carboxylic acids [361].

Lignin, a complex compound, consists of *p*-coumaryl, sinapyl, or coniferyl alcohols that hydrolyze to produce phenols, cresols, syringols, guaiacols, and catechols. At subcritical conditions, these phenolics can undergo dehydrogenation and dehydration into coke. Above critical conditions, these phenolics degrade to form gases through the generation of intermediates such as aldehydes, alcohols, ketones, and carboxylic acids [359].

Lignin alkali initially undergoes hydrolysis to form phenol and formaldehyde, which gets converted into gaseous products [362]. In other pathways, compounds such as formaldehyde and phenol may also undergo cross-linking to form resins through reactions with reactive sites in supercritical water conditions. Hence, lignin not only produces low-molecular molecules but also produces high molecular weight char or tar [363]. The product composition and yield are influenced by a number of design and operation parameters. Key parameters include temperature, pressure, time, heating rate, reactor type, and the nature of the catalyst.

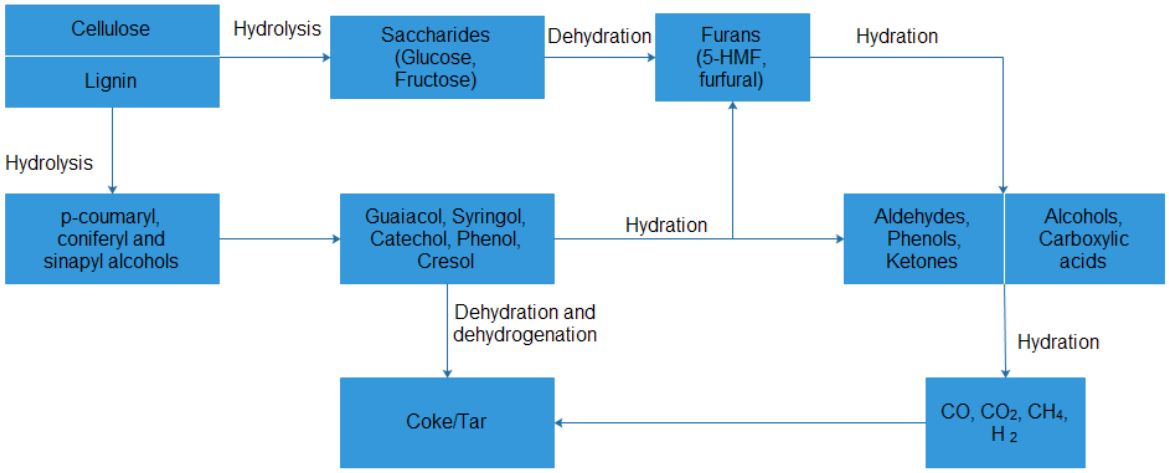

Figure 5: Hydrothermal gasification of biomass to gaseous products via aqueous intermediates (Adapted from Madenoğlu et al. [359])

As SCWG proceeds to the critical point of water, the gasification of biomass into H_2 and CH_4 occurs through reactions (a) and (b):

$$C_6H_{12}O_6 + 6\ H_2O \rightarrow 6\ CO_2 + 14\ H_2 \quad \text{(a)}$$

$$C_6H_{12}O_6 \rightarrow 3\ CH_4 + 3\ CO_2 \quad \text{(b)}$$

H_2 formation is endothermic while CH_4 is somewhat exothermic. As per Le Chatelier's principle, H_2 would dominate CH_4 at elevated temperatures; however, CH_4 would be favorable at high pressures. Thus, free radical reactions are favored at high temperatures and low pressures during

gas formation [364]. Higher temperatures lead to higher conversion but reduce SCWG's energy efficiency. Hence, it is desirable to achieve gasification at lower temperatures with the help of catalysts. The types of catalysts used for SCWG are discussed in detail in the next section.

SCWG involves methanation (c), steam reforming (d) and water-gas shift (e) reactions.

$$CO + 3H_2 \rightarrow CH_4 + H_2O \quad (c)$$

$$C_6H_{10}O_5 + H_2O \rightarrow 6\,CO + 6\,H_2 \quad (d)$$

$$CO + H_2O \rightarrow CO_2 + H_2 \quad (e)$$

The extent of gasification is expressed in terms of gasification efficiency, which is a measure of the fraction of H_2 or C in the gaseous product to that in the feeding stream. Carbon gasification efficiency (CGE) increases with temperature, reaching ~100% at 700 °C, while H_2 efficiency exceeds 100% and reaches ~158% efficiency at 740 °C. The enormous increase in H_2 efficiency is attributed to the abstraction of H from H_2O, which depicts the role of water as a reactant and medium. In a continuous reactor, gas yields are presumed to be unaffected by the reaction time after complete biomass conversion into gases [355, 365]. In batch reactors, reaction time has a profound effect on yield [366]. When reaction time increases from 30 to 120 min, the gaseous yield falls. Heating rates also affect yield in batch reactors. High heating rates tend to have high gaseous yields [367]. The percentage of biomass in the input stream also changes the product yield [368-370]. As biomass concentration increases, a high temperature is required to achieve complete gasification [368]. In general, CGE ranges from 92-100% for lower feed concentrations and drops to 68-80% above 10%. CH_4 yields increase with biomass concentration, and a gas mixture of CO_2 and H_2 tends to form at low biomass concentrations [369]. Experiments involving hydrothermal gasification technology without catalysts are summarized in Table 11 using references [371-381].

Table 11: Experiments in the hydrothermal gasification of model compounds or biomass without catalysts

Model compounds/ Real biomass	Operating conditions	Reactor/device/ tubing	Key findings/remarks/ observations	Ref.
Glucose, fructose	300-400 °C, 25-40 MPa	Continuous	The decomposition of glucose produced fructose (isomerization), 1,6-anhydroglucose (dehydration), and erythrose and glyceraldehyde (C-C bond splitting). Fructose didn't form 1,6-anhydroglucose and showed no isomerization into glucose. The proposed mechanism for products involved C-C bond cleavage by reverse aldol condensation and Lobry de Bruyn–Alberda van Ekenstein transformation.	[371]
Glucose	600-767 °C, 25 MPa	Continuous tubular	At 1.8 wt% glucose, a H_2 yield of 11.5 mol/mol glucose was reported. High CE (91%) and low TOC (23 ppm) indicated complete conversion of glucose into gaseous products, which was attributed to the enhanced water-gas shift reaction and flow stability.	[372]
Glucose	175-400 °C, 25 MPa	Continuous	Decomposition kinetics studies showed that the reaction order fell from 1.0 at 448 K to around 0.7 at 673 K. This was attributed to a shift of reaction from an ionic mechanism to a radicalic one.	[373]
Wheat straw, walnut shell, and almond shell	420-440 ˚C, 25 MPa	Batch	Wheat straw showed the highest hydrogen gasification (23%) and carbon gasification (44.92%) efficiencies. With an increase in reaction time, the gasification efficiencies increased. Total gas yield increased up to 30 min and remained constant thereafter.	[374]

Fruit wastes, Agro wastes	400-600 ˚C, 15-45 min	Tubular batch	Temperature was the dominant factor in the gasification of biomass. A longer reaction time improved thermal cracking reaction. At 45 min, H_2 yield was 0.91 mmol/g compared to 0.69 mmol/g at 15 min.	[375]
Wood residues	500-600 ˚C, 20-42.5 MPa	Autoclave	Biomass with lower lignin and higher extractives produced more gaseous products. With increased pressure, carbon gasification efficiency reduced.	[376]
Ulva macroalgae	400-550 ˚C; 25 MPa	Batch	A short residence time (7 min) was sufficient for a suitable conversion rate. At 550 ˚C, H_2, and CH_4 exceeded 15 mol%.	[377]
N-hexadecane	525-605 ˚C; 15-22 MPa	Tubular	With an increase in temperature, yields of H_2 and CO_2 improved, suggesting an improved water-gas shift reaction. A reduction in pressure improved the yields of gaseous products.	[378]
Beet-based distillery wastewater	300-375 ˚C	Batch	After 45 min of reaction time, the H_2 mole fraction reached 48.8% at 375 ˚C. At a longer reaction time, the water-gas shift reaction reached equilibrium, indicating a gradual increase in H_2 along with a moderate reduction in CO and CO_2 fractions.	[379]
Phenol and alanine	400 ˚C; 22-26 MPa	Batch	With 60 wt% alanine, the highest H_2 yield was reported. The reaction mechanism involved the decomposition of alanine to aldehyde, acids, and gases. The aldehyde and phenol condensed to form phenolic resin tar.	[380]
Marine biomass	300-600 ˚C	Batch	With biomass loading of 0.08 g ml^{-1}, corresponding H_2 and CH_4 yields were 10.37 mol/kg and 6.34 mol/kg at 600 ˚C. An increase in temperature and decrease in biomass loading improved gasification yield.	[381]

3.7.1 Catalytic hydrothermal gasification

Effective degradation of biomass into low-molecular weight gaseous compounds requires high operating temperatures (up to 600 °C). High temperatures result in a high yield; however, the high temperature lowers process energy efficiency. Hence, gasification at a lower temperature is desirable and is often carried out by catalyst. The use of catalysts improves the yield and quality of fuels. It is also known to enhance gasification performance at mild conditions, thereby showing huge promise as a suitable candidate for supercritical hydrothermal gasification. As for hydrothermal liquefaction, the literature highlights two types of catalysts, homogeneous and heterogeneous, and they are discussed below.

3.7.1.1 Homogeneous catalysts

The use of homogeneous catalysts such as alkali metals (NaOH, Na_2CO_3, K_2CO_3, $KHCO_3$, etc.) on sub- and supercritical gasification of biomass, as shown in Table 12, has been widely reported in the literature [156, 290, 382-393]. Such catalysts are often used to improve the water-gas shift reaction. The catalytic effect of K_2CO_3 was reported in a number of studies for the catalytic SCWG of a broad range of model compounds and biomass types [359, 382, 394-398]. K_2CO_3 shows activity through the formation of $HCOO^-K^+$ [367, 399, 400]. The process involves the release of CO_2 and H_2 via formic acid as an intermediate through reactions (f-j):

$$CO + H_2O \rightarrow HCOOH \leftrightarrow CO_2 + H_2 \quad \text{(f)}$$

$$2KHCO_3 \rightarrow H_2O + K_2CO_3 + CO_2 \quad \text{(g)}$$

$$K_2CO_3 + H_2 \rightarrow KHCO_3 + KOH \quad \text{(h)}$$

$$KOH + CO \rightarrow HCOOK \quad \text{(i)}$$

$$HCOOK + H_2O \rightarrow KHCO_3 + H_2 \quad \text{(j)}$$

NaOH has also been found to enhance the water-gas shift reaction and favor H_2 formation and gasification efficiency [383, 401-407]. Hydrogen gas was believed to form through the release of CO and carboxylic acids through the decarbonylation of hydroxylated carbonyl compounds, followed by the generation of hydrogen gas through the water–gas shift reaction. Another H_2 production route was believed to occur through the reaction of sodium salts of simple carboxylic acids with water. In addition, the catalytic effect of KOH is due to the enhanced water-gas shift reaction through formic acid as an intermediate [156, 384]. Despite the potential of alkali catalysts for high hydrogen yield, they cause plugging, fouling, and corrosion [408]. An experiment with a SCW fluidized bed system for biomass gasification at 923 K and 30 MPa showed no reactor plugging up to 30 wt% glucose and 18 wt% corn cob [409]. In addition, the positive effects of natural mineral catalysts such as trona, dolomite, and borax have been realized with SCWG [410]. The rapid dissemination of knowledge of this technology provides future possibilities for scale-up operations. Onwudili et al. [406] predicted the possibility of scale-up for H_2 in a semi-continuous mode through the elimination of CO_2 as Na_2CO_3. Thus, Na_2CO_3 acted as both catalyst and C sequestration agent. A study by Lin et al. [404] involved the integration of a water-hydrocarbon reaction, a water-gas shift reaction, CO_2 absorption, and various pollutants in a single process, HyPr-RING (Hydrogen Production by Reaction Integrated Novel Gasification).

Table 12: Homogeneous catalyst use for the hydrothermal gasification of model compounds or biomass

Model compounds/ biomass	Operating conditions	Reactor/device /tubing	Catalysts (with/without support)	Key findings/remarks/observations	Ref.
Humic acid	375- 600 ˚C, ~24 MPa	Fixed-bed batch	K_2CO_3	The catalyst increased the gas yield to 1.64 mol/kg. However, the H_2 yield decreased more than it did without catalytic SCWG.	[397]
Timothy grass	450-650 ˚C; 23-25 MPa	Tubular	KOH, K_2CO_3, NaOH	KOH acted as the best catalyst in increasing H_2 and CO yield via the water-gas shift reaction. The yield of 8.91 mol/kg was obtained.	[386]
Wood and char products from pyrolysis	450 ˚C, 27 MPa	Batch	K_2CO_3	K_2CO_3 increased the yield of H_2 through the water-gas shift reaction.	[398]
Cellulose, lignin alkali	300-600 ˚C	Batch	K_2CO_3	At 600 ˚C, maximum yields of H_2 and CH_4 were obtained in the presence of a catalyst. The catalyst promoted gasification and prevented char formation.	[359]
Xylose	600 ˚C, 42.5 MPa	Batch	K_2CO_3	The catalyst improved the carbon gasification efficiency (86%) at 600 ˚C and 20 MPa. Maximum H_2 and CO_2 yields were obtained using a catalyst.	[387]
Lignin, cellulose, waste biomass	650 ˚C, 26 MPa	Batch	K_2CO_3	A high temperature (~650 ˚C) and catalyst loading (~100%) resulted in a high H_2 yield.	[388]
Horse manure	400-600 ˚C, 23-25 MPa	Tubular batch	Na_2CO_3, K_2CO_3, NaOH	A high H_2 yield was observed at 600 ˚C after 45 min. A H_2 yield with a 2 wt% catalyst followed the order: Na_2CO_3>K_2CO_3>NaOH.	[389]
Paper waste sludge	450 ˚C	Batch	K_2CO_3	The catalyst resulted in a H_2 yield of 7.5 mol/kg through the water-gas shift reaction. It also enhanced H_2 and CO_2 production, while not affecting CH_4 much.	[390]

Model compounds/ biomass	Operating conditions	Reactor/device /tubing	Catalysts (with/without support)	Key findings/remarks/observations	Ref.
Mannose	700 ˚C, 20 MPa	Batch	K_2CO_3	The catalyst improved the H_2 yield to 10.34 mol mol^{-1} from mannose. Acetic acid was the main component in the aqueous phase during gasification.	[391]
Lactose	550-700 ˚C; 22.5 MPa	Continuous	NaOH, KOH, Na_2CO_3	Catalysts inhibited char formation and promoted H_2 at low temperatures. The main gases produced were H_2 and CO_2.	[392]
Phenol	400-600 ˚C, 20-42.5 MPa	Batch	K_2CO_3	The catalyst, at high temperatures, enhanced gasification. The reaction produced a CH_4-rich gas along with CO_2, H_2, and CO.	[393]
Pyrocatechol	500 °C, 25 MPa	Tumbling and tubular	KOH	At 600 °C (2 min) or 700 °C (1 min), 99% of the feedstock was gasified.	[156]
Cotton stalk, corncob, tannery waste	500 °C, 3 °C/min	Autoclave	K_2CO_3, Trona, red mud	The catalyst improved in the H_2 yield through an accelerated water-gas shift reaction and the methane reformation. Fe-based catalysts show potential for gasification.	[382]
Para-formaldehyde	400 °C	Bomb	NaOH	The primary reactions were the Cannizzaro reaction and the self-decomposition of HCHO. The Cannizzaro reaction dominated with increased OH^- in the homogeneous phase.	[383]
Wastewater (organics)	450-550 °C, 25 MPa	Continuous	KOH	Maximum H_2 generation was achieved by accelerating the water-gas shift reaction rate. The H_2 amount in the gas phase increased with oxidants in a limited range due to the competing oxidation and gasification reactions.	[384]
n-hexadecane (*n*-C_{16}) and organosolv-lignin	273 °C, 30-40 MPa	Bomb	NaOH	The catalyst showed no effect on the conversion of *n*-C_{16} and promoted the formation of 1-alkenes and H_2. The H_2 yield with NaOH was almost four times higher than that without a catalyst (with and without O_2).	[385]

Model compounds/ biomass	Operating conditions	Reactor/device /tubing	Catalysts (with/without support)	Key findings/remarks/observations	Ref.
Rosa Damascena residues	500-600 °C, 35-45 MPa	Batch	K_2CO_3, Trona	The gaseous products consisted mostly of H_2, CO_2, and CH_4. Total yields of combustible gases were more than the CO_2 yield. Aqueous gasification products had carboxylic acids as the main component. High temperatures increased total gaseous yields but decreased aqueous products. Conversions amounting to 90% gaseous and 8% aqueous at 600 °C were reported.	[394]
Cauliflower residue, acorn, tomatoes residue, extracted acorn and hazelnut shell	600 °C, 35 MPa	Continuous	K_2CO_3, Trona	The catalyst resulted in a mixture of gases like H_2, CO_2, CH_4, CO, and a small amount of C_2 compounds. The H_2 yield (mol gas/kg C in feed) of acorn was 7 times more in the presence of Trona (53.5 mol H_2/kg C in feed) than that without catalyst. The use of Trona was realized as a more economical catalyst than commercial ones.	[395]
glucose	500 °C	Batch	NaOH	An increase in H_2 yields of 135% with NaOH vs. non-catalytic process at a water-biomass ratio of 3.	[401]
Dewatered sewage sludge	400 °C, ~ 22.1 MPa	Batch	NaOH	NaOH not only promoted the water-gas shift reaction but also captured CO_2, driving the reaction with Ni catalyst towards more H_2.	[402]
Acetic acid; phenol	600 °C, 40 MPa	Tubular flow	NaOH	H_2 and CO_2 yields were highest at a 0.2 wt% of NaOH; this can be attributed to the hydrogenation of phenol to benzene to cyclohexane.	[403]
Organics	600 -700 °C, 12-105 MPa	Micro-autoclave	NaOH	The process involved a novel H_2 generation method (HyPr-RING). A higher temperature and pressure increased H_2 yield, although the effect of temperature was greater.	[404]
Glucose, molasses, rice bran	330-390 °C	---	NaOH	NaOH improved H_2 yield during the water-gas shift reaction by inhibiting tar/oil and char and promoting	[405]

Model compounds/ biomass	Operating conditions	Reactor/device /tubing	Catalysts (with/without support)	Key findings/remarks/observations	Ref.
				CO- intermediate compounds. H_2 yield increased with reaction temperature and time.	
Glucose	200 °C, 2 MPa to 450 °C, 34 MPa	Batch	NaOH	Half the optimum H_2 gas yield was achieved at 350 °C and 21.5 MPa, and > 80% (v) H_2 gas at 450 °C and 34 MPa. Apart from H_2, methane constituted ≥10% (v). The H_2 generation rate followed the order: glucose > cellulose, starch, rice straw > potato > rice husk.	[406]
Organosolv lignin	400 °C, 30 MPa	Batch-type bomb	NaOH	The H_2 yield was four times higher than without catalysts due to partial oxidation and decomposition of lignin to H_2.	[407]
Hard-shell nut residues	300-600 °C, 8.8-40.5 MPa	Batch	Trona, dolomite, borax	Gaseous product (wt%), H_2, and CH_4 yields followed the order: almond shell > walnut shell > hazelnut shell. Activities were in the order: trona > borax > dolomite. The aqueous phase contained acetic acid for all biomass types and exhibited the highest yield with walnut shells.	[410]

3.7.1.2 Heterogeneous catalysts

Though homogeneous catalysts can accelerate water-gas shift reactions, they cause problems related to plugging, corrosion, and fouling [367]. Heterogeneous catalysts, however, have high hydrogen selectivity, recyclability, and CGE [400]. The literature reports three types of heterogeneous catalysts used for SCWG: activated carbon, transition metals, and oxides. The carbon derived from plants, shells, and wood has been used as a heterogeneous catalyst for supercritical water gasification due to its high stability in reducing environments along with a high degree of dispersion [154, 411-413]. These carbons include activated carbons like charcoal, coconut shells, and coal-activated carbon. The catalytic effect of activated carbon is thought to be due to the adsorption of the reacting species onto the carbon surface [414]. Although carbon forms a good catalyst support with no solid acid-base properties, the lack of metallic support results in reduced metal dispersion on the carbon surface.

Several studies have described the application of transition metal catalysts (supported/unsupported) in SCWG reactions, i.e., Raney nickel [157, 415-419], ruthenium [420, 421], and other noble metals. According to Huo et al. [422], the activity and selectivity of a porous Ni catalyst for cellulosic conversion to methane is believed to occur through pyrolysis, hydrogenation, and methanation. Nickel supports, with the aim of improving CGE, have been reported in the literature [401, 423-429]. de Vlieger et al. [424] showed that a high dehydrogenation activity of Pt-Ni catalysts resulted in high H_2 through the suppression of CH_4 and acetic acid. Another study used a fixed bed Ni/Ru catalyst to develop a wastewater clean-up facility [430].

Ni/Ni supports, though economical, are usually unstable and suffer from the effects of sintering in both batch and continuous mode [153]. The combined effect of catalyst structural changes and limited life performance of Ni deactivate it in hydrothermal media [431]. A study on the supercritical water gasification of wood at 300-410 °C and 12-34 MPa for 90 min resulted in complete gasification, though the Raney Ni surface was found to have carbon deposits [432]. Elliott et al. [433] performed experiments to improve an Ni catalyst by adding Ag, Ru, Sn, and Cu. Also, the effect of Ce loading to inhibit carbon deposition during the SCWG of glucose was studied in an autoclave reactor at 673 K and 24.5 MPa. With the Ce loading content of 8.46 wt%, the maximum H_2 yield and selectivity were recorded [434]. Ni has shown activities with other compounds such as lignin and cellulose [296, 435-437]. Another known transition metal, Ruthenium (Ru), is known to be a highly active catalyst for low temperature catalytic gasification reactions [438-444]. Catalytic gasification involves the dehydrogenation of reacting species onto a catalyst surface and the scission of C-C or C-O bonds. Further breakdown of C-C produces synthesis gas, which proceeds through water-gas shift and methanation, whereas C-O breaks down into alcohols and organic acids [400]. Ruthenium is also known for high metal dispersion due to reduced metal loadings. Ni or Ru supported on zirconia, titania, γ-alumina, or activated carbon are highly stable at severe oxidizing and corrosive reaction environments [153, 438, 445-457]. Nonetheless, a few reports highlight the poisoning effect of Ru/C, presumed to be from the presence of S in the form of S^{2-} and SO_4^{2-} [458-460].

Other works have studied Pt as a catalyst on aqueous phase reforming reactions [461] and ZrO_2 for SCWG [385, 462]. Finally, oxides of Cu, Mn, Co, Al, Ca, Zr, Ce, and Ru have been shown to be effective for catalytic SCWG [463-467]. It is interesting to note that the reactor materials, made of alloys, affect the reaction. The designs of the “new” Hastelloy [155, 365] and Inconel [468, 469]

reactors use heavy metals, which show catalytic activity towards water-gas shift reactions and methanol reforming. Yu et al. [470] studied the SCWG of glucose at 600 °C and 34.5 MPa in reactors made up of the new Hastelloy and Inconel. The gasification efficiency in the new Hastelloy reactor and the Inconel reactor dropped to ~ 85% and ~ 68%, respectively, with a 0.8 M increase in glucose concentration, and Inconel was found to catalyze the water-gas shift reaction.

Heterogeneous catalysts tend to undergo sintering, which deactivates catalysts. A recent study discussed the use of a bimetallic catalyst in hydrothermal processes [471]. The use of a dual metal-support catalyst was reported for supercritical water gasification with the aim of improving H_2 yield [472]. Table 13 illustrates the use of heterogeneous catalysts for the hydrothermal gasification of various biomass compounds.

Table 13: Heterogeneous catalysts used for the hydrothermal gasification of model compounds or biomass

Model compounds/ biomass	Operating conditions	Reactor/ device /tubing	Catalysts (with/without support)	Key observations	Ref.
Glucose	750 ˚C, 30 MPa	Batch	Ni/Zr $(Ce,Y)O_2$-δ	The highest H_2 yield (22 mol /kg) was obtained. The catalyst provided hydrothermal stability and had anti-carbon deposition properties. The addition of CeO_2 improved gasification efficiency.	[429]
Glucose	450-700 ˚C,	Parr type stirred vessel	Ni/MgO, Ni/ZnO, Ni/Al_2O_3, Ni/TiO_2	Ni/MgO had a superior effect on the gasification efficiency, attributed to the enhancement of the water-gas shift reaction.	[418]
Biocrude	500-700 ˚C	Continuous tubular	Dual metal (Ni, Ru)-dual support (Al_2O_3, ZrO_2)	The highest carbon gasification efficiency (92%) was obtained. High temperatures favored H_2 yield while high concentrations resulted in higher CH_4.	[472]
Plastics	450 ˚C, 10-38 MPa	Batch	RuO_2	20 wt% RuO_2 resulted in a carbon gasification efficiency of 99 wt% and a hydrogen gasification efficiency of over 100%. In the presence of the catalyst, the water-gas shift reaction and steam reforming occurred simultaneously.	[444]
Pine wood, wheat straw	300-500 ˚C,	Tubular batch	Ni	The catalyst accelerated methanation and water-gas shift	[419]

Model compounds/ biomass	Operating conditions	Reactor/ device /tubing	Catalysts (with/without support)	Key observations	Ref.
	23-25 MPa			reactions. The lower biomass concentration was easily hydrolyzable.	
Glucose	500 ˚C, ~ 27.5 MPa	Continuous flow tubular	Ni Ru/γ-Al_2O_3	At 500 ˚C, the catalyst produced the maximum H_2 (0.68 mol mol^{-1} carbon-fed) and highest gasification efficiency (> 0.98 mol mol^{-1}). The catalyst showed good activity and stability.	[454]
Microalgae	385 ˚C, 26 MPa	Batch	Raney Ni, Nickel/α-alumina	The catalyst improved the yield asymptotically (80-90%) over time. The main gas products obtained followed the order: $CH_4 > CO_2 > H_2 > CO$	[455]
Valine	500-710 ˚C; 28 MPa	Fixed-bed	AC, Ni–Y/AC, Ni–Pt/AC, and Ni–Pd/AC	Ni-Y/AC achieved a carbon gasification efficiency of 98.1% at 600 ˚C, and total gas yield increased with temperature. The catalyst disintegrated amines in the effluent.	[456]
Sugarcane bagasse	360 ˚C; 18 MPa	Micro-reactor	Cu with γ-Al_2O_3-MgO	The unpromoted catalyst resulted in the highest yields of H_2 (10 mmol/g of biomass) and gas (41 mmol/g).	[467]
Glucose	400 °C		Ni/activated carbon (AC), Ni/MgO, $Ni/CeO_2/Al_2O_3$, Ni/Al_2O_3	An 81% H_2 yield was reported with Ni/activated carbon (AC), 62% with Ni/MgO, 60% with $Ni/CeO_2/Al_2O_3$ and 52% with Ni/Al_2O_3. H_2 yield increased by 6.9% with AC and 36.9% with Ni/AC.	[401]
Glucose	500 °C, 30 MPa	Autoclave	Raney nickel and K_2CO_3	Gaseous products were H_2, CO_2, CH_4, and C_2H_6. H_2 yield doubled with K_2CO_3. Ni improved CH_4 yield.	[408]
Corn, potato starch gels, and sawdust	710 °C	Hastelloy C-276 tubing	Coconut shell AC	Gases like H_2, CO_2, CH_4, CO, and a little C_2H_6 were obtained Gas yield (>2 L/g) with 57 mol% H_2 was reported at the highest temperature.	[411]

Model compounds/ biomass	Operating conditions	Reactor/ device /tubing	Catalysts (with/without support)	Key observations	Ref.
Corn starch	650 °C, 28 MPa	Hastelloy C-276 tubing	Coconut shell AC	Gases such as H_2, CO_2, and CH_4 with little CO resulted from the reaction. The catalyst remained active over a 6 h period.	[412]
Chicken manure	700 ˚C 30 MPa	Fluidized bed	Activated carbon	The catalyst improved the H_2 yield of 25.2 mol/kg at 600 ˚C. The catalyst increased the carbon gasification efficiency at low temperatures.	[413]
Glycerol, glucose, and cellobiose	600 °C, 34.5 MPa	Inconel 625 tubing	Spruce wood charcoal, macadamia shell charcoal, coal activated carbon, and coconut shell AC	Complete conversion of glucose (22% by wt in water) to H_2 achieved at a weight hourly space velocity (WHSV) of 22.2 h^{-1}. The carbon catalyst was deactivated after < 4 h without swirl in the entrance region of the reactor.	[154]
Microcrystalline cellulose and organosolv lignin	400-600 °C	Quartz	Ni, Fe, Cu, Zn, Zirconium wires, ruthenium powder, and Raney nickel slurry	Exhibited highest H_2 yields (16.0 mmol/g) from Ni (surface area/biomass weight ratio of 240 mm^2/mg); H atom content in the product gas stream was 70%, with > 60% of C atoms gasified.	[417]
Cellulose and glucose	325 °C	batch	Ni	The maximum CH_4 yield of 73.8% was achieved in the presence of 0.1 mol of Zn and 1.0 g of porous Ni catalyst with at 325 °C for 2 h. A porous Ni catalyst was effective for the conversion of glucose into CH_4. Acetoin, hydroxyl-2-propanone, and 1,2-ethanediol acted as liquid intermediates for the formation of CH_4 during the reaction.	[422]

Model compounds/ biomass	Operating conditions	Reactor/ device /tubing	Catalysts (with/without support)	Key observations	Ref.
Glucose	350-410 °C	Batch	α-Al_2O_3, carbon nanotube (CNT), and MgO supports, SiO_2, Y_2O_3, hydrotalcite, yttria-stabilized zirconia (YSZ), and TiO_2	The highest carbon conversion was achieved from α-Al_2O_3, carbon nanotube (CNT), and MgO supports; modest activities from SiO_2, Y_2O_3, hydrotalcite, YSZ, and TiO_2; and no activities from zeolites were observed. The maximum hydrogen selectivity with 20% Ni/α-Al_2O_3 at 380 °C was found.	[423]
Ethylene glycol	450 °C, 25 MPa	Continuous	Al_2O_3 supported Pt and Pt–Ni	Methanol, ethanol, and acetic acid were the main liquid by-products. The deactivation of Pt and Pt–Ni catalysts occurred due to the hydroxylation of the Al_2O_3 surface by acetic acid.	[424]
Glycerol	450-575 °C, 25 MPa	Inconel-625	Ni supported La_2O_3, *α*-Al_2O_3, γ-Al_2O_3, ZrO_2, and YSZ	Ni/YSZ was found to be effective for gasification but caused higher methanation. The maximum H_2 yield from Ni/La_2O_3 was reported. Reactions with moderate space velocities ($WHSV$ = 6.45 h^{-1}) and 5% glycerol showed higher hydrogen selectivity and yield.	[425]
Sugarcane bagasse	400 °C	batch	Ni/CNTs and Ni–Cu/CNTs	The high internal surface of CNTs had a noticeable effect. Ni/CNT nanocatalysts improved the hydrogen yield by a factor of 5.84. The promoted Ni/CNT with 7.5 wt% copper had 25.9% reduction in CH_4.	[426]
Polyethylene glycol contaminated wastewater	390 °C, 24 MPa	Inconel 625	Ni/ZrO_2	Gas yield and CGE increased with Ni loadings but decreased with PEG concentration.	[427]
Glucose, organic	600-750 °C,	Bench-scale	RuNi/γ-Al_2O_3 or	A γ-Al_2O_3-supported Ni catalyst was found to be	[428]

Model compounds/ biomass	Operating conditions	Reactor/ device /tubing	Catalysts (with/without support)	Key observations	Ref.
waste, and sludge hydrothermal liquefaction process	24 MPa	continuous down-flow tubular	RuNi/activated carbon (AC)	effective in catalyzing the SCWG of a simulated aqueous waste feedstock. However, the catalyst showed deactivation during the SCWG of real waste. An AC-based catalyst exhibited higher stability and activity in the SCWG of real waste.	
Composite refuse derived fuel (RDF)	650 ˚C, 45 MPa	Hastelloy	RuO_2/γ-Al_2O_3	The presence of a catalyst improved carbon gasification efficiency up to 99 wt%. In addition, H_2 and CH_4 yields increased.	[443]
Macroalgae	440 ˚C, 25 MPa	Batch microreactor	Fe-Ni-Ru/γ-Al_2O_3	The highest H_2 yield of 12.28 mmol/g was obtained with a 2 wt% catalyst. Hydrogen selectivity was 0.74.	[452]
Glucose	500 ˚C	Quartz capillaries (batch)	Ru/Al_2O_3	With a catalyst, the gas yield improved with longer reaction time. Phenols and arenes were found to be stable in supercritical water and thus showed little decomposition. The catalyst inhibited char formation.	[453]
Sugarcane bagasse	400 ˚C, 24 MPa	Batch micro-reactor	γ-Al_2O_3 with Cu	With increased Cu loading, CO, CO_2, and H_2 increased. However, the addition of potassium reduced gas yield. A catalyst with 20% Cu and 2.5% potassium on alumina was reported to be highly selective.	[465]
Alkali lignin	400-600 ˚C	Batch	Ru/C	Higher temperature, longer reaction time, higher water density, and lower reactant concentration favored biomass gasification. A gasification efficiency and carbon conversion efficiency of 73.74% and 56.34% were achieved.	[421]
Wood	300-410 °C,	Batch	Raney Nickel	The highest CH_4 yield of 0.33 g/g wood was observed.	[432]

Model compounds/ biomass	Operating conditions	Reactor/ device /tubing	Catalysts (with/without support)	Key observations	Ref.
	12-34 MPa			Complete gasification was achieved after 90 min.	
Organosolv-lignin	400 °C, 37.1 MPa	Tube bomb	Ru/TiO_2, Ru/C, Ru/γ-Al_2O_3	Ru/TiO_2 showed stable activities; Ru/C exhibited high lignin gasification; Ru/ γ -Al_2O_3 lost its activity despite having higher activity initially.	[438]
Organosolv-lignin	250-400 °C	Tube bomb	Ru/TiO_2	Ru resulted in high CH_4 yield with no solid product; there was a rapid degradation of formaldehyde into gases such as CH_4, CO_2, and H_2.	[441]
Cellulose and sawdust	500 °C, 27 MPa	Autoclave	Ru/C, Pd/C, CeO_2 particles, nano-CeO_2 and nano-$(CeZr)_xO_2$	The treatment of 10 wt% cellulose or sawdust with CMC in the presence of Ru/C yielded 2-4 g H_2 and 11-15 g H_2/100 g feedstock.	[446]
Glucose	600 °C, 24 MPa	Continuous-flow tubular	(Ni, Ru, Cu and Co) and promoters (e.g., Na, K, Mg, or Ru) supported on(γ-Al_2O_3, ZrO_2, and AC)	A H_2 yield of 38.4 mol/kg glucose was obtained with Ni20/γ-Al_2O_3 (γ-Al_2O_3 with 20 wt% Ni); Mg and Ru were the effective promoters of the Ni/γ-Al_2O_3 catalyst and reduced deposits of coke and tar during reaction.	[448]
Glucose	650 °C, 28 MPa	Tubular flow	Ni/AC, Ni–Y/AC, Ni–Fe/AC and Ni–Co/AC	A Ni–Y/AC catalyst showed high gasification performance among the catalysts studied. Fe and Co loading into the Ni/AC did not improve H_2 yield; Y loading into the Ni/AC was presumed to prevent coke formation.	[450]
Glucose and cellulose	400-440 °C,	Batch	ZrO_2	Hydrogen yield almost doubled with the addition of ZrO_2.	[462]

Model compounds/ biomass	Operating conditions	Reactor/ device /tubing	Catalysts (with/without support)	Key observations	Ref.
	30-35 MPa				
Glucose, cellulose, heterocyclic compounds, paper sludge, and sewage sludge	400 °C, ~30 MPa and 500°C, ~50 MPa	Inconel 625	RuO_2	Gases such as H_2, CH_4, and CO_2; were obtained. RuO_2 was not affected by nitrogen compounds; carbazole was gasified completely.	[463]
Cellulose, xylan, and lignin	400 °C, 25 MPa	Batch	Ni	A decrease in gas production was observed from lignin mixtures; H_2 yield dropped from the reaction of cellulose intermediates with lignin.	[157]
Glycerol	700-800 °C	Tubular fixed-bed	Ru/Al_2O_3	A near-theoretical yield of 7 mol of H_2 was observed.	[420]
Microalgae	400 ˚C, 28 MPa	Continuous	Ru/C	A good catalytic activity persisted over 55 hours, after which sulphur poisoning deactivated the catalyst.	[460]
Industrial waste streams	300-375 ˚C	Batch	MnO_2, CuO and Co_3O_4	The catalytic activity followed the order: Co_3O_4 > CuO > MnO_2. High temperature (375 ˚C) and longer reaction time (45 min) favored H_2 production.	[464]
Fruit pulp	400-600 ˚C	Batch	Ru/C	With a biomass ratio of 2.5%, the highest H_2 yield was 54.8 mol/kg biomass. The gasification efficiency was 150.8%.	[451]
Phenol water	350 ˚C, 20 MPa		Ni ($Ni/C/Al_2O_3$)	There was no deactivation of catalysts at 2 g L^{-1} of phenol concentration. Catalyst activity improved with time and the conversion of phenol reached 100%.	[457]
Black liquor	350-450 ˚C, 25 MPa	Batch	CeO_2	The catalyst decreased the production of carbonaceous solids; however, the H_2 yield was largely unaffected, as the catalyst was mainly involved in hydrogenation reactions.	[466]

Model compounds/ biomass	Operating conditions	Reactor/ device /tubing	Catalysts (with/without support)	Key observations	Ref.
Furfural	200-400 ˚C, 23-25 MPa	Batch	Cu+Zn, Co+Ni, Cu+Ni Zn+Ni	Two elements with different combinations showed improved gasification efficiency compared to single metal catalysts.	[471]

3.8 Hydrothermal carbonization

Hydrothermal carbonization (HTC) converts biomass into a value-added product (solid fuel) at a comparatively low temperature (180-250 °C) and saturated pressure (2-10 MPa) [473-476]. The resulting product has carbon content similar to lignite with mass yields varying from 35 to 60% [477-481]. The obtained aqueous phase has most of the dissolved organics in the form of carbon with a minimal amount of gas [477, 482, 483]. The process is influenced by the nature of its feedstock as well as loading and process conditions [473, 479, 480, 482]. The carbonization improves the heating value and dewatering capability of the feedstock [484]. Process efficiency and dewatering capacity are improved by boosting the solid yield and recycling, respectively [484]. In addition, solid loading has a positive effect on product distribution [479, 480], and the process design is positively affected by internal heat recovery [485-487] as the HTC reaction heat is usually low [488]. Carbonaceous materials from hydrothermal carbonization are used in super capacitors and fuel cells for energy storage. The application of hydrothermal carbonization material in energy storage, conversion, and fuel cells is presented in Table 14 [489-503].

Hydrothermal carbonization (HTC) is widely used to convert lignocellulosics into solid hydrochars, which have better physico-chemical characteristics than raw feedstock [504]. HTC technology uses batch and semi-continuous systems, both of which have rendered it less economically viable.

Figure 6 provides insight into the reaction pathways with key products for hydrothermal carbonization [126]. The blend of phenols, organic acids, and ketones form biocrude through hydrothermal liquefaction. At critical conditions of water, reactions pertaining to free radicals become prevalent and gasification becomes favored, leading to the formation of CH_4 and H_2 [342]. To facilitate the formation of a solid product such as char, the process temperature must be controlled to avoid liquefaction and gasification. The glucose dehydration to form 2,5-hydroxy-methylfurfuraldehyde followed by aldol condensation outlines the formation of substances like carbon spheres [473, 477, 505]. The chemistry involving reactions such as oxidation, esterification and etherification on the hydroxymethyl group and reactions such as oxidation, reduction and aldol on the formyl group have been reported [506]. Also, solid-solid interactions, as in the case of torrefaction, have been investigated [507]. The composition of HTC is also supported by reaction pathways through liquid and solid state to form coke and char, respectively [477, 508].

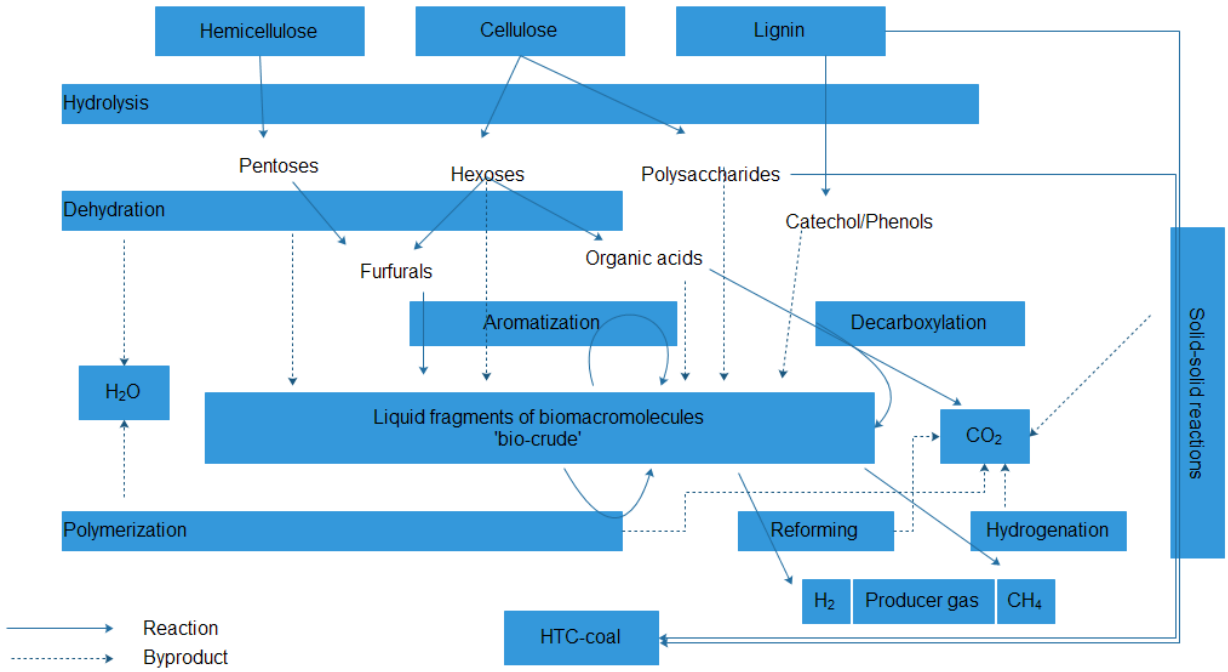

Figure 6: Reaction pathways involved in hydrothermal carbonization (Adapted from Kruse et al. [126])

HTC is also used in char production as it has high energy content, good grindability, and high hydrophobicity [509]. Using spectroscopic methods, a hydrochar microspheres-based chemical model the discernible core and the shell of hydrochar particles, which is shown in Figure 7 [510]. In the formation of hydrochar microspheres via hydrothermal carbonization of saccharides, sucrose and starch hydrolyze to form corresponding monosaccharides such as glucose and or fructose [248]. Starch also produces maltose, and the fructose is obtained by glucose isomerization [248]. The monosaccharides such as glucose and fructose break down into lower molecular weight compounds like organic acids, thereby lowering pH [511]. The hydronium ions produced act as a catalyst for oligosaccharide degradation into the corresponding monosaccharides, which further undergo a series of reactions involving ring C-C bond breaking and dehydration into furfural compounds [512]. The compounds thus generated undergo further decomposition to form aldehydes, acids, and phenols [512]. Following the series of reactions, the monomers and the decomposition molecules undergo condensation and polymerization into polymers [513]. The polymerization reactions are enhanced by aldol condensation or intermolecular dehydration [510]. This reaction phenomenon also causes polymer aromatization. As their concentration approaches the critical supersaturation point, nucleation occurs, which further grows through diffusion at the surface of the chemical species that are linked to the microspheres via hydroxyl, carboxylic, and carbonyl groups [514]. As a result of these reactions, carbonaceous microspheres with stable oxygen groups in the form of pyrone or ether are produced [510].

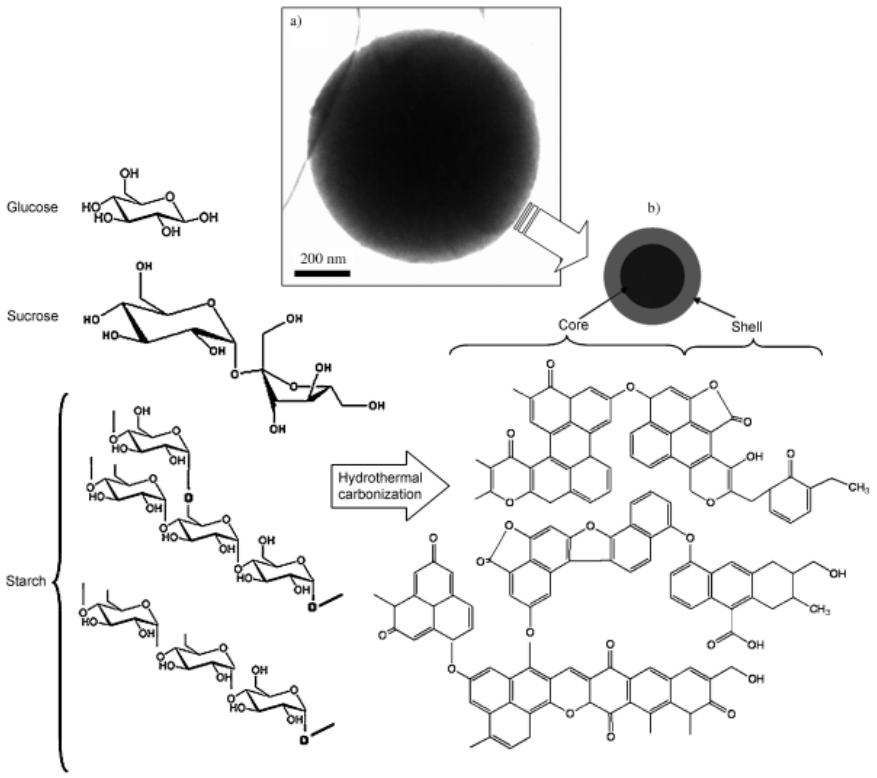

Figure 7: Diagram showing hydrophilic/hydrophobic core-shell structure of the hydrochar microspheres via hydrothermal carbonization (Adapted from Sevilla et al. [510])

The HTC process leaves the char less dusty, which improves pelletization characteristics [515, 516]. The commercial realization of HTC has suffered because of its high temperature and pressure requirements, which increase costs. Pellet quality is measured in terms of mechanical durability, that is, its ability to remain intact during handling or storage [517]. Reza et al. [518] reported that pellet durability improved when HTC temperature increased. Hoekman et al. [516] reported that pellets obtained from hydrochar show good durability at temperatures as low as 200˚C. Durability can further be enhanced at higher temperatures, but high temperatures produce pellets that are more brittle. Similarly, a temperature below 200˚C produces less durable pellets, as the pellets swell when immersed in water. Nonetheless, hydrochar from HTC produces highly stable, water-resistant pellets [516].

The high cost of commercial HTC technology comes from the need for hydrochar to bind torrefied or raw biomass. Hydrochar is as an effective binder because of the furan and phenolic resins obtained from the degradation of hemicellulosics and cellulosics [516]. Hence, hydrochar improves the durability and pelletization characteristics of other biomass feedstocks. Liu et al. [519] studied the durability and combustion characteristics of hydrochar/lignite pellets. They concluded that hydrochar, along with lignite, improved the tensile strength of blended pellets, especially with a hydrochar fraction > 50%.

There are logistics associated with the large-scale commercial use of HTC pellets. Commercial HTC technology should have applications that include technical and economic benefits beyond commercial biomass. HTC biochar can be used as a solid biofuel. The industrial application of

HTC biochar uses pelletization technology and thus the transportation, handling, and storage of pellets affecting its mechanical durability are important in industry from an economical point of view [520]. Pellet crumbling leads to problems that reduce combustion efficiency and increase emissions [520]. Another logistic problem originates from HTC's hydrophobicity, which influences the mechanical durability of pellets. Also, with the aim of making HTC technology more environmental friendly in order to develop it commercially, the treatment of spent liquor through anaerobic digestion [521-526] and the influence of the recirculation of spent liquor have been studied [527-530]. Recirculation helps increase the mass and energy yields of the hydrochar product, which further affects the economy of the process.

Recently, a pilot-scale study was proposed for the HTC of lignocellulosics into solid fuels, which shows the relevance of solid fuel production from wet biomass [531]. More than 80% of energy yields are obtainable through the HTC of woody biomass at pilot scale, which indicates how much energy content from the feed is converted into solid fuel [532]. Hence, the future of HTC is promising in terms the conversion of wet biomass to solid fuels [533, 534]. Hydrochar has several applications such as fuel source, catalysts, soil amendment, adsorbent, and energy storage [535]. However, recent research interests are oriented towards the production of hydrochars that have application in industry [162, 536]. Comments on the application of HTC for biochar production provided in Table 14 were obtained from various sources [533, 535, 537-546].

Table 14: Application of material from HTC in energy storage, conversion, and fuel cells

Model compounds/ Biomass	Applications	Ref.
Loblolly pine wood chips	Used continuous HTC process through the fast HTC reactor with a retention time of 20-30 s. Hydrochar showed high energy densification and pelletization characteristics. At 290 ˚C, hydrochar yield was 85% based on dry feedstock.	[537]
Bagasse from land plant (Grindelia)	HTC performed on plant after biocrude was extracted and hydrochars were pelletized. The HHV increased by up to 26 MJ/kg at 260 ˚C.	[538]
Woody biomass and agro-residues	Hydrochar pellets showed high mechanical strength and their moisture content decreased to < 2%. Pellets had increased mechanical durability and combustion characteristics, suggesting their suitability as solid fuels.	[539]
Cassava rhizome	Biomass hydrochar at 200 ˚C showed thermal characteristics similar to a low-rank coal with an HHV of 23.7 MJ/kg, suggesting its potential as a renewable fuel.	[535]
Bamboo	The combustion characteristics of biomass increased along with its HHV. At 260 ˚C, the HHV increased from 17.1 MJ/kg (raw biomass) to 20.3 MJ/kg.	[540]
Rapeseed husk	Microwave-assisted HTC resulted in a hydrochar HHV of 21.57 MJ/kg, suggesting its potential application as a solid fuel.	[541]
Bio-oil	The HHV from hydrochar produced from the HTC of bio-oil was 4.35-5.29 times higher than the initial feed, signifying a new approach to remove unstable components of bio-oil through the production of high energy-rich hydrochars.	[542]
Sludge	The addition of acetic acid as a catalyst improved the HTC reaction rates, thereby increasing the HHV of hydrochar to 20.2 MJ/kg on average. Other catalysts studied with this biomass were borax and zeolite.	[543]
Eucalyptus bark	A higher temperature improved the HTC of biomass, resulting in hydrochar with high fixed carbon and HHV as well as improved thermal stability. The HHV values for hydrochar lay in the range of 27-28.2 MJ/kg, showing potential for solid fuel application.	[533]
Corn stalk	Corn stalk was transformed into hydrochar at a reaction severity of 5.05-8.29. As it increased to 7.11, the hydrochar had properties similar to those of coal. The hydrochar yield ranged from 71% to 36%.	[544]
Cellulose, xylan, lignin	The optimum temperature for greatest energy efficiency was 220 ˚C. Cellulose and hemicellulose had a significant impact on the properties of solid fuel. An increase in carbon	[546]

Model compounds/ Biomass	Applications	Ref.
	contents and fixed carbon was reported following hydrothermal carbonization. The calculated calorific values of hydrochar were 23-26 MJ/kg at 220 ˚C.	
Sludge	Acetic acid was an effective catalyst for this biomass. Hydrothermal carbonization of mixtures of sewage, acetic acid, and cassava pulp had energy contents of 28.5 MJ/kg, which are comparable to natural coals, showing potential to use these mixtures as a fuel for combustion.	[543]
Sludge residue	The carbon content of hydrochar obtained had energy densification ratios of 1-1.5 and energy yields of 60-100%. At higher temperatures, solid yield dropped to ~40%.	[545]
Cellulose, potato starch, and eucalyptus wood sawdust	Showed good capacitance retention ability (175 F/g).	[489]
D-glucose	HTC nanospheres were employed as anodes in Li^+ and Na^+ batteries.	[490, 491]
Cellulose	Ni/C material was prepared by hydrothermal carbonization and the resulting PtRu/C anode electrocatalysts showed high performance for DMFC, unlike Vulcan XC72 carbon.	[492]
Glucose	Glucose in situ hydrothermal carbonization from carbon riveted PtRu/C catalyst were used in methanol fuel cells.	[493]
Digested sludge	Exhibited potential for solid fuel due to increased C and FC (fixed carbon) content. Reduced C-O and aliphatic C-H with an increase in aromatic C-H from C*H*$_x$ functional group were observed.	[494]
Sewage sludge	Resulting solid fuel showed higher FC and lower volatile matter, hydrochars with a fuel ratio up to 0.18, and HHVs of 0.98-1.03. The removal of 60% of the nitrogen and sulphur resulted in a cleaner fuel.	[495]
Black liquor	Improved yield, HHV, C recovery, and total energy recovery efficiency of solid fuel at 265 °C.	[496]
Chitosan	A facile carboxylated chitosan hydrothermal process resulted in N-doped carbon-coated $CoSnO_3$ composites with improved lithium storage properties and a reversible capacity of 650 mAh g^{-1} even after 50 cycles.	[497]

Model compounds/ Biomass	Applications	Ref.
Microalgae (*S. Platensis*) and glucose mixtures	Synthesized microporous N-doped carbon materials (areas up to ~2200 $m^2 g^{-1}$) based on HTC and chemical activation processes. While working with neutral LiCl electrolyte, the porous carbons produced at 700-750 °C showed a retention of 80% of the capacitance at a current density of 20 A g^{-1}.	[498]
Commercial sugar	Carbon microspheres (5-10 μm diameter) and uniform nanopores were synthesized by HTC-assisted microwave together with KOH activation. This process resulted in a superior specific capacitance (about 179.2 F/g) at a current density of 1 A/g and cycling performance over 1000 charging/discharging cycles with a KOH/C of 1:1 and a microwave irradiation level of 70%.	[499]
Polytetrafluoroethene waste	A $CaCO_3$-assisted template carbonization method was developed as a means of disposing PTFE waste and the resulting nanoporous carbon materials showed the potential for super-capacitor application.	[500]
D (+) glucose	Electrical double layer capacitors were formed from the 1-ethyl-3-methylimidazolium tetrafluoroborate and carbon electrodes; they showed ideal polarizability ($\Delta V \leq 3.2$ V), a short charging/discharging time constant (2.7 s), and a high specific series capacitance (158 F g^{-1}).	[501]
Glucose	A graphene/AC nanosheet composite was obtained by HTC together with KOH treatment. Nanosheet had specific capacitance of 210 F g^{-1} in aqueous electrolytes and 103 F g^{-1} in organic electrolytes.	[502]
Hazelnut shells	Nanoporous carbons behaved as anode materials for lithium ion batteries; the best cycling performance in Li cells was reported by HC-MA formed by MgO templating of hydrochar.	[503]

3.9 Issues with hydrothermal technologies

3.9.1 Economic considerations

Economic considerations are important, both with respect to a novel technology itself and with implementation. The economic viability of a plant helps determine the profitability of a technology and the costs associated with optimizing it.

Based on an economic assessment, the competitiveness and feasibility of a process can be compared to known conventional technologies. Though several techno-economic assessments have been done for thermochemical-based conversion processes such as fast pyrolysis and conventional gasification [547-564], cost analyses are available for biomass-based hydrothermal-based HTL [143, 565-568] and HTG [569-571] processes. The Pacific Northwest National Laboratory (PNNL), under the sponsorship of the National Advanced Biofuels Consortium (NABC), performed bench-scale HTL and upgrading experiments for woody biomass. The techno-economic study included the development of a large-scale commercial HTL and upgrading platform for bio-oil production for two cases, a state-of-technology (SOT) case with experimental results from the HTL process, and a goal case that assumed plausible future improvements for mature HTL technology [567]. The results showed that production costs were lower for the goal case, which assumed decreasing organics loss to the aqueous phase that led to higher product yields and reduced wastewater treatment costs. The cost results from the SOT case highlighted that the bio-oil production cost, based on the current HTL process, is not competitive compared to petroleum-based gasoline. Although the results from the goal case look promising for bio-oil production from woody biomass through HTL, the lack of process knowledge and concepts has financial risks. The main factors influencing the bio-oil production cost are feedstock cost, product yield, and upgrading equipment cost. The identification of key parameters will be necessary in a future research study.

Techno-economic studies on bench-scale experiments for lipid-extracted microalgae (LEA) liquid fuels through hydrothermal liquefaction (HTL) and upgrading processes have also been undertaken [572]. The results show that the HTL process is promising for the production of liquid fuel compared with conventional gasoline and diesel. However, uncertainties in feedstock cost had a major influence on production cost. Other key factors influencing production cost were product yield and equipment cost for upgrading. Faeth et al. [573] reported that costs for a continuous HTL process can be reduced through lower residence times. In another study, catalytic hydrothermal gasification (CHG) was performed for the conversion of wet LEA to methane together with wastewater treatment through HTL [574]. The coupled HTL and CHG improved biocrude yield and overall economics. Jones et al. [575] evaluated the economics of hydrothermal liquefaction (HTL) and catalytic upgrading of whole algal biomass to obtain renewable diesel fuel. In their study, the feedstock cost had the most significant impact on diesel fuel cost. The economic study highlights the need to look for improved cultivation, harvesting, and dewatering methods to reduce feedstock costs.

The feasibility of SCWG has setbacks due to current hydrogen costs. It costs around three times as much to obtain H_2 through direct biomass gasification than through the steam methane reforming (SMR) of natural gas [576]. The cost of obtaining H_2 from natural gas via SMR is 1.5-

3.7 US $/kg (assuming a 7 US$/GJ natural gas price) and 10-14 US$/GJ from biomass [577]. The high operating and capital costs for high-pressure supercritical water systems poses economic challenges. The lack of understanding of SCWG technology, together with net positive energy and economic considerations, limits the ability to obtain hydrogen from commercial SMR. However, there have been a few techno-economic studies on supercritical water gasification technology for biomass and algae. In 1997, General Atomics came up with first cost estimate for an SCWG using sewage sludge with dry matter contents of 20% and 40%; however, their estimate was based on a supercritical water oxidation (SCWO) plant because there is relatively little known about the novel SCWG technology [578]. In 1999, Amos calculated cost estimates for starch waste with a 15% dry matter content and product gas cleaned by expensive membrane technology [579]. The membrane alone made up more than 35% of the purchased equipment costs. In 2002, Matsumura et al. [569] estimated the costs for supercritical gasification using water hyacinths with a 5% dry matter content. Their estimate included only the investment costs for bulk plant components and left out the costs of piping, engineering, services, etc. Including these costs raises the total investment costs fourfold. Gasafi et al. [570] studied the economics of SCWG using sewage sludge as feedstock with the aim of producing hydrogen. According to their findings, the hydrogen cost production was about 35.2 € GJ^{-1} if no revenues from sewage sludge disposal, which were significantly higher than the cost of hydrogen obtained through electrolysis (26.82 € GJ^{-1}), are considered. In 2013, Brandenberger et al. [580] estimated costs for microalgae cultivated in ponds and photo-bioreactors for synthetic natural gas (SNG) production using SCWG and reported that the economic challenges are due to the cost of algal biomass production, which are 94% of the required capital investment. In 2014, the results from a techno-economic analysis of glucose and sewage sludge for hydrogen production via SCWG were studied [571]. The authors of that study found that there were no profits associated with a glucose feed concentration of 15% until the price of hydrogen goes beyond 5 $/kg. The SCWG technology still needs to be optimized through a proper understanding of process concepts and plant components to improve economic efficiency.

More research is needed on hydrothermal processing technology to make it economically feasible.

3.9.2 Gaps in knowledge

The reactor configuration and design have a crucial role in the process run and affect process reaction kinetics. The main challenges in reactor design are related to enhancing heat integration, handling plausible poor heat transfer due to contact between the incoming reactor effluent with the reactor feed owing to its high viscosity, and decreasing costs of the reactor system itself when operating at high pressures [581]. These challenges require an experimental analysis of required heat transfer coefficients at various locations in the process to determine proper heat integration. Moreover, the type of material for the HTL reactor design needs to be evaluated by taking into account harsh reaction conditions and possible corrosive effects. Considerable research is needed to improve the suitable liquid hourly space velocity (LHSV) in the HTL reactor system. The pump needs to be able to handle high solids content. The feasibility of separating bio-oil and water at the reactor temperature and pressure is yet to be determined. This is important because efficient bio-oil separation from an aqueous phase will increase the yield of bio-oil.

A study of prevailing reaction rates and products from biomass processing through hydrothermal technologies will help us understand how to optimize reactor design. HTL bio-oil yield is

influenced by factors such as temperature, feed solid content, the nature of the biomass, and residence time. A detailed characterization of all the products obtained from hydrothermal processing (i.e., bio-oil, aqueous, gaseous, and solid products) is required. Considerable effort is needed to comprehend bio-oil stability and quality and thereby better understand ongoing process reactions and upgrading needs. This effort would also be important when options for transporting bio-oil offsite (when an upgrading plant is not co-located with HTL plant) are identified. The characterization methods, which use equipment such as GC/MS, NMR, and HPLC for product analysis, are critical to understanding the nature of the reactive species influencing product quality and yield. However, analytical techniques such as chromatography cannot accurately predict high molecular weight compounds due to the technique's low resolution and limited selectivity.

A study on the continuous flow system is needed to understand process development for commercial applications. The catalyst has an important role in determining process yield and performance. There are research gaps with respect to catalyst maintenance, stability, plausible regeneration, and subsequent lifetimes. Improving the long-term use of catalysts is essential both to improve their performance and to minimize deactivation during reactions.

Supercritical water gasification, another hydrothermal processing technology, is a promising approach for handling wet biomass. However, an analysis of SCWG design suggests that the feasibility of the process depends on feed type and concentration. Clogging, plugging, and char formation are major problems in the SCWG of biomass. In addition, the limited dissolution of inorganic salts in biomass under supercritical water conditions causes precipitation during SCWG and these salts combine with char and plug the reactor. Though continuous stirred reactors and fluidized beds can handle plugging problems, there are underlying issues with the complex design and the high energy demands in the process. Thus, an efficient SCWG reactor system design is still being developed. Another technical challenge is in selecting material to avoid corrosion in the reactor. The extreme environments in the SCWG process require materials capable of preventing corrosion. In addition, pumping biomass at high concentrations is an issue. In order to optimize the process, efficient and better energy recovery equipment is needed. The wide use of metal catalysts such as Ni and Ru in the SCWG of biomass are aimed at improving H_2 production; however, they are known to cause a methanation reaction and produce CH_4. The selectivity towards H_2 production and, in turn, the stability of the catalyst at supercritical conditions, presents a challenge. Catalyst poisoning, loss, and deactivation during SCWG pose technical challenges and suggest the need for catalyst supports to prevent unwanted side reactions and enhance H_2 yields.

Process optimization and research in the areas of hydrothermal processing will likely improve product yield and thus profitability.

3.10 Conclusion

Hydrothermal processing technologies have significant potential for biomass with high moisture content. We conducted an extensive literature review to understand the current state of various hydrothermal processing technologies. Studies differ with respect to their analysis of experimental results yet provide in-depth understanding for future process development. In general, hydrothermal processing precludes an energy-intensive pretreatment step for bioconversion to

useful products. This review focused on different hydrothermal processing technologies, namely the liquefaction, gasification, and carbonization of individual biomass fractions/whole biomass, and their effects on process conditions. The nature and yield of products from hydrothermal technologies depends on factors such as catalyst, feedstock type, the nature of the solvent, and process conditions. The nature of biomass in terms of protein, carbohydrates, and lipid fractions determines the compositional yield of the product type. The effect of a catalyst on product yield cannot be dismissed, as it changes the compositional characteristics of the product obtained. Thus, the choice and selection of catalyst for a particular application is important in view of its major influence on the yield and desired properties of the final product. Hydroprocessing technologies have not yet been commercialized due to a number of technological gaps and economic constraints.

Technological gaps with respect to various plant components include reactor design for process development and optimization in order to achieve a thermal efficiency high enough to attain an economic process. A synergistic effect of the individual components in the process design is crucial for efficient operation. Considerable challenges remain in the area of catalyst recycling and regeneration in order to improve the lifetime and efficiency of the hydrothermal process. Along with technological constraints, there are economic bottlenecks. As the technology uses high pressure equipment, the process has high capital investments.

If economically feasible, a process can be practically achievable. However, cost studies are not enough to support the development of large-scale processes. Commercialization requires testing with different feedstocks to understand the process. In addition, integrating a techno-economic analysis with energy tools helps understand energy flow and consumption, which have a direct impact on cost. Internal recovery of heat and power in an integrated system would reduce external energy demands and costs, thereby improving technology costs. A sensitivity analysis combined with Monte Carlo simulations for risk analysis would help evaluate the technology properly. Although hydrothermal technologies have several challenges, such as environmental concerns, depletion of fossil fuel reserves, etc., research towards specific fuels targeted for the transportation sector and as raw materials for the chemical industry continues. In view of this, hydrothermal technologies hold significant promise, and research and development continues to overcome the barriers associated with the technology for plausible market integration in future.

4 Analytical Model to Predict Microalgae Yields in Open Pond Raceway Systems Based on Local Solar Irradiance

Significant micro-algae research continues to be conducted globally based on the potential for these single cell plants to meaningfully address growing global challenges related to clean air, clean water, food, and energy. The primary objective of this section is to develop a data-intensive analytical model to predict the cultivation of algae biomass at a scale of 2,000 tonnes dry biomass per day in OPR systems applicable to Canada's cold climate regions. The key specific objectives of this study are:

- To analyze Canadian site-specific climate data to determine the different model parameters in an OPR system applicable to Canada's cold climate regions;
- To develop a bottom-up analytical model to predict the cultivation of algae biomass in OPR systems located in different sites;
- To conduct the comparative analysis of algae biomass yields between selected OPR sites;
- To perform sensitivity analyses of various parameters such as thermal energy, harvesting period, inoculum concentration on the predicted biomass yield; and
- To estimate the impact of supplementing solar light with artificial light on the predicted biomass yield.

4.1 Methods

A flowchart for the development of the SATOPR (SATellite Open Pond Raceway) algae cultivation model can be seen in Figure 8.

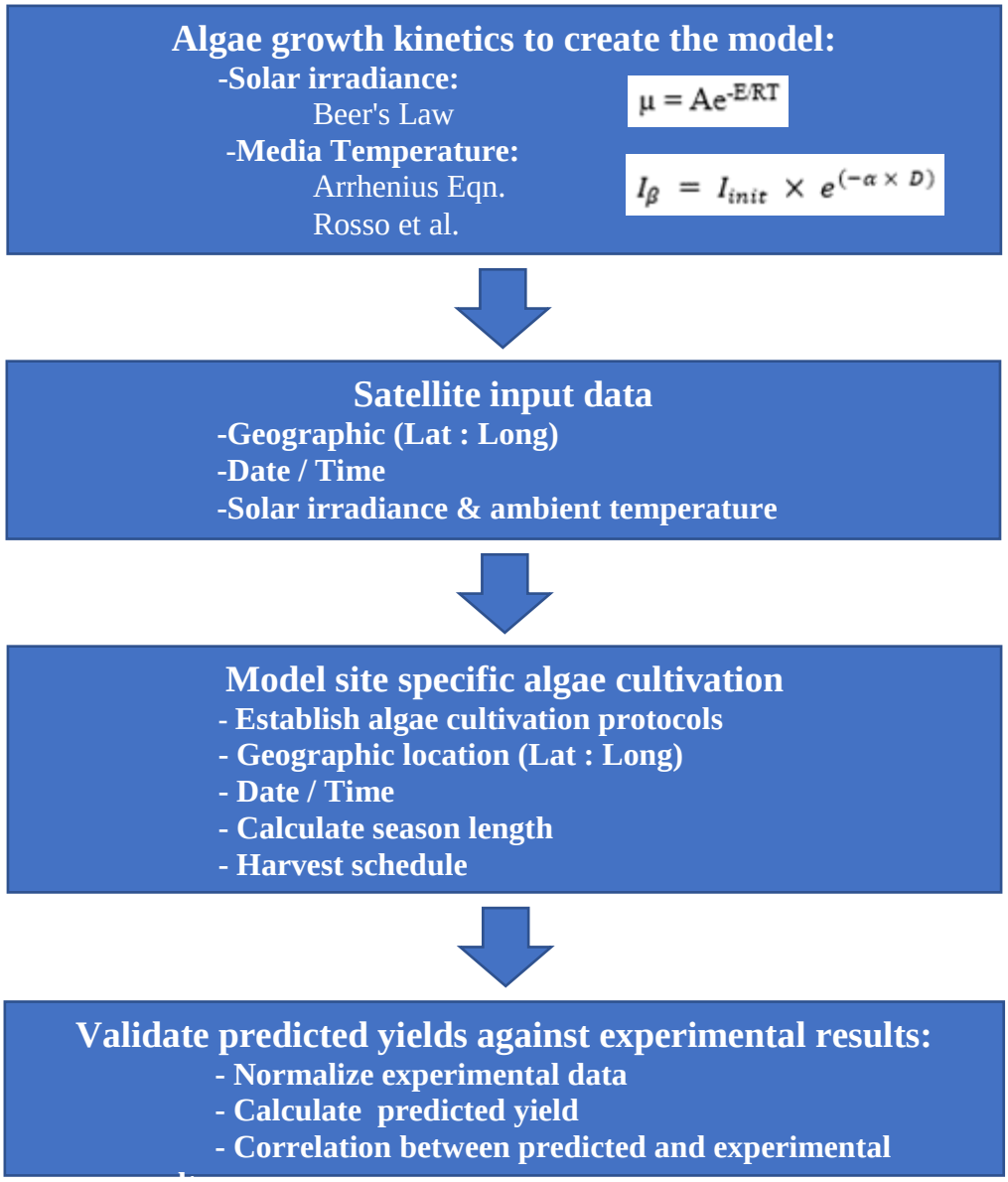

Figure 8: Flowchart for the SATOPR algae cultivation model

Satellite meteorological data is available for geographical locations in Canada, as well as other regions around the globe [582]. The two key parameters required by the model include solar irradiance and media temperature [583]. These parameters are discussed in more detail below.

Because of our interest in evaluating and comparing algae yield results from various locations and our need to validate our model, we selected 2014 as the year for which we would calculate the annual yields of our OPR systems. This period coincided with experimental data sets from different locations that we would use for validation.

4.2 Algae species – *Nannochloropsis oceanica*

The analytical model was created with the intention to fix certain key variables including the algae species to be cultivated. Since the experimental data sets involved the cultivation of the algae species *Nannochloropsis oceanica*, this is the species cultivated in our modeled cases. In a study by Singh et al., the maximum growth rate achieved under varying light wavelengths and intensities was 0.64 d^{-1} under phototrophic and 0.66 d^{-1} in mixotrophic conditions [584]. Sandnes et al., in agreement with Singh et al., found that specific growth rates increase with temperature, peaking at between 25-29 ºC, with growth quickly destabilizing beyond 30℃ [585]. Likewise, the optimal temperature would increase as light intensity increases up to 28 ºC at 80 µmol photons m^{-2} s^{-1} with a recorded growth rate of 2.3 d^{-1}. Maximal specific growth rate achieved in the study was 1.6 d^{-1}, the culture density at which the cell mass reaches its highest output rate of biomass for specific culture conditions.

4.2.1 Algae growth kinetics

The accumulation of autotrophic algae biomass is a function of the growth rate of live algae cells, a corresponding rate at which algae cells die, which in turn is directly influenced by metabolic activity determined by media temperature and access to energy (light) and nutrients. The associated kinetics can be represented mathematically in the following equation, provided by Jayaraman and Rhinehart [586]:

$$B = B_L + B_D \tag{2}$$

The total biomass (B [g/L]) is the sum of live (B_L) and dead algae cells (B_D). Given the relatively brief period between harvesting periods in OPR systems, the quantity of dead cells relative to live ones is assumed to be negligible ($B_D = 0$). Thus, the growth rate (μ) of the algae biomass would equal the change in biomass related to the change in time (dB_L/dt), which is normally recorded as grams per liter per day (g/L/d) in Eqn. 3.

$$\mu = \mathrm{d}B_L/\mathrm{dt} \tag{3}$$

Or, the increase (change) in biomass that occurs over a change in time is represented as Eqn. 4:

$$\mathrm{d}B_L = \mu\,(\mathrm{dt}) \tag{4}$$

However, the growth rate (μ) is attenuated by a biomass production attenuation coefficient (K_P), Eqn. 5:

$$\mathrm{d}B_L = K_P\mu\,(\mathrm{dt}), \tag{5}$$

which is the product of multiple functions that control the metabolic activity of the algae cells including light intensity ($f[I]$), media temperature ($f[T]$), and the availability of nutrients, particularly carbon, in the form of CO_2 ($f[C]$), nitrogen in the form nitrates ($f[N]$), and phosphates ($f[P]$), as seen in Eqn. 6.

$$K_P = f(I)f(T)f(C)f(N)f(P) \tag{6}$$

4.2.2 Light intensity

Light provides the energy for autotrophic algae growth and varies with depth, wavelength, suspended particles (other algae cells), light intensity, and incident angle. The amount of light (intensity) entering the media is affected by diurnal and seasonal variations. Li et al. provide a mathematical analysis of the stoichiometrically derived algal growth model [587]. For our model, we assumed uniform mixing within the system with light penetration being reduced (extinguished) as depth increases. According to the Beer-Lambert Law for liquids, we can calculate light intensity at any depth in a pond based on algae biomass concentration [586, 588-591]. Light intensity (I_β) (also percentage of light), recorded as Wm^{-2}, transmitted through the absorbing media is equal to the impinging light intensity (I_{init}) multiplied by the exponent of the negative total pond extinction coefficient (α) multiplied by the depth of the pond (D), as shown in Eqn. 7.

$$I_\beta = I_{init} \times e^{(-\alpha \times D)} \tag{7}$$

The total pond turbidity extinction coefficient (α) is equal to the sum of the nonalgal turbidity extinction coefficient (K_n) and the algae turbidity extinction coefficient (K_a) multiplied by the associated initial algae biomass concentration (B_{init}) as seen in Eqn. 8:

$$\alpha = (K_n) + (K_a)\, B_{init} \tag{8}$$

where the extinction coefficient for nonalgal turbidity (K_n) is assumed to equal zero for clear water, and (K_a) has been estimated by Jamu and Piedrahita as 0.014 [592]. Therefore, Eqn. 9 for (I_β) becomes:

$$I_\beta = I_{init} \times e^{(-K_a \times B_{init} \times D)} \tag{9}$$

To calculate the average light intensity throughout the water column, we altered our formula to Eqn. 10 [586]:

$$I_{avg} = \left(\frac{I_\beta}{(K_a \times B_{init} \times D)}\right) (1 - e^{(-K_a \times B_{init} \times D)}) \tag{10}$$

To complete the calculation that determines the influence of the photosynthetic light response rate $f(I)$ on the biomass production attenuation coefficient (K_P), we used Jayaraman and Rhinehart's Eqn. 11 [586]:

$$f(I) = 9.34 \times (1 - e^{(-0.0044 \times I_{avg})}) - 1.60 \tag{11}$$

4.2.3 Media temperature

In an analogous way to determining the influence of light intensity on algae growth, we are able to account for the effect of media temperature. In our research study, we considered two alternative approaches to these calculations. In our first model [T_1], we applied the temperature dependence $f(T_1)$ forwarded by James and Boriah [586] and Jayaraman and Rhinehart [593] in Eqn. 12:

$$f(T_1) = e^{(-K_t \times (T_m - T_{opt})^2)} \tag{12}$$

Temperatures are recorded in kelvins (-273.16 °C) and matched with species-specific growth rate data, where K_t is the temperature extinction coefficient, which is equal to T_{opt}^{-2}, T_m is the pond temperature, and T_{opt} is the optimal growth temperature. For *Nannochloropsis oceanica*, K_t was determined to be 0.00001. When we apply the pond water temperature dependence on algae, we can predict an increase in growth rate up to the optimal temperature followed by a gradual decline.

In a second model $[T_2]$, temperature dependence follows the kinetics proposed by Rosso [594] and later supported by Bechet [595], Chen [596], and Ras [597] in Eqn. 13:

$$f(T_2) = \frac{U_{opt} \times (T - T_{max}) \left((T - T_{min})^2\right)}{(T_{opt} - T_{min})\Big((T_{opt} - T_{min})(T - T_{opt}) - (T_{opt} - T_{max}) \left(T_{opt} + T_{min} - (2\,T)\right)\Big)} \quad (13)$$

Rosso postulates in his model that a more accurate approximation of the effects of changes in temperature ($f\,[T_2]$) may be achieved by including cardinal or important species-specific temperatures, T_{min} and T_{max}, along with a specific optimum growth rate (U_{opt}) achieved at the optimal temperature (T_{opt}). T_{min} is the temperature below which no growth is observed. T_{max} is the temperature above which no growth is observed.

Our research compared these two models to evaluate the concurrence of predicted results with experimental ones.

Fluctuations in pond temperatures have been extensively studied and show that solar radiation can effect thermal changes that could be harvested for energy. Processes that govern heat transfer in ponds involve complex, inter-related parameters including wavelength-specific angular incident solar radiation, particulate matter, salt concentrations, reflectivity, heat capacity, density, air temperature, water transparency, composition of the pond bottom ground properties, wind, evaporation, convection, long-wave radiation to the sky, conduction, light and heat transmission through water, annual periodic sinusoidal flux, and underground water movement [598, 599]. In all of the associated calculations, to arrive at a predictive result, each variable introduces the potential for errors and relatively large standard deviations, the sum of which may be very significant.

Even if site-specific surface water temperatures were available, significant assumptions are still made. OPR systems have a significantly different limnology and thermal properties than large open lakes and streams. Available government data sets are often linked to larger bodies of water where complex environmental factors interact to govern actual temperatures.

Given the complex science involved in surface water temperature, our model needed a good proxy for surface media temperature in shallow ponds. Our hypothesis was that ambient air temperature would provide such a proxy. To test this theory, we analyzed the NREL experimental data set we had selected, in which pond media and ambient temperatures were logged every 15 minutes. We correlated this information to daily mean temperatures and determined that the average media temperature was approximately 4.5 degrees cooler than the daily ambient mean temperature, with a standard deviation of 1.99. This finding concurs with experimental cultivation results by Dahmani et al. on *Chlorella pyrenoidosa* in a small OPR system 0.4 m deep [600].

We also assumed that average media temperature had to consistently be above -2 °C, the minimum growth temperature (T_{min}) for *Nannochloropsis oceanica* to commence algae cultivation [585, 597]. Optimum growth temperature (T_{opt}) has been established at 26.7 °C, maximal growth temperature (T_{max}) at 33.3 °C, and optimal growth rate at 1.8 per d.

4.2.4 Nutrient availability (C, N, P)

The consumption of nutrients by the growing algae, represented by $f(C), f(N)$, and $f(P)$, can be modeled kinetically using the Monod equation where $f(C_x)$ represents each nutrient: carbon from CO_2 (C), nitrogen from nitrates (N), and phosphate (P) [601]. The change in nutrient concentration (C_x) recorded in g/L over time (t) can be represented by Eqn. 14:

$$\frac{\mathrm{d}C_x}{\mathrm{dt}} = -K_x\, r_x\, K_p\, B_{init} \tag{14}$$

where K_x is the species-rate constant, r_x is the rate of nutrient consumption, K_p is the biomass production attenuation coefficient, and B_{init} is the initial biomass concentration. The influence of each nutrient can then be expressed as Eqn. 15:

$$f(C_x) = \frac{C_x}{K_x^h + C_x} \tag{15}$$

where K_x^h represents the half concentration of a specific nutrient species (x) and plays a key role in contexts where nutrients are added only at the beginning of a growth period. As nutrients are used up, the algae eventually shift into a deprived nutrient state. For our research, we maintain that each nutrient will be maintained in surplus concentrations throughout the cultivation period. Although production protocols with respect to maintaining these conditions will vary among researchers, they will be consistently adhered to between production platforms. Where N and P concentrations may be readily adjusted using ammonia (NH_3) and di-ammonium phosphate (DAP or $[NH_4]_2HPO_4$), C is generally maintained by the infusion of CO_2 by sparging this gas into the media. However, this could also be effected through the addition of bicarbonate. Interestingly, the addition of CO_2 affects the OPR system pH. For simplicity, we assumed that the pH was maintained by controlling the infusion of CO_2. The effect of this nutrient is expressed as Eqn. 16:

$$f(CO_2) = \frac{1}{(1+e^{\lambda(pH-pH_{opt})})} \tag{16}$$

Since our assumption for this research project is that nutrients will be kept in surplus, each function related to these nutrients will equal 1. Therefore Eqn. 6 above becomes Eqn. 17:

$$K_P = f(I) f(T) \tag{17}$$

Given the foregoing, to predict change in biomass over time we calculate the following using Eqn. 18 from Jayaraman and Rhinehart [586]:

$$\frac{d_B}{d_t} = K_p \times B_{init} \times f(I) \times f(T) \tag{18}$$

To calculate the production of biomass, we rearrange the formula:

$$B = B_{init} + K_p \times (B_{init} \times f(I) \times f(T)) \quad (18)$$

The SATOPR model involved using daily mean photosynthetically active radiation (PAR) and ambient near-surface satellite data for our selected site. Given the daily flux in both parameters during any given day and our assumption that there would be a suitable correlation between ambient temperatures and our OPR media temperature there was uncertainty that we would be able to draw a meaningful correlation between modeled results and experimental results. Where satellite data was provided daily, experimental results provided flux at 15 minute intervals.

Once the SATOPR model was constructed, we applied it for an entire year's growing period (330 days). Predicted algae production was measured in g/L based on a weekly harvesting regime with the initial inoculum cell concentration set at 0.2 g/L.

4.3 Results and discussion

This work reports on the development of a novel, data-intensive analytical model to be able to predict algae OPR productivity in Canada. Although day-to-day conditions may be difficult to predict, we can consider historical weather data at specific sites to construct site-specific models. The SATOPR model is based on satellite site-specific irradiance and temperature data, then validated and benchmarked against species-specific/operating protocol-specific experimental OPR data.

4.3.1 Validation

Our model was validated by testing it using the much more granular experimental data. The validation experimental data set was accessed from the ATP3 (Algae Testbed Public-Private-Partnership) Program conducted at the ASCATI (Arizona Center for Algae Technology and Innovation)/NREL (National Renewable Energy Laboratory), located in Mesa, AZ, from June 20 through July 26, 2014 [602]. The analysis provided us with 2772 data points. Since the first week of data was based on a three-day cultivation cycle and started at a higher initial concentration, it was not included in our model.

The SATOPR adjusted K_p (biomass production attenuation coefficient) achieves a statistically closer correlation between the modeled and experimental results for different locations. We theorized that this accounts for variance in respiration and photosynthetic flux between sites.

Under the summer 2014 UFS protocol from which the experimental data was taken, *Nannochloropsis oceanica* ASU algae strain KA32 Pond 2 was studied. The algae were cultivated in a 1 m^3 OPR system with a nominal pond depth of 25 cm, media circulated by paddlewheel. Algae were harvested weekly. Data logging took place using a YSI 5200 monitor and control system. Pond variables included pH, temperature, oxidative reduction potential (ORP), dissolved oxygen, conductivity/salinity, and PAR from a local LI-COR sensor. PH was set at 8.0 and salinity at 0 ppt [603].

Research studies have determined that to cultivate algae in OPR systems, a minimum solar irradiance of 4.65 kWh m^{-2} is required [604, 605]. Radiation source information was accessed from the NASA/GEWEX Surface Radiation Budget (SRB) Project. The Global Modeling and Assimilation Office (GMAO) provided the meteorology source information. Canadian

sunrise/sunset calculations were obtained from the National Research Council Canada (NRC) and SunEarth Tools.

Validating the model necessitated bringing together several sets of experimental raw data into a single data source file synchronized in time [606]. The data set selected included PAR solar data that was correlated to the rest of the data sets. The data sets included instantaneous (5 min and 15 min intervals), harvesting (weekly), weather (15 min), and operating data (twice d^{-1}, 5 days wk^{-1}). A relatively contiguous set of records for the key variables of interest included date, time, pH, media temperature, dissolved oxygen, algae strain, pond ID, and algae dry weight. Although rigorous experimental protocols were in place, gaps were observed in some of the data streams.

For the selected study period, biomass concentration (g L^{-1}) was plotted against time (days) for each week. From the slope of this graph, we obtained the experimental growth rate for each week of cultivation over a four-week period. Where experimental parameters such as solar irradiance, media temperature, pH, and dissolved oxygen were measured and logged every 15 minutes during a weekly cultivation and harvesting regime (representing some 672 data points), only 4 or 5 data points represent biomass concentration during the same seven-day cultivation period between harvests.

Experimental data was used to determine a level of concurrence and validation with formulas that predict algae growth and to establish values for species-specific constants as discussed above. As Figure 9 shows, there is good correlation between experimental and predicted algae productivity.

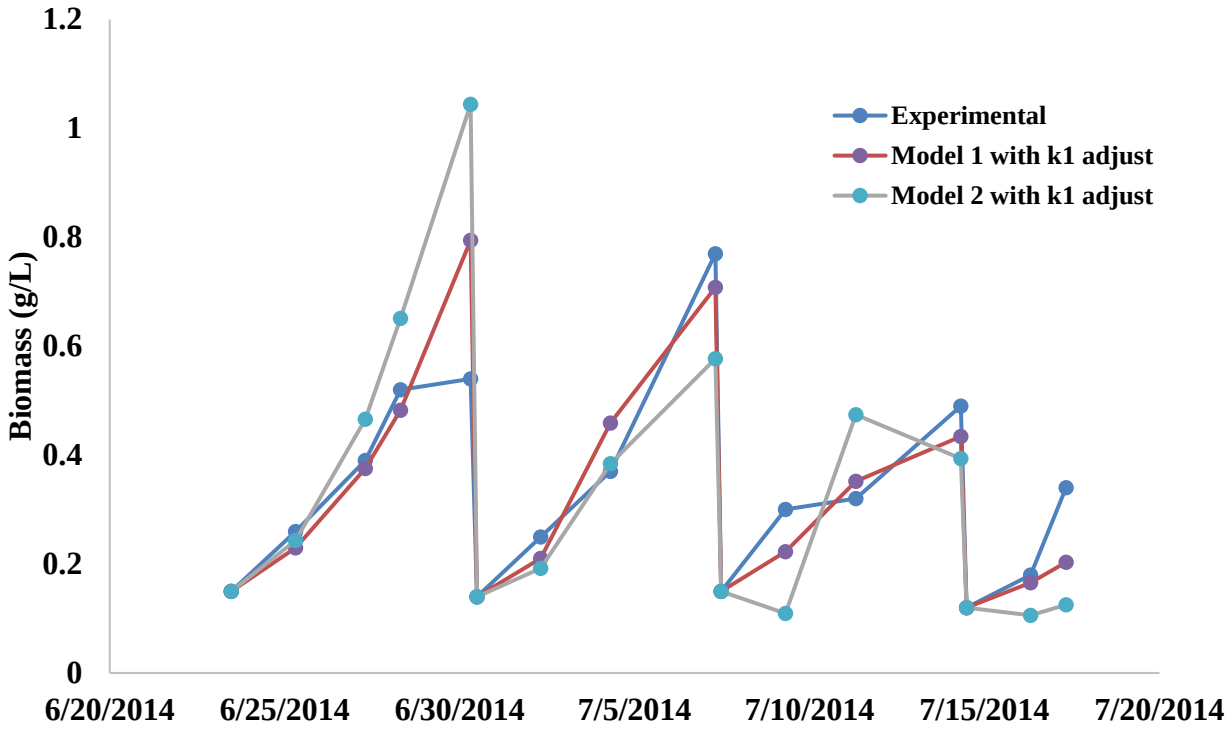

Figure 9: Algae growth – experimental vs. modeled data (Mesa, AZ Jun 23 – Jul 17, 2014)

The experimental data was correlated to the predicted results, with the values for K_t and K_p adjusted in the analytical formulas to minimize the standard deviations between modeled and experimental data sets and to provide agreement with an experimental yield of 2.14 g. Recorded standard deviations for models T_1 and T_2 were 0.1017 and 0.4389 for K_p values 0.000755 and 0.000647, respectively (see Table 15). K_t was set at 0.000011. The findings for K_p are consistent with the acknowledged greater sensitivity of $f(T_2)$ to temperature changes compared with $f(T_1)$.

Table 15: Model coefficients for the case where biomass yield equals experimental yield (2.14 g)

Model	K_t	K_p	Standard Deviation	Experimental (g)	Model 1 (g)	Model 2 (g)
$f(T_1)$	0.000011	0.000755	0.1017	2.14	2.14	
$f(T_2)$	0.000011	0.000647	0.4389	2.14		2.14

With the functional model development completed, work focused on correlating the model's results using NASA satellite data sets for the same location and time for both solar irradiance and local ambient climatic conditions. The next step in our analysis was to determine a similar correlation between experimental results with NASA satellite solar irradiance and air ambient temperature data. Like our initial analysis, the predicted results correlated well with experimental results. See Figure 10.

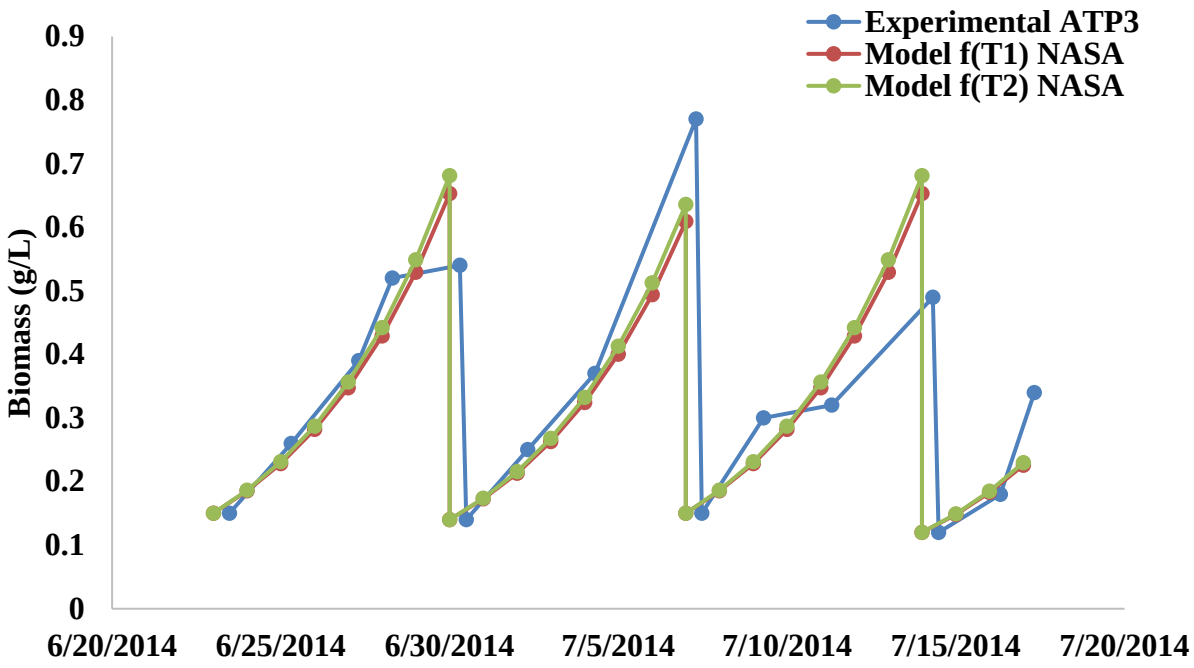

Figure 10: Algae growth – Experimental vs Model – Mesa, AZ – June 23 – July 17, 2014

Model adjustments were made to K_p in the analytical formulas to minimize the standard deviations between modeled and experimental data sets and to provide agreement with the experimental yield (2.14 g). The recorded standard deviation for model T_1 and T_2 were 0.00878 and 0.00681 for K_p values 0.034543 and 0.019813, respectively. K_t was maintained at 0.000011 (see Table 16).

Table 16: Model coefficients for the case where biomass yield equals experimental yield (2.14 g) based on NASA data

Model	K_t	K_p	Standard Deviation	Experimental (g)	Model 1 (g)	Model 2 (g)
$f(T_1)$	0.000011	0.034543	0.00878	2.14	2.14	
$f(T_2)$	0.000011	0.019813	0.00681	2.14		2.14

4.3.2 Modeled results

The SATOPR model was run for four different sites and the following results are provided: Mesa, AZ (Figure 11), Medicine Hat, AB (Figure 12), Fort Saskatchewan, AB (Figure 13), and Great Slave Lake, NWT (Figure 14).

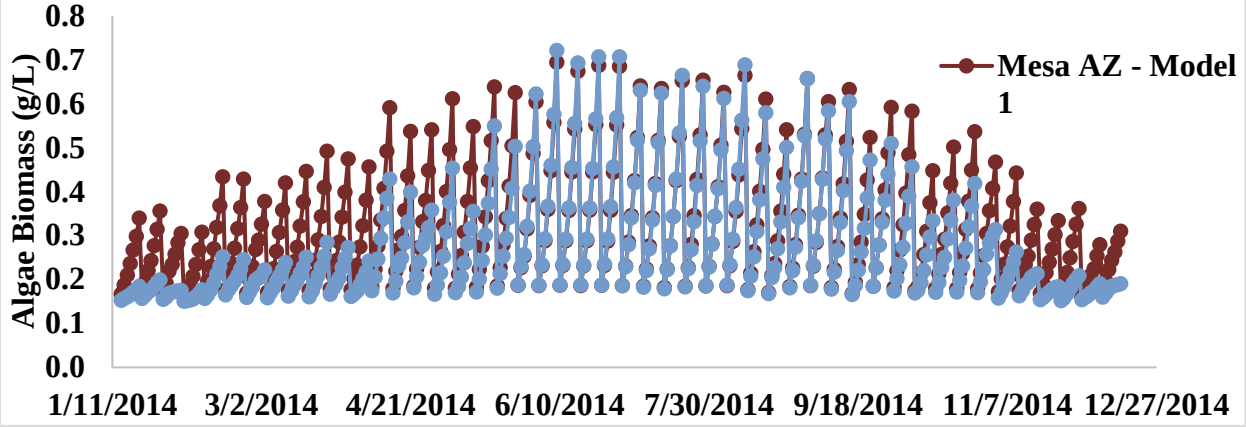

Figure 11: Predicted annual algae growth from 2 models, Mesa, AZ, 2014

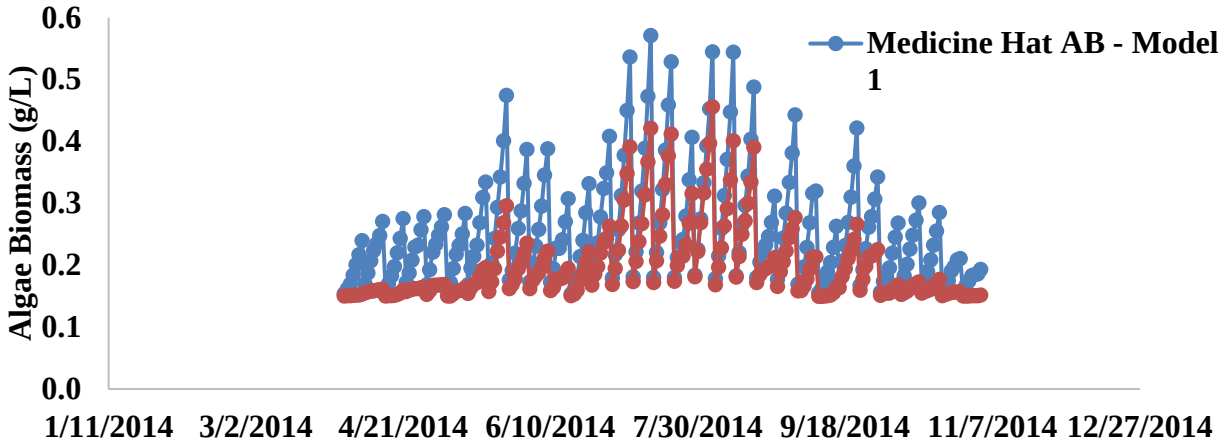

Figure 12: Predicted annual algae growth from 2 models, Medicine Hat, AB, 2014

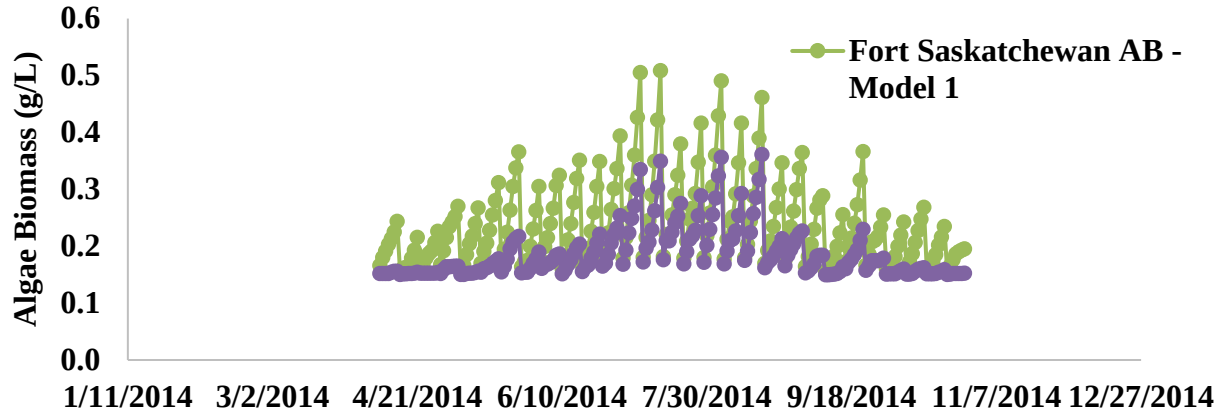

Figure 13: Predicted annual algae growth from 2 models, Fort Saskatchewan, AB, 2014

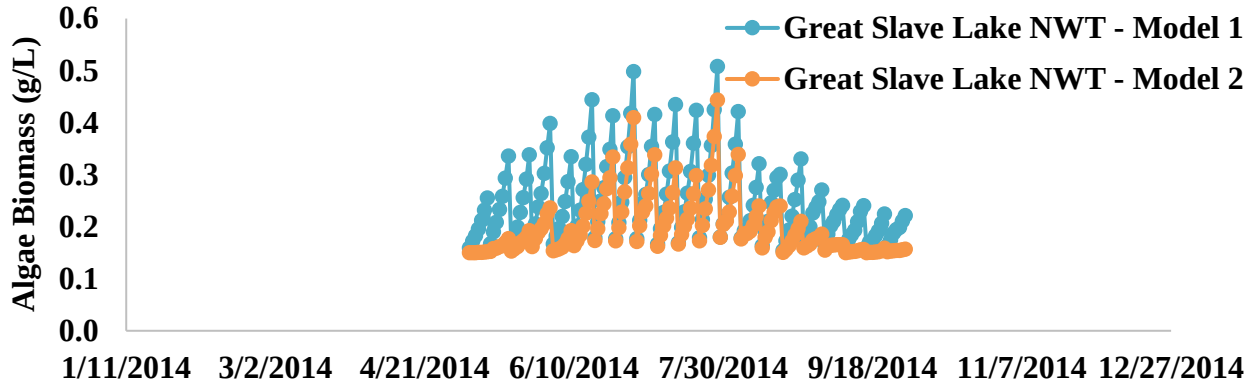

Figure 14: Predicted annual algae growth from 2 models, Great Slave Lake, NWT, 2014

4.3.2.1 The effect of temperature

It is interesting to note that in Mesa, AZ (Figure 11), where media temperatures fluctuate relatively closely around the optimum growth media temperature, there is little difference in results between approaches in calculations from model T_1 and model T_2 (June through August). However, as media temperatures continue to decrease across the shoulder and winter seasons, the predicted difference in results becomes much more pronounced. A year-long consistent experimental study would be required to determine which temperature model more accurately predicts yield outcomes across a broader range of cultivation media temperatures.

Predicted results based on the two approaches for calculating the impact of $f(T)$ are seen to be significantly different from one another in the above graphs, with the annualized results presented in Table 17.

Table 17: Predicted results – 7-day harvest schedule

Harvest Schedule		**Weekly**			**Optimized Media T = 26.7℃**			
LOCATION	**Growing (days)**	**Growing (weeks) # harvests**	$f(T_1)$ **Predicted Biomass** ***g/L/yr***	$f(T_2)$ **Predicted Biomass** ***g/L/yr***	$f(T_1)$ **Predicted Biomass** ***g/L/yr***	$f(T_2)$ **Predicted Biomass** ***g/L/yr***	$f(T_1)$ **Biomass Factor Increase**	$f(T_2)$ **Biomass Factor Increase**
Mesa, AZ	336	48	23.6	17.3	37.4	33.8	1.58	1.95
Med Hat, AB	217	31	8.2	3.9	19.8	18.1	2.41	4.64
Ft Skwn, AB	203	29	7.0	2.6	17.6	16.2	2.51	6.23
GrtSlvLk, NWT	147	21	5.6	2.8	12.5	11.5	2.23	4.11

The SATOPR model's power becomes apparent in that parameters may be changed to consider cultivation alternatives. Table 3 shows that not only are we able to establish the advantage of constructing the OPR in Mesa versus the alternative Canadian sites, we can also see the predicted dramatic impact of maintaining a constant optimum media temperature.

4.3.2.2 The effect of harvest schedule

With the model, we were also able to change from a weekly harvest schedule to waiting until the algae density in the biomass reaches a certain threshold (i.e., 5 g/L) (see Table 18). The model construction allows us to conduct simulations that predict optimized harvest yields. A review of Tables 17 and 18 shows that for Mesa, AZ, adopting a weekly harvesting schedule versus choosing to harvest at 5 g/L may result in a 15% increase in annual yield as per model $f(T_1)$ calculations. At Fort Saskatchewan, the same model calculations forecast a 15% improvement by adopting a 5

g/L harvest schedule over a weekly schedule. The results suggest that for OPR systems with greater media temperature flux, a density harvest schedule will outperform a weekly harvest schedule.

Table 18: Predicted results – Harvest schedule based on cell density

Harvest Schedule		**Density > 5 *g/L***			
LOCATION	**Growing (days)**	**# harvests**	$f(T_1)$ **Predicted Biomass *g/L/yr***	**# Harvests**	$f(T_{2)}$ **Predicted Biomass *g/L/yr***
Mesa, AZ	336	57	20.1	44	15.3
Med Hat, AB	217	27	8.8	14	4.4
Ft Skwn, AB	203	25	8.0	11	3.6
GrtSlvLk, NWT	147	18	5.9	10	3.1

4.3.2.3 Predicting land requirements

From the constructed SATOPR model, we have extracted a great deal of valuable comparative information from four sites of interest that proves useful for a future techno-economic analysis. Under the prevailing local climatic conditions provided by satellite, we were able to determine the amount of land required for the OPR system to produce 1000 tonnes/yr of dry biomass at each location (see Figure 15).

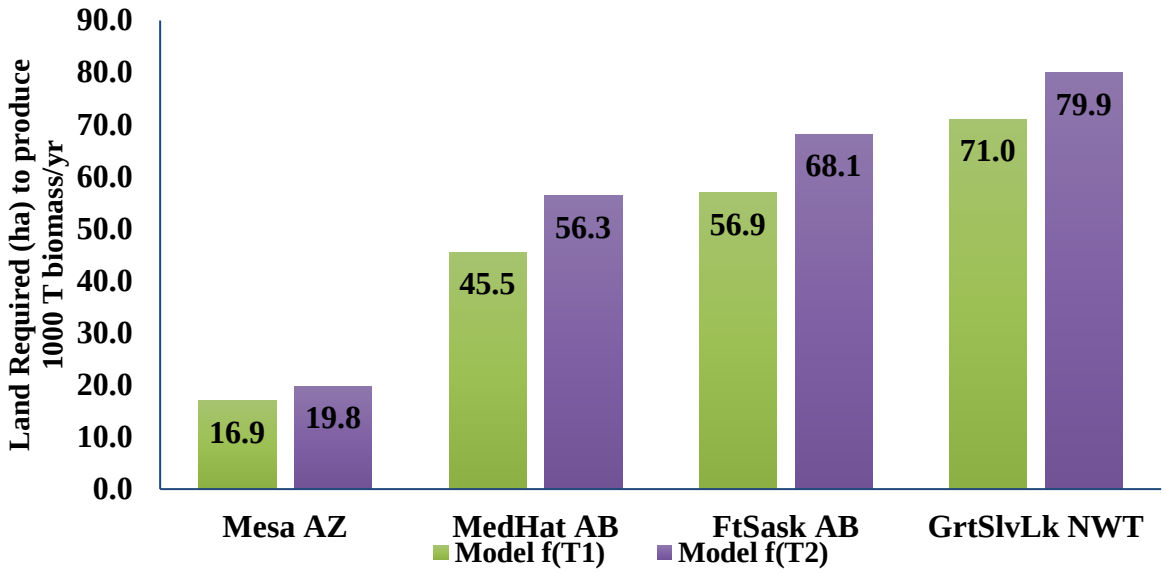

Figure 15: Predicted land requirement to produce 1000 tonnes biomass/yr

We predicted that a land area of 17-20 hectares in Mesa, AZ can produce a similar amount of biomass as 57-68 hectares at Fort Saskatchewan. Simple math provides the amount of land area required to meet our research objective, the cultivation of 2000 tonnes/day algae (i.e., 1,000 tonnes/yr/330 d/yr = tonnes/day [predicted]; 2000 tonnes/day [objective]/tonnes/day [predicted] = multiplication factor to be applied).

4.3.2.4 The effect of inoculum concentration

The model also proves useful in assessing the impacts of increasing the concentration of the inoculum for each subsequent growth period on yield and land requirements to produce 1000 T algae/yr (see Figures 16 and 17). Figure 16 shows a linear and direct relationship between initial inoculum concentration and annual biomass yield. In Figure 17, the model predicts that increasing the inoculum concentration from 0.2 g/L to 3.5 g/L reduces the requirement for land to an inflection point. If the inoculum concentration exceeds the higher concentration by more than 0.5 g/L, the requirement for land begins to increase again. The model also predicts that impacts of inoculum changes increase the further from the equator the OPR is located.

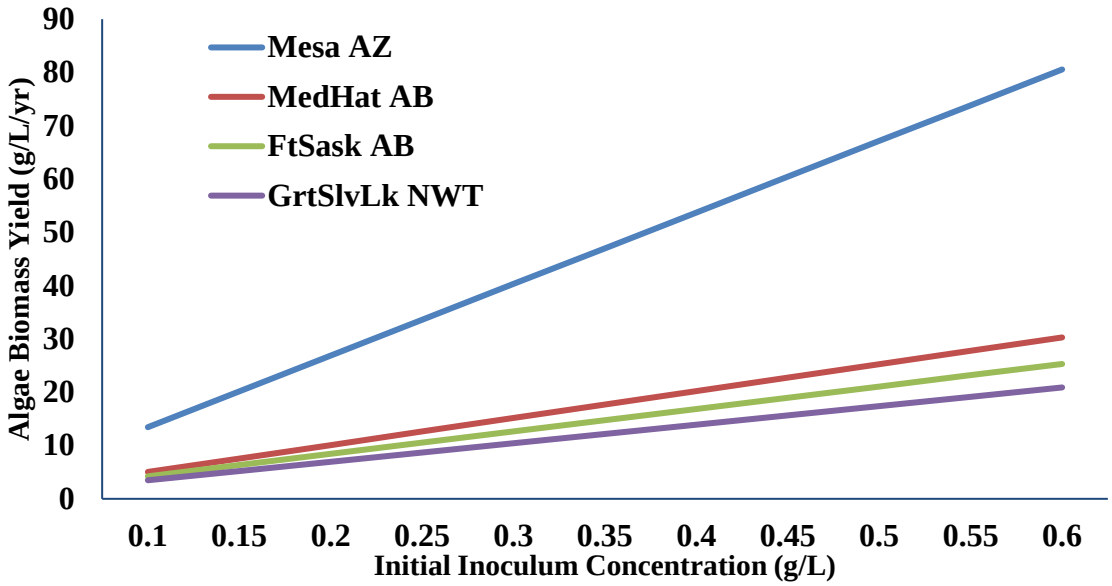

Figure 16: Predicted effect on biomass yield by increasing inoculum concentration (Model f [T_2])

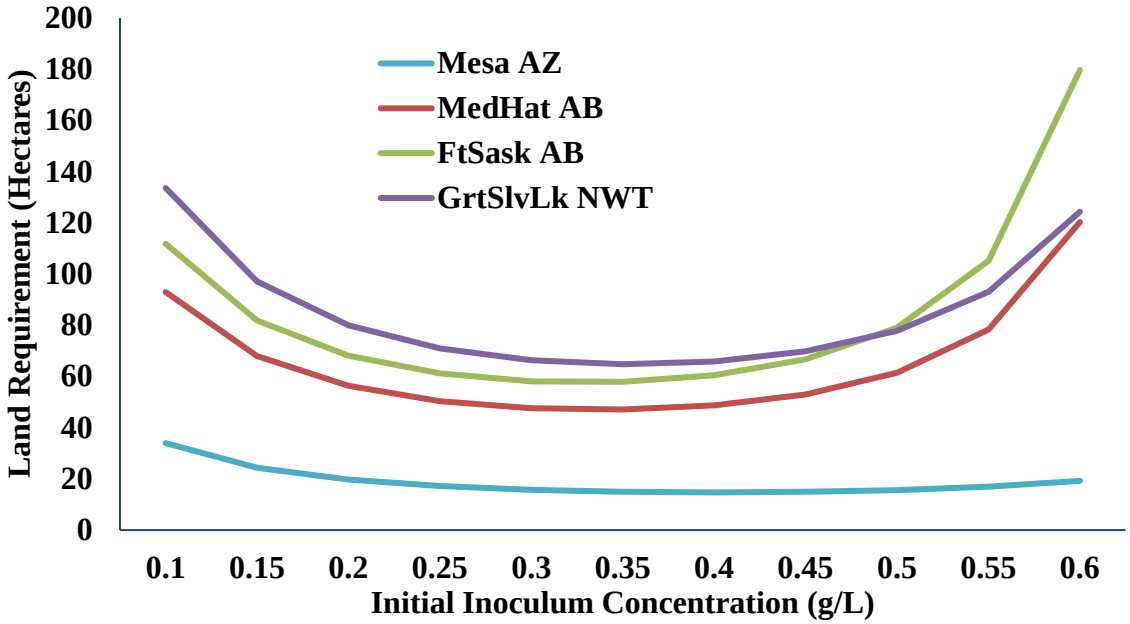

Figure 17: Predicted effect on hectares of land required to produce 1000 tonnes biomass/yr by increasing inoculum concentration (Model $f\ [T_2)]$)

4.3.2.5 The effect of incremental media temperature increases

We also assessed the impacts of incremental increases in media temperature on algae production and land requirements to produce 1000 tonnes/yr (see Figures 18 and 19). For the presented results, the incremental increase in temperature is applied throughout the year. Given that the media temperature at Mesa is already near the optimal level for much of the year, the addition of more than a few degrees of heat to the media would have adverse effects on annual production. Given the more northerly Canadian latitude for the other three OPR systems, it is relatively easy to generalize that these systems could benefit from the application of much higher levels of thermal energy to maintain optimized algae growth.

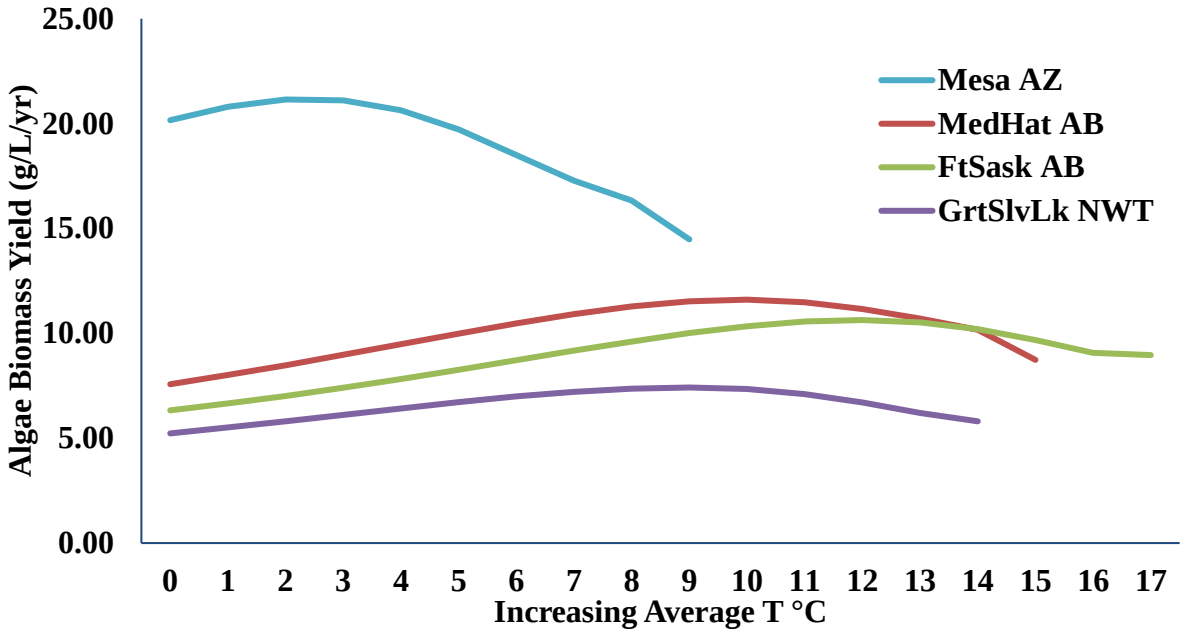

Figure 18: Predicted impact of increasing media temperature on algae biomass yield (Model $f\ [T_2]$)

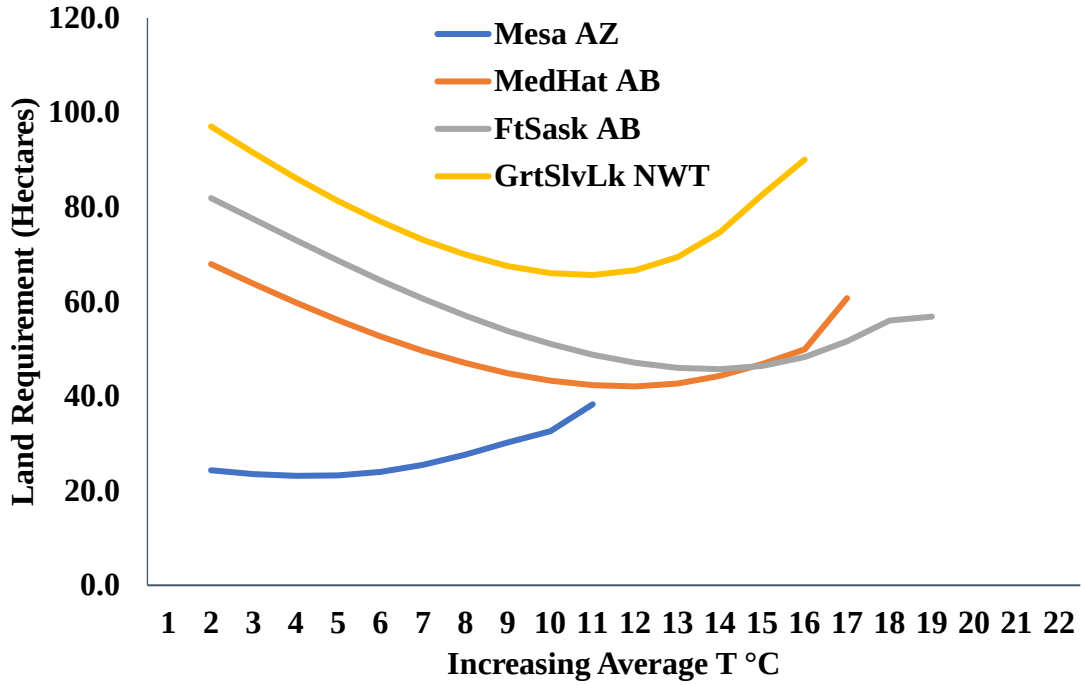

Figure 19: Predicted impact of increasing average media temperature on land requirement (Model $f\ [T_2)]$)

As seen earlier in the current study, the model can be adapted to maintain the media temperature at its optimum level to support algae growth. Calculations and analyses may also be conducted to

determine the amount of thermal energy required for this purpose along with associated costs, depending on the source of heat used.

4.3.2.6 The effect of supplementing light

Similarly, the model allows for the consideration of supplementing ambient light with LED and other sources of light to shift growth toward optimal levels. A simulation was conducted in our original correlation model wherein the system was optimized for the least amount of constant intensity light required to produce an equivalent amount of biomass. The model predicted that where $f(T_1)$ was fixed and optimized, the 2.14 g of biomass produced during the trial period could be achieved using a light source producing a constant 431 Wm^{-2}. Under $f(T_2)$ conditions, the same outcome would be achieved with a 215 Wm^{-2} light source (see Table 19).

Table 19: Predicted minimum constant light required to achieve the same yield as experimental (2.14 g), holding K_p constant for $f(T_1)$ and $f(T_2)$, respectively, and K_t and media T constant.

Model	K_t	K_p	Standard Deviation	Experimental (g)	Model 1 (g)	Model 2 (g)	Light ($W\ m^{-2}$)
$f(T_1)$	0.000011	0.000755	0.088935	2.14	2.14		431
$f(T_2)$	0.000011	0.000647	0.207232	2.14		2.14	215

The same model predicts that under $f(T_1)$ conditions, using a constant 1000 Wm^{-2} light source would improve the yield from 2.14 g to 2.56 g. Under $f(T_2)$ conditions, the same 1000 Wm^{-2} light source would improve the yield from 2.14 g to 5.08 g. Consistent with our understanding that light becomes limiting after a certain point, when the light source is changed to 580 Wm^{-2}, the $f(T_2)$ scenario still predicts a yield of 4.28 g (see Table 20).

Table 20: Predicted maximum biomass yield when light intensity is varied holding K_p constant for $f(T_1)$, and $f(T_2)$, respectively, and K_t and media T constant.

Model	K_t	K_p	Standard Deviation	Experimental (g)	Model 1 (g)	Model 2 (g)	Light ($W\ m^{-2}$)
$f(T_1)$	0.000011	0.000755	0.329437	2.14	2.56		1000
$f(T_2)$	0.000011	0.000647	0.072253	2.14		4.28	580
$f(T_2)$	0.000011	0.000647	0.106228	2.14		5.08	1000

As highlighted in the discussion, the SATOPR model demonstrates its ability to predict algae cultivation productivity in different geographies. However, it is also unique and useful for simulating outcomes for optimization scenarios such as changing harvesting schedules, applying units of heat to the media, augmenting natural light with artificial light and adjusting inoculum concentrations.

4.4 Conclusions

The objective of our research was to develop an analytical model that would prove useful in the prediction of algae biomass production for OPR sites in Canada. This work has demonstrated the successful development a data-intensive model whose results show good correlation with published data. The key parameters in developing the SATOPR model are media temperature and solar light intensity. Given the global reach of satellites, using this data source to predict OPR system performance both in Canada and the rest of the globe makes the model both unique and beneficial for comparative analyses of OPR system performance. The uniqueness in the development of SATOPR is that satellite data has never before been used in an attempt to model OPR algae yields. Because of its ability to predict localized algae yields, SATOPR may be used as an initial algae cultivation site screening tool, an alternative and complementary analysis tool useful for comparing system performance between locations. We have also demonstrated how the model provides additional supportive analytic capabilities that can be useful for techno-economic analyses and life cycle assessments. Future research with this model would benefit from access to timely experimental yield data (i.e., 15-minute incremental results that could be matched with other model parameter results that are provided at these same intervals). This would enable more accurate analysis and assist in refining capabilities in the SATOPR model. It is anticipated that the ultimate value of the model will be revealed as results from the model are correlated with experimental field data from multiple sites using identical species and operating protocols.

5 Techno-economic Assessment of Algae Biomass Production in Cold Climates

This section presents a comparative TEA of discrete cultivation systems that produce wet algae biomass (20% solids by weight). Three algae cultivation systems producing similar amounts of algae biomass were evaluated using published results and our modeled results. A sensitivity analysis was conducted for the key operating parameters associated with each approach. The analysis provides valuable insights into factors that are common between systems and those that are different. The first OPR system was modeled as located at Mesa, AZ. A second identical system was modeled in the northerly Canadian context at Fort Saskatchewan, AB. A third cultivation system based on PBR closed environmental technology providing optimized temperatures and lighting was modeled at Fort Saskatchewan. Using an analytical model constructed by Pankratz et al. to arrive at system costs, we selected Fort Saskatchewan as the reference point given the opportunity to co-locate with industrial CO_2 producers and the potential to offset associated greenhouse gas (GHG) emissions [607]. Fort Saskatchewan, in Alberta's Industrial Heartland (see Figure 20), is home to one of Canada's largest petrochemical processing regions, producing millions of tonnes of CO_2 annually [608]. There may be opportunity for \$20 CDN tonne^{-1} CO_2 emissions credits as of January 2017 from the province of Alberta. These credits would increase to \$30 CDN tonne^{-1} in January 2018 [609].

Every tonne of algae biomass produced sequesters 1.8 tonnes of CO_2 [8, 106]. Although not used in this study, Fozer et al.'s findings indicate that 2.02 tonnes and 2.09 tonnes CO_2 sequestered for each T of algae biomass cultured in OPRs and PBRs, respectively, would be more appropriate for calculations [610]. However, given the limited validation of Fozer's findings, we used 1.8 tonnes to predict the potential for qualifying algae biomass to receive carbon credits of \$28 US tonne^{-1} in 2017 and \$42 US tonne^{-1} in 2018 and beyond. Given the absence of published research related to the cultivation of algae in cold climate, the main objective of this study is to conduct the cost of algae cultivation yield in cold climate like Canada through development of techno-economic models. Specific objectives include:

- Estimating the cost of producing algae at the commercial scale at Fort Saskatchewan, AB, via OPR cultivation through the development of data-intensive techno-economic models;
- Estimating the cost of producing algae at the commercial scale at Fort Saskatchewan, AB, via PBR cultivation through the development of data-intensive techno-economic models;
- Conducting comparative economics between OPR algae cultivation in Canada and in a hot climate;
- Conducting comparative economics between PBR algae cultivation in Canada and OPR algae cultivation in a hot climate; and
- Conducting sensitivity analysis to study the impacts of varying parameters on the overall cost of algae production through the two production systems.

Figure 20: Map showing location of Fort Saskatchewan

5.1 Methods

This study focuses on a comparison between the two broad categories of cultivation technologies (OPR and PBR). OPR and PBR systems (see schematic Figure 21) are relatively similar in design. However, given the diversity of PBR technologies, we have selected a columnar PBR to represent this group (see schematic Figure 22). To develop the techno-economic model, it is important to analyze the energy and mass flows between unit operations and to calculate the associated operating costs.

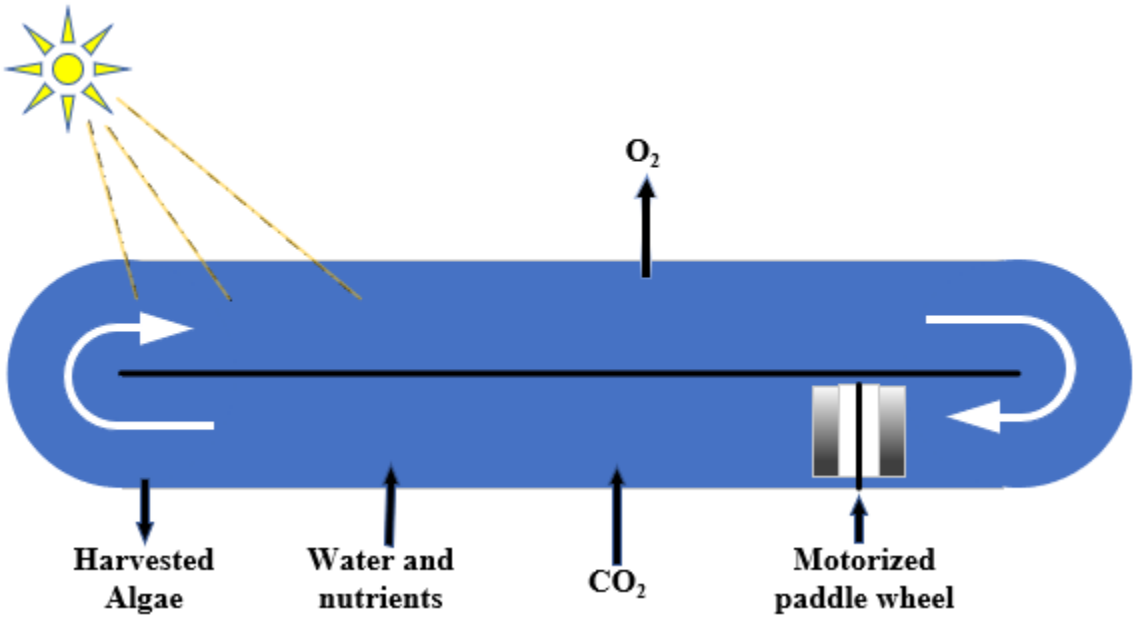

Figure 21: Schematic of open pond raceway (OPR) algae cultivation system

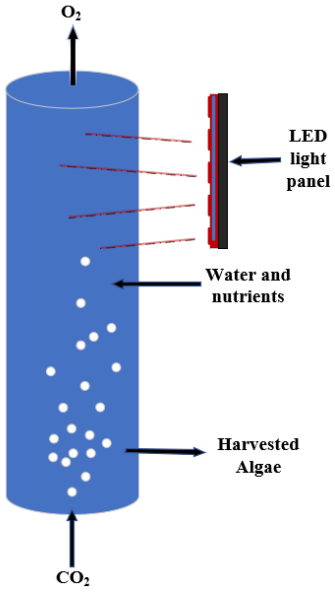

Figure 22: Schematic of photobioreactor (BPR) algae cultivation system

More specific details follow below. Figure 23 is a flow diagram that identifies the key inputs, systems, and processes that precede algae cultivation and lead to wet algae biomass production (i.e., 20% solids by weight). The 20% solids represent both the dewatering that can be achieved through a centrifugation process and also the amount of dewatering that would be required for potential downstream thermochemical processing by hydrothermal liquefaction. The single-celled microalgae plants in the inoculum system require access to dissolved CO_2 and primary nutrients like nitrogen, phosphorus, potassium, and sulphur to grow using the sun's radiant energy to replicate. Upon reaching a high cell density (e.g., wt 0.05% solids, the density at which algae would normally be harvested at), the media is transferred to a much larger cultivation vessel where much more water is added to bring the algae concentration down to wt 0.01% solids [611]. Again, CO_2 and nutrients continue to be added to ensure growth and replication continue. Over time, because of evaporation (in OPR systems) and blowdown (the constant removal of a small portion of the growth media to prevent ionic buildup in the media), additional makeup water will be required. When the algae culture reaches a prescribed cell density (e.g., wt 0.05% solids), it is time to harvest and dewater the algae biomass from the media. In a preliminary step, the algae cells are allowed to settle to the bottom of the cultivation system, helping to concentrate the algae.

The remaining unit operation technologies found in the process diagram (dewatering, harvesting and storage) are assumed to be identical between systems. The concentrated cells are drained off and pumped through a micro-filtration system that removes much more of the water and recycles it back into the cultivation vessel. However, more water must be removed by a centrifugation process to get the algae biomass to a desired 20% solids concentration for later downstream thermochemical processing. Because the algae biomass cannot be processed immediately following harvesting, the media is chilled for a short period before being transferred for post cultivation processing.

For the purpose of techno-economic assessment, the mass and energy balances were calculated for key inputs, including equipment for media circulation, nutrients, dewatering, and artificial lighting that may apply with each cultivation technology. Nutrient requirements for the algae cultivation are based on the stoichiometric macro-elemental quantities found in the resulting biomass: 54% C, 1.8% N, and 0.22% P. An additional 20% of these quantities were added to ensure that a nutrient surplus was maintained. Commercially available diammonium phosphate (DAP) provided the necessary phosphorous and anhydrous ammonia (NH_3)-supplemented nitrogen already available from the DAP. Carbon in the form of CO_2 is assumed to come from neighboring industrial processes. OPR construction and operating costs are based on values provided by Davis et al. [611]. The associated calculations are based on a data-intensive analytical model described in a paper by Pankratz et al. [607]. Table 21 provides a list of calculated key cost factors.

Table 21: Key cost factors

Items	Open raceway pond (OPR)	Photobioreactor (PBR)
Capital Costs (x $1000)		
Production ponds	1,866,235	
Photobioreactors (PBR)		691,773
Inoculum ponds	189,568	
Building for PBRs		69,923
CO_2 delivery	76,533	
Circulation	84,775	
Dewatering	277,064	154,091
Storage	62,405	20,576
Land	268,985	233
Indirect costs	1,528,370	508,666
Total Capital Invested	**4,353,935**	**1,439,262**
Cultivation Costs ($/tonne biomass)		
CO_2	100	100
NH_3	17	17
DAP	7	7
Power	58	54
Chilling	4	4
Fixed costs	208	66
Capital depreciation	189	69
Average Income Tax	129	42
Average Return on Investment	576	190
MBSP	**1,288**	**549**

The satellite (SATOPR) model simulates OPR cultivation results for any site-specific geographic area. Algae growth kinetic formulas were applied including the Beer-Lambert Law to account for the impact of sunlight on algae growth and the equation forwarded by James and Boriah to account for media temperature to predict algae production [593].

Calculations are indexed to 2016 USD and based on site-specific climatic factors, cultivation days, and local land, nutrient, and energy pricing. The following were made: algae minimum growth temperature -0.2 C; maximum growth temperature 33.3C; and optimum growth temperature 26.7 C [597]. The cost of land is assumed to be $3000/acre [611]. However, industrial land near CO_2 emitters at Fort Saskatchewan is reported above $75,000/acre [1]. For an OPR system, the considerable land that would be required at commercial biomass production levels would enable more favorable pricing.

[1] http://www.loopnet.com/for-sale/fort-saskatchewan-ab

The cost of electricity is projected at $0.68/kWh with CO_2 cost of $45/tonne at 90% utilization efficiency from a local natural gas-fired power plant without consideration of a potential gas purification step prior to use for cultivation [611]. The average algae productivity is 16 g/m^2/d and 1250 g/m^2/d for the OPR and PBR systems, respectively [607]. The OPR pond depth is 25 cm [611].

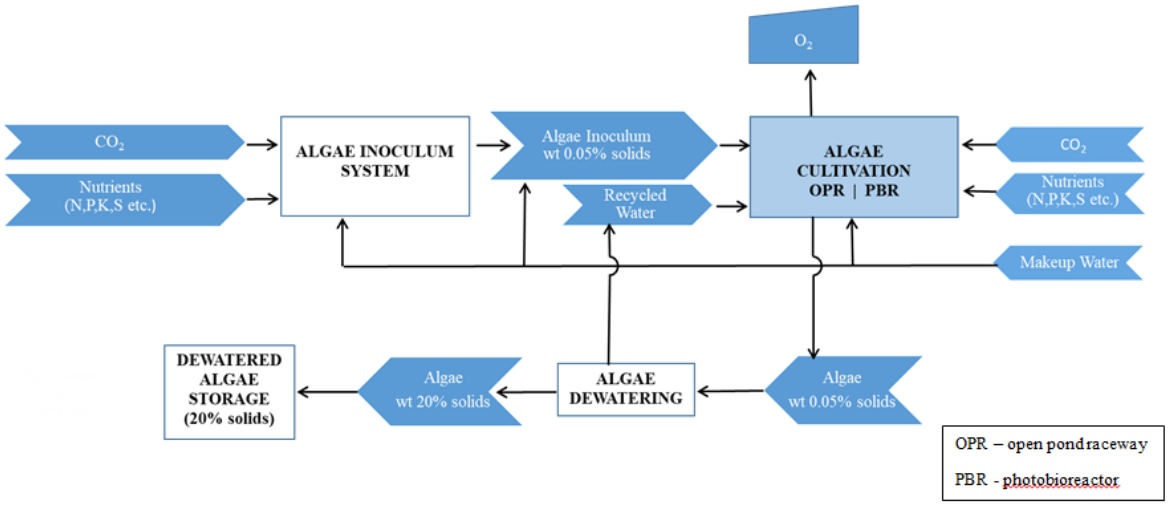

Figure 23: Simplified process flow diagram showing algae biomass cultivation activities

An OPR system at commercial scale (2000 tonnes/day), based on 10-acre ponds, was modelled and collocated with access to CO_2 at a landfill site producing electricity from landfill methane, using a combined heat and power (CHP) system, near Fort Saskatchewan. The commercial scale was chosen to match feedstock input requirements in downstream processing. Pond sizing was based on values presented by Davis et al. [612]. The CHP generation was modelled around the regional landfill methane production. However, calculated power generation was insufficient for operations, and therefore electricity was only accessed from the Alberta grid. Similarly, CO_2 was accessed from neighboring petrochemical facilities. OPR construction and operating costs are from the National Energy Research Laboratory (NREL) report by Davis et al. [612].

A columnar photobioreactor (PBR) system was also modeled at the same Fort Saskatchewan site and required only 14 acres of land [607]. The PBR design allows for consistent lighting and temperature control, thus enabling more optimized cultivation conditions. Enclosing the PBR systems in a temperature-controlled building reduces culture contamination and enables more effective control of media temperature. Thousands of low-cost cultivation media bags each containing approximately 7 m^3 of media (Bob Mroz, Hy-Tek Bio LLC, Dayton, MD, personal communication, Feb 20, 2017) are connected to an automated management system to monitor and control system parameters including nutrient delivery, LED lighting, electrical conductivity, pH, gas exchange, and media mixing (Bob Mroz, Hy-Tek Bio LLC, Dayton, MD, personal communication, Feb 20, 2017). Algae culture densities achieved in this controlled environment are more consistent and considerably higher than those achieved in OPR systems, up from 16 g/m^2/d (0.1 g/L/d) to 1250 g/m^2/d (5 g/L/d), a factor of 50. The productivity of this design is

consistent with the high-density productivity described by Apel et al. at 4 g/L/d [613]. Apel et al. report having attained algal cell densities of up to 67 g/L. The SATOPR model for predicting the cultivation of biomass was not required for this scenario since there is no reliance on ambient solar irradiance and temperatures. These parameters can be controlled throughout the entire growing period.

Although site-specific literature values for costing are available, for comparative purposes it is important that these values be correlated to experimental results based on local solar irradiance, media, and ambient temperature values. The modeled results were compared to experimental results and showed good correlation, confirmed by the analysis of standard deviations.

5.2 Harvesting, downstream dewatering, and storage

In each scenario, after cultivation, biomass is harvested, dewatered, and placed into cold storage to retain its value for additional downstream processes not covered in this study. Harvesting in the OPR system commences at 0.5 g/L, at which time 80% of the media is drawn off and dewatered [612]. The system is refilled with recycled water and topped up with fresh makeup water, thus resetting the remaining concentration to 0.1 g/L algae concentration. In the PBR system, harvesting begins once the algae reach a targeted 5.0 g/L density. At this predicted steady state, 10% of the algae media is harvested every 2.4 hours (i.e., 10x/day) [607].

In both OPR and PBR systems, preliminary dewatering takes place through gravity settling to increase the biomass concentration to 10 g/L [612]. This is followed by a secondary dewatering operation and continues through microfiltration and centrifugation to achieve a final concentration of 200 g/L (20% solids by weight) required for downstream processing [614]. In each case, water removed by dewatering is recirculated back into the cultivation media. Given that there will be continual water loss through evaporation, hydrolysis during photosynthesis, and post-cultivation processes, a certain amount of makeup water will be added to replenish the losses and to mitigate the potential for ionic buildup in the media. It is assumed that the makeup water has a negligible impact in the TEA. For OPR systems, although it is estimated that 2.1 L of water is required for the production of 1 kg of algae biomass, the associated cost of the water will be insignificant related to the MBSP. For PBRs, the water requirement is estimated to more than 100 times less [607].

5.3 Techno-economic assessment

Capital operating and production costs for the production of algae are based on a 30-year facility lifetime. The internal rate of return (IRR) is modeled at 10% [611]. Capital costs include land, construction/installation, engineering, and contingency costs. Land requirements include cultivation system space for open ponds systems, buildings, roadways, administrative, processing, and laboratory requirements. For OPR systems, this also includes civil work, creating, shaping raceway burns and leakage control, installation of piping, pumps, paddle wheels, settling area, inoculum ponds, etc. [611].

For PBRs, construction and installation with pumps, piping, supervisory control and data acquisition (SCADA systems), light emitting diode (LED) lighting systems, chillers, along with

buildings[2] that would enclose them would be included (Bob Mroz, Hy-Tek Bio LLC, Dayton, MD, personal communication, Feb 20, 2017).

Dewatering assets include membrane filtration units, centrifuges, and chillers along with biomass storage prior to downstream processing. Operating costs include energy for circulation of media, sparging for CO_2, nutrient supplementation, chilling, lighting, pumping, filtration and centrifugation, water costs, staff salaries, system maintenance, and transport of algae biomass for downstream processing. Fertilizer costs are projected to represent less than 5% of the cost of production and therefore do not appear in our results

For each system, the sum of each of the above costing factors leads to the calculation of minimum biomass selling price (MBSP).

5.4 Results and discussion

5.4.1 Validation

OPR biomass productivities were predicted using the SATOPR analytical model developed by Pankratz et al. in which satellite climatic data for 2014, including ambient temperature and solar irradiance at Fort Saskatchewan, was used[3][607]. OPR modeled results were validated using ATP[3]'s algae cultivation experimental data sets[4]. The modeled PBR system was validated through Hy-Tek Bio LLC's experimental results in cooperation with the University of Maryland (Bob Mroz, Hy-Tek Bio LLC, Dayton, MD, personal communication, Feb 20, 2017)[5], which demonstrated volumetric productivity algae yields of 5 g L^{-1} d^{-1}.

5.4.2 Techno-economic results

Table 22 presents techno-economic assessment results for key metrics including a calculated minimum biomass selling price (MBSP) for each of the two algae cultivation systems discussed above. With the SATOPR model we predicted the duration of the growing season for OPR systems at both locations and determined annual yields for that time period.

With the analytical SATOPR model, we can visualize the algae cultivation results. As shown in Figure 24, Fort Saskatchewan's climate supports algae growth for 203 days when the mean growing media temperatures remains above -2°C and produces 13.0 g/L/y of biomass. Meanwhile, the PBR system, which is not limited by either ambient temperatures or solar irradiance, will function 365 days of the year and is predicted to produce 1825 g/L/y of biomass.

The SATOPR analytical model was able to predict yields based on a regimented 7-day harvesting routine. A number of other harvesting regimes were run and predicted the opportunity to achieve more optimized outcomes [607]. For this study, the model was run to harvest biomass from the

[2] Estimate source from www.sprung.com and www.altusgroup.com
[3] These data were obtained from the NASA Langley Research Center (LaRC) POWER Project funded through the NASA Earth Science/Applied Science Program.
[4] https://openei.org/wiki/ATP3
[5] https://www.umces.edu/feng-chen

OPR systems on the day cell density was determined to be above 0.5 g L^{-1} and dilute the remaining algae back to 0.2 g L^{-1} as a starting concentration.

Table 22: Key metrics for annual biomass production

Items	Units	OPR Ft.Sk., AB	PBR Ft.Sk., AB
Average productivity	g/m^2/d	16	1250
Land required	m^2	1243	0.5
MBSP	/$/tonne	$1,288	$550
Total capital investment	$/tonne	$6,593	$2,179
Land cost (at $3000 ($75000)/acre))	$/tonne	$407 ($10,183)	$ 0.4 ($8.8)
System water volume	m^3	90.193	0.231
Annual cultivation days	Days	203	365
Annual productivity	g/L/y	13.0	1825

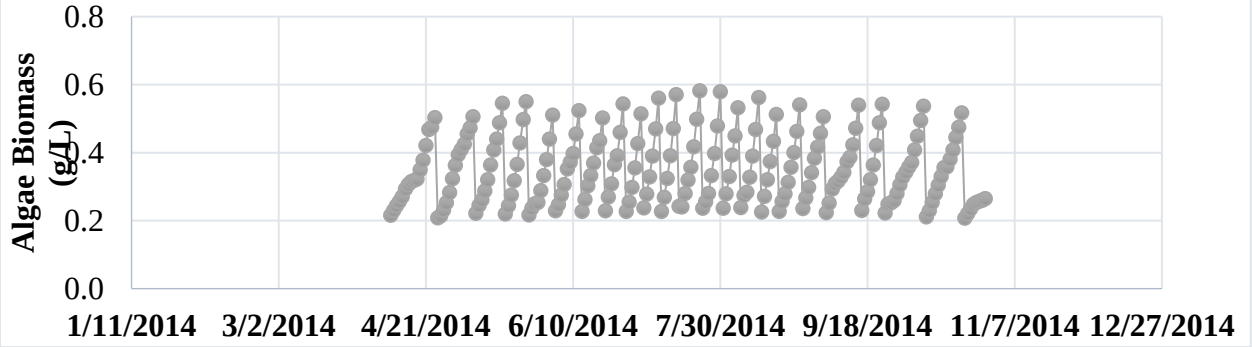

Figure 24: Predicted annual algae OPR growth at Fort Saskatchewan, AB – 2014.

As shown in Figure 24, in Fort Saskatchewan, AB, summer harvests would occur every 5th or 6th day. Meanwhile, algae were harvested in a semi-continuous manner for the PBR system by withdrawing 10% of the media every 2.4 hours, or 10 times each day. This regime enables the system to maintain a much higher media algae density. The PBR system was modeled to produce algae by providing light 24 h/d using LEDs. However, we explored the possibility of improved economics by using available sunlight. Assuming that 40% of our light (daylight hours) could come from sunlight, we determined that when the PBR takes advantage of sunlight, the MBSP would improve by 2.70 $/tonne (a 0.5% change in MBSP).

The analytical model also predicted that cultivating algae biomass in Fort Saskatchewan, AB, would require 555 m^2/tonne with an OPR system, vs. 0.5 m^2/tonne via a PBR system. The

cultivation area to produce 2,000 tonnes/day of biomass with an OPR system requires over 82,000 ha and only 32 ha with a PBR system. See Table 23.

Table 23: Key metrics for annual biomass production of 2000 tonnes/day (660,000 tonnes/yr) biomass

	Units	OPR Ft.Sk., AB	PBR Ft.Sk., AB
System water required	m^3 x 1000	59,527	153
Land required	ha	82,038	32
MBSP	$/tonne	$1,288	$550
Annual cultivation days	Days	203	365

5.5 Sensitivity analysis

A sensitivity analysis was conducted for each of the key cultivation factors found in both the OPR and PBR systems. Table 24 provides a list of theses variables and allows us to make comparisons between OPR and PBR cultivation systems and demonstrates the sensitivity that changes to each parameter will have on the cost of producing biomass.

Table 24: Key variables with associated impact on MBSP per tonne of biomass

Items	**OPR Ft. Sk. AB**	**PBR Ft. Sk. AB**
Open raceway pond avg. productivity ($gm^{-2}d^{-1}$) Mesa AZ (40:25: 15) Ft Sk.AB (34:21:13)	($384) : $0 : $735	-
PBR avg. productivity (g/L/d) (8 : 5 : 3) equivalent to $gm^{-2}d^{-1}$ (2000:1250:750)	-	($134) : $0 : $238
Scaling PBR capacity (L PBR^{-1}) (20K, 6.8K, 3.5K)	-	($190) : 0 : $268
Composition + Productivity ($gm^{-2}d^{-1}$) (HPSD@35 : HCSD@25 : HLSD@15)	($11) : $0 : $248	($11) : $0 : $248
CO_2 (cost/tonne) ($0 : $100 : $120)	($100) : $0 : $20	($100) : $0 : $20
Land (cost/acre) ($1000 : $3000 : $75000)	($29) : $0 : $1045	$0 : $0 : $1
Total capital investment (-25% : 0 : +25%)	($415) : $0 : $243	($81) : $0 : 81
Leakage control (shift from in-situ clay to fully lined)	$0 : $0 : $421	-
Scaling cultivation area (acres) (10000 : 5000 : 1000)	($18) : 0 : $112	-
On-stream factor, days/yr (360 : 330 : 300)		
On-stream factor, days/yr (220 : 203 : 185)	($117) : $0 : 114	
On-stream factor, days/yr (360 : 365 : 330)		$0 : $0 : 26
Flue gas vs. CO_2	($49) : $0	($49) : $0
Labor costs (-50% : 0 : +50%)	($64) : 0 : $64	($26) : $0 : $26

Items	OPR Ft. Sk. AB	PBR Ft. Sk. AB
CO_2 recycle (30% : 0%)	-	-
N recycle (90% : 0%)	-	-
Power cost ($/kWh) ($0 : $0.068 : $0.10)	($58) : $0 : $28	($54) : $0 : $25
Increasing cultivation media T 10 Deg.C using low grade heat.	($530) : $0	-
Staff – # PBR's each person can manage (5000 : 2500 : 1000)	-	($26) : $0 : $78
Alberta carbon credit ($/tonne biomass)	($28)	($28)

Figures 25 and 26 show tornado sensitivity analyses of both the OPR and PBR cultivation scenarios considered in this study.

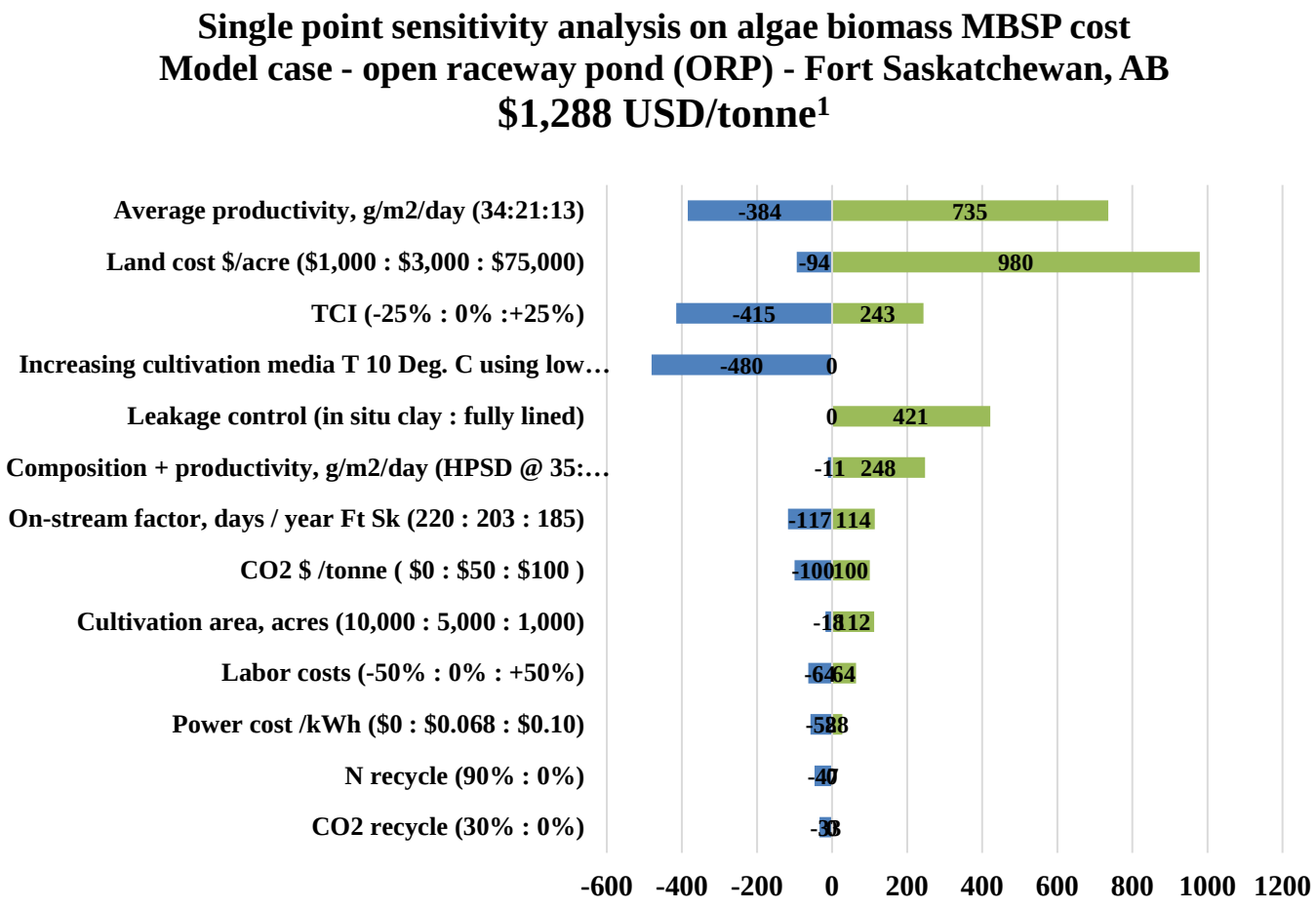

Figure 25: Sensitivity analysis of algae biomass cost for OPR located at Fort Saskatchewan, AB

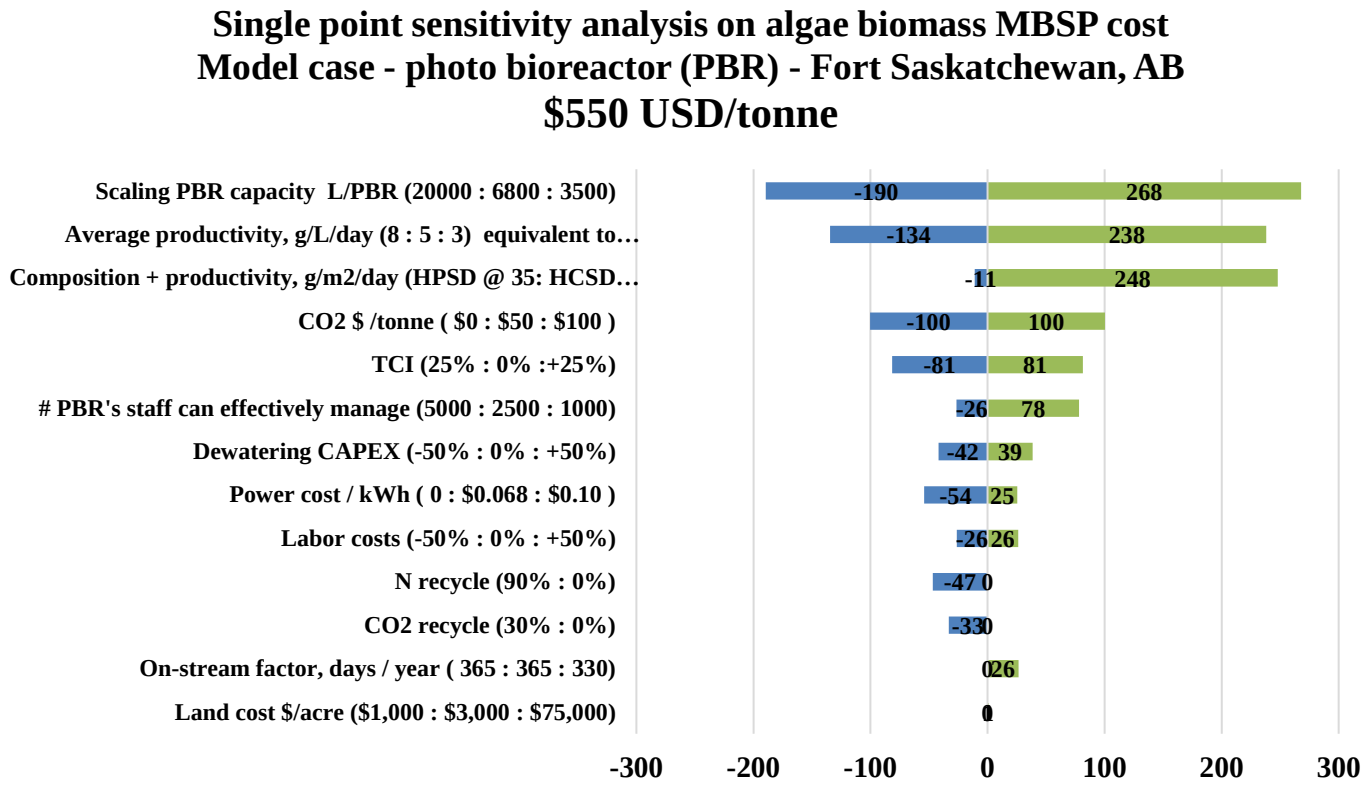

Figure 26: Sensitivity analysis of algae biomass cost for PBR located at Fort Saskatchewan, AB

In the OPR systems (Figures 25), average productivity is found to have the greatest sensitivity with respect to minimum biomass selling price (MBSP). Increasing productivity in the OPR system by 60% from 21 $gm^{-2}d^{-1}$ to 34 $gm^{-2}d^{-1}$, would reduce the MBSP by $384/tonne (17%). If yields fail to achieve the current average production of 21 $g/m^2/d$ and fall by 60%, to 13 $g/m^2/d$, biomass cost is predicted to increase by $735/tonne (33%). For the PBR technology, a 60% increase in yield from 1250 $g/m^2/d$ to 2000 $g/m^2/d$ (8 g/L/d) would reduce the biomass price by $123/tonne (21%), whereas a decrease in yield to 750 $gm^{-2}d^{-1}$ (3 g/L/d) would increase the biomass price by $267/tonne (45%).

Land cost, introduced earlier, may have a significant impact on the MBSP and this impact highlights the importance of siting, especially for OPR systems. The significance of this can be seen when land prices are negotiated from our assumptive $3,000/acre down to $1,000/acre with a realized MBSP benefit of $94/tonne. The same land priced at $75,000/acre would increase the MBSP by $980/tonne. It becomes obvious that land price is a major sensitivity factor affecting the MBSP in OPR systems, yet this same factor (changing land price from $1,000/acre to $75,000 /acre) plays only a minor role in a PBR system with an impact of $1/tonne on the MBSP.

Fluctuations in total capital investment (TCI) for OPR systems would see the MBSP price fall by $415/tonne when TCI decreases by 25% and increase by $243/tonne when TCI increases by 25%.

For the Canadian PBR system, TCI fluctuations of 25% result in an $81/tonne MBSP swing in both directions.

Given the tremendous amount of available low-grade heat from industrial operations, there is an opportunity to shift media temperature closer to optimum growing temperature for OPR systems. Success in raising media temperature by 10 ºC would significantly improve yield and reduce the MBSP by approximately 1/3 ($480/tonne). The offset not considered in this calculation would be engineering/capital costs required to provide heat transfer. Choosing to use full leakage control for the OPR would increase MBSP $421/tonne. Neither of these factors would apply to PBRs.

Building on the topic of productivity, biomass composition, a factor influenced by cultivation and harvesting practices, also impacts the MBSP. Batch harvests considered in this study for OPR systems may be taken in early, mid, and late cultivation states. An early harvest would result in nominal nutrient depletion. For mid-harvest, no additional nutrients would be added, and the batch would be maintained an extra 3-5 days to achieve a mid-nutrient depletion state. A late harvest would occur 6-9 days post early harvest, thereby using up more primary nutrients. This regime corresponds to composition and nitrogen (N) availability in the media as follows: low N state promotes high protein (HPSD) composition, mid N promotes high carbohydrate (HCSD), and high N promotes high lipid (HLSD) composition. The trade-offs between states in the sensitivity analysis indicate that a mid-harvest regime (our assumption for this study) may strike an appropriate balance between yield and value for downstream processing. Choosing HLSD would provide a nominal $1/tonne reduction in the MBSP. High lipid composition biomass would produce higher heating values but at the cost of significant biomass yield, thereby increasing the associated biomass MBSP by $248/tonne. Depending on plans for downstream processing, an economic decision would be made to determine which harvest regime would provide the greatest economic benefit from a cost/benefit perspective. While the choice of early, mid, or late harvest has significant production cost implications, the costs are not ones where we can differentiate between the cultivation technologies employed since the impacts are assumed to be identical for both OPR and PBR systems.

The on-stream factor is related to the percentage of time a given facility is anticipated to operate annually. Currently, this figure ranges widely between cultivation technologies and is affected by culture crashes, pond upsets, pond freeze-up, maintenance, and other factors. This study predicts a 90% on-stream factor to be consistently attainable. Economic analysis indicates that a 10% change from the predicted 203-day on-stream factor will affect the OPR MBSP by 9%. The price will increase by $114/tonne if the system remains on stream 185 days (the on-stream factor decreases by 10%) and decrease by $114/tonne if the system operates 220 days (the on-stream factor increases by 10%). Given the much higher degree of system control with the PBR, a 99% on-stream factor is proposed. For PBRs, since we contemplate they operate year-round, we only considered the case in which only a 90% on-stream factor is achieved, and this would result in an increase in the MBSP by 5% (or $26/tonne).

Similarly, since CO_2 is common to both cultivation technologies, it is not a differential factor by itself between ORP and PBR technologies. At $50/tonne for the purchase of CO_2, it ranks 8th for costs in OPR systems and 4th for the PBR system. At 90% utilization, and the requirement for 1.8 T of CO_2 for every tonne of algae biomass produced, this translates into $100/tonne MBSP. The

price can be reduced by $100/tonne if the CO_2 is free and goes up by $100/tonne if the CO_2 price increases to $100/tonne.

Considerable engineering work has been conducted on OPR algae cultivation system design in order to predict the impact of enlarging pond size from the existing 5,000 wetted acres and scaling to 10,000 acres [611]. At the scale of the OPR system in this study, 5,000-acre wetted areas were proposed. Doubling the wetted areas to 10,000 acres would improve the MBSP by $18/tonne, whereas reducing the size to 1,000 acres would increase costs by $112/tonne. For the PBR system, the design size could theoretically be tripled. Interestingly, tripling the PBR cultivation volume is predicted to provide the strongest benefit of the weighted sensitivity factors by improving the MBSP by $190/tonne (34%).

Each of the cultivation systems considered would be similarly affected by CO_2 and N recycling and improve the MBSP by $41-47 for N and $33-38 for CO_2.

Labor cost sensitivities on the MBSP range from 4-5% between scenarios based on a 50% salary fluctuation. These fluctuations represent a potential MBSP change of +/- $64, and +/- $26/tonne for the OPR and PBR systems, respectively.

Given that electrical power has economic and environmental impacts, both of which affect the ability to use carbon credits, it is useful to evaluate its economic sensitivity. For the OPR siting, we determined the possibility of accessing free electricity from combined heat power (CHP) plants run on methane from an adjoining municipal solid waste (MSW) plant as part of their parasitic load (electricity not transmitted to consumers but used at the source location). To understand the potential impact, we conducted more detailed calculations for the cultivation sites at Fort Saskatchewan [615-617]. Approximately 200,000 tonne/yr of MSW are produced in the region with the potential to generate 9.6 MW power. However, the PBR system requires 98 MW of power. Hence, the CHP would produce less than 10% of the energy required by the PBR system and approximately one-third of the power requirement for the OPR system. However, obtaining power at no cost from this source would provide a benefit of $58/tonne for the Fort Saskatchewan OPR and $54/tonne for the PBR system.

There are several important insights to be gained from the comparison of TEAs of autotrophic OPR and PBR systems sited in Fort Saskatchewan, AB.

In terms of the potential to reduce the MBSP, the most important common factor is increasing average productivity (yield). Whether yield is calculated by g/L/d or $g/m^2/d$ or other productivity metrics, the results are the same. Given that PBRs have been shown to outperform OPR systems by a factor of 50, it is more likely that greater productivity gains will be realized in the PBR than the OPR system. It may be argued that gains made by using a PBR are linked directly to the higher level of control of all biological system parameters than is possible in OPR systems.

The total capital investment (TCI) is important. Every parameter in an algae cultivation system affects the amount of capital that must be invested to both create and operate the system. This knowledge is instructive to algae cultivation system architects and designers; by focusing on every design detail, they can eliminate unnecessary costs.

Access and co-location with cheaper nutrient sources and power for operations will reduce the MBSP.

While OPRs have reached an upper limit with respect to scaling, tremendous opportunities for scaling and resulting reduced MBSPs may be possible by using PBR systems.

Designing algae cultivation systems to take advantage of automation will lower the MBSP.

From a techno-economic perspective, carbon credits, especially when the algae industry struggles to gain traction, will enable companies to begin operations while they find long-term economic footing.

The study does not support the placement of an OPR algae cultivation system at Fort Saskatchewan, AB, from a techno-economic perspective. Although summer growing conditions are favorable because of both long days and warm temperatures, the actual growing season is too short. There may be an opportunity to capitalize on industrial low-grade heat to augment growing conditions. However, unless the added heat allows both the growth media to be maintained at close to optimal growing temperatures and cultivation at least an additional 60 days annually, the MBSP would remain (potentially) double that of an OPR system in Mesa, AZ.

Co-locating either the OPR or the PBR system on an MSW site is a great strategy, providing the electricity generated is free and considered a parasitic load with no negative environmental impacts. It would be important to match the scale of operations to the available electricity. Furthermore, power generated from the landfill methane would produce flue gases with adequate CO_2 generated to support biomass growth. Any CO_2 absorbed in this way would mitigate the CO_2 emissions and potentially qualify for associated carbon credits. Heat generated through the production of power as well as landfill geothermal heat could be used to optimize media temperatures for an OPR system. This could also increase the number of on-stream days. The 0.9 MW CHP (combined heat and power) engines assumed in this study release 8.5 million BTU hr^{-1} and close to 1 T CO_2 hr^{-1}. Siting at or near landfills may provide access to lower-priced land.

The cumulative gain from extracting benefits at every level will lead to a more favorable and sustainable techno-economic MBSP for algae biomass. It may be argued that OPR cultivation systems still provide the most economic means of producing algae biomass. This study, however, determined that PBR systems will outperform OPR systems in Canada. Given that PBR systems may be sited adjacent to CO_2 producers to access this free key nutrient, the systems will have a 10-20% economic advantage over OPR systems.

While OPR systems may only be viable in specific geographic regions with moderate temperatures and good solar radiation most days, the advantage of PBR systems is that they can be sited anywhere.

An opportunity for future research would be to conduct a Monte Carlo simulation to determine the probability of positive outcomes in each cultivation technology in the next 5 years. The results of the current analysis suggest that the future development and refinements to PBR systems may lead to more ubiquitous deployment of algae cultivation around the globe and eventually to a lower and more sustainable MBSP than offered by current OPR technologies. Sensitivity factors that can dramatically impact the MBSP in PBR systems may be easier to positively alter and control than

similar sensitivity factors in OPR systems. As outlined in this study, it is conceivable with PBR technologies, over a five-year horizon, to triple the size of the current bioreactor and increase average productivity from 5 g/L/d to 8 g/L/d while reducing capital investment by 25%. Attaining these goals could place algae biomass MBSP well below $200/tonne.

5.6 Conclusions

A comparative techno-economic analysis (TEA) for cultivating algae biomass feedstock for downstream processing into diluent and hydrogen has been conducted for an open pond raceway (OPR) system and a "closed" photobioreactor (PBR) system. The key factors that affect the economics of OPR systems are not the same as those for PBR systems. The findings of this comparative research are that the MBSPs for a tonne of algae biomass produced from OPR and PBR cultivation systems in Fort Saskatchewan, AB, are $1,288/tonne, and $550/tonne, respectively.

This analysis has revealed that in Canada a PBR cultivation system has the potential to produce algae biomass at a significantly lower MBSP than an OPR system at the same location. In fact, it is projected that the PBR MBSP could rival that of OPR systems located in even the most favorable climatic locations. Environmental and operating parameters have been identified and show potential for continuing to improve MBSP and are recommended for further study.

6 Comparative Techno-Economic Analysis of the Production of Diluents from the Thermochemical Conversion of Algae

This section focuses on thermochemical approaches to microalgae use, specifically microalgae HTL and pyrolysis, to comparatively assess the production of chemicals from this biomass, which are used as diluents for oil sands applications. The research comparatively assesses the techno-economics of pyrolysis and HTL-based platforms for diluent production from algal biomass. Hence, the specific objectives of this study are to:

- Develop a detailed process model for algal-based HTL and pyrolysis followed by upgrading to produce diluents;
- Provide capital cost estimates for 2000 tonnes/day diluent production using HTL and pyrolysis-based diluent pathways;
- Determine the optimum plant capacity for algal HTL and pyrolysis-based diluents;
- Analyze the influence of biochar from pyrolysis on pyrolysis-based diluent production;
- Perform a sensitivity analysis to understand the effects of key parameters on process economics; and
- Perform an uncertainty analysis using the Monte Carlo approach to identify the uncertainty associated with the product value of diluent.

6.1 Thermochemical process design

Unlike algal biodiesel production, which relies mostly on specific algal strains and is aimed at lipid accumulation solely to increase biodiesel yield, thermochemical approaches, namely pyrolysis and HTL, convert not only the lipid portion of microalgae but also other biomolecules like carbohydrates and proteins in whole algae [618]. In general, microalgae achieves concentrations from 0.01 to 0.1% (mass fraction basis) and thus requires concentrating to render it compatible for pyrolysis and HTL [619]. The latter requires that algal biomass undergo filtration or centrifugation whereas the former requires additional thermal drying.

6.1.1 Algal pyrolysis

Pyrolysis, a type of thermochemical process, involves operating conditions at atmospheric pressure in a temperature of 300-700 °C or higher in an oxygen-free environment that lead to the thermal disintegration of dry organic feed (moisture content below 10%) [620]. The major products from pyrolysis include bio-oil (organic liquid), gas, and char (solid), the amounts of which depend on operating conditions, the nature of the feedstock, and the reactor used. Fast and flash pyrolysis, which involves a high heating rate and a short residence time at 450-550 °C, increases the organic liquid mass yield from 50 to 70% w/w [621]. However, extensive drying is required before biomass is input to the system in order to reach high heating rates.

Fast pyrolysis for bio-oil production has been studied for a number of microalgae strains [622-626]. For instance, Gong et al. [625] and Harman-Ware et al. [623] employed *Scefnedesmus sp.*, *Chlorella vulgaris*, and *Dunaliella salina* for fast pyrolysis and produced bio-oil with a higher heating value (HHV) of 18–25 MJ/kg. Microalgae pyrolysis has three steps [627]. In the first step, light volatile compounds and water are removed at a low temperature (130-165 °C, depending on the algae). The second step is de-volatilization at 140-540 °C, wherein organic molecules are

decomposed in this order: polysaccharides, proteins, lipids. The final step occurs above 540 °C, which causes the carbonaceous substances in the residuals to decompose. A general process scheme for the pyrolysis algal platform is modeled in this study. Figure 27 shows the main unit blocks for the pyrolysis system: feedstock processing, fast pyrolysis, hydrotreating, and a hydrogen production plant. The particles are fed to the fast pyrolysis reactor to produce oxygenated liquids. The resulting fast pyrolysis oil is hydrotreated to produce stabilized bio-oil, which can be used as diluent. The off-gases from all processing areas are used with natural gas to obtain the requisite hydrogen for hydrotreating.

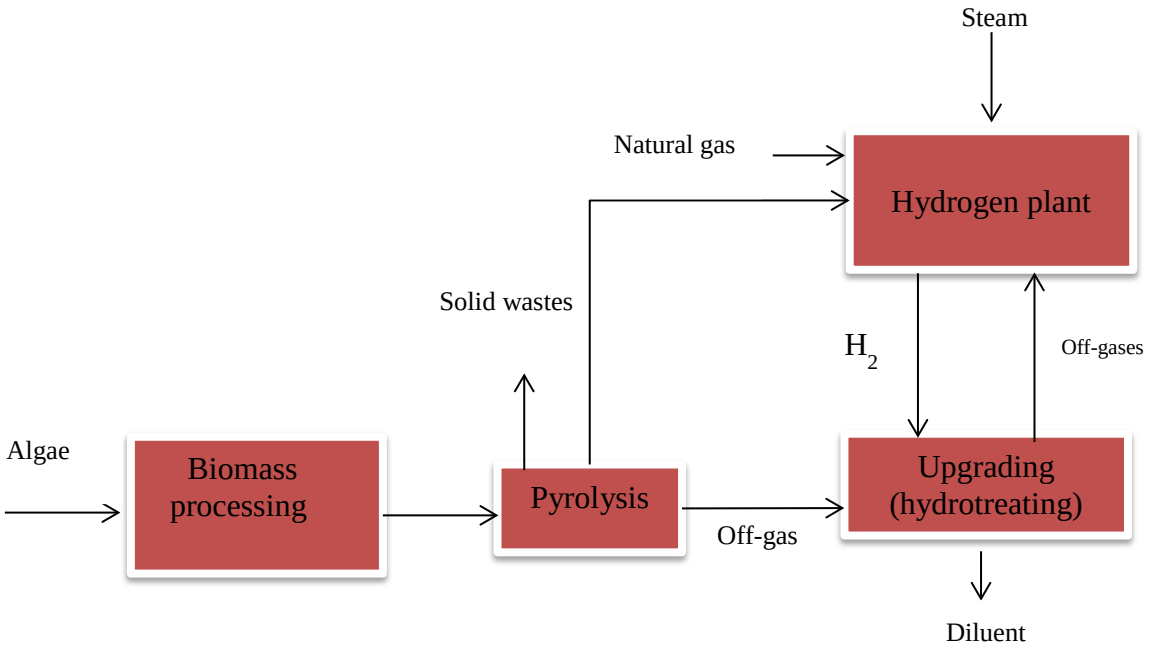

Figure 27: Block diagram for the thermochemical algal pyrolysis pathway

6.1.2 Algal HTL

Hydrothermal liquefaction (HTL) converts wet biomass (moisture content above 50% by mass) to liquid biocrude with or without a catalyst at temperatures in the range of 280–370 °C and pressures of 10–25 MPa [628-630]. HTL process conversion efficiency is influenced by process conditions such as temperature, pressure, residence time, and the nature of the feedstock. HTL oil, characterized by 10–20% w/w oxygen and nitrogen, has an energy density of 30-37 MJ/kg [631]. HTL processing is best suited for wet feedstocks like algae as the drying requirement is avoided. Early studies on microalgae hydrothermal liquefaction involved the use of a batch reactor at high algal concentration at 300 °C and resulted in oil yields of 37 wt% and 57-64 wt% for *Botryococcus braunii* and *Dunaliella tertiolecta*, respectively [632, 633]. Most HTL studies have been performed in batch reactors; nevertheless, continuous-scale processing is needed to realize HTL biocrude production at a commercial scale. Yang et al. studied HTL characteristics through the liquefaction of the main components of low-lipid microalgae such as crude proteins, crude polysaccharides, and their mixtures [247]. They demonstrated that polysaccharides contributed less than 5% towards bio-oil formation whereas proteins contributed up to 16.29%. Jazrawi et al.

and Roussis et al. demonstrated the use of two-stage HTL, the feasibility of which was further investigated by Costanzo et al. by comparing it with single-stage HTL at the laboratory scale, which aims to lower the content of nitrogen in biocrude [634, 635, 636]. They illustrated that the two-stage processes are suited to high lipid-containing microalgae. Hognon et al. comparatively analyzed the HTL and pyrolysis of *Chlamydomonas reinhardtii* and showed a possible approach to recover the aqueous phase for cultivation purposes [627]. Their study on re-using an aqueous medium for microalga growth shows great potential; however, the authors determined that the high levels of organics in the aqueous phase required treatment before the aqueous medium could be used for cultivation. During the HTL process, water acts as both solvent and reactant. The operating conditions of water in HTL are closer to water's critical state (Tc = 374 °C and Pc = 22.1 MPa), which reduces the dielectric constant and increase the solubility of the organics [368]. The reaction mechanism in HTL involves biomass de-polymerization, subsequent biomass decomposition into monomers via a series of reactions (decarboxylation, dehydration, cleavage, and deamination), followed by fragments recombination [127].

A general process scheme for an HTL algal platform was modeled in this study. Figure 28 (a) shows the main unit blocks in the HTL system developed for woody biomass in a previous study [637]. This model considered as a biomass feedstock whole tree wood chips with an initial moisture content of 50% and the resulting process entailed further preprocessing to reduce solid loadings to 8.2 wt% at the inlet of HTL reactor. Algal processing facilities are different from lignocellulosic biomass-based processes [638]. There is no pre-processing requirement for algal biomass suited for direct processing [137]. Moreover, algal biomass production and conversion platforms are co-located and dependent. The conversion platforms do not require that algal biomass be transported to a downstream facility and hence avoid the costs associated with off-site transportation, as noted also by Davis et al. [639]. Figure 28 (b) shows the main unit blocks for the HTL system in the current study. As shown in Figure 28 (b), after harvesting and dewatering, algal slurry is pumped into the HTL reactor where it is separated into biocrude, aqueous phase, and gases. Biocrude is further separated from other process streams. The HTL biocrude is fed to the hydrotreating section for further upgrading to the desired product. The process off-gases from all processing areas are directed to a hydrogen plant for H_2 production for hydrotreating.

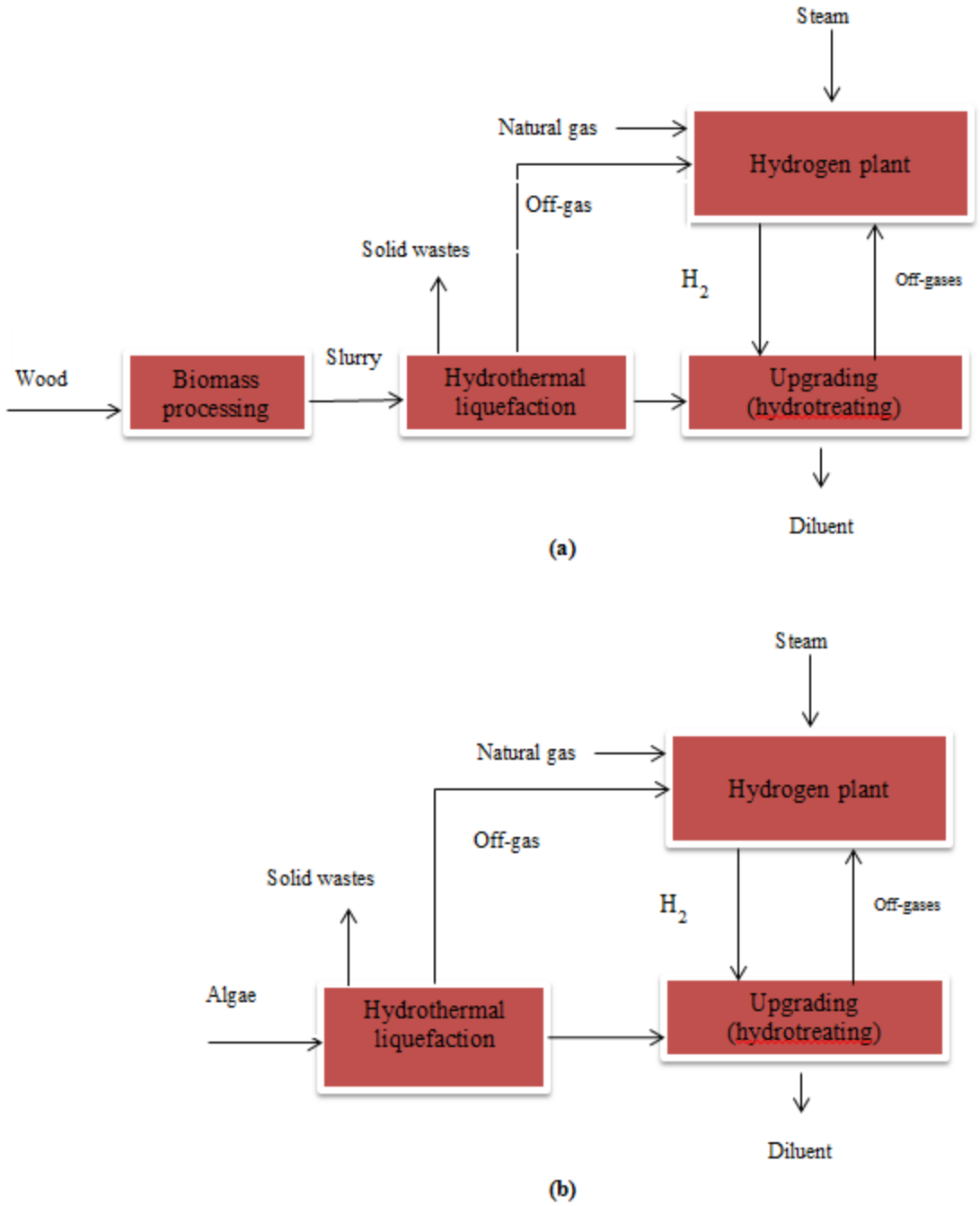

Figure 28: Block diagram for the thermochemical (a) wood and (b) algal hydrothermal liquefaction pathways

6.2 Materials and methods

Techno-economic assessment involves the development of data-intensive techno-economic models using the process models to estimate the product value of diluent. The process models are developed in Aspen Plus and the equipment costs are derived from the Aspen Icarus Economic Evaluator [640, 677]. The rate of return on investment is calculated through a discounted cash flow of rate of return (DCFROR) analysis for a 20-year plant life. The assumptions used in the analysis of the HTL and pyrolysis plants are discussed in this section. It is assumed that the plant uses 2000 dry tonnes/day of microalgae for both platforms. Biomass concentration results for algal HTL in other studies are 10-20% [641, 642]. It is known that 20% of the algal biomass obtained from the initial processing steps can be transported with a positive displacement pump [643]. The process off-gases are used in the hydrogen generation plant for hydrogen production. The thermochemical plant analysis uses an n^{th} design, which does not consider special financing needs [638]. Tang et al.'s algae compositional characteristics of algae, as provided in Table 25, were used in this study [644]. Traditionally, microalgae has higher nitrogen content than lignocellulosic biomass; this is mainly due to the presence of proteins[645]. Thus, a significant amount of nitrogen can be found in the resulting biocrude, leading to issues during biocrude upgrading and combustion [646].

Table 25: Composition of the algal feedstock considered in this study, derived from Tang et al. [644]

Parameters	**Algal biomass**
Algae	*Nannochloropsis*
HHV, MJ/kg (dry basis)	20.5
Wt% (dry basis)	
C	49.27 ± 0.93
H	7.27 ± 0.12
N	6.29 ± 0.09
S	0.83 ± 0.01
O	36.34

6.2.1 HTL model development

The developed process model includes areas for hydrothermal liquefaction (HTL), hydrotreating, and hydrogen production as shown in Figure 29. The process flow simulation is developed based on material and energy balances, chemical equilibrium, and the thermodynamic properties of the system. The model is developed in a steady-state process simulator engine in Aspen Plus that simulates several pieces of equipment interlinked via mass, work, and energy streams. The input assumptions in the development of hydrothermal liquefaction for diluent production are provided in Table 26.

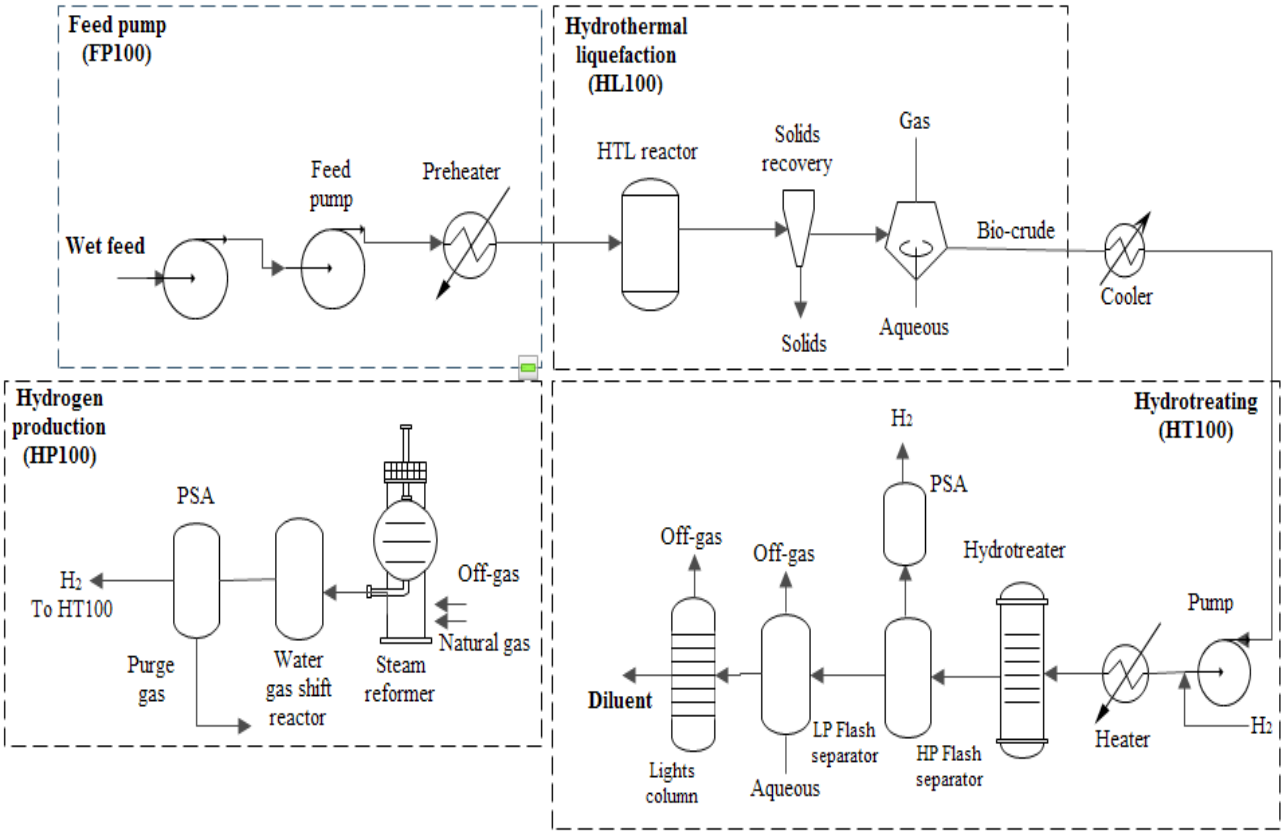

Figure 29: Process model development for an algal hydrothermal liquefaction plant

Table 26: Hydrothermal liquefaction process assumptions and properties

Algal biomass flow rate, dry tonnes/day	2000
Algal biomass % (dry w w^{-1})	20
Hydrothermal liquefaction [628]	
Temperature, ˚C	350
Pressure, MPa	20.3
HTL biocrude yield (wt%)	40.3
HTL biocrude moisture content (%)	5.52
Hydrotreating (Single-step) [638, 648]	
Temperature, ˚C	400
Pressure, psia	1500
Hydrogen production plant [567]	
H_2, g/g dry bio-oil	0.043

6.2.1.1 Hydrothermal liquefaction

The wet microalgae is initially pumped to a pressure of 18 MPa and directed through heat exchangers to achieve a temperature of 350 °C. This algal slurry is then preheated by incoming hot effluent from the HTL reactor. Under these conditions, water exists below the supercritical point and thus can dissolve most of the organics in the biomass stream. The HTL reactor is modeled through the RYield block in the process simulator. The product yield distributions for process design were obtained from a study that used GC/MS analysis and elemental balances [638]. Biocrude yields typically ranges from 35-65 wt% [647]. Brown et al. reported the highest bio-oil yield of 43 wt% for the hydrothermal liquefaction of microalga *Nannochloropsis* sp [647]. Faeth et al. reported a biocrude yield of 44 wt% for typical algal HTL [573]. Juneja et al. considered optimal conditions for HTL biocrude productivity of 37% to be 340 °C [648]. The effluent passes through the HTL reactor where the organic molecules present in the biomass are converted to biocrude. The effluent then passes through a filter where the solid residues are separated in the form of ash and disposed of [567, 640, 649]. The filtered effluent stream is recycled through a heat exchanger that allows heat recovery and preheats the incoming feed stream. The cooled effluent is further depressurized and enters a three-phase separator that separates the incoming stream into organic (biocrude), aqueous, and gaseous phases. The generated off-gases (carbon dioxide, hydrogen, and smaller molecules) are used as fuel gases in the hydrogen generation plant. The aqueous phase, which consists mainly of small polar organics including water molecules, is directed to a wastewater treatment facility [618, 646, 649]. The biocrude is hydrotreated and undergoes further deoxygenation in the presence of catalysts.

6.2.1.2 Biocrude hydrotreating

The raw biocrude obtained from HTL has high amounts of nitrogen and oxygen that needs to be reduced to meet desired product characteristics. The raw biocrude from HTL is pressurized before it comes in contact with hydrogen. The incoming stream is fed to the hydrotreating reactor, which uses a single-stage hydrotreating unit to produce stabilized biocrude. The hydrotreater is modeled through the RYield block in the process simulator. This analysis uses the product yield distribution results from experimental work by Jones et al. [638].

The resulting stream is cooled and directed to high-pressure flash units. The effluent is separated into the aqueous phase, upgraded biocrude, and off-gases. The gas phase, consisting of light hydrocarbon molecules and other gases, undergoes H_2 recovery in a pressure swing adsorption column (PSA). The organic liquid phase is passed through a low pressure flash unit to remove gaseous components present in the oil phase. The upgraded biocrude is further stabilized through a debutanizer column, which removes the light components in the biocrude. The overhead gas from debutanizer column, along with PSA off-gases, is directed to the hydrogen production plant. The aqueous waste stream is assumed to be discharged to a wastewater treatment plant [618, 646, 649]. The off-gases from the hydrotreating section are sent to the hydrogen production plant.

6.2.1.3 Hydrogen production

Hydrogen is produced through conventional steam reforming. Some of the off-gases from the process areas are used as fuel gas in the reformer burner. The rest is used in steam reforming together with superheated steam for hydrogen generation, which also uses makeup natural gas.

The steam reformer produces syngas, which is directed to a water-gas shift reactor (WGSR) to increase the amount of hydrogen. The resulting gas is cooled, and the water vapor is condensed. The cooled gas is directed to the PSA to produce highly purified hydrogen [567]. The tail gas from the PSA column is sent to the reformer burner. Steam is produced when the fuel gas is cooled in the burner and a portion of the steam is used in steam reforming.

6.2.2 Pyrolysis model development

The process model includes biomass processing, pyrolysis, hydrotreating, and hydrogen production, as shown in Figure 30. The modeling is performed in Aspen Plus using mass and energy balances. The economic analysis uses the Aspen Icarus Evaluator, which estimates equipment cost through sizing and investment analysis spreadsheet calculations. The input assumptions in the development of pyrolysis for diluent production are provided in Table 27.

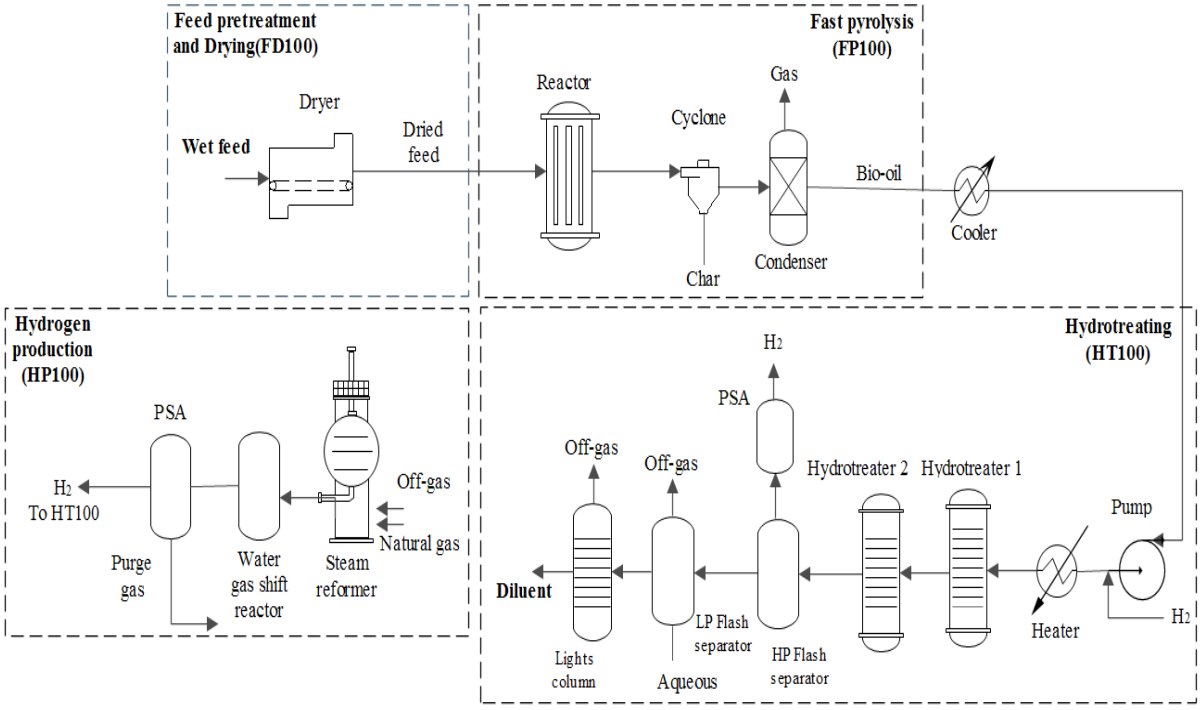

Figure 30: Process model development for an algal pyrolysis plant

6.2.2.1 Feedstock preparation

To avoid an energy penalty, algal biomass must be pre-conditioned before it is passed through the pyrolyzer to avoid energy penalty. Without pre-conditioning, the yield will decrease, thereby increasing the heat requirements [650]. Feedstock drying is the key for thermochemical processes like pyrolysis because the presence of moisture in biomass entails more heat. Algal biomass is dried to a moisture content of <10% in order to reduce the water content in the resulting fast pyrolysis bio-oil product [650].

Table 27: Pyrolysis process assumptions and properties

Items	Values
Biomass flow rate, dry tonnes/day	2000
Algal biomass % (dry w w^{-1})	20
Pyrolysis [627]	
Temperature, ˚C	500
Pressure, MPa	0.102
Hydrogen production plant	
H_2, g/g dry bio-oil	0.043

6.2.2.2 Fast pyrolysis

Fast pyrolysis of algal biomass allows the rapid transfer of heat at a considerably low residence time. The dried algal biomass from the feed pretreatment area is sent to a circulating fluidized pyrolysis reactor at 520 °C. Sand acts as the fluidization medium during the process run and the reaction time is <1 s. Following pyrolysis, solid (biochar) particles are removed by cyclones entrained in effluents. The resulting pyrolytic bio-oil is recovered through the condensation of vapors. The bio-oil product yield distribution for algal pyrolysis is obtained from an experimental study [651]. A typical oil product yield from fast pyrolysis ranges from 55-65 wt% [652]. The non-condensable gases, consisting of methane and other gases, are directed to the hydrogen production plant for hydrogen production for hydrotreating purposes.

6.2.2.3 Bio-oil hydrotreating

Hydrotreating, an exothermic reaction process, is used in the oil and gas industry for the selective removal of oxygen, nitrogen, and sulphur [653]. Traditionally, algal bio-oils have high amounts of nitrogenous compounds. Nitrogen removal presents challenges during bio-oil upgrading that contribute significantly to upgrading costs [555]. Bio-oil from the pyrolysis reactor is hydrotreated in the presence of hydrogen in a two-step process. The first step involves mild hydrotreatment in a catalytic reactor to stabilize the pyrolytic bio-oil using cobalt molybdenum (CoMo) [654]. The resulting liquid product passes through a two-step hydrotreater operating at a lower space velocity and higher temperature than the first stage; this hydrotreater also uses CoMo. The second-step product is separated into organic liquid products, wastewater, and off-gases. The off-gases from the hydrotreating units are directed to the pressure swing adsorption, which allows hydrogen recovery. The PSA tail gas, consisting of light hydrocarbons and other gases, is passed to the hydrogen plant for hydrogen generation. The resulting aqueous phase is discharged through wastewater treatment.

6.2.2.4 Hydrogen production

The hydrogen plant in the pyrolysis facility is same as that in the HTL plant. The off-gases from all processing areas are employed as fuel gas. The hydrogen is produced through conventional

steam reforming, which uses a series of water-gas shift reactors and a PSA column to produce the required hydrogen for hydrotreating.

6.2.3 Techno-economic asessment

The developed process model uses HTL and pyrolysis pathways for economic analysis, and the Aspen Icarus Evaluator then maps and sizes the unit equipment. The techno-economic assessment considers an n^{th} plant scenario, which means that the process is mature and commercially available. Based on the total purchased equipment cost (TPEC) estimates, the total project investment (TPI) was obtained with the factors laid out by Peters et al. [655]. The total installed cost (TIC) was evaluated by multiplying the TPEC by an installation factor. The parameters used to estimate the TPI from the TPEC are provided in Table 28. The capital cost distribution and production plant capacity factors were obtained from Shahrukh et al. and Agbor et al. relevant to a biomass handing plant [656, 657]. A 10% contingency factor was considered in order to cover unexpected expenses at the project startup [658, 659]. The annual operating costs are divided into both fixed and variable costs. The variable costs are the costs for raw materials, catalysts, and utilities. A price of 100 /tonne is considered as a revenue for biochar obtained from pyrolysis [660]. The biomass feedstock cost was obtained from a study by Davis et al. [639]. The price of electricity was taken from the literature [661, 641] and catalyst prices were obtained from a study by Zhu et al. [572]. The fixed costs are the labor and maintenance costs. Alberta-specific wage rates were applied for labor and supervision [662, 698]. The product value was estimated through the DCFROR analysis. An inflation rate of 2% was assumed for the analysis. Table 29 shows the lists of economic assumptions used in the study of thermochemical technologies for diluent production.

Table 28: Plant capital cost calculation factors

Project investment cost factor estimates	
Installation factor	3.02
Total installed cost (TIC)	302% of TPEC
Indirect cost (IC)	89% of TPEC
Total direct and indirect costs (TDIC)	TIC + IC
Contingency	10% of TDIC
Fixed capital investment (FCI)	TDIC + contingency
Location cost	5% of FCI
Total project investment (TPI)	FCI + location cost

Table 29: Economic analysis assumptions

Items	Values
Plant life (yr)	20
Cost year	2016
Capital cost distribution [656, 657]	
Year 1 (%)	20
Year 2 (%)	35
Year 3 (%)	45
Production plant capacity factor	
Year 1	0.7
Year 2	0.8
Year 3 and beyond	0.85
Internal rate of return (%)	10
Maintenance cost ($)	3% of TPI
Operating charges ($)	25% of operating labor cost
Plant overhead ($)	50% of operating, labor, and maintenance costs combined
Subtotal operating cost, SOC ($)	Sum of all operating costs including raw material and utility costs
G & A cost ($)	8% of SOC
Solid disposal cost ($/tonne) [572]	41.91
Wastewater disposal cost ($/tonne) [640]	0.76
Stream factor (%) [572]	90

6.2.4 Sensitivity and uncertainty study

During plant operation, process parameters may vary. Hence, a sensitivity analysis was conducted to study the effects of changes in parameters on product value. The product value was estimated by varying a parameter by ±20%. Varying one parameter at a time would help in understanding the effects of individual parameters; however, in reality, many parameters are likely to change at the same time, the effects of which were studied through a Monte Carlo simulation using 10,000 iterations. This approach was used to determine the product value based on probability distribution in the process design.

6.3 Results and discussion

6.3.1 Techno-economic assessment

The process economics for hydrothermal liquefaction and pyrolysis takes into account biomass costs, capital cost, and process operating costs. These costs are then applied in a discounted cash flow of return analysis to estimate the product value of the diluent at a net present value of zero using a rate of return of 10%. The cost analysis was carried out for a plant capacity of 2000 dry tonnes/day.

6.3.1.1 Cost estimates

A 2000 dry tonnes/day algal HTL plant has a TPEC of 111.5 M$ and an FCI of 479.5 M$, which is considerably higher than a pyrolysis plant using the same quantity of feedstock, as shown in Table 30. A similar cost estimate was obtained for thermochemical platforms in a study by Ou et al. [649].

Table 30: Cost estimates for hydrothermal liquefaction and pyrolysis plant facilities

	Hydrothermal liquefaction	Pyrolysis
Total purchased equipment cost (M $)	111.5	85.1
Total project investment (M $)	503.5	384.6
Operating cost (M $)	356.1	397.2
Production cost ($/L)	1.60	1.69

The breakdown of cost estimates for hydrothermal liquefaction and pyrolysis is shown in Figure 31. The hydrothermal liquefaction costs were estimated at 70.7 M$, which is 63.4% of the total purchased equipment cost. Similar cost estimates, in the range of 64.3-75 M$, were reported in hydrothermal liquefaction studies for a 2000 dry tonnes/day plant [640, 663]. Estimated hydrotreating costs are 16.5 M$, or 14.8% of the total purchased equipment cost, and a hydrogen production plant costs 20.4 M$ or 18.3% of the TPEC. The highest cost is the capital cost of the hydrothermal liquefaction unit because of the shell and tube reactor design, which allows the unit to operate at elevated temperature and pressure compared to other processing areas of the HTL plant [649]. The capital cost estimates for a plant capacity of 2000 dry tonnes/day for algal pyrolysis are shown in Figure 31. The fast pyrolysis equipment cost estimate is 33.9 M$, or 33.9% of the overall purchased equipment cost. This cost estimate is within the range of values reported in the literature [640, 664]. The hydrotreating and hydrogen plant equipment costs ae 26.60% and 28.93% of equipment costs, at 22.6 M$ and 24.6 M$, respectively.

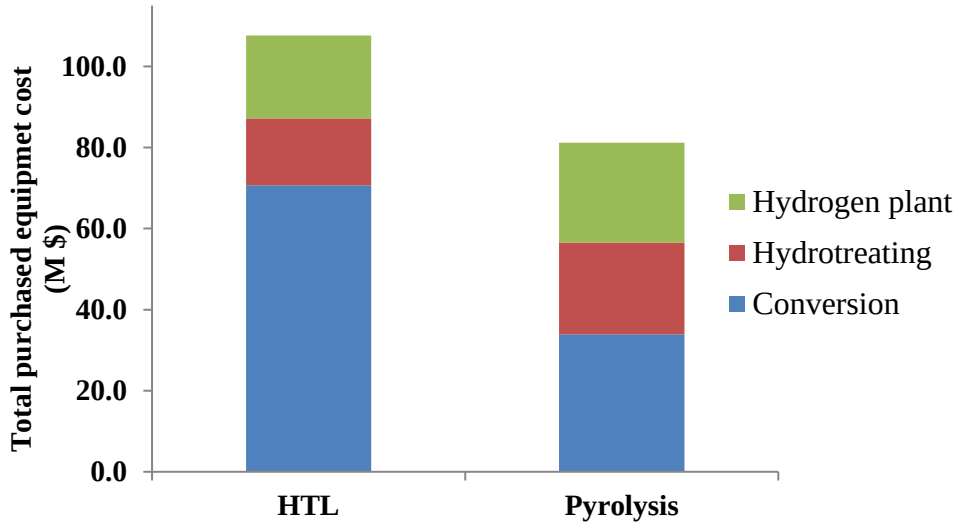

Figure 31: Total purchased equipment cost for hydrothermal liquefaction and pyrolysis plant facilities

Based on the results, the HTL process capital investment is higher than that of fast pyrolysis, as also reported previously [663]. Also, the capital cost of hydrotreating for HTL is lower than that for a fast pyrolysis plant. This is in agreement with previous studies on hydrothermal liquefaction and fast pyrolysis [640, 663]. It is obvious that the process differences in the two thermochemical processes have significant differences in economics.

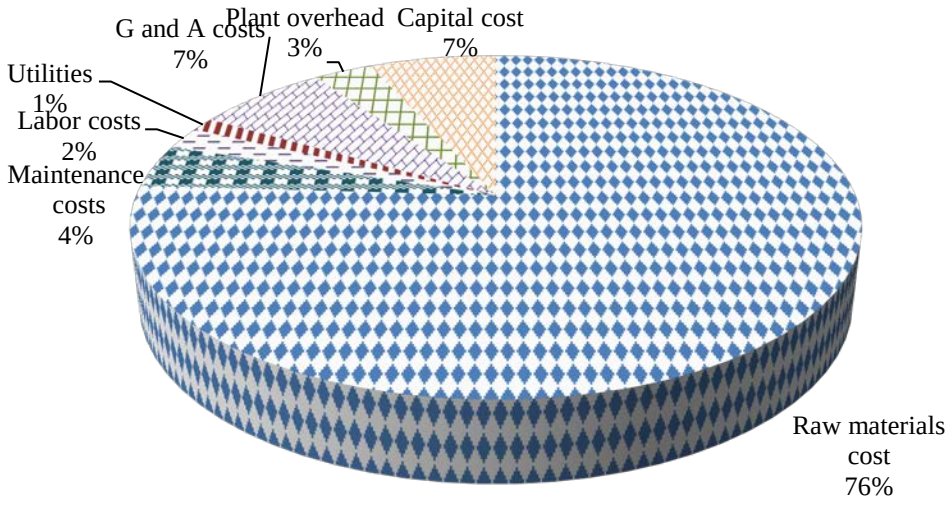

(a)

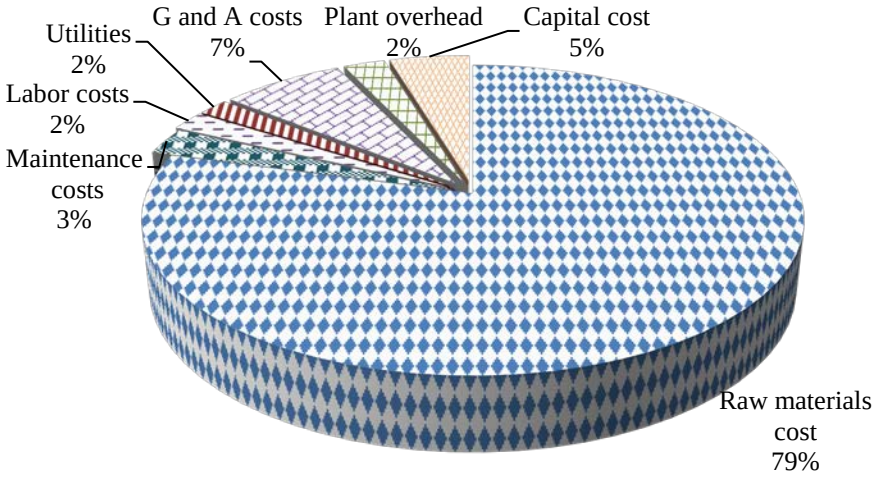

(b)

Figure 32: Breakdown of operating costs for (a) HTL plant facility and (b) pyrolysis plant facility

The breakdown of operating costs for HTL and pyrolysis plants is shown in Figure 32. The annual plant operating cost includes raw materials, labor, maintenance, overhead, and utilities as well as general and administrative charges, for both plant configurations. The raw material cost makes up most of the operating costs. This estimate is in accordance with a previous study by Jones et al.,

who provided a design case for continuous HTL and subsequent catalytic hydrotreating of whole algae, with biomass constituting 74% of the product cost [638].

Figure 33 shows the parameter cost breakdown of the product value of diluent from HTL and pyrolysis. The raw material accounts for a significant portion to the product value of diluent, which is attributed in this study to the higher cost of biomass.

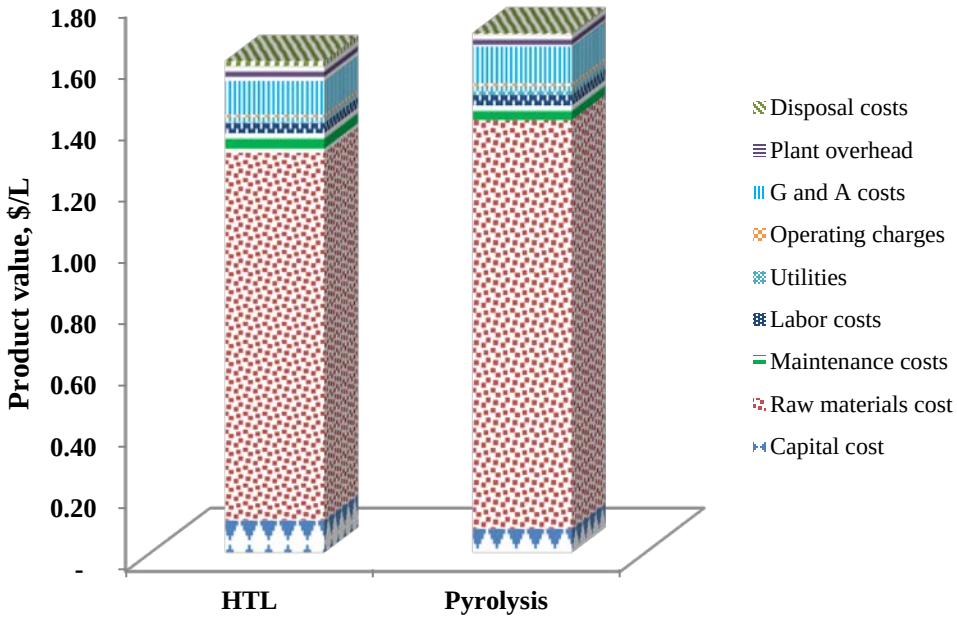

Figure 33: Contribution of HTL and pyrolysis operating costs to the product value of diluent

6.3.1.2 Cost comparison with previous studies

We performed a techno-economic analysis for a proposed plant in western Canada. There are a few studies on algal-based thermochemical pathways with a focus on producing transportation fuels, and cost estimates vary considerably. Lundquist et al. estimated the value of algal-based products up to 2.09 $/L [665]. Other studies reported cost estimates in the range 0.88-24.60 $/L [662]. The differences in costs are due to differences in algal processing costs. This study obtained a product value of 1.60 $/L for diluent from algal hydrothermal liquefaction. Product values for hydrothermal liquefaction products (biocrude) vary in the literature from approximately 1.39 to 2.72 $/L for different algal feedstocks [230, 638, 648, 666]. Orfield et al. studied an algal bio-refinery concept using hydrothermal liquefaction and reported an algal oil cost of 1.64 $/L [666]. Another HTL study on microalgae using different cultivation systems showed product costs of 1.66-2.20 $/L for biomass costs of 510 to 673 $/tonne [667]. Hence, the product value obtained in this analysis for hydrothermal liquefaction for diluent production is in accordance with previously reported studies.

For a pyrolysis plant, a product value of 1.69 $/L is estimated for a processing plant capacity at 2000 dry tonnes/day. The product value from a study by Thilakaratne et al. for a pyrolysis plant facility ranges from approximately 1.65-1.98 $/L for algal feedstocks [555]. Thus, the product value obtained in this analysis is in good accordance with values reported in another study. In general, literature studies show a minimum fuel selling price of pyrolysis bio-oil from different feedstocks in the wide range of 0.53-2.11 $/L, which could be due to different system configurations, assumptions in parameters, and process inconsistencies owing to market uncertainties [650, 668-671].

The product value obtained in this analysis for pyrolysis is higher than for HTL, as also reported by Tews et al. [640]. The same authors compared the hydrothermal liquefaction and pyrolysis of forest residue and obtained the higher bio-oil product value of 3.09 $/gallon gasoline equivalent for pyrolysis compared to 2.0 $/gallon gasoline equivalent for hydrothermal liquefaction at a processing capacity of 2000 dry tonnes/day [640]. de Jong et al. studied the economic feasibility of HTL and pyrolysis for renewable jet fuel production and found that the product price was lower for HTL than for pyrolysis [672].

Instead of using raw microalgae as a feedstock, defatted microalgae (a by-product of biodiesel through lipid extraction) can be used as investigated in a study by Ou et al. [649]. The elemental composition of this feedstock is known to show similarities with raw microalgae, other than lower carbon and higher nitrogen levels [649]. Hence, the lower cost of this biomass feedstock has advantages as feedstock for both HTL and pyrolysis. The cost of diluent obtained from crude oil distillation is 0.7 $/L [673]. On comparison, the cost of diluent production through current technological platforms does not compete. Hence, a robust system with special focus on reducing algal costs and increasing product yield would offer significant benefits.

6.3.1.3 Plant capacity

The effects on the product value of diluent with changes in plant capacity are shown in Figure 34. The figure shows the unique behavior of diluent's product value, which falls rapidly at plant capacities of 500-3000 dry tonnes/day. In hydrothermal liquefaction, the product value of diluent falls from approximately 1.82 to 1.56 $/L when plant capacity is changes from 500-3000 dry tonnes/day. For pyrolysis, the product value falls from roughly 1.94 $/L at a capacity of 500 dry tonnes/day to 1.65 $/L at a capacity of 4000 dry tonnes/day. A similar trend for the production of pyrolysis oil from switchgrass was observed by Lerkkasemsan and Achenie [674]. With increasing plant capacity, the curve flattens, signifying that the reduction in cost is minimal. Hence, as plant capacity increases, the product value decreases, however, its feasibility depends on the amount of algae that can be produced. This trend has also been observed for algae-derived diesel [675]. The key factor affecting plant size is biomass availability. Thus, biomass plant facilities are developed at a small scale [676]. Larger plants require several equipment units to run the process [640]. Despite the economic benefits from large-scale thermochemical systems, large continuous-scale systems for diluent production have not yet been demonstrated, and there are issues in achieving heat transfer to the reactors [677].

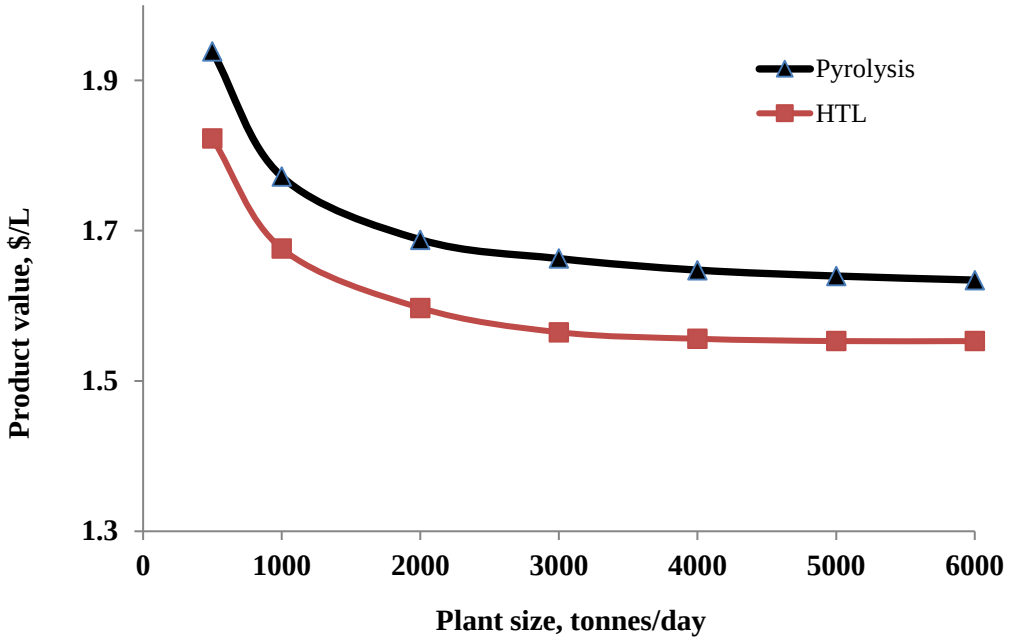

Figure 34: Plant capacity profile showing changes in product value when plant size is varied for (a) hydrothermal liquefaction and (b) pyrolysis

6.3.1.4 Influence of biochar from pyrolysis as a revenue or heating source

If biochar from fast pyrolysis is regarded as a selling product, the revenue depends on the selling price. The biochar selling price was varied from 0-500 $/tonne [660]. Diluent cost is sensitive to biochar price, as shown in Figure 35.

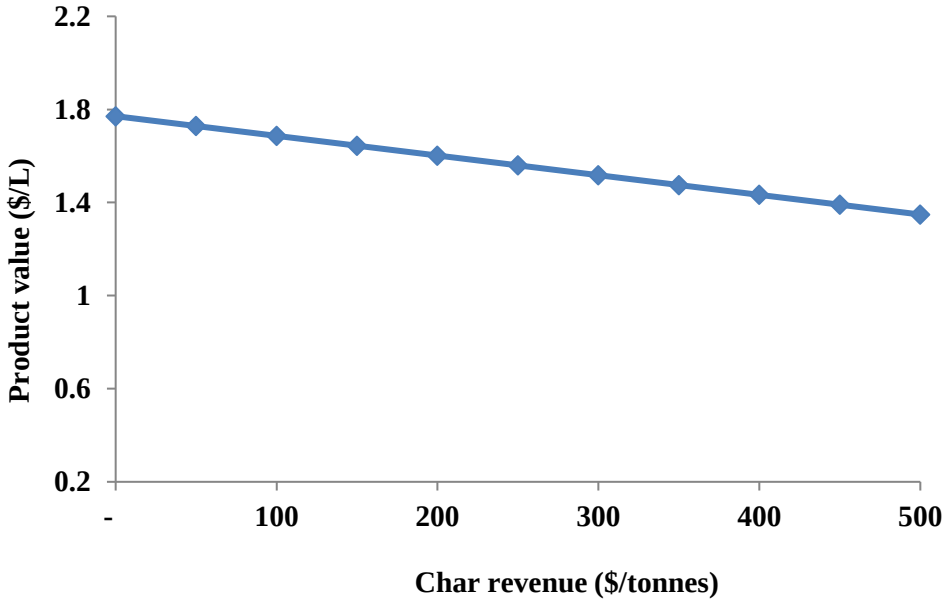

Figure 35: Change in product value of diluent with changes in char revenue in fast pyrolysis

The product value of diluent in this study can be further reduced by combusting biochar. The energy obtained from biochar can be used to obtain sufficient energy for algal biomass drying and heat supply to the pyrolysis reactor [678]. The use of biochar as an energy source in the system has a product value at 1.67 $/L. Such a process is advantageous, however, offers challenge in terms of process integration and has safety issues [678, 679].

6.3.2 Sensitivity analysis

Variations in economic parameters in the operation of a thermochemical facility are assessed in a techno-economic analysis through sensitivity analysis. It assessed the impact of economic parameters on the product value of the diluent for both thermochemical pathways. The results of the sensitivity analysis are shown in Figure 36. The results were determined by considering a range of ±20% for the parameters studied [555]. It is obvious that algal diluent yield has the highest impact on the product value followed by algal biomass cost for both thermochemical platforms. The factors influencing product yield include phase separation efficiency, and the yield will decrease if there is a considerable loss of organics to the aqueous phase during the phase separation. Other factors influencing the yield include the nature of the algae, solid content in feed, process operating conditions, and upgrading methods [638]. The reduced biocrude/bio-oil yield lowers the diluent yield due to organics loss to the aqueous phase. Hence, final product yields are affected by yields from biocrude and upgrading as well as separation efficiencies [649]. A variation of ±20% in product yield for HTL leads to product value ranging of 1.33-1.99 $/L. With a decrease in product yield to 80% from the base case, the product value increases by about 24%. A fluctuation of ±20% in yield also has the highest impact on the product value for pyrolysis. An increase in diluent yield by 20% reduces the product value to 1.41 $/L. Brown et al. also determined product yield from pyrolysis to be the most influential parameter [669]. This finding necessitates improved technologies to reduce product yield losses during the process run.

The second most influencing parameter in both thermochemical platforms is algal biomass cost. Microalgae cost depends on growth, cultivation, and harvesting costs. There are uncertainties in the cost estimates with current thermochemical technologies. The production costs of raw algal biomass could reach 3000 $/tonne, which could considerably influence the product value of diluent [8]. Thilakaratne et al. considered algal biomass costs of 0.35-7.32 $/kg; this range is due to the differences in cultivation, the nature of the strain, and extraction techniques, as well as facility location [555]. A 20% increase in biomass cost increases the product value of diluent from both HTL and pyrolysis by roughly 14%. This means that there is a need to develop robust methods for algal cultivation and harvesting technologies and make more effort to determine the market competitiveness of algae.

Algal thermochemical technology development is still at the nascent stage and hence there are uncertainties in capital cost estimates. A 20% increase in the IRR and total capital investment for HTL increases the product value by approximately 3% and 2.5%, respectively. The capital costs are the highest for HTL algal processing technology. Algal processing may be optimized by lowering temperature and residence time, which will reduce the capital costs of the high-pressure equipment used for HTL processing. Research and development efforts could look for alternatives to assess the feasibility of HTL systems to further lower costs. For pyrolysis, a 20% increase in IRR and total capital investment increases the product value by roughly 2% and 1.7%, respectively.

The catalyst cost depends on catalyst type, space velocities, lifetime, and price. The other parameters have less impact on the overall product value of diluent for both thermochemical plant configurations.

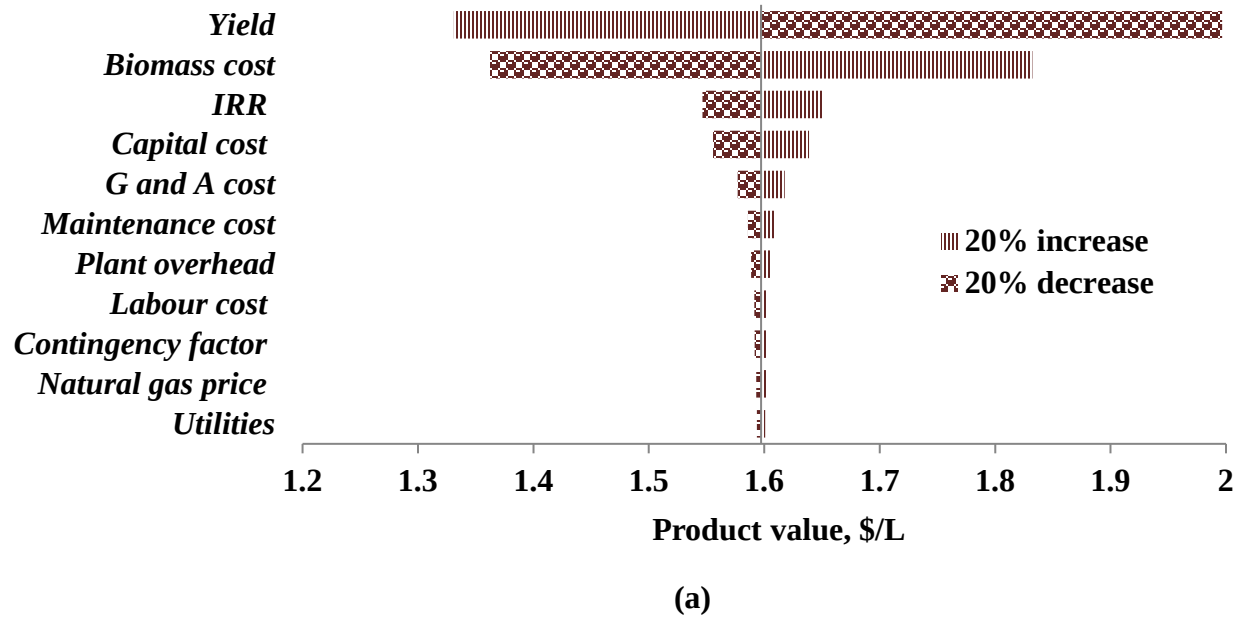

(a)

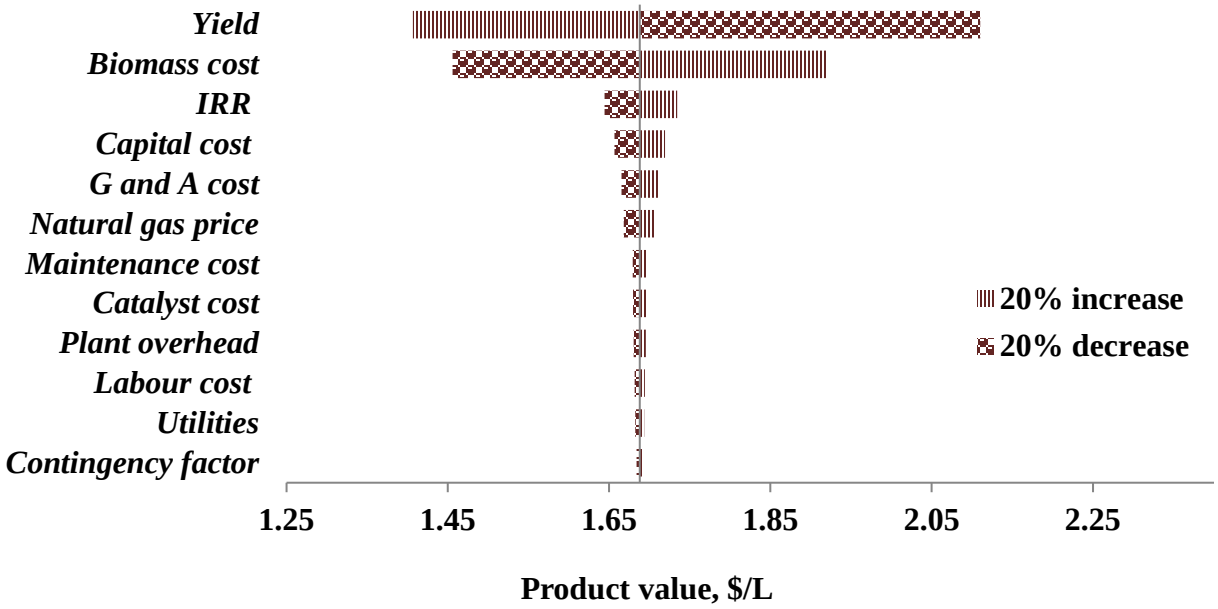

(b)

Figure 36: Sensitivity analysis results for factors influencing the product value of (a) hydrothermal liquefaction and (b) pyrolysis

6.3.3 Uncertainty analysis

The lack of data and knowledge of advanced thermochemical processes such as HTL and pyrolysis may result in uncertainties in cost estimation. The sensitivity analysis determined the effects of changing a single parameter on the product value at a given time. For the uncertainty analysis, a Monte Carlo simulation was performed for a 2000 dry tonnes/day algal thermochemical plant. ModelRisk software was used and 10,000 iterations were run involving random values from all given parameters that impact the product value. The uncertainty analysis uses all costs including raw material, capital, labor, maintenance, operating charges, general and administrative charges, utilities, plant overhead, and disposal costs. Uncertainties in the range of 80-125% were considered on the cost parameters. The product values from the uncertainty analysis for both thermochemical pathways are shown in Figure 37. The simulations for hydrothermal liquefaction and pyrolysis for algal biomass result in product values of 1.60 ± 0.09 $/L and 1.69 ± 0.11 $/L, respectively, at 95% confidence.

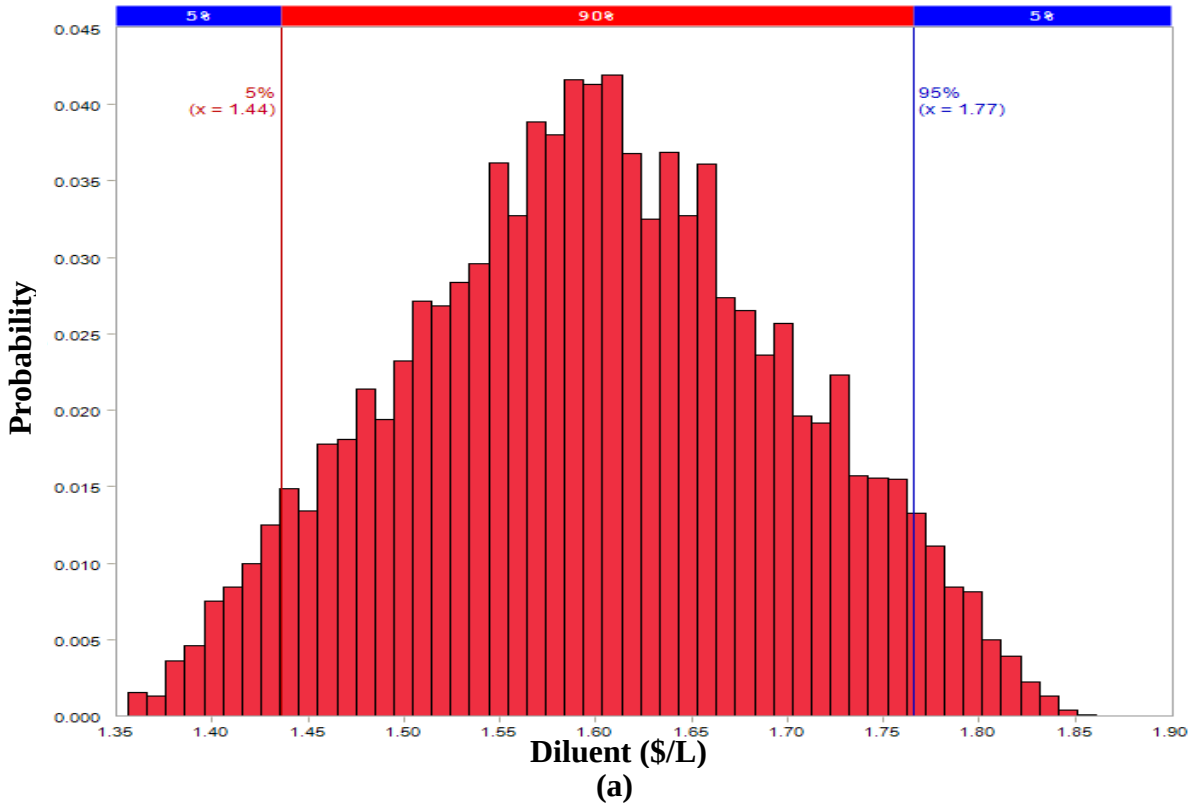

(a)

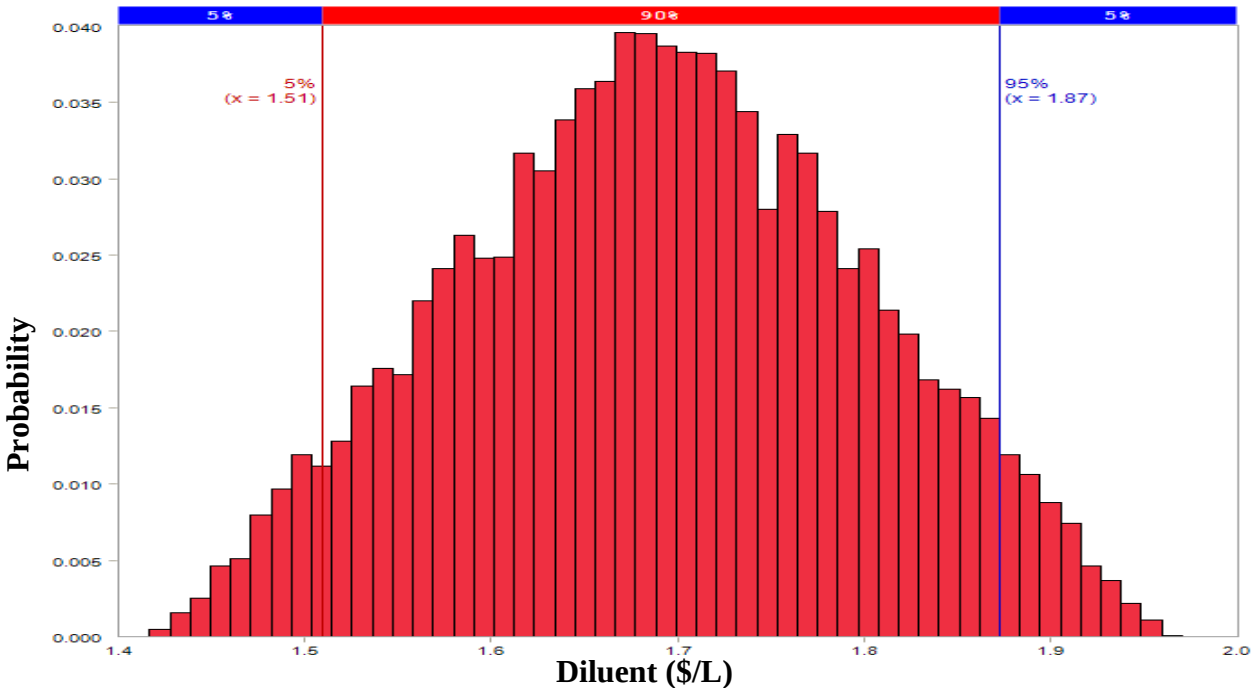

(b)

Figure 37: Uncertainty analyses for diluent production through (a) hydrothermal liquefaction and (b) pyrolysis

6.4 Key perspectives

HTL is a high-pressure technology, whereas fast pyrolysis is a low-pressure process [663]. Testing the application of the thermochemical liquid products obtained from algal-sourced biomass is limited, as previous studies have focused mostly on lignocellulosic biomass. For hydrothermal liquefaction, woody bio-oils show boiler firing efficiency analogous to petroleum distillates [680]. Though HTL has shown promise at the bench scale, it still faces challenges due to high capital costs and pumping difficulties [681]. Nonetheless, HTL systems have been demonstrated at the pilot scale, and they have yet to be developed commercially [663]. Upgrading HTL biocrude likewise has yet to be demonstrated [663]. A few techno-economic studies have been done to investigate the feasibility of HTL developments [572, 640, 663].

Pyrolysis, on the other hand, has been widely tested on a small scale at both pilot and commercial levels using lignocellulosic biomass [682]. Scale-up has also been performed using flash and fast pyrolysis to improve bio-oil yield and reduce char production [646]. Other techno-economic studies have demonstrated the potential of energy recovery and bio-oil processing from waste biomass via pyrolysis [681]. With such fast pyrolysis commercial systems being made available, fast pyrolysis bio-oil upgrading has been successfully achieved at lab or an engineering scale.

Additional research and development is required to fully understand the potential of thermochemical platforms. In both cases, liquid product properties need to be improved through improvements in HTL upgrading, catalyst stability, and product quality [630, 663]. Improvements in catalysis design to attain high performance and lifetimes will ameliorate process developments [654]. As a hydrogen production plant adds to capital costs, co-locating the conversion plant and hydrotreating system with an existing refinery would allow process off-gases to be used in the refinery for hydrogen production, thereby lowering thermochemical system costs [663]. Zhu et al. showed that the integration of a refinery with a hydrothermal liquefaction plant or a pyrolysis system could reduce the final product value by about 25% or 15%, respectively [663]. However, final product specifications need to be determined to illustrate this integration with an oil refinery. Detailed characterizations of crude and upgraded products in terms of densities, compound nature and types, boiling point curves, and acid number require investigation. For thermochemical systems such as HTL, it is also imperative to identify reactor limitations with respect to heat transfer and corrosion. For pyrolysis, reducing preprocessing steps will lower costs [654].

In order to make the process economically attractive, non-technological data such as carbon tax, premium, and royalty are required. Research efforts should involve optimizing the process model together with supplementing non-technological mechanisms to support technological development.

6.5 Conclusions

A techno-economic study on microalgae-to-diluent production via two thermochemical plant configurations, namely HTL and pyrolysis, was conducted. Microalga-based diluents are technologically feasible; however, costs need to be lowered to make diluent cost competitive. HTL has been explored in continuous-process reactors at high concentrations of algae. HTL biocrude is regarded as having lower oxygen content than algal pyrolysis biocrude. In terms of the technological aspects, this study showed that algal-based HTL is a promising pathway with respect to product quality. However, HTL is still at its nascent stage of development, whereas pyrolysis is

a mature and industrialized technology. The choice and specificity of biomass present major problems and prospects for both pathways. Microalga is a potential biomass feedstock for the production of diluents in both thermochemical routes.

A process outline for assessing the viability of commercializing advanced thermochemical processes was presented. The modeling and cost results provided useful insights into the development of large-scale development approaches. In the future, with burgeoning industrial demands for products from biomass, algae show a great promise for diluent production for oil sands industrial applications.

7 A Comparative Analysis of Hydrogen Production from the Thermochemical Conversion of Algal Biomass

Hydrogen is considered a potential energy resource, and biomass, because it is renewable, is emerging as a vital energy source. The purpose of this section is to perform a techno-economic assessment of large-scale hydrogen production from algal biomass. The specific objectives are:

- To develop a detailed techno-economic model to evaluate the product value ($/kg) of hydrogen derived from microalgae using thermal gasification and supercritical gasification;
- To determine the hydrogen product value with respect to plant capacity;
- To conduct sensitivity and uncertainty analyses of several cost parameters that influences the product value.

The results will provide key insights into the techno-economic feasibility of producing hydrogen from high moisture containing feedstocks such as microalgae.

7.1 Thermal gasification

Microalgal biomass is seen as a promising candidate for biofuel production as a future energy source. Thermal gasification, a known thermochemical method, occurs at a temperature of 800-1000 °C and involves partial oxidation of biomass in the presence of gasifying agents such as steam, oxygen, and air [683, 684]. The syngas thus produced is a mixture of H_2, CH_4, CO_2, and CO. In general, gasification is suitable for biomass with a moisture content <15%. There are several studies on the gasification of biomass [685-688] but only a few that focus on microalgae [689, 690]. Microalgae require drying because high moisture content materials reduce gasifier efficiency and syngas energy content. A study based on biomass-based integrated gasification combined cycle showed that a moisture content of less than 10 wt% is required to achieve high temperatures during gasification, thus improving energy efficiency [691]. The gasifier used for microalgal conversion is a vertical fluidized bed. However, such reactors pose challenges in terms of scalability and ensuing carbon loss, so they are commercially infeasible [692, 693]. A horizontal bed reactor improves heat transfer by allowing significant contact time, which can reduce the char formation. This reactor design is simple and easy to operate and can improve carbon conversion [694]. Using air as a gasifying agent is more advantageous than other known gasifying agents such as pure oxygen and steam that make the process long, expensive, and complex.

There are very few studies on algal thermal gasification for biofuel production. Hirano et al. studied the gasification of *Spirulina* at 850-1000 °C into syngas that consisted of H_2, CO_2, CO, and CH_4 [695]. Their study showed that temperature has a key role in increasing hydrogen and carbon conversion efficiency. A study by Minowa et al. involving the gasification of *C. vulgaris* at 350 °C in the presence of a Ni-catalyst was aimed at producing higher levels of CH_4 than H_2; the study showed the significance of catalysts for higher carbon conversion efficiency [632]. Raheem et al. studied air gasification of *Chlorella vulgaris* in a horizontal tube configuration and reported 950 °C as an optimal temperature [696].

7.2 Supercritical water gasification

The unique properties of supercritical water are the basis of supercritical water gasification technology. Beyond the critical point (374 °C, 22.1 MPa), water shows different properties than at ambient conditions [697]. Supercritical water has a smaller dielectric constant than water at ambient conditions. Consequently, supercritical water behaves like an organic solvent, thereby improving the solubility of organics and preventing the formation of byproducts such as tar and char. In addition, the chemical reactions occur in a single fluid medium that would otherwise happen in a multiphase environment under normal conditions [698]. Supercritical water has high reactivity, which further increases the hydrogen yield. Some of the advantages of the SCWG process are: biomass does not need drying (in fact, water acts as a high reactive medium for SCWG); high hydrogen and considerably low carbon monoxide yields are achieved; the unique properties of supercritical water often result in less tar and char formation.

The experimental setup had a liquefaction step to precipitate the insoluble organics to prevent problems in the feed line. Amos [699] estimated the costs of hydrogen production for starch waste (15 wt% dry matter) at a throughput of 7500 kg/h (wet basis). The costs did not include the feed supply lines, and the gas cleaning was done through membrane technology, which made up >35% of the purchased equipment costs. Another study performed a similar cost estimate for water hyacinths (5 wt% dry matter) at a throughput of 42.67 kg/h [569]. The gas cleaning approach involved a CO_2 absorber with water as the scrubbing medium. The investment costs consisted mainly of bulk plant components, and costs related to engineering, assembly, etc., were not incorporated. Gasafi et al. studied the economics of the SCWG of sewage sludge (20 wt% dry matter) for hydrogen production at a throughput of 5 t/h and found that SCWG could be competitive if the revenues associated with the sewage sludge disposal as a waste product were considered [570]. The study lacked the information on what scale the plant could be commercially built to produce hydrogen via supercritical water gasification. Recently, Mosuli et al. studied the economics of producing renewable hydrogen from glucose (15 and 25 wt%) and sewage sludge (15 wt%) [571]. These studies show the potential of SCWG for hydrogen production from a range of high moisture feedstocks. However, the techno-economics of algae produced through SCWG has not been studied.

7.3 Methods

An understanding of the techno-economics of hydrogen production from algal biomass requires an analysis of the mass and energy flows of the different unit operations in the plant design. The techno-economic assessment was done through development of process models using Aspen Plus Simulator to estimate the product value of hydrogen [700]. The analysis considers a base plant capacity of 2000 tonnes/day of dry algal biomass feedstock for hydrogen production through thermochemical technologies, based on studies at large scale [701, 702]. The thermochemical plants have the infrastructure to take in biomass as it is produced, and the production and conversion facilities are co-located [702].

7.3.1 Process model description

The development of a process model for producing hydrogen via thermal gasification and supercritical gasification is discussed in this section.

7.3.1.1 Gasification

Algal thermal gasification consists of drying, pyrolysis, and gas cleanup, as shown in Figure 38. Drying occurs at a temperature range of 0-150 °C, which is aimed at improving the product's calorific value. The dried biomass is subjected to a temperature of 500 °C; this produces syngas comprising H_2, CH_4, and CO. For the purpose of gasification, a fluidized bed gasifier is suitable as it provides enhanced mass and heat transfer and a high heating value, resulting in high efficiency [703]. The water-gas shift reaction enriches H_2 yield by using CO and H_2O to form H_2 and CO_2. The syngas undergoes gas treatment, that is, the gas is cleaned and sulphur is removed. The conversion of microalgae to syngas involves gasification reactions, that is, the water-gas shift reaction, methanation, and the Boudouard reaction [703].

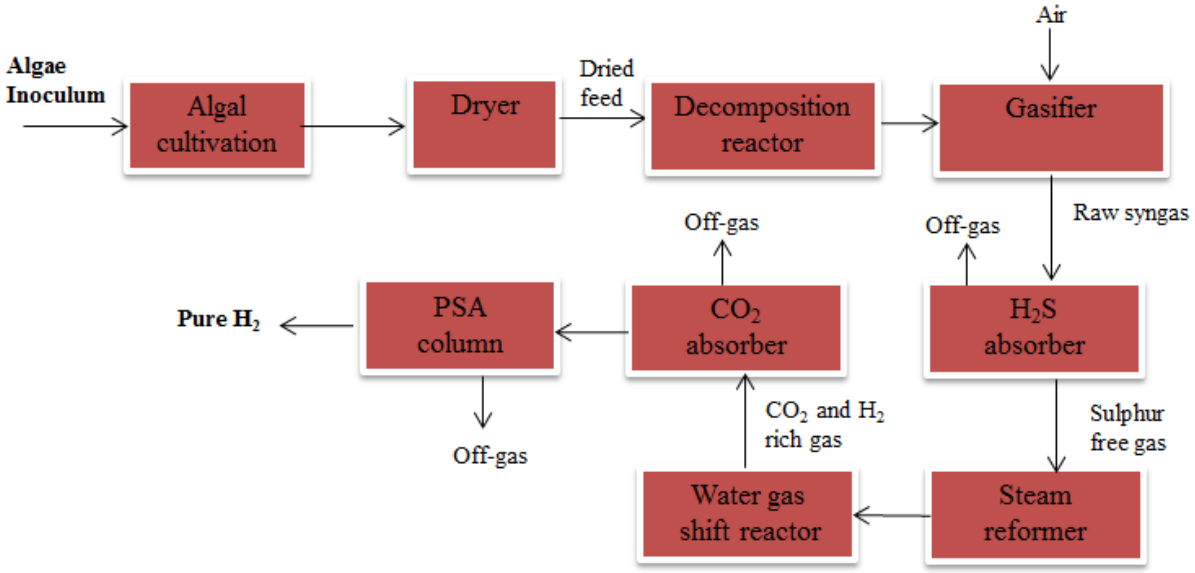

Figure 38: Block diagram for thermal gasification pathway for hydrogen production

7.3.1.2 Supercritical water gasification (SCWG)

The simplified flowsheet (shown in Figure 39) includes the following major unit operations: feed preparation, supercritical water gasification of wet biomass to syngas, and purification of syngas into hydrogen. The modeled reactor system has a pre-hydrolysis reactor, a pseudo-critical minerals separator, and a supercritical water gasification reactor. The pressurized feed initially passes through the pre-hydrolysis reactor where the non-conventional components of biomass are broken down. This is followed by a minerals separator step at the pseudo-critical point of ~ 380 ˚C to remove salts, whose presence would cause plugging and clogging downstream. The resulting stream is directed to the supercritical water reactor, which operates at 600 ˚C. The sulphur in the biomass is captured in the form of H_2S in an absorption column by using Selexol (dimethyl ether of polyethylene glycol). The sulphur-free gas is allowed to pass through reactors, i.e., a steam reforming reactor with high and low temperature water-gas shift reactors (WGSRs). CO_2 is further removed through its absorption with Selexol. Once the CO_2 has been removed, the H_2-rich product

gas passes through pressure swing adsorption (PSA). The process model has been described in detail by the authors in an earlier paper [704].

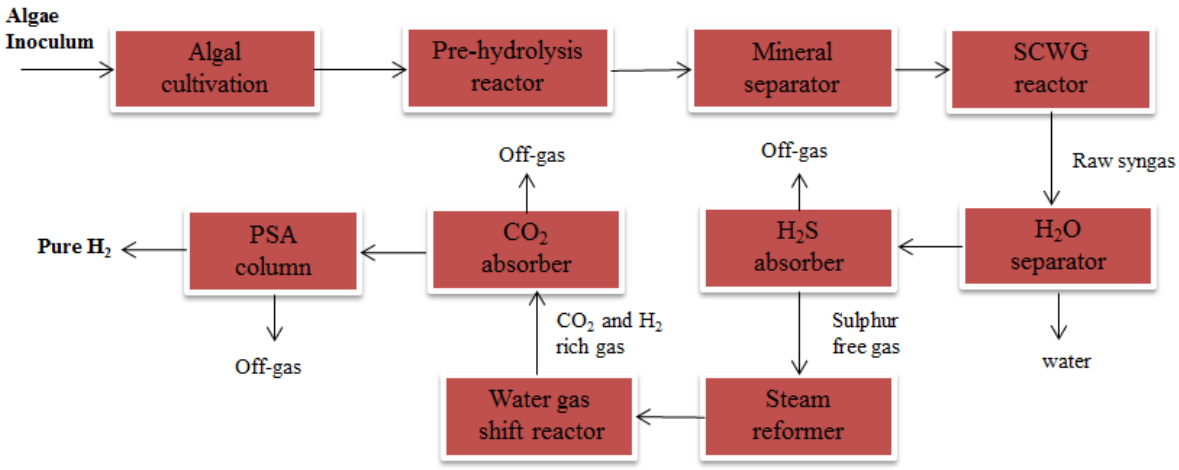

Figure 39: Block diagram for supercritical water gasification pathway for hydrogen production

7.3.2 Techno-economic assessment

The techno-economic assessment determines the product value (PV) using the plant's capital and operating costs. In this analysis, the life of the plant is assumed to be 20 years. The Aspen Icarus Process Evaluator is used to calculate the total purchased equipment costs, which are used to determine the product value through a discounted cash flow rate of return (DCFROR) analysis. Following process model development, the unit equipment is mapped and capital costs are obtained. Based on total project capital investment, the fuel product value at a net present value of zero is determined.

7.3.2.1 Capital cost estimate

The total capital cost is obtained by combining individual purchased equipment costs with installation factors and indirect costs. The indirect costs include engineering, construction, and contingency costs. The simulation results are used for economic analysis. The process model is used to map unit operations, which are sized to determine overall costs. An installation factor, which includes electrical, piping, and other installations, is needed for the total purchased equipment costs. The installation factors obtained from the process model are usually lower than the standard factors as suggested by Peters et al. [655]. Hence, an installation factor of 3.02 is considered more suitable for solid-liquid chemical plants and is used to calculate the total installed cost (TIC), as shown in Table 31. The indirect costs (IC), as a percentage of the total purchased equipment costs (TPEC), include engineering and supervision costs (32%), legal and contractors' fees (23%), and project construction expenses (34%). The total direct and indirect costs (TDIC) are the sum of the total installed costs and indirect costs (IC). A project contingency of 15% of the total direct and indirect costs (TDIC) is applied. A location factor of 10% is added to calculate the

total project investment (TPI) [705]. The present analysis assumes that there are no special financing requirements resulting from the project's working capital and longer startup times.

Table 31: Capital cost factors for capital cost estimate for a thermochemical plant [655]

Estimates for total project investment cost factors (in 2016 dollars)	
Installation factor	3.02
Total installed cost (TIC)	302% of TPEC
Indirect cost (IC)	89% of TPEC
Total direct and indirect costs (TDIC)	TIC + IC
Contingency	15% of TDIC
Fixed capital investment (FCI)	TDIC + Contingency
Location cost	10% of FCI
Total project investment (TPI)	FCI + location cost

7.3.2.2 Operating cost estimate

Annual operating costs are made up of fixed and variable costs. The fixed costs include operating labor, maintenance, and administrative expenses. The variable costs are the operating supply costs such as feedstock, chemicals, and utilities. The labor cost is the salaries of operators and supervisors. Hourly wages in Alberta were 26.11 $/h and 33.57 $/h for operators and supervisors, respectively A total of 8 staff (7 operators and 1 supervisor) are required per shift for the operation of a 2000 tonnes/day supercritical water gasification plant [700] and three shifts per day are considered [706-708]. The plant utility costs, such as electricity cost, are taken to be 0.067 $/kWh based on the average electricity price in Alberta. Other costs that are crucial for plant operation include maintenance and overhead costs. The maintenance cost is usually considered to be 2-10% of the total project investment cost; the present economic analysis considers this cost to be 3% of the TPI [700, 709, 710]. Operating charges are 25% of operating labor costs [710]. Plant overhead is assumed to be 50% of operating labor and maintenance costs [710]. Plant overhead mainly refers to the facilities, payroll, overhead, services, etc. General and administrative (G&A) expenses, specified as 8% of operating costs, refer to general administrative expenses, research and development, product distribution, etc. [700, 710]. The construction of the thermochemical plant is considered to make up 20%, 35%, and 45% of the total capital cost during the first, second, and third years, respectively [656, 657]. Other costs pertaining to the plant's overall techno-economic analysis were obtained from the literature [711, 712]. Table 32 shows the economic assumptions used in the development of the techno-economic model for thermochemical technologies for hydrogen production.

Table 32: Economic assumptions during the development of the techno-economic model

Parameters	Values	References
Plant life (year)	20	[709]
Cost year basis	2016	
Capital cost distribution		[656, 657]
Year 1 (%)	20	
Year 2 (%)	35	
Year 3 (%)	45	
Production plant capacity factor		[656, 657]
Year 1	0.7	
Year 2	0.8	
Year 3 and beyond	0.85	
Internal rate of return (%)	10	[709]
Maintenance cost ($)	3% of TPI	[700]
Operating charges ($)	25% of operating labor cost	[700]
Plant overhead ($)	50% of total operating labor and maintenance cost	[700]
Subtotal operating cost, SOC ($)	Sum of all operating costs including raw material and utility cost	[700]
G & A cost ($)	8% of SOC	[700]
Solid waste revenues ($/tonne Nitrogen)	500	[711]
Wastewater disposal cost ($/tonne)	1.16	[712]

7.3.2.3 Product cost estimate

The product value of hydrogen ($/kg) is determined using a discounted cash flow rate of return (DCFROR) analysis at a discounted internal rate of return (IRR) of 10% over a 20-year plant life [709]. For currency conversion, a US$/CAD$ exchange rate of 1:0.77 (Bank of Canada exchange rate, March 2016) was used. All cost numbers in this study are in US$ 2016. An inflation rate of 2% was considered for the present economic analysis [656, 713, 714].

7.4 Results and discussion

The results obtained from the techno-economic process model developed for hydrogen production from two thermochemical technologies are discussed, followed by sensitivity and uncertainty analyses.

7.4.1 Process modeling results

The process model results show that from an algal biomass SCWG plant with a capacity of 2000 tonnes/day, approximately 209 tonnes/day of hydrogen is produced, corresponding to a percentage yield of 10.5%. This is in agreement with values reported in other studies (8.4-11.2%) [570, 571, 715, 716]. Gasafi et al. studied the hydrogen production from sewage sludge via SCWG and reported a hydrogen yield of 8.39% [570]. Lina et al. estimated a hydrogen yield of 10% from

the SCWG of palm oil waste [715]. The details of the developed process simulation model results and the influence of key operating parameters on syngas yield have been described in earlier work by the authors [704].

7.4.2 Techno-economic modelling results

The cost estimates for the hydrogen production for a plant capacity of 2000 tonnes/day using algal feedstock via SCWG and thermal gasification are given in Table 33. The total purchased equipment cost for supercritical water gasification is 56.2 M$, which corresponds to a total capital investment of 277.8 M$. For thermal gasification, the installed capital cost is 131.48 M$, with a total capital investment of 215.3 M$. The purchased equipment cost obtained in this study for supercritical water gasification is in good agreement with that found in an earlier study on the SCWG of 15 wt% glucose for renewable hydrogen production and a reported total purchased equipment cost of around 62 M$ for a 2000 tonnes/day plant [571].

Table 33: Cost estimates for hydrogen production using thermochemical technologies (in 2016 US dollars)

Parameters	SCWG	Thermal Gasification
Installed capital cost (M$)	169.6	131.48
Total capital investment (M$)	277.8	215.3
Cost of hydrogen ($/kg)	4.59	5.66

The supercritical water gasification unit and water-gas shift reactor together incur the highest total purchased equipment cost (30.2 M$), followed by the gas purification unit (25.9 M$). Spath et al. studied the process model and economics for hydrogen produced through biomass gasification at a plant capacity of 2000 dry tonnes/day and reported total purchased equipment costs for processing and gas purification at approximately 39-41 M$ (2016 US dollars) [717]. For thermal gasification, feed handling and drying contributed 10.1 M$ whereas gas cleanup, compression, sulphur removal, and steam methane reforming unit contributed 24.5 M$. The cost parameter contributions to the product value of hydrogen for supercritical water gasification and thermal gasification are shown in Figure 40. It is clear that the raw material cost contributes highest to the overall product value of hydrogen from biomass for both thermochemical processes. Similar results were reported in a study on synthetic natural gas (SNG) production via SCWG, which found >94% of algal biomass production to be attributed to production cost [580].

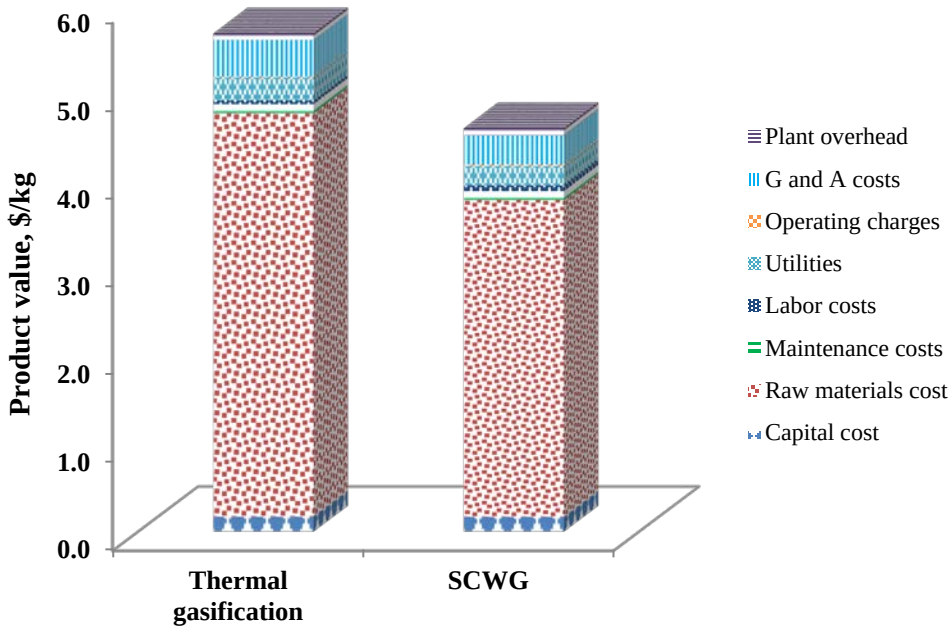

Figure 40: Breakdown of product values of hydrogen for SCWG and thermal gasification of biomass

7.4.3 Plant capacity profile

The plant capacity profile versus the product value of hydrogen is shown in Figure 41. As the plant capacity increases, the product value decreases and then flattens out. This trend is the result of the trade-off between capital, raw materials, and labor cost. The flat trend shown in the graph indicates that the product value of hydrogen does not change with any increase in plant capacity beyond a capacity size of 2000 dry tonnes/day, signifying the economies of scale. The optimum plant capacity is found in the trade-off between the biomass transportation cost and plant capital cost.

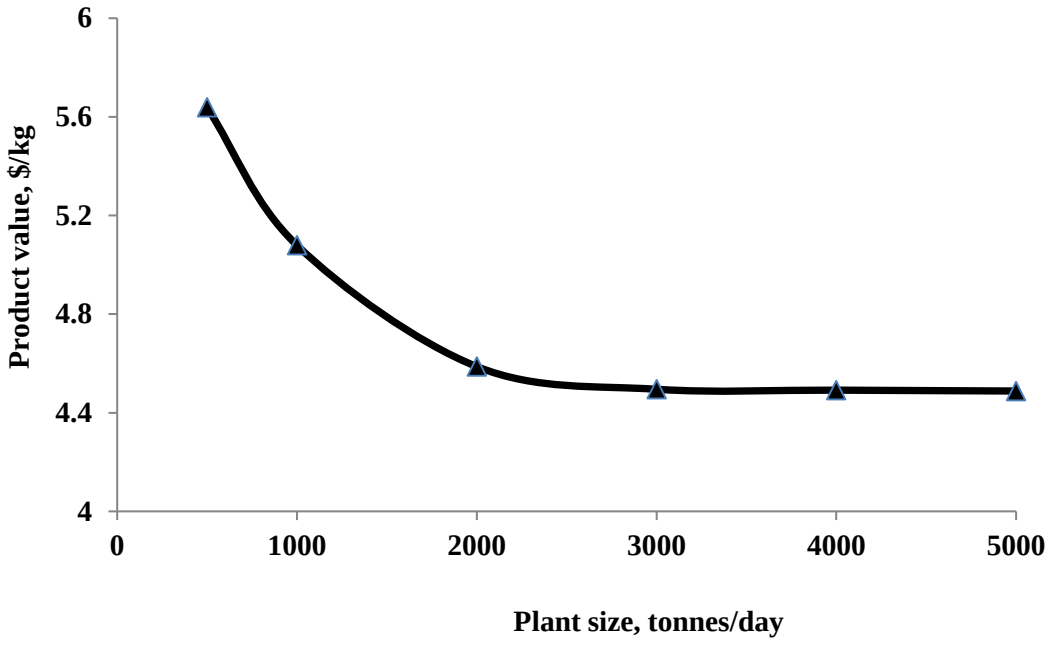

(a)

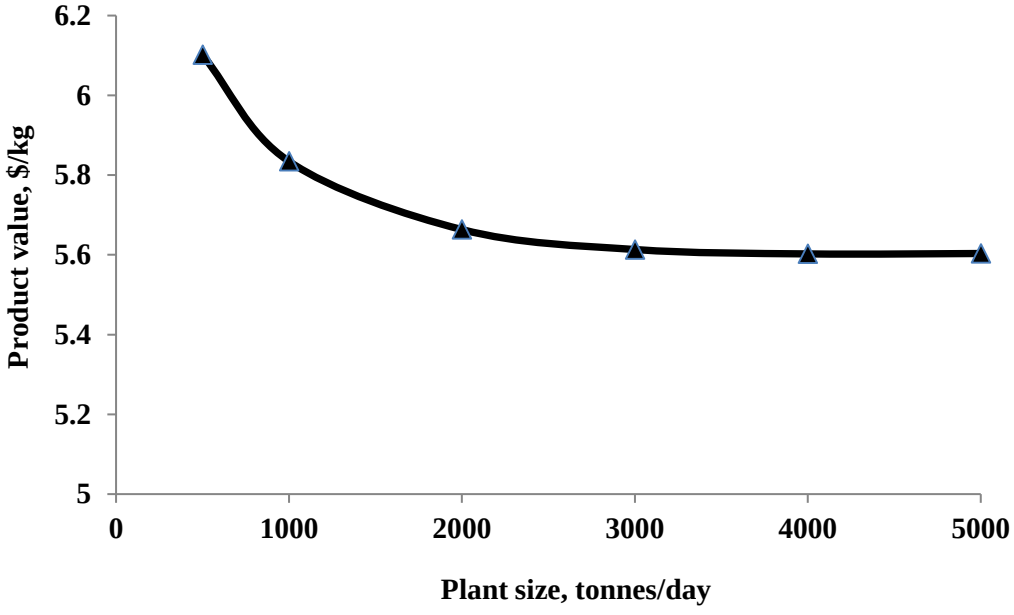

(b)

Figure 41: Effect of plant scale factor on the product value of hydrogen for (a) supercritical water gasification (b) thermal gasification

7.4.4 Comparison of hydrogen costs with those from the literature

To the best of the authors' knowledge, there are no studies on the production of hydrogen through supercritical water gasification in Western Canada. Some authors have done studies on the

supercritical water gasification of different feedstocks. Mosuli et al. showed that no profit can be realized with a glucose feed concentration of 15% until the hydrogen price is more than $5/kg [571]. Matsumura reported hydrogen production costs of $58.89/GJ (based on currency conversion and 2% inflation) [569]. The current study found a product value of $4.59/kg ($38.16/GJ) assuming the LHV of hydrogen to be 120.21 MJ/kg, which is in good agreement with values reported in the literature [569, 580]. The differences in product value arise due to the location-specific nature of the plant design. Sarkar et al. studied a gasifier for biohydrogen production using forest residues and straw and reported $1.17/kg and $1.29/kg of H_2 at a plant capacity of 2000 dry tonnes/day [550]. Brandenberger et al. studied the economics of synthetic natural gas (SNG) using microalgae from SCWG from raceway ponds (RP) and tubular and flat-panel (FP) photobioreactors through a process named SunCHem [580]. For the most optimistic cases, this study estimated SNG production costs of approximately $37-127/GJ based on different algal production costs. The main downsides to large-scale implementation of microalgae-based biofuels are the high investment costs and energy requirements during cultivation and harvesting [718, 719]. Brandenberger et al. analyzed the base case scenario for SNG production from microalgae, with an algal production cost of $ 2.84-7.33/kg , and found it to be not viable economically [580]. Different cost estimates for microalgae biomass production have been reported in the literature. van Beilen estimated $5-15/kg for algal biomass production in raceway ponds [719]. Williams and Laurens reported large-scale production costs of $0.41/kg under optimized conditions [720]. In Western Canada, most hydrogen is obtained from natural gas with a cost of $0.78/kg [676]. A thermochemical plant using 2000 dry tonnes/day algae as a feedstock is not economical. However, alga's carbon neutrality and its ability to take up CO_2 make it potentially an attractive option.

7.4.5 Drying using hydrogen gas

The chemical reactions in the gasification of microalgal biomass require moisture removal or dewatering, as high moisture in biomass such as algae reduces the efficiency of the gasifier. Hydrogen gas can also be used to dry algae. A European refinery used high purity hydrogen for drying purposes in certain unit operations [721]. Another study on industrial processes employed gaseous hydrogen for drying as an energy efficiency alternative [722]. In this study, the potential of using hydrogen as an energy source for drying was investigated for gasification. The product value of hydrogen increased to $5.90/kg when hydrogen was partly used as a drying energy resource. However, the product value increased as a result of a decrease in the overall yield of hydrogen produced.

7.5 Sensitivity analysis

Because the technology is still developing, an understanding is needed on how economic parameters influence product value in order to improve process efficacy. A sensitivity analysis was done by selecting cost variables that impact the product value estimate. The influence of cost variables on the product value of hydrogen is important in view of the uncertainties. The chosen parameters are those associated with biomass, utility, labor, maintenance, plant overhead, and G&A costs including IRR, hydrogen yield, and plant capital costs. Sensitivity analysis is done by varying cost parameters by ± 20% while the other parameters remain fixed. The key sensitive parameter is the hydrogen yield obtained during the process. A 20% increase in product yield reduces the product value by $0.76/kg and $1.30/kg for SCWG and thermal gasification, respectively. Thilakaratne et al. [555] also found product yield to be the most sensitive parameter

in the techno-economic assessment of microalgae for both thermal drying and partial mechanical dewatering processes. The other significant parameter is biomass feedstock cost. A ±20% variation in biomass cost changes the product value by > 20% for both processes. The cost of algal biomass depends on the availability of biomass, which relies on optimized design and performance of algal production methods that improve biomass productivity. Also, there are uncertainties in the cultivation and harvesting of microalgae for biofuel production [723]. Thus, algal production methods vary with location and capital costs, and algal production costs range from $30-70/kg for photobioreactors [724] and $0.24-15/kg for raceway ponds [719]. Manganaro et al. studied the doubling time in a techno-economic assessment of algae production and found that a 10% decrease in doubling time reduced the price of algae by ~ $0.92/gal, and thus research into the inhibiting impacts on microalgae doubling time is required [725].

The next most important sensitivity parameter is internal rate of return (IRR), followed by the plant capital cost. The product value of hydrogen through thermal gasification ranges from $5.54-$5.79/kg with a ±20% variation in IRR. The product value increases with increasing IRR. Another key factor is the capital cost; it influences the capital investment of the plant, which in turn affects return on investment. With a ± 20% variation in capital costs, the product value for thermal gasification ranges from $5.59-$5.73/kg. However, other cost variables such as utility, labor, maintenance, G&A, and plant overhead have little or no impact on product value.

The influence of key parameters on the product value of hydrogen is provided in Figure 42. The analysis shows that the product value of hydrogen can be significantly reduced either by increasing product yield or by reducing microalgae biomass cost, as also reported by Thilakaratne et al. [555].

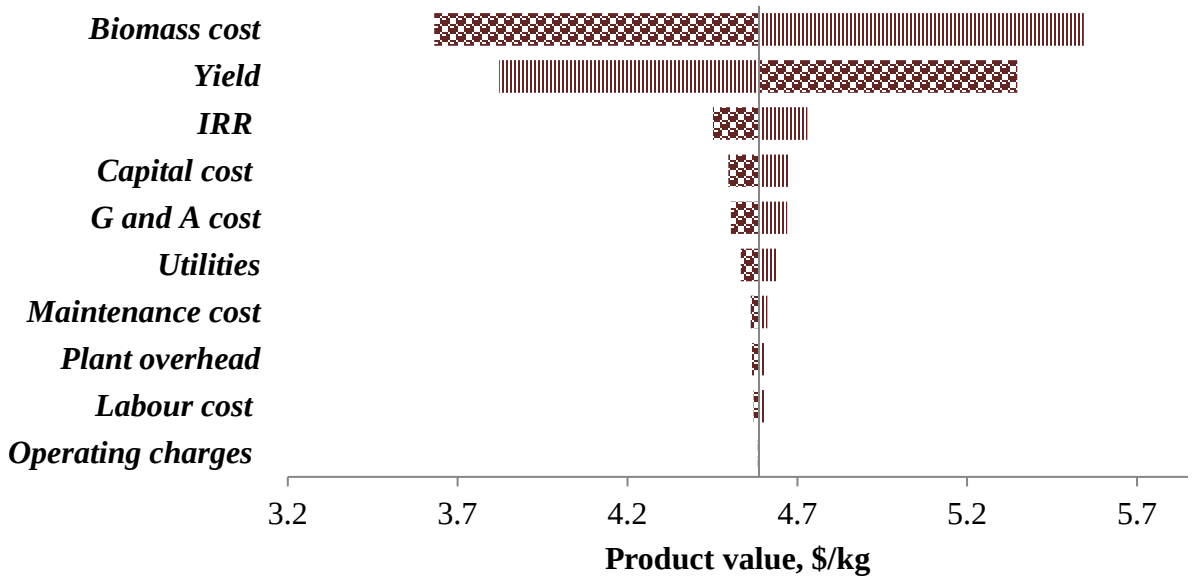

(a)

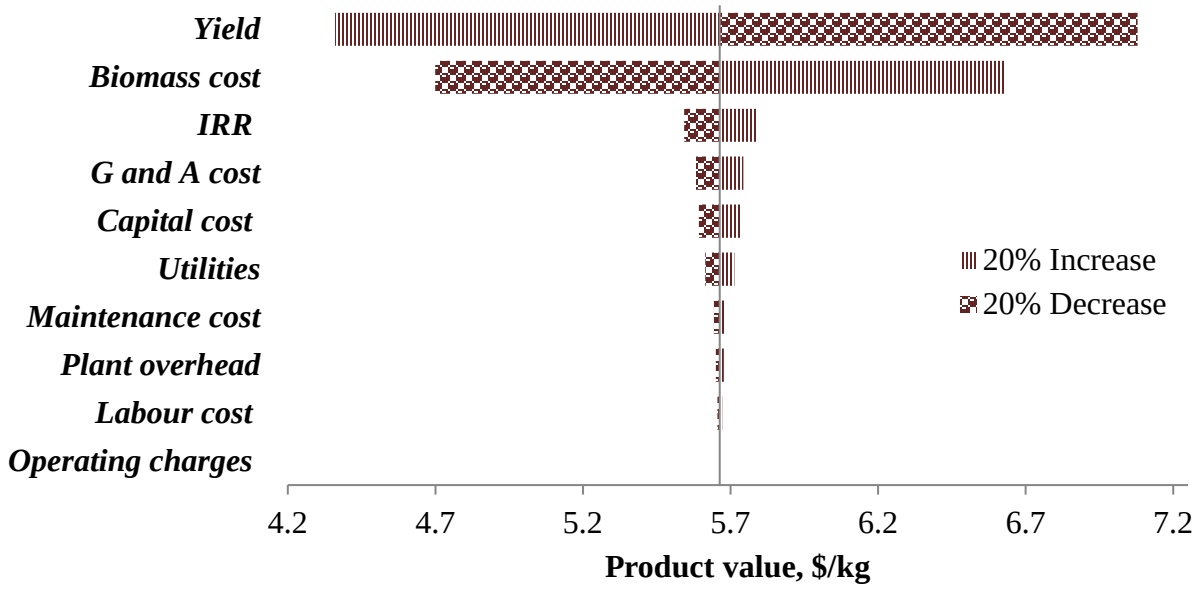

(b)

Figure 42: Sensitivity analysis on the product value of hydrogen for (a) supercritical water gasification and (b) thermal gasification

7.6 Uncertainty analysis

The lack of accurate data and relative uncertainty in techno-economic parameters constrains accurate data prediction and modeling and thus production cost estimates. In order to address these uncertainties, a Monte Carlo simulation was performed based on relative volatilities in the estimation of economic parameters. For this purpose, a ModelRisk software was used to run the simulation. The simulation was performed for 10,000 iterations to obtain accurate data. The Monte Carlo simulation results for the cost of hydrogen at a plant capacity of 2000 tonnes/day are $4.59 ± 0.10/kg and $5.66 ± 0.10/kg at an assumed 95% confidence level for supercritical water gasification and thermal gasification, as shown in Figure 43.

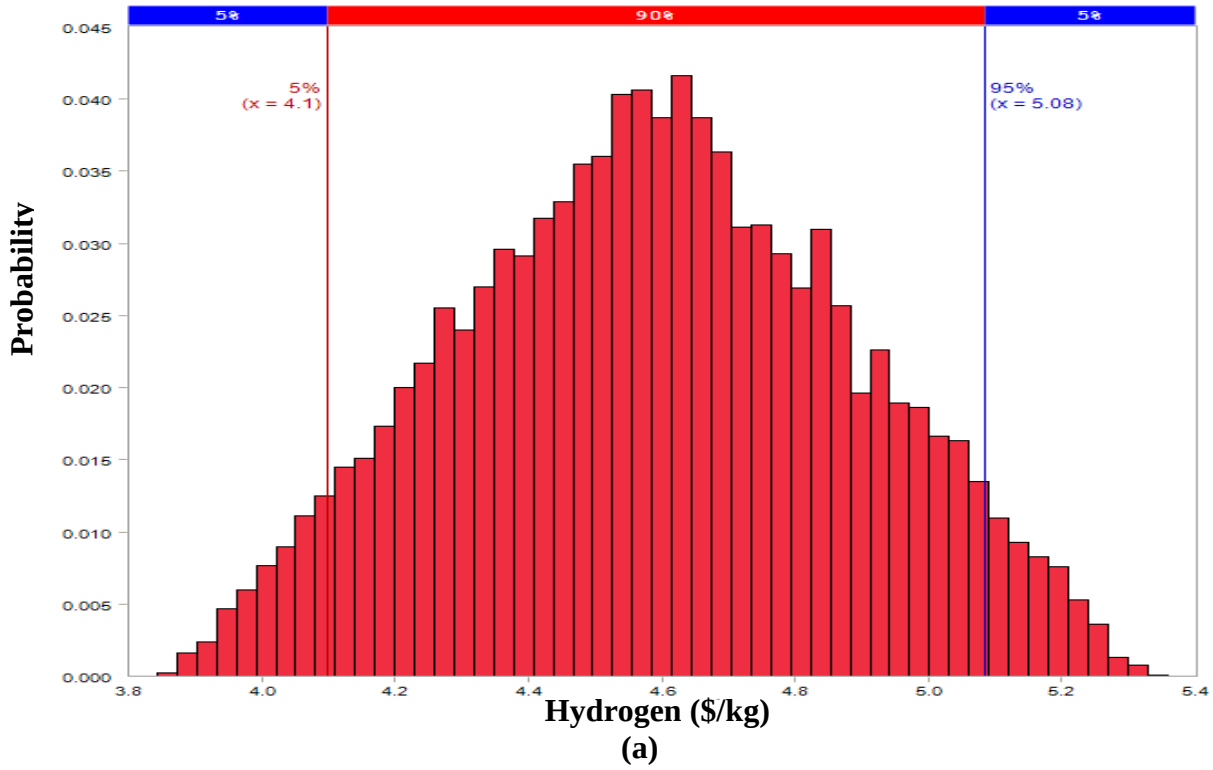

(a)

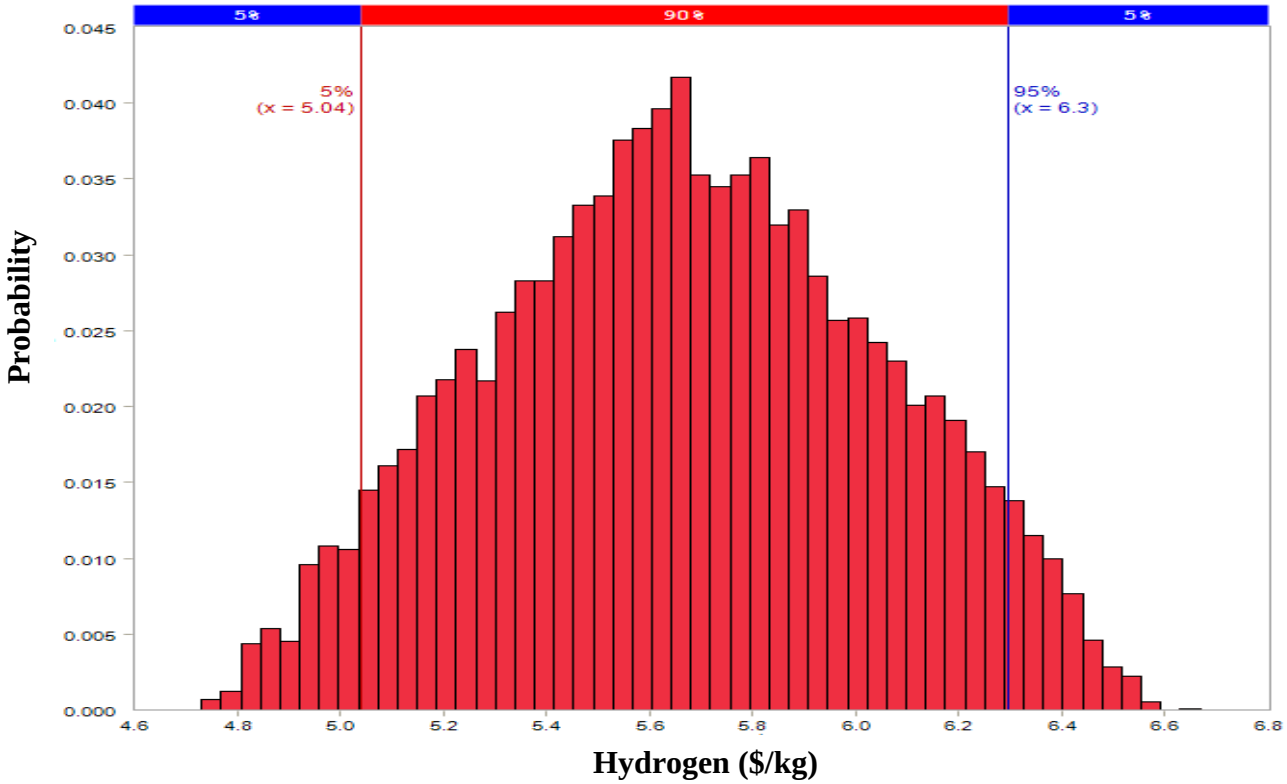

(b)

Figure 43: Uncertainty costs in the product value of hydrogen produced through (a) supercritical water gasification and (b) thermal gasification

7.7 The impact of industrial CO_2 on the product value of hydrogen

To mitigate problems with rising atmospheric CO_2 levels, biological CO_2 use has gained industrial attention. Photosynthetic microalgae has the ability to use flue gas CO_2 in the form of a carbon source [726]. This inherent feature of algae can be employed to produce biomass with high growth rates. This means that the algal cultivation can rely on CO_2 from a number of industrial sources. This may transform future hydrogen industry as algae are known to have high fixation efficiencies [727]. This could be desirable for the industrial sector in the jurisdictions where there is a carbon tax associated with the release of CO_2 in the environment. In jurisdictions like Alberta, effective levies on CO_2 emissions are in the range from $10/tonne to $30/tonne [728]. The companies paying these levies might be willing to dispose of their CO_2 if there is an opportunity to do this at a lower cost than the carbon levy. The algae conversion facility might benefit from companies willing to pay to take up the industrial CO_2. Every tonne of algal biomass takes away 1.8 tonnes of CO_2 [729].

The impact of using industrial CO_2 on the product value of hydrogen is also assessed in this study. The CO_2 ($/tonne) payment to the algae conversion facility was varied from $0-40/tonne and its impact on the product value of hydrogen was studied for both thermochemical routes. Figure 44 shows the influence of paying for CO_2 use on the product value of hydrogen. The assumption in this analysis is that industrial CO_2 is directly used by the algae conversion facility and does not need any purification. Also, it is assumed that the industrial facility is located near the algae conversion facility, so there is no transportation cost. For a supercritical water gasification plant and thermal gasification, the product value of hydrogen can be reduced to $2.60/kg H_2 and $3.65/kg H_2, respectively, when payment for CO_2 use is increased to $40/tonne. Hence, relying on industrial CO_2 for algal biomass growth reduces the product value of hydrogen for both thermochemical technologies.

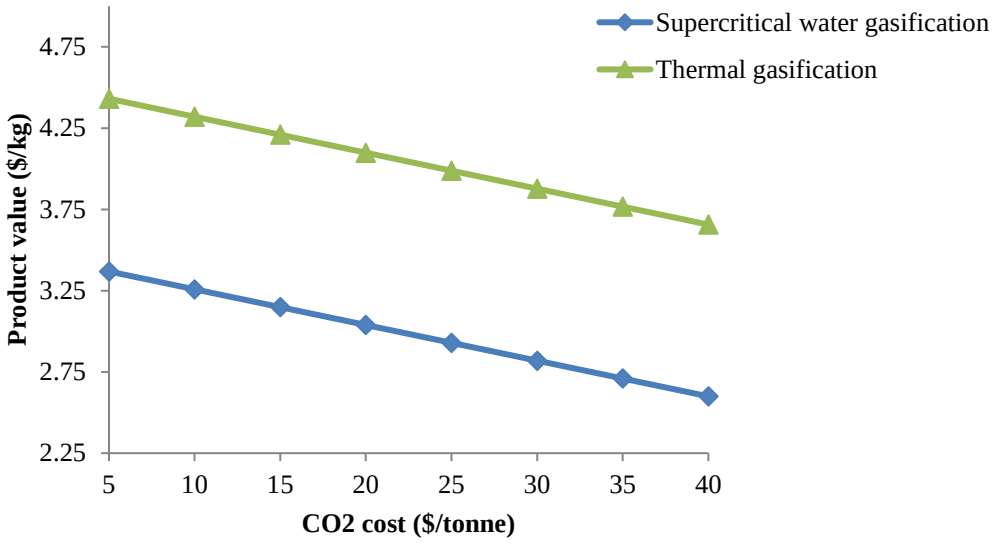

Figure 44: The effect of the cost of industrial CO_2 on the product value of hydrogen

7.8 Future perspectives

As discussed in this paper, algal gasification for hydrogen production can occur through two gasification technologies, thermal gasification and supercritical water gasification. SCWG has limitations with respect to the use of high pressure equipment including continuous pumping, plugging, etc. [138, 730]. The availability of algal biomass is a major concern as its cultivation and growth depends on several factors such as nutrients, water, CO_2, temperature, sunlight, etc., as well as doubling time. Manganaro et al. [725] studied the techno-economics of microalgae production and reported doubling time to be the most sensitive parameter on the sale price of algae; it can be lowered by improving mixing or increasing pond velocity. Also, co-locating an algal plant near industry would make use of industrial CO_2 emissions in algal biomass cultivation [731]. Moreover, the presence of NOx and SOx in industrial emissions does not negatively impact algal growth as NOx is converted to NO_2, which acts as a nitrogen source, and SOx has no influence on algal growth below concentration levels of 400 ppm [732, 733]. Thus, flue gas components can be used as nutrients for algal cultivation. Algae are characterized by high moisture containing feedstocks (70-90 wt%) that require drying for thermal gasification. Thermochemical pathways are high-energy processes. During the process run, energy can be lost due to limitations in heat exchanger design [734, 735]. The CO_2-rich gas obtained after gas cleanup can be recycled for algal cultivation. Algal companies claim lower costs of microalgae and biofuels production, though this assertion has not been proven in published literature [719, 720, 724, 736].

7.9 Conclusion

Algae is a promising biomass feedstock for energy production. Hydrogen production from algae is considered to be an option for obtaining energy as the process is believed to offer highly energy efficient operation, use, and storage. Moreover, using CO_2 from an industrial source and obtaining a tipping fee for using the CO_2 for algae cultivation reduce the cost of hydrogen production in the thermochemical plant. The harvesting of energy from algae via a thermochemical approach results in a high conversion rate and efficiency. A system was developed to produce hydrogen based on two different gasification technologies. A techno-economic assessment of supercritical water gasification and thermal gasification shows that a 2000 dry tonnes/day plant needs total capital investments of 277.8 M$ and 215.3 M$ with hydrogen product values of $4.59 ± 0.10/kg and $5.66 ± 0.10/kg, respectively. These costs are higher than the natural gas-based hydrogen. The sensitivity analysis indicates that algae feedstock cost and yield are the key sensitive parameters in the economics of the process, which highlights the importance of algal biomass availability. Supercritical water gasification holds tremendous potential because of its ability to handle wet biomass, thereby avoiding the cost-intensive drying step. The economic assessment suggests that the feasibility of the technology depends heavily on the cost of algal biomass and the yield obtained. Increasing algal biomass yield requires developing novel algal biomass production and cultivation systems including new reactor designs, harvesting approaches, and highly productive algal species. Hence, further process optimization research is essential to increase fuel production. If there is a payment from the CO_2 producer to the algae conversion facility, the cost of hydrogen production comes down significantly.

8 Development of Life Cycle Water Footprints for Production of Diluent and Hydrogen from Algae Biomass

The water consumption of the entire life cycle of a product needs to be assessed because water is a scarce resource. The aim of this section is to analyze the life cycle water consumption of diluent and hydrogen production from algal biomass used as raw material. The specific objectives are to:

- Develop a method to estimate the water footprint for diluent and hydrogen production from algal biomass for four different conversion pathways. These thermochemical conversion methods that can be applied to algal biomass produced either through ponds or PBRs are:
  - the production of diluent through fast pyrolysis and the hydrotreating of algae feedstock;
  - the production of diluent through the hydrothermal liquefaction and hydrotreating of algae feedstock;
  - the production of hydrogen through the gasification of algae feedstock and enrichment of syngas; and
  - the production of hydrogen through the hydrothermal gasification (HTG) of algae feedstock and enrichment of syngas.
- Conduct sensitivity and uncertainty analyses to study the changes resulting from variations in input parameters on the life cycle water footprints of diluent and hydrogen production from algae.

8.1 Method

Calculating the water footprint from the production of diluent and hydrogen from algal biomass involves an analysis of the life cycle of the biomass from well to tank (which means all the steps from resource acquisition for biomass cultivation to the final production of chemicals of interest, excluding their consumption). The International Organization for Standardization suggests through their ISO 14040 norms a life cycle assessment framework that consists of a goal and scope definition, life cycle inventory, and impact assessment and interpretation [737]. First, the goal and scope define the system boundaries of the cases that will be analyzed and include details on possible impacts (negative or positive) for industry or government. The life cycle inventory is the part of the study in which all the information necessary for the analysis is assembled and all the input assumptions are made. Finally, the computation and analysis permit the assessment of environmental impacts and a better interpretation of the results of the study. This study adopts a functional unit of 1 MJ of diluent (for the fast pyrolysis and HTL analyses) and 1 MJ of hydrogen (for the gasification and HTG analyses). More specifically, for the resource of interest in this study, the results are presented in terms of L of water/MJ of diluent or H_2. In other words, the functional unit is the amount of water required to produce 1 MJ of the product of interest in a wheel-to-gate approach. Different base cases were established so that the importance of each variable in the final results could be measured. Once this was done, an uncertainty analysis was conducted through a Monte Carlo simulation to determine the influence of the uncertainties of some inputs on the results.

It is necessary to consider the unit operations involved in algal biomass production, thermochemical conversion through fast pyrolysis, hydrothermal liquefaction, hydrothermal gasification or conventional gasification, and hydrotreating to obtain diluent (in the cases of fast pyrolysis and HTL). The basic unit operations for fast pyrolysis and HTL are the production and dewatering of algal biomass, drying (for fast pyrolysis only) and thermochemical conversion of

the feedstock, and hydrotreating to produce diluent. The conversion pathway for fast pyrolysis is shown in Figure 45 and for HTL in Figure 46. For gasification and HTG, the unit operations are cultivation and dewatering, drying (for gasification only) and thermochemical conversion, and hydrogen production. The conversion pathways for thermal gasification and hydrothermal gasification are presented in Figures 47 and 48, respectively. In both fast pyrolysis and HTG, it is assumed that the cultivation and conversion facilities are closely located and that the impact of transportation between units is negligible. This analysis uses data gathered from the literature on the cultivation and conversion of algal biomass (and other types of biomass, when case studies for algae are not conclusive), information obtained from industry, and information obtained through models developed by the authors in Aspen Plus [738]. Some key assumptions were made for the analysis conducted in this paper. First, it was assumed that the algae production facility capacity is 2000 dry tonnes of biomass per day; this figure is used in earlier studies on large-scale biomass-based systems [739, 740]. Second, the thermochemical conversion plants have the infrastructure to use everything that is produced as it becomes available. Third, the production facilities and conversion plants are adjacent to each other and the impact of biomass transportation is negligible. Fourth, the inoculum systems of ponds have a negligible contribution to the overall water consumption of the process. Fifth, the electricity input to each stage of the process indirectly contributes to the overall water consumption, since water is required for energy generation. And last, water loss due to evaporation in PBRs is negligible, considering that PBRs are closed systems (versus open ponds).

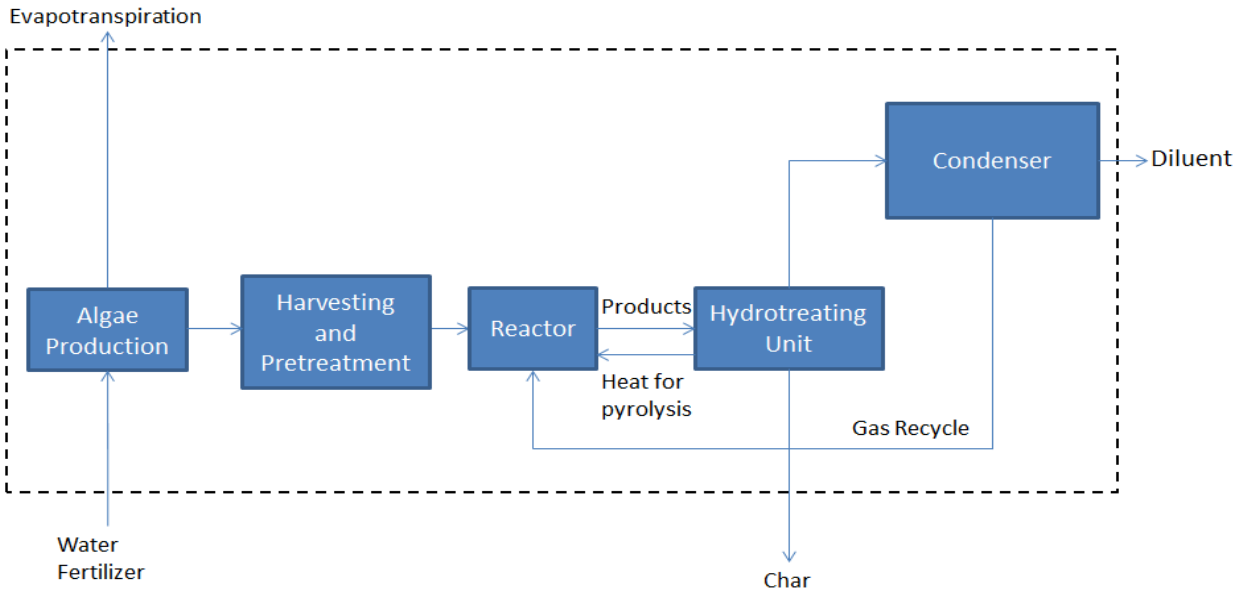

Figure 45: System boundary for pyrolysis

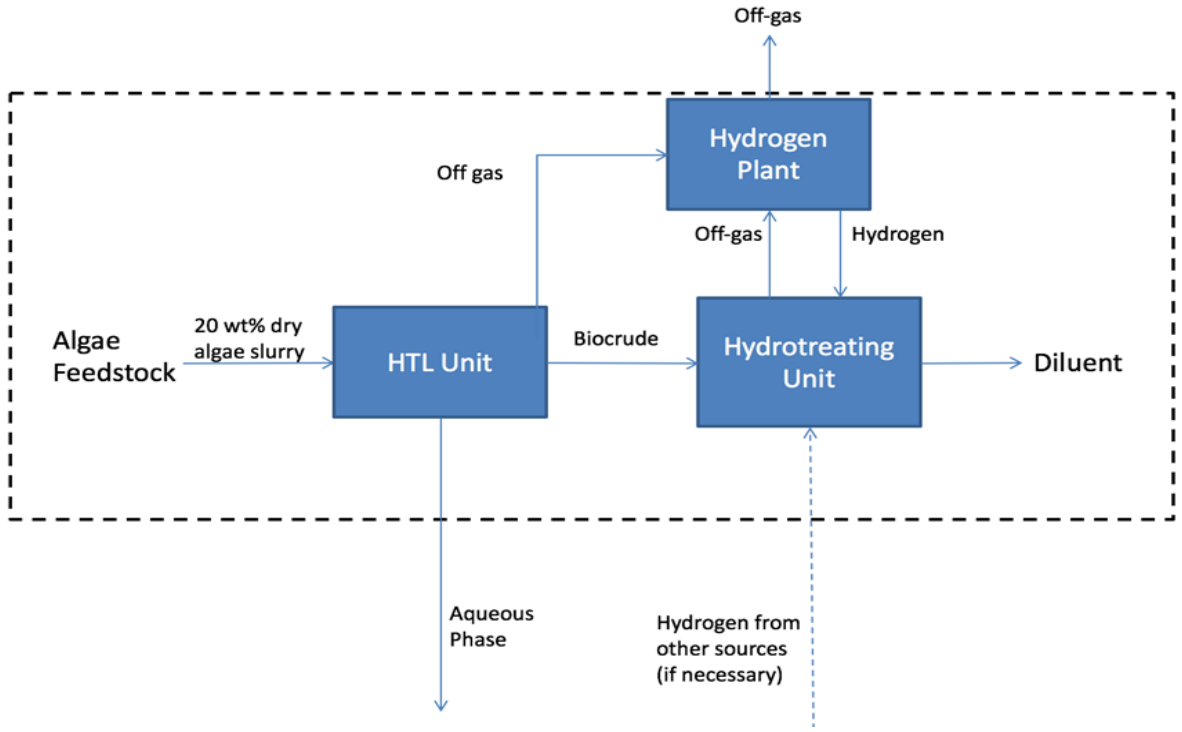

Figure 46: System boundary for hydrothermal liquefaction

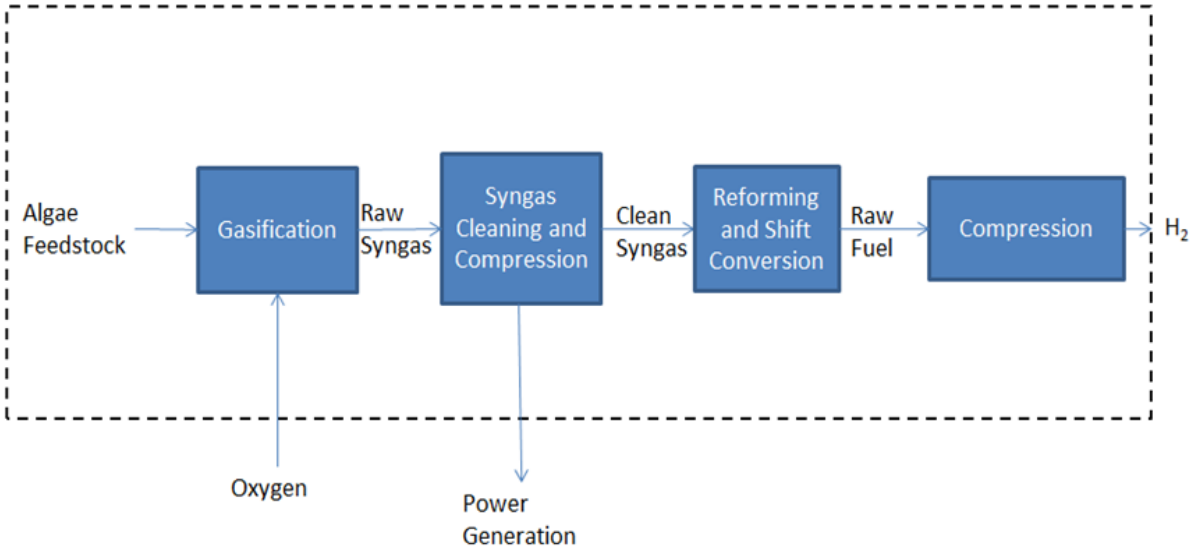

Figure 47: System boundary for thermal gasification

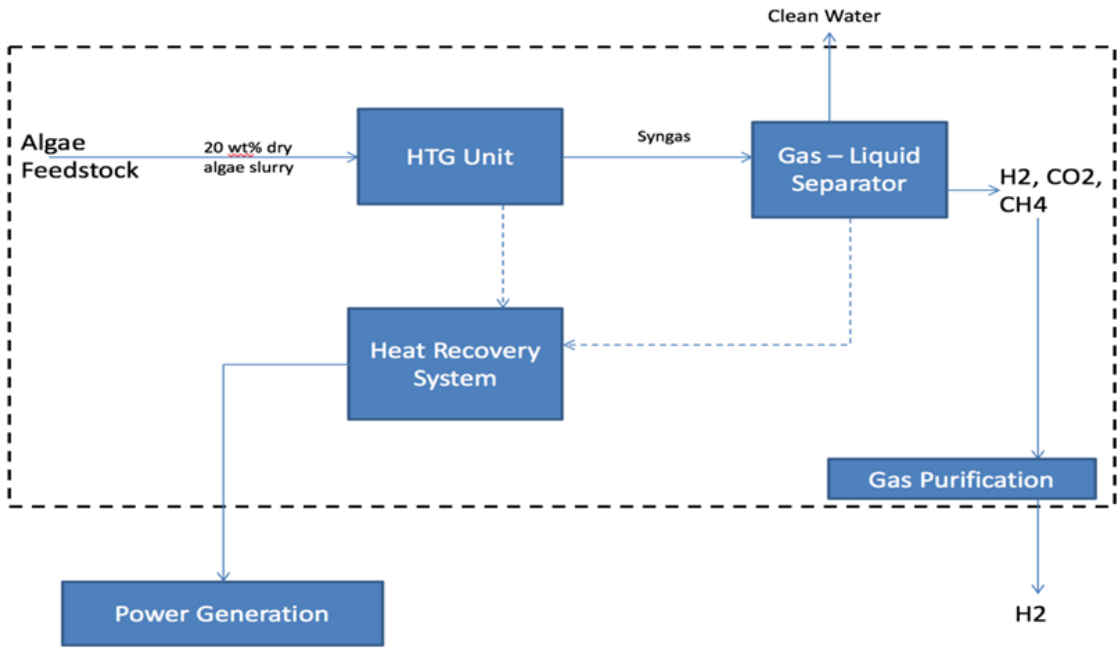

Figure 48: System boundary for hydrothermal gasification

A water footprint assessment for algae cultivation was conducted for two options. The first is the use of raceway ponds, which is currently the most common method of algae cultivation and consists of a recirculation channel where the feedstock, immersed in a liquid solution, is guided through the channel, thereby avoiding sedimentation [8]. The other method is the use of photobioreactors (PBRs), an innovative technology in which biomass is cultivated in enclosed systems, which increases the level of control the operator has over the parameters and makes it possible to maximize biomass production [741]. Of the four thermochemical conversion pathways considered in this study, two are for the production of diluent and two for hydrogen. In this study, the life cycle water footprint refers to both direct and indirect consumption of water during the processes used to produce algal biomass and to convert it to diluent or hydrogen. Direct consumption of water is defined as the total amount of water required during the entire biomass production phase and the subsequent thermochemical conversion processes, such as losses due to evaporation or blowdown of water at the steam generation or cooling stages. Indirect consumption refers to the amount of water used during fertilizer production (ammonia and diammonium phosphate, in this case) and electrical energy input for the various unit operations [742]. Surface or ground water can be used as sources for both direct and indirect uses.

8.2 Water requirement inventory

Water requirements calculated in this inventory are categorized based on the unit operations that make up the entire production pathway of algal biomass to diluent or hydrogen.

8.2.1 Production of biomass

This section presents the input parameters related to the production of algae feedstock for the two main methods of algae cultivation, ponds and photobioreactors.

8.2.1.1 Ponds

Raceway ponds are common in the algae facilities currently in operation [743]. Hence there are many studies that explore in depth the operating conditions and production optimization methods in ponds [743-746]. However, most of the literature in this area concentrates on facilities built in warm locations with high solar radiation all year and generally good conditions for algae cultivation in an open-air setting [729]. This study considers a pond facility in central Alberta, Canada, and assumes that production is limited to the warm months of the year, approximately 175 days. For ponds, some of the main sources of water loss are transpiration and evaporation, system blowdown, and losses during harvesting and drying. While some of these losses can be mitigated (for example, through water recycling feeds designed for the system), evapo-transpiration is a challenge in the dry climates and low precipitation rates in Alberta [747]. Hence water replacement rates may be relatively high in this cultivation method. To estimate the average evaporation during summer, it was assumed that summer conditions in Alberta are similar to late spring/early autumn in Arizona (where detailed data on algae cultivation are available), so that an average evaporation rate can be adopted for this study. The evaporation data from Arizona were compared with data measured in the Wabamun Lake area in Alberta [748].

For our study, we assumed a large-scale facility capable of producing 2,000 T of dry algae/day, with the same basic characteristics of operation and production described in a recent study [639]. Daily alga production is assumed to be 25 g/m^2/d in a facility divided into farms of 20.2 million m^2 dedicated to pond cultivation only and a total footprint per farm (including processing and storage) of 30.8 million m^2. A design with 400,000 m^2 modules containing 50 raceway ponds of 8 000 m^2 each is also assumed. The media in these ponds would be mixed by paddlewheels and the alga concentration kept at 0.1 g/L, or 0.01 wt%. An inoculum system is also part of the design; its goal is to guarantee the production of a high-concentration media for insertion into the ponds, which maintains the culture at the desired concentration. This inoculum system is negligible in size compared to the main system and does not account for a considerable percentage of the water consumption. The data for the water footprint analysis of algae cultivation in ponds were acquired from multiple sources, from industry partners to extensive studies of algae cultivation. Empirical data for what can be expected in Alberta, such as evaporation rate and number of days of harvest per year, help more accurately estimate water requirement. The calculated water footprint for the production of algae through ponds was 1,564 L of water/kg of algae. The details of algae cultivation in raceway ponds as reported by [639] or derived from their data are provided in Table 34.

Table 34: Basic operational data for algae cultivation in ponds [639]

Operation	Value	Unit
Average daily algae production	0.025	$kg/m^2/d$
Pond cultivation area/farm	20.2 million	m^2
Pond depth	0.25	m
Pond motion velocity	0.2	m/s
Volume harvested daily	20	%
Size of module ponds	100	acres
Net evaporation rate/day	0.5	%
Blowdown – replacement of media/day	0.5	%
Media loss at harvesting	0.2	%
Number of days of harvest/year	175	days
Pumping	0.75	kW/acre
Paddlewheel	1.35	kW/acre
Pumping to/from dewatering	1000	kW/module pond
Energy demand (membranes)	0.04	kWh/m^3
Inlet flow rate (membranes)	76000	m^3/day
Energy demand (centrifuges)	1.35	kWh/m^3
Inlet flow rate (centrifuges)	6000	m^3/day

It is also important to consider the water footprint of the electricity consumption of the facility. In this case, the highest energy-consuming equipment are the pumps used to carry the algae solution through the ponds, the paddlewheels used to stir the ponds, and the drying apparatus used to increase the algae concentration to 20% dry weight before it is sent for thermochemical conversion. The drying consists of pumps, membranes for the first and most basic phase of the dewatering process, and centrifuges that guarantee the desired 20 wt%. The water consumption factor is adopted based on data for Alberta, Canada, where most of the electricity generation is coal-based. For ponds, the processes that require the highest amounts of water are the initial filling of the modules, water loss to evaporation, and blowdown.

8.2.1.2 Photobioreactors

PBRs are a promising alternative to ponds; however, there is not much information available on them in the literature. PBRs may be able to optimize algae production and resource allocation, since they allow more control of the operating parameters, such as temperature and light applied to the media [743]. They also require a smaller cultivation area than ponds for the same amount of algae produced. PBRs can be designed and built in many different sizes. For this study, a tank size of 6,800 L and a daily production of 20 kg of algae, like the one used by HY-TEK Bio, was assumed. This design consists of a hollow tank that has an airlift system to help with the mixture of the media [741], with a bubble sparging mechanism containing CO_2 for the photosynthesis process. The algae concentration in a system of this type is assumed to be between 3 and 5 g/L, up

to 50 times higher than in ponds. Because of the limited data available on this equipment, a consistent set of parameters provided by industry was used and validated with data from various studies [41, 749, 750]. The same assumptions were made for PBRs as for a pond producing 2000 T of algae per day. PBRs have negligible losses to evaporation since the culture remains in an enclosed space isolated from the environment. Other losses (i.e., water loss during harvesting) can be mitigated through systems controls. As expected, the water footprint for the cultivation of algae via PBRs is considerably lower than that for ponds; PBRs consume only 25 L of water/kg of algae produced. Table 35 gives the details of the basic operational data for algae cultivation in PBRs.

Table 35: Basic operational data for algae cultivation in PBRs (source: HY-TEK Bio)

Operation	Value	Unit
PBR tank size	6800	L
PBR production/day	20	kg/day
Volume harvested each time	10	%
Number of harvests	10	#/day
Area occupied/PBR	8	m^2
Blowdown	6435	m^3/day
Harvesting	2145	m^3/day
Compressor – Power/PBR	6.25	kW
LED lights' power/PBR	0.9	kW
Chiller for storage power	10	kW
Chiller for storage power/PBR	0.01	kW
Airlift system	3.9	kW/acre
Water consumption factor for electricity generation	1.08	L of water/kWh

In terms of electricity consumption, PBRs require considerably more energy than ponds [639, 751]. This is due to the equipment necessary for the proper functioning of the system, such as the compressors to regulate the pressure and the many LED lamps that both transmit light and provide heat to the culture at all times of the day. This equipment would allow the cultivation of algae year round even in cold winter climates like Alberta's. The PBR algae cultivation processes that require the most water are the initial filling of the tanks, replacement of blowdown water, and electricity generation.

8.3 Fast pyrolysis

Fast pyrolysis is a thermochemical conversion method commonly used to convert biomass to bio-oil. It is a thermal decomposition process that occurs in high temperatures in the absence of oxygen in 0.5 to 10 seconds (flash pyrolysis lasts less than 0.5 second and conventional pyrolysis takes 5 to 10 minutes). Fast pyrolysis yields relatively high amounts of bio-oil [551, 752]. In this method, biomass is dried to a moisture content of <10% to decrease the water content in the fast pyrolysis bio-oil [562].

Biomass feedstock that only goes through dewatering leaves the cultivation facility with approximately 20 wt% dry biomass and must go through extra drying before being fed into the fast pyrolysis reactor. Feedstock with a moisture content of 5-10 wt% is preferred for fast pyrolysis

[753]. Other important parameters in the pyrolysis reaction are particle size, temperature, pressure, and residence time. Once prepared, the dried biomass is sent to a fluidized bed pyrolysis reactor at 520 °C [654] with particles smaller than 2mm. Following reaction, biochar is removed by cyclones, resulting in a bio-oil yield of approximately 59.9 wt% (dry basis) depending on the feedstock [679]. For this study, a yield of 26130 kg/hr was estimated using process model [754]. The fast pyrolysis values related to the water footprint generated by the cooling, ash quenching, steam condensing, and steam producing processes are extracted from the literature, given that there is no significant difference in water requirement for this equipment no matter which feedstock is used. Most of the water used in these processes is recycled, but there is an estimated loss of 3% due to factors such as blowdown and evaporation. Steam condensing is the main contributor to the water footprint [679]. Water is indirectly consumed through the generation of the electricity necessary to operate the plant during pre-treatment and pyrolysis. For the fast pyrolysis of algae, a process model was developed in Aspen Plus to estimate the entire plant's electricity consumption and generation, and the results for water requirements for algal pyrolysis are provided in Table 36. With the higher heating value (HHV) of diluent at approximately 34 MJ/kg, when all the factors shown, the hydrotreating factors (Table 5) are considered and all their contributions are added, the total water footprint from the production of diluent through fast pyrolysis is approximately 0.12 L/MJ of diluent.

Table 36: Water requirements for pyrolysis of algae

Operation	Value	Unit	Source
Bio-oil cooling*	0.027	L water/kg bio-oil	[679]
Bio-oil vapor cooling*	0.003	L water/kg bio-oil	[679]
Steam condensing*	1.077	L water/kg bio-oil	[679]
Steam system*	0.026	L water/kg bio-oil	[679]
Ash quenching*	0.233	L water/kg bio-oil	[679]
Recycle gas compression	10400	kW	This study
Feedstock grinding	5600	kW	This study
Other auxiliary	1248	kW	This study
Electricity generated	19600	kW	This study

*Water consumption derived from the flow rates of the plant described by Ringer et al. [679]

8.4 Hydrothermal liquefaction

HTL is a thermochemical conversion process that converts biomass to biocrude in the presence of large amounts of water [755]. During the process, macromolecules are broken down into small molecules that are unstable and can recombine, with a good portion of the oxygen present in the biomass being removed [127]. The method is used to produce diluent and does so through medium temperature and high pressure reaction in a high concentration of water; biocrude is its main

product [630, 709, 755]. In hydrothermal liquefaction, biomass is pumped to 18 MPa and passed through heat exchangers to increase the algal stream temperature to 350 °C [709]. At this temperature, water exists slightly below the supercritical point, which allows dissolution of biomass organics [137]. The incoming effluent is fed into the HTL reactor, which converts biomass components into biocrude. The output from the HTL reactor is filtered to obtain solid residue in the form of biochar. The filtered effluent passes through a heat exchanger to recover heat before moving to a three-phase separator unit to produce aqueous, bio-oil, and gaseous phases [567]. The biocrude undergoes hydrotreating, where it is deoxygenated [756].

Hydrothermal liquefaction happens at medium temperatures and high pressures and generates mainly the liquid product known as biocrude but also gases and an aqueous phase [285]. In this study, it is assumed that 2,000 T (dry basis) of biomass is processed .A diluent yield of 28600 kg/hr was estimated on Aspen Plus for the HTL case [754]. Since for HTL no extra drying is necessary after cultivation, the feedstock fed into the HTL reactor is 20% dry content. Thus about 80% of the water can be recycled after the cooling and depressurization of the reaction effluents [757]. The remaining water is sent to a wastewater treatment plant. The direct water footprint generated by HTL is affected by the cooling system and the boiler feed water, since these systems consume high amounts of water. Zhu et al. show that the differences in water requirement for the cooling system and boiler feed are negligible regardless of feedstock, and thus in this study we used their water consumption values for the cooling system and boiler feed [567]. HTL also indirectly requires water for the electricity necessary to operate the equipment. However, electricity can be generated by burning the methane-rich off-gas, and this energy can be used in the HTL system, thereby reducing indirect water consumption [567]. Table 37 shows the water requirements for HTL of algae. With the higher heating value (HHV) of diluent at approximately 34 MJ/kg, when all the factors shown in plus the hydrotreating factors are considered and all their contributions are added, the total water footprint from production of diluent through HTL is approximately 0.20 L/MJ of diluent.

Table 37: Water requirement for the HTL of algae

Operation	Value	Unit	Source
Cooling water makeup	4.32	L water/kg diluent	[567]
Boiler feed water makeup	0.72	L water/kg diluent	[567]
Water purged/day	1.17	L water/kg algae	[567]
Feed pre-treatment	4.3	MWe	This study
Steam reforming	1.28	MWe	This study
Other auxiliary	0.11	MWe	This study
Electricity generation	-1.9	MWe	This study
Water consumption factor for electricity generation	1.08	L water/kWh	[758, 759]

8.5 Upgrading of bio-oil/biocrude

The bio-oil and biocrude produced during fast pyrolysis and HTL, respectively, go through the hydroprocessing phase to remove oxygen and increase the stability and heating values of the products, which make them more attractive commercial options. These reactions use hydrogen and a catalyst [654], which contribute to the water footprint of the process, due to the steam reforming involved in the production of hydrogen. The most traditional hydroprocessing method is the one used to convert bio-oil/biocrude to biofuel, which requires hydrotreating or hydrocracking, depending on the thermochemical conversion pathway [742, 760-763]. However, for the production of diluent, only hydrotreating is required. Conditions for the hydrotreating of fast pyrolysis and HTL products are slightly different, since they have different characteristics. The water requirements for the hydrotreating of bio-oil generated through fast pyrolysis are shown in Table 38.

Table 38: Water requirement for hydroprocessing after the pyrolysis of algae

Operation	Value	Source
Cooling water required (L water/kg diluent)*	0.08	[762]
Boiler feed required (L H_2O/kg diluent)*	0.82	[762]
Natural gas (MJ/kg diluent)*	12.18	[762]
Electricity (kWh/kg diluent)*	0.410	[762]
Water use factor (L H_2O/kWh)	1.08	[758, 759]

*Derived based on the values for hydroprocessing bio-oil to biodiesel

For the upgrading of biocrude from HTL, the body of knowledge is still limited. Studies have been conducted in this area by Elliot et al., Elliott, Kumar et al., and Tews et al. [137, 680, 709, 756]. No large-scale facility has been built for this purpose, but the hydrotreating process for HTL products is in theory simpler than the hydrotreating process for fast pyrolysis products, since biocrude has a lower oxygen content than bio-oil [764]. Biocrude goes through only one hydrotreating step and requires less energy and reactant than the hydrotreating of bio-oil [765], which requires two steps. In the developed process model, the hydrotreating of biocrude involves a reaction of hydrogen in a fixed bed reactor at temperatures around 400 ^oC; around 78-85% of the product has diluent properties. The main parameters of the reaction are given in Table 39.

Table 39: Parameters of hydroprocessing after the HTL of algae

Operation	Value	Unit	Source
Light hydrocarbons	0.008	wt%	This study
Diluent	0.815	wt%	[766]
Electricity	3.8	MWe	This study
Water consumption factor for electricity generation	1.08		[758, 759]

8.6 Gasification

The gasification of biomass is a thermochemical conversion process that converts feedstock into gaseous products through reactions in high temperatures (up to 850 ^{o}C) and atmospheric pressure. Biomass enters the system at 5-10% moisture content. Oxygen (or steam) and a catalyst agent are also used in the reaction [767]. Gases such as CH_4, H_2, CO_2, and CO are produced from the gasification reaction, as are tar and char. The hydrogen concentration can be increased through reforming and shift conversion [768]. In this study, the estimated hydrogen yield through gasification is 6475 kg/hr. An earlier study of the gasification process and the current status of production and water use in a hydrogen plant gives details on losses due to blowdown and evaporation. These losses are assumed to remain constant for the entire stream (from drying to output of final product) and are estimated to be around 2.2% of the flow [717]. The indirect water footprint from the electricity required to operate the equipment in the plant can be offset by the electricity generated in the steam plant, which uses off-gases from the gasification process. It is estimated that of the approximately 35 MWe necessary to operate the facility, only about 10 MWe needs to be extracted from the grid. The details of the water requirement for the different operations involved in the gasification of algae are provided in Table 40.

Table 40: Water requirement for the gasification of algae

Operation	Value	Unit	Source
Cooling water and utilities*	1.78	L H_2O/kg H_2	[717]
Steam system and power generation*	0.49	L H_2O/kg H_2	[717]
Gas clean-up and compression*	1.48	L H_2O/kg H_2	[717]
Gasification and tar reforming*	0.05	L H_2O/kg H_2	[717]
Drying and handling*	20.96	L H_2O/kg H_2	[717]
Feed handling and drying	742	kW	[717]
Gasification, tar reforming, quench	3,636	kW	[717]
Compression and sulphur removal	21,871	kW	[717]
Steam methane reforming, shift, and PSA	630	kW	[717]
Hydrogen compression	3,899	kW	[717]
Steam system and power generation	-25,583	kW	[717]
Steam system and power generation – required	660	kW	[717]
Cooling water and other utilities	1,110	kW	[717]
Miscellaneous	3,255	kW	[717]
Water consumption factor for electricity generation	1.08	L H_2O/kWh	[758, 759]

*Water consumption derived from the flow rates of the plant described by Spath et al. [717]

With the higher heating value (HHV) of hydrogen at approximately 34MJ/kg, when all the factors shown in Table 7 are considered and their contributions are added, the total water footprint from the production of hydrogen through gasification is approximately 0.19 L/MJ of hydrogen.

8.7 Hydrothermal gasification

HTG is a thermochemical conversion pathway that uses the benefits of supercritical conditions of water in a solution as a reactant, making water itself a reaction partner to the feedstock. First, the bonds between the biomass macromolecules are broken through hydrolysis, then new molecules are formed in the presence of a catalyst agent [352]. The reaction normally happens at intermediate temperatures (300-410 ^{o}C) and high pressures (12-34 MPa), while the biomass initial concentration remains between 10 and 30 wt% [432] (for this study it is assumed to be 20 wt% after the cultivation phase). Generally, the product yield (syngas) from HTG is considerably higher than from gasification, and in this case was estimated at 9285 kg/hr. Syngas is then purified into H_2. The syngas is cleaned using Selexol and then sent to water-gas shift reactors to enrich the H_2. A co-generation facility for power generation is also commonly built with the HTG plant [570, 769, 770]. The co-generation plant uses off-gases from processing areas to produce electricity [570].

In terms of the direct water consumption, it was assumed that the tar reforming and gas compression phases had footprints comparable to their counterparts in the gasification pathway. The cooling system, steam feed, and HTG reaction estimates are taken from Matsumura, whose study considers different types of biomass [569]. These values are assumed to have a negligible difference compared to those for algae biomass. The indirect water footprint from electricity consumption was estimated through the developed process model for all the equipment necessary to run the plant. Interestingly, the power generation possible in an HTG facility is so high that it compensates for the power requirement of the entire plant, making it possible to sell energy to the grid and consequently lead to a slightly negative water footprint in terms of the balance between electricity consumed and generated. Table 41 gives the details of the water requirement for different operations for the HTG of algae.

Table 41: Water requirements for the hydrothermal gasification of algae

Operation	Value	Unit	Source
Cooling, steam, and HTG reaction	8.06	L H_2O/kg H_2	[569]
Tar reforming	0.049	L H_2O/kg H_2	[717]
Gas clean-up and compression	1.23	L H_2O/kg H_2	[717]
Hydrogen/syngas ratio	9.3		This study
Total plant power requirement	74662	kW	This study
Generated power	-92,462	kW	This study
Grid electricity requirement	17,800	kW	This study
Water use factor	1.08	L H_2O/kWh	[758, 759]

With the higher heating value (HHV) of hydrogen at approximately 142 MJ/kg, when all the factors shown in Table 8 are considered and their contributions added, the total water footprint from the production of hydrogen through HTG is approximately 0.05 L/MJ of hydrogen.

8.8 Results and discussion

Base case scenarios were developed to understand the water footprints of each cultivation method coupled with each conversion pathway. We compared algae cultivation methods and thermochemical conversion pathways according to their final results for the unit operations and the final water requirement for each base case scenario. We then varied the values of some input variables within a specified range so that the most significant ones could be identified. Lastly, an uncertainty analysis was conducted through a Monte Carlo simulation to estimate changes in results from the uncertainty of the inputs.

8.8.1 Base case scenario

The base case scenarios give the details of individual unit operations: biomass production and dewatering, harvesting, bio-oil or biocrude production followed by hydrotreating (fast pyrolysis or HTL) or hydrogen production (gasification and HTG). Different process unit operations for diluent production through fast pyrolysis and HTL, respectively, are listed in Table 42. Table 43 shows the results of water use efficiency for the unit operations in the production of hydrogen through gasification and HTG, respectively.

Table 42: Life cycle water footprint for the conversion of algae biomass to diluent

Unit operation (L H_2O/MJ diluent)	Pond cultivation followed by pyrolysis	PBR cultivation followed by pyrolysis	Pond cultivation followed by HTL	PBR cultivation followed by HTL
Biomass production	137.67	2.24	133.95	2.18
Biomass harvesting and fertilization	0.007	0.001	0.008	0.002
Conversion	0.071	0.071	0.19	0.19
Hydroprocessing	0.046	0.046	0.013	0.013
Total	137.79	2.36	134.15	2.20

Table 43: Life cycle water footprint for the conversion of algae biomass to hydrogen

Unit operation (L H_2O/MJ hydrogen)	Pond cultivation followed by gasification	PBR cultivation followed by gasification	Pond cultivation followed by HTG	PBR cultivation followed by HTG
Biomass production	141.94	2.31	99.43	1.61
Biomass harvesting and fertilization	0.001	0.001	0.001	0.002
Conversion	0.19	0.19	0.05	0.05
Total	142.13	2.50	99.48	1.66

The difference in water consumption for algae cultivation compared to every other unit operation is huge. In fact, it is more than 99% of the total consumption whether ponds or PBRs are used. Hence, any future system modelling aiming for lower water consumption rates must focus primarily on the cultivation side. The results show much higher water consumption in the algae biomass derived from pond cultivation than from PBRs. This was expected since photobioreactors offer a more controlled setting, where evaporation is negligible. Waste through blowdown and harvest are also significantly lower in PBRs than in ponds. On the other hand, the water footprint of PBRs from electricity use is considerably higher than that of ponds. This could be due to the high electrical demand for the equipment used in PBR cultivation (i.e., lighting, compressors, etc.). The higher electricity consumption in PBRs, however, is not enough to compensate for the high water footprint from the cultivation of algae in ponds. It is noticeable that the footprints of the thermochemical conversion methods are very small compared to the footprint of the cultivation phase. This is because the standard for any thermochemical plant design includes many opportunities for water recycling, and the concentration of algae in the solution that enters the plant is considerably higher than during cultivation. It is clear from the results that water consumption mitigation steps are important in the algae thermochemical conversion life cycle. Work by Yang et al. suggests means of achieving some reduction goals and reducing water consumption by up to 80% [771]. Some measures that could mitigate the water footprint of algae cultivation include designing a system that includes feedback piping (to recycle water to other parts of the system) and developing a more efficient system that does not require large amounts of water.

The electricity consumption is less than the electricity generated for hydrothermal gasification, which results in a water footprint of -0.015 L H_2O/MJ hydrogen. This causes the water consumption footprint of HTG to be lower than in the other thermochemical conversion pathways. This is because the power generation of the hydrogen plant works in conjunction with the HTG facility. The water consumption footprint of gasification and HTG is generally lower per unit of energy produced because the higher heating value of hydrogen (142 MJ/kg) is much higher than that of diluent, a low energy product of approximately 34 MJ/kg.

8.8.2 Other scenarios – Sensitivity analysis

The effects of the main inputs and contributing factors on the study results were analyzed by introducing different scenarios within specified ranges. Table 44 lists all the considered scenarios in this study for an analysis of ponds and PBRs.

Table 44: (a) Scenarios for sensitivity analysis of ponds, (b) Scenarios for sensitivity analysis of PBRs

a. Scenarios for sensitivity analysis of ponds	
1	Decrease in pond depth design by 10%
2	Increase in pond depth design by 10%
3	Decrease in evaporation rate/day by 10%
4	Increase in evaporation rate/day by 10%
5	Decrease in replacement of media by 10%
6	Increase in replacement of media by 10%
7	Decrease in media loss at harvesting by 10%
8	Increase in media loss at harvesting by 10%
9	Decrease in the number of days of harvest/year by 10%
10	Increase in the number of days of harvest/year by 10%
11	Decrease in product yield (for all thermochemical conversion methods) by 10%
12	Increase in product yield (for all thermochemical conversion methods) by 10%

b. Scenarios for sensitivity analysis of PBRs	
1	Decrease in PBR tank size by 10%
2	Increase in PBR tank size by 10%
3	Decrease in media loss at harvesting by 10%
4	Increase in media loss at harvesting by 10%
5	Decrease in the number of harvests/day by 10%
6	Increase in the number of harvests/day by 10%
7	Decrease in electricity consumption by 10%
8	Increase in electricity consumption by 10%
9	Decrease in harvest volume by 10%
10	Increase in harvest volume by 10%
11	Decrease in product yield (for all thermochemical conversion methods) by 10%
12	Increase in product yield (for all thermochemical conversion methods) by 10%

Figures 49 to 52 show the sensitivity analysis results for the four thermochemical conversion methods and two cultivation options.

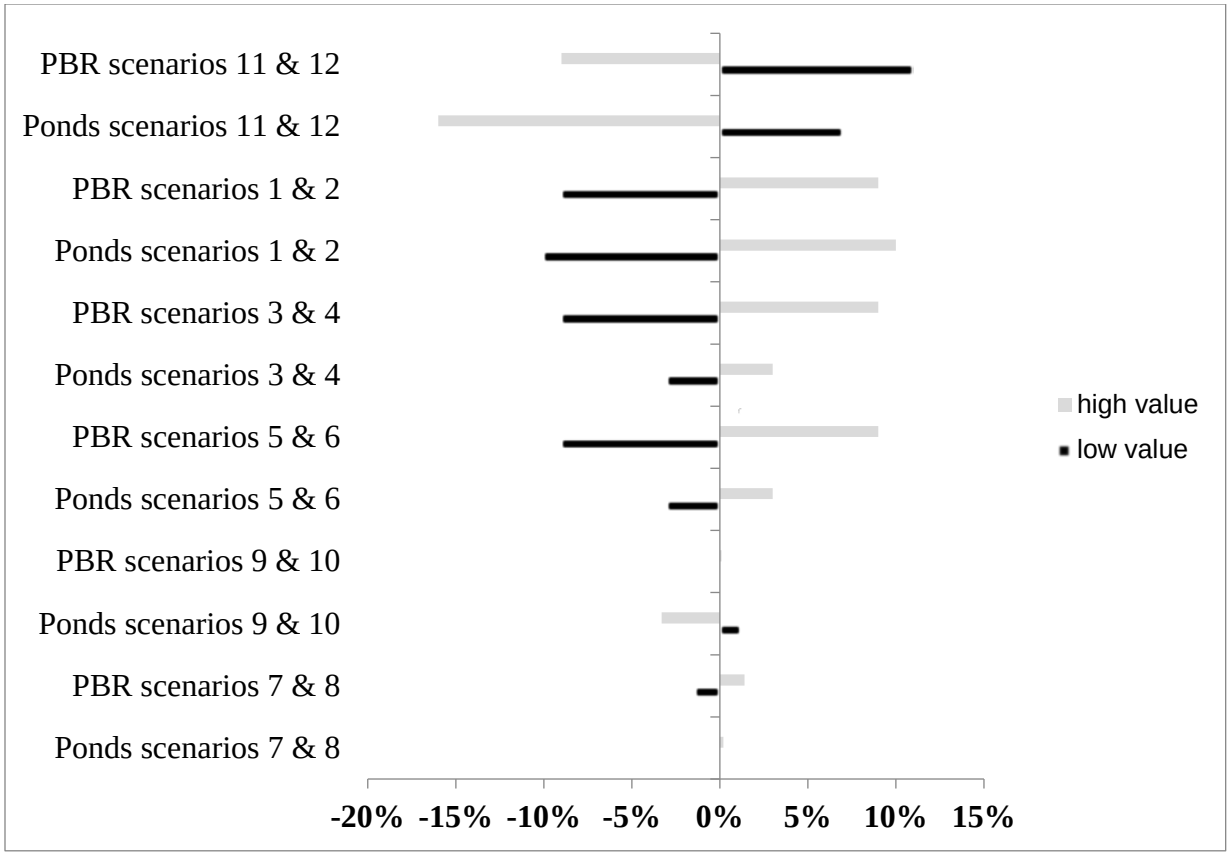

Figure 49: Sensitivity analysis for algae conversion to diluent via pyrolysis

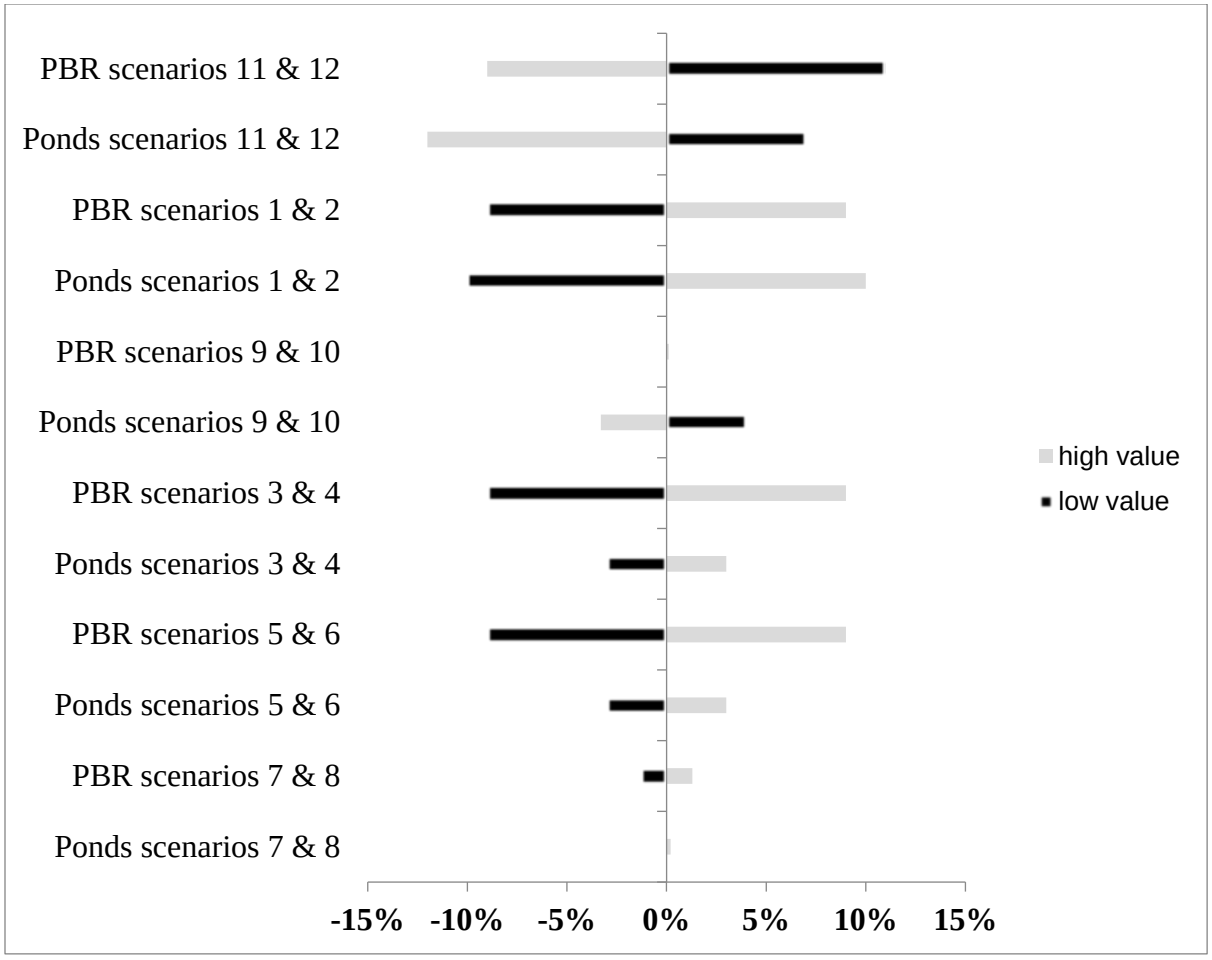

Figure 50: Sensitivity analysis for algae conversion to diluent via HTL

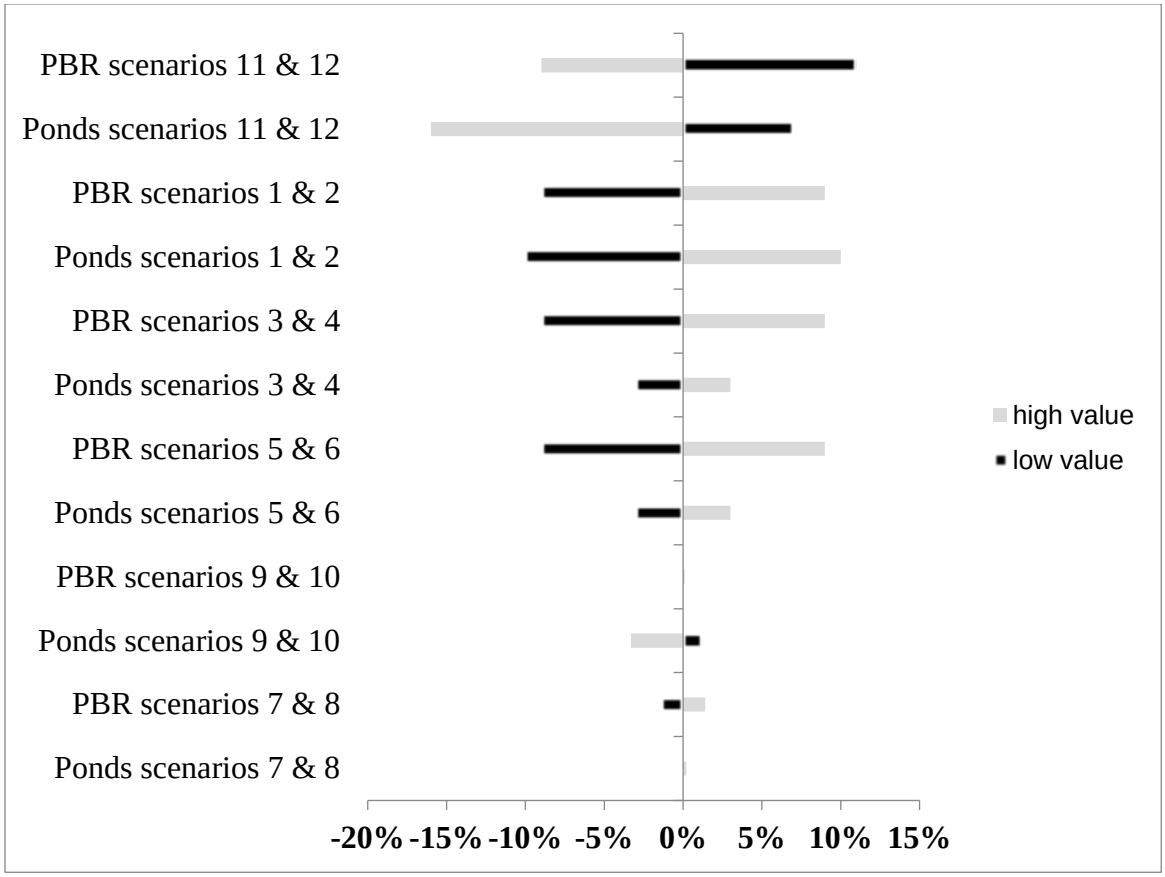

Figure 51: Sensitivity analysis for algae conversion to hydrogen via gasification

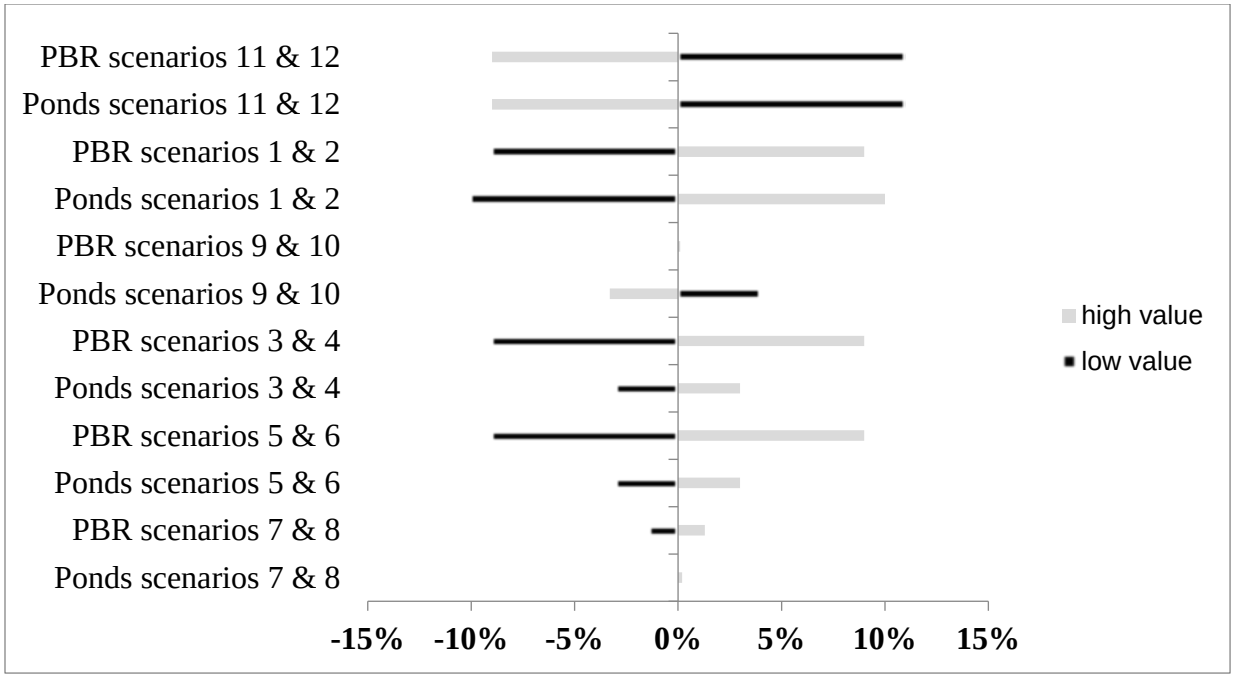

Figure 52: Sensitivity analysis for algae conversion to hydrogen via HTG

The results presented in the base case scenarios clearly show that biomass cultivation is the unit operation with the highest water footprint, in an order of magnitude of almost 1000:1 to any other variable. Therefore, it makes sense that any sensitivity analysis should focus on cultivation parameter variations and their impacts in final outputs. Since large design changes to a system are not always practical [772], for this sensitivity analysis it was assumed that none of the input variations were below -10% or above 10%.

From the results, it is noticeable that five inputs for ponds and five for PBRs were significant when varied by 10%. Only two areas did not change the results significantly, media harvesting for ponds and harvest volume for PBRs. Almost all input variables chosen for the sensitivity analysis directly affect the results, meaning that a positive variation to the input led to an increase in water footprint. The only exceptions were the yield of the desired product and the yearly cultivation period for ponds. Unlike in ponds, where water footprint-related electricity consumption is minor, the electricity consumption of PBRs is a matter of concern. In fact, the sensitivity analysis showed a minor contribution of the electricity consumption to the outcome of the water footprint in PBRs (a variation of around 1.5%). This variation might not be as high as the ones generated by some other inputs, but it was significant enough to be considered in the uncertainty analysis.

8.9 Uncertainty analysis

For this study, an uncertainty analysis was conducted using a Monte Carlo simulation. The simulation was done through a ModelRisk software execution (as described by Vose et al. and Habibi [773, 774] that randomly selected variables within the established range of 100000 iterations. When the relationship between variables is known and there are uncertainties in both

published and estimated information, a triangular probability distribution is commonly adopted, since in a distribution of this type the central value is estimated while the maximum and minimum values are fixed. This distribution is used for every input considered in the uncertainty analysis. The triangular distribution also assumes that the majority of the data is centered around the estimated value.

Uncertainty is commonly estimated by identifying the significant inputs through sensitivity analyses and then assigning a suitable uncertainty to each based on the information available. In this study, significant inputs with known estimated uncertainty ranges were varied during the Monte Carlo simulation. Significant inputs with unknown uncertainty had ranges of ±10% attributed to them. Table 45 shows the water use efficiency values for diluent from fast pyrolysis and HTL at various percentiles. Table 46 shows the water use efficiency values for hydrogen from gasification and HTG, also at various percentiles. The low deviation from the median of each case can be seen by calculating the difference between the median and the values on both extremes for a particular case. For example, for the fast pyrolysis of algae grown in ponds, the deviations for the 5% and 95% extremes from the median are -9.81% and 10.88%, respectively. For the gasification of algae produced in photobioreactors, the deviations for the 5% and 95% extremes from the median are -10.38% and 11.63%, respectively. With all the uncertainties in the variables considered in the Monte Carlo simulation, the results on the 50% mark were very close to the results obtained in the base case scenarios. There were some (negligible) deviations of a few percentile points from the original cases. It is also noticeable from Tables 45 and 46 that the spread of results is concentrated around the median. Therefore, the results of this study for the base case scenarios can be considered accurate considering the uncertainty of the inputs used.

Table 45: Percentile values of uncertainty distribution plots for diluent production

	Water use efficiency of diluent production via fast pyrolysis and hydroprocessing		**Water use efficiency of diluent production via HTL and hydroprocessing**	
Percentile	**Ponds L H_2O/MJ diluent**	**Photobioreactors L H_2O/MJ diluent**	**Ponds L H_2O/MJ diluent**	**Photobioreactors L H_2O/MJ diluent**
5%	124.09	2.10	121.60	1.95
15%	128.78	2.18	125.44	2.02
25%	131.75	2.23	127.76	2.07
50%	137.60	2.33	133.99	2.16
75%	143.67	2.43	139.83	2.26
85%	146.94	2.48	142.90	2.30
95%	152.44	2.56	148.18	2.37

Table 46: Percentile values of uncertainty distribution plots for hydrogen production

	Water use efficiency of hydrogen production via gasification		Water use efficiency of hydrogen production via HTG	
Percentile	Ponds L H_2O/MJ diluent	Photobioreactors L H_2O/MJ diluent	Ponds L H_2O/MJ diluent	Photobioreactors L H_2O/MJ diluent
5%	129.25	2.23	89.28	1.48
15%	133.64	2.31	92.63	1.53
25%	136.44	2.36	94.77	1.57
50%	141.87	2.47	98.94	1.64
75%	147.46	2.58	103.33	1.71
85%	150.54	2.63	105.68	1.75
95%	155.58	2.71	109.70	1.80

8.10 Conclusion

Water may be abundant in many locations, but it is a very valuable resource. Since other uses of water take priority over biomass production, it is important to reduce water consumption in this activity. The cases of algae cultivation explored in this study present challenges considering the high amount of water used in the production of diluent and hydrogen. The process that requires the most water is the cultivation phase, which is responsible for more than 99% of consumption. This study develops life cycle water footprints including the detailed unit operations involved in pathways. The study also shows that a viable cultivation method based on photobioreactors uses less water than ponds to produce algae. While PBRs are more expensive and complex than ponds, they offer savings in water consumption, nutrients, and land required, which could make them a feasible alternative. In all pathways studied, the water footprint for algae cultivated in PBRs was less than 25% of that for ponds. The difference between different thermochemical conversion methods when the same cultivation method is considered tends to be small, though not negligible. The thermochemical conversion pathway with the lowest water footprint was HTG, with about 60% of the footprint of HTL (the one with highest footprint).

In the future, with increasing demand from industry for products derived from biomass with a lower carbon footprint, algae are one of the likeliest prospects. Some of the technologies discussed in this paper are still novel and can be improved on many levels (economic, resources required, efficiency, etc.). The results presented in this study will help others understand the resource allocation necessary for algae cultivation and processing, which in turn will help to make better choices on areas to invest or formulate policy.

9 Comparative Life Cycle Assessment of Fuel and Chemical Production from Microalgae Cultivated in Canadian Open Raceway Ponds and Photobioreactors

Life cycle assessment (LCA) is a useful tool to evaluate the environmental impacts associated with a product, process, or service. This section aims at estimating life cycle GHG emissions associated with diluent and hydrogen production from microalgal systems through thermochemical technologies in Western Canada. Using theoretical models, a cultivation system of microalgae at industrial scale of 2,000 tonnes/day in open raceway ponds and photobioreactors is presented for processing biomass into hydrogen and diluent. A number of conversion pathways for the biomass are considered with varying results owing to differences in production technologies and assumptions. The specific objectives and uniqueness of this study are to:

- Conduct a comparative LCA based on the conversion of microalgae feedstock cultivated in ORP and PBR systems in Canada via hydrothermal liquefaction and pyrolysis to produce diluent; and via hydrothermal gasification (HTG) and thermal gasification (TG) to produce hydrogen;
- Provide GHG emissions information to the Canadian and Alberta governments, as well as to commercial investors to help them make better informed decisions related to industry investments, financial matters, and legislation.

9.1 Method

An LCA, according to the ISO 14040/44 principles. framework, and guidelines, is developed to evaluate energy and GHG emissions [831, 832]. LCA involves the identification and quantification of mass and energy balances by looking at system inputs and outputs at each of the process stages to identify the associated environmental impacts.

9.1.1 Goal and scope definition

The goal of the current LCA study is to evaluate and compare two algae cultivation scenarios and four thermochemical conversion pathways leading to the production of diluent and hydrogen. Each activity involved in these processes is energy intensive and has associated GHG emissions. The LCA follows an “attributional” approach wherein environmental impacts are evaluated by introducing changes to a process, thereby providing comparative results based on a 100-year time horizon. The engineering models of diluent and hydrogen production from the microalgae are used to conduct LCAs of four different conversion pathways. The analysis involved energy and material requirements for various sub-processes including cultivation, dewatering, and conversion systems for all pathways studied.

The LCA is set in the geographical context of Fort Saskatchewan, AB. The region is recognized for the energy-intensive industrial petrochemical processing facilities associated with oil sands activities. Figure 53 shows the main systems included in the assessment. The functional unit to which the input and output requirements are scaled up is 1 MJ of energy. Together with LCA, the net energy ratio (NER) is determined as the ratio of output energy to input fossil-fuel energy. The current calculations do not include the environmental impacts associated with the initial construction of the algae cultivation ponds and photobioreactor systems.

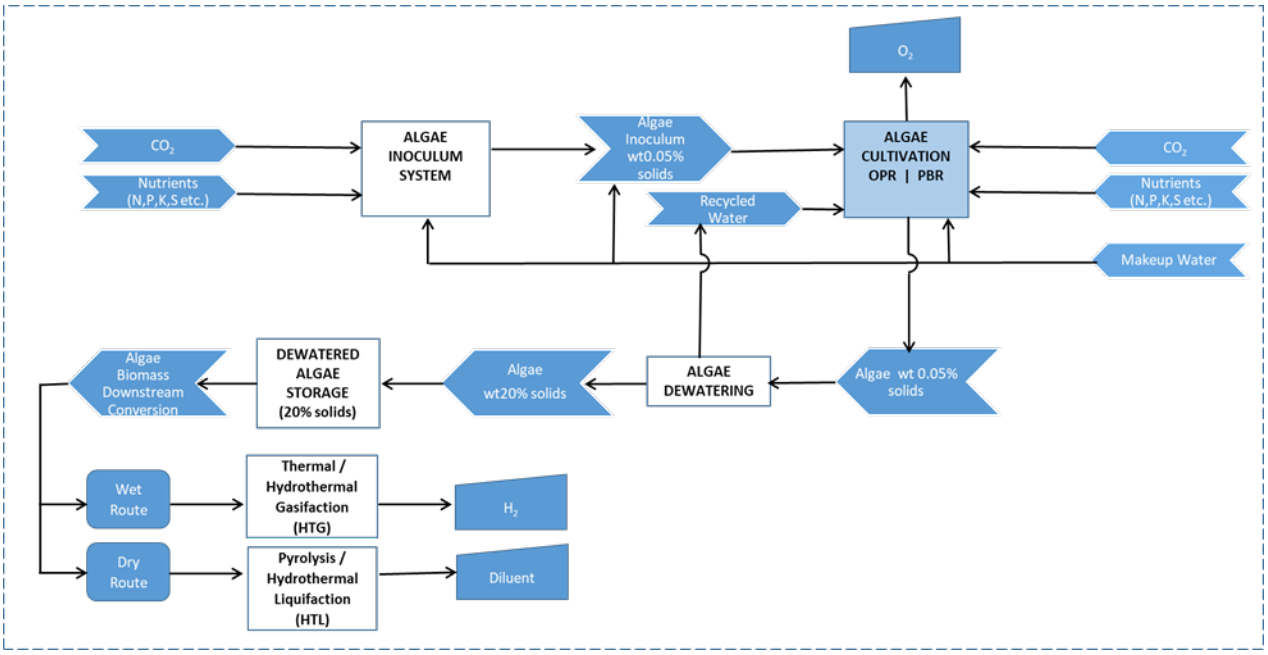

Figure 53: System boundary of thermochemical pathways considered for diluent and hydrogen production

9.1.2 Life cycle inventory assessment

A life cycle inventory assessment was conducted for all stages from algae cultivation to thermochemical processes that deliver 1 MJ of product. Algae cultivation has been modeled around ORP and PBR systems. Much of research to date for algae-to-energy systems has been conducted at bench to demonstration scale [833].

Microalgae are cultivated in an aqueous media. Nutrients such as carbon dioxide (CO_2) derived from local industry, nitrogen (N), and phosphate (P), as well as light and temperature are required to support algae growth. Diammonium phosphate (DAP), a commercial fertilizer, is considered the source for P and ammonia (NH3) for nitrogen (N). The inventory calculations include the upstream GHG emissions associated with the production of these fertilizers. GHG emissions from direct land use, water use in algae cultivation, dewatering via settling, and the use of ultrafiltration and centrifugation produce biomass with 20% solids are evaluated. GHG emissions from the use of equipment such air compressors for sparging CO_2 into the media, pumps and paddlewheels for circulation, LED lighting in the PBR system to promote growth, and algae processing are included. Table 47 provides a summary of parameters and input requirements considered in the inventory assessment. Productivity is based on experimental lab scale results. Land and water requirements are based on productivity, site climatic conditions and assumptions related to cultivation operations. Water loss due to blowdown is related to replacement of media to prevent buildup of ion concentrations within the media.

Table 47: Data related to the production of 1 kg of algal biomass

Parameters	OPR	PBR	Units
Productivity	5.8	1825	g/L//yr
Land	1.24	0.00048	m^2/kg/yr
Water	1.06	0.023	m^3
Cultivation period	203	365	d//yr
Water loss – evaporation	0.5	0	%/d
Water loss – blowdown	0.5	0.5	%/d
Water loss – harvesting	0.2	0.2	%/harvest/tonne
Harvests	11	365	#/year
Potential for cultivation crash	5	1	%

The ORP system was modeled using Olivares et al.'s values [834] and extrapolated using site-specific satellite climatic data from the predictive analytical model developed by Pankratz et al. [835]. The ORP operating performance was predicted based on Fort Saskatchewan metrological data including local daily temperature and irradiance values. 80% of the OPR algae was harvested when densities rose to 0.5 g/L cell density at which time pond algae density was returned to 0.2 g/L.

The PBR system input and output requirements are determined based on a unique columnar photobioreactor design [836] providing a fully controlled algae growth environment. CO_2 is sparged into the PBR providing both access of photons of light to penetrate deeper into the media and also continuous mixing of media for nutrient exchange. Lighting is provided by flashing tuned LEDs providing photons at wavelengths that optimize growth. Under these optimized conditions, cultivation yields are predicted at 5 g/L/day. The productivity associated with this particular design would be consistent with other high density productivity as described by Apel et al [613] and Mata et al [49].

Furthermore, since PBR systems are enclosed, negligible evaporative water loss takes place. Apart from water losses due to evaporation, blowdown, and harvesting, water and remaining nutrients are recycled into the cultivation system. CO_2, N, and P were modeled to be provided at 20% surplus over actual cultivation requirements. Harvesting the PBR biomass is semi-continuous; 10% of the biomass is removed for processing every 2.4 hours, thereby holding cell density at approximately 5 g/L. Dewatering the algae feedstock after cultivation in both ORP and PBR systems follows literature values provided by Davis et al. [837]. The algae biomass undergoes settling through a hollow fiber membrane ultrafiltration process followed by centrifuging to concentrate the biomass to 200 g/L in preparation for downstream thermochemical conversion (described later in this study).

As seen in Table 48, the key energy requirements from the technosphere are related to system operations including the paddlewheel, sparging, dewatering pumps, and LED lighting. In this study, the 2016 Alberta electricity generation mix emission intensity factor of 0.83 kg/kWh was considered [838]. Given the large areas of land that may be impacted if algae cultivation for 2000

tonnes dry biomass takes place using ORP systems, this, too, is given consideration in the study. Transportation is not included in the scope of this study since the selected location for the algae cultivation is modeled adjoin the refineries that both produce the commercial nutrients and also use the biomass output of production. The focus in this study has not been placed on a specific species of algae to be cultivated given that a number of strains of algae, among thousands, have been identified for their capacity for both high growth yield and lipid content [33, 35].

Table 48: OPR and PBR system assemblies with input/output operations

ASSEMBLIES	OPR	PBR	Units
Algae inoculum system			
INPUTS			
Makeup water	0.398		m^3
Land for inoculum	0.12		m^2
Nutrients	0.24		kg
Energy – electrical	0.0257		kWh
OUTPUTS			
O_2 from hydrolysis of water	0.14		kg
Inoculum media moved to cultivation	0.214		m^3
Water loss	0.184		m^3
CO_2 lost to air	0.038		kg
N loss to water blowdown/air	0.0016		kg
Algae cultivation system			
INPUTS			
Inoculum media with water	0.214		m^3
Makeup water	2.15	0.012	m^3
Land for cultivation	1.2	0.00048	m^2
Nutrients	2.4	2.4	kg
Energy – electrical	0.257	0.785	kWh
OUTPUTS			
O_2 from hydrolysis of water	1.4		kg
Water loss	1.84	0.011	m^3
CO_2 lost to air	0.38	0.38	kg
N loss to water blowdown/air	0.016	0.016	kg
Algae dewatering – Ultra/micro filtration membrane			
INPUTS			
Cultivation media (10 g/L)	0.0155	0.0000	m^3
Energy – membrane filtration	0.11	0.020	kWh
OUTPUTS			
Algae biomass (130 g/L)	0.0012	3.8E-06	m^3
Water for recycling	0.014	0.000046	m^3
Algae dewatering – centrifuge			
INPUTS			
Algae biomass (130 g/L)	0.0012	3.8E-06	m^3
Energy – centrifuge	0.27	0.048	kWh

ASSEMBLIES	OPR	PBR	Units
OUTPUTS			
Algae biomass (200 g/L – 20% solids)	0.00078	2.5E-06	m^3
Water for recycling	0.00042	0.0000013	m^3
Algae storage – chilling			
INPUTS			
Energy – chilling biomass/kg	0.0073	0.0073	kWh
HTL conversion			
Hydrothermal liquefaction	3.50		kWh/kg
Hydrotreating	0.45		kWh/kg
Pyrolysis conversion			
Pyrolysis	11.17		kWh/kg
Hydrotreating	2.89		kWh/kg
SCWG conversion			
Gasification	13.28		kWh/kg
TG conversion			
Gasification	22.88		kWh/kg

*Units/kg dry biomass (nitrogen surplus) under lower heating value calculations. Inoculum based on 10% of cultivation values.
*Assume the use of naturally occurring algae species that performs similar to species grown in other parts of the world. Will remain dormant in ponds during winter period.

The algae cultivation model was developed to produce dry biomass at 2,000 tonnes/day incorporating design features found in the literature based on site-specific satellite meteorological data. The modeled OPR system to produce this biomass located in Alberta would encompass an area of some 82,000 ha (8.8 townships) whereas using the modeled PBRs to produce the same biomass would require approximately 50 ha. Similarly, the OPR-modeled system would require 4.3 million m^3 of water, whereas the PBR system would only require 23.2 thousand m^3. In both cases, given that every tonne of biomass requires 1.8 tonnes of CO_2, producing 660,000 tonnes biomass annually results in the uptake of nearly 1.2 MT of CO_2 [8, 106]. While published algae biomass yields vary tremendously, the model assumes that 0.1 g/L/d for the ORP systems and 5 g/L/d for the PBR systems are achievable. The downstream processing LCA calculations were made using Aspen Plus. The life cycle assessment is conducted based on the steps outlined in ISO 14040 [813]. The inventory values are translated to GHG emissions per functional unit using a IPCC one-hundred-year time horizon emissions factor [814].

9.1.3 Life cycle analysis approach

The engineering approach used to model the cultivation and downstream processing of the algae biomass followed the processes shown in the system process flow diagram (Figure 53). The model computes material and energy balances for each unit operation. The cultivation section was constructed in Excel with downstream thermochemical conversion modeled with more rigorous computations with the use of Aspen Plus software. Cultivation yields were predicted based on experimental yield data found in literature and industry interviews, coupled with stoichiometric calculations and making assumptions on suitable surplus nutrients (20%) being available to ensure maximum productivity. Where the calculated LCA outcomes are based on a certain amount of

uncertainty associated with the chosen theoretical conditions, the computed GHG emission values are useful for comparing a variety design and process configurations. They are also useful for further sensitivity analysis around high environmental emission processes where performance improvements are desired.

9.2 Results and discussion

The LCA results are summarized in this section. First, emission results for algal cultivation are discussed, by comparing unit operation environmental impact results from OPR and PBR cultivation and dewatering processes. Then unit process thermochemical conversion results are compared. The aggregate results from these comparative calculations are presented in the subsequent section.

9.2.1 Algal cultivation

The environmental impacts associated with algae cultivation in both ORP and PBR systems are discussed here. Figure 54 provides a breakdown of emissions associated with unit operations for both OPR and PBR algae production systems. For the ORP system, the GHG emissions are calculated to be 0.8 tonne/CO_{2eq}. Fertilizer accounts for 0.24 tonne/CO_{2eq} (30%) and electricity 0.56 tonne/CO_{2eq} (70%); water use was calculated at a factor of 1.9E-5 T CO_{2eq} (<1%). The calculated net result would be 1.0 tonne of CO_2 removed from the atmosphere.

For the PBR cultivation system, the profile is similar, with GHG emissions of 0.9 tonne/CO_{2eq}. Fertilizer again accounts for 0.22 tonne/CO_{2eq} (23%) and electricity 0.71 tonne/CO_{2eq} (76%); water use was calculated at a factor of 1.0E-7 tonne/CO_{2eq} (<1%) (EcoInvent – SimaPro). The calculated net result would be 0.9 T of $CO_{2\text{-}eq}$ removed from the atmosphere for every T biomass produced. Under both scenarios, we see that electricity still accounts for the majority of the energy requirements associated with the algae cultivation processes. Although the electricity use differs significantly, outcomes are relatively close.

In the case of OPR systems, the paddlewheel and pumping systems involved in moving water long distances because of the vast areas required for the pond systems comes relatively close to the relatively minor use of pumps, but a much greater amount of energy is required to drive the artificial lighting systems. In spite of these details, the results remain better than those published by Verma et al. at 0.42 and 0.39 tonne of CO_{2eq} removed from the atmosphere for every tonne biomass produced based on using *Nannochloropsi sp* and *A. platensis* algae species [782].

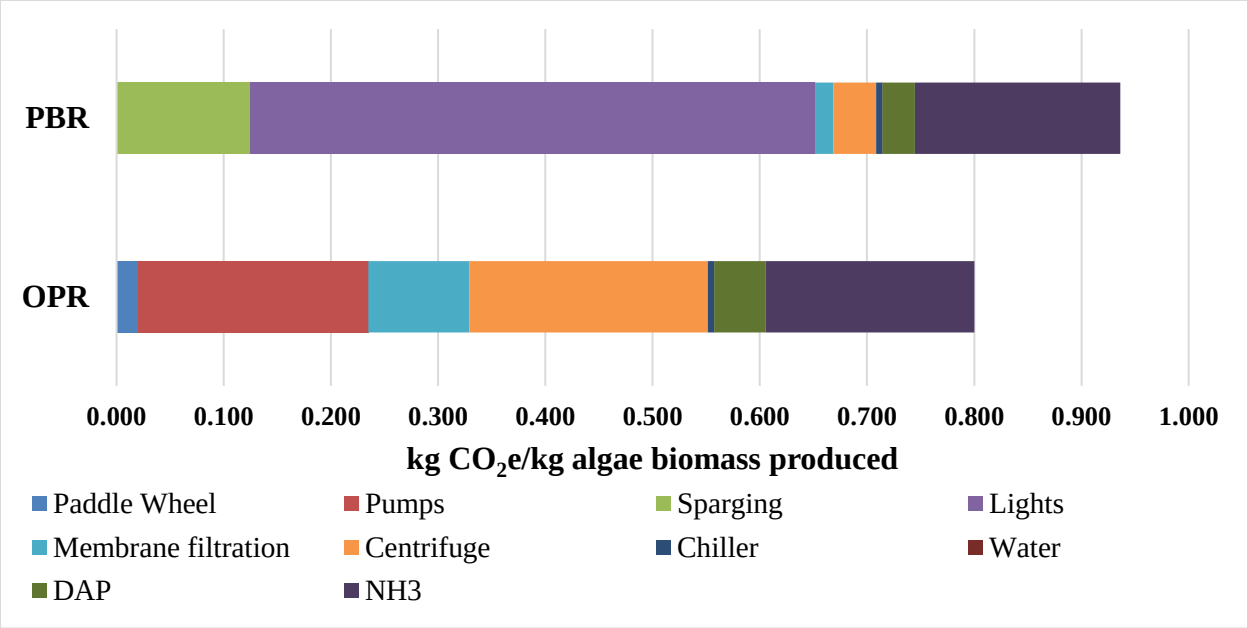

Figure 54: Algae biomass production – CO_{2eq} emissions by factor

Because of the commercial scale of the operations modeled, it is also useful to compare CO_2 sequestration through algae cultivation with carbon sequestration from existing forests in the region. Spruce and aspen trees may be harvested every 80 years and yield 180 m^3/ha or 2.25 m^3/yr where 1 m^3 of wood has approximately 200 kg C [839]. This calculates to 0.265 kg CO_2 sequestered m^2/yr. For our modeled OPR algae cultivation system, 0.804 kg CO_2 is sequestered at m^2/yr, representing an approximate 5-fold increase in CO_2 sequestration. The PBR system results in 2008 kg CO_2 sequestered at m^2/yr or an approximate 12,174-fold increase in CO_2 sequestration.

9.2.2 Process conversion

The GHG emissions for algal biomass diluent production from HTL and pyrolysis, as well as hydrogen production from SCWG and TG, are discussed in this section. The GHG emissions from the HTL pathway are 29.6 g $CO_{2\text{-eq}}$/MJ, as shown in Figure 55. 60.13% of these GHG emissions are from the hydrothermal liquefaction unit and the rest from the hydrotreating section of the hydrothermal liquefaction plant. The high energy consumption in the high temperature and pressure reactor in the HTL plant is attributed to higher GHG emissions than the hydrotreating plant. Diluent production through HTL has advantages in that it can use high moisture containing microalgae, thereby avoiding energy and corresponding emissions pertaining to microalgal drying. The GHG emissions for a fossil-fuel based product are more than 67% (90.8 g $CO_{2\text{-eq}}$/MJ) higher than HTL diluent [840].

The pyrolysis pathway results in 81.1 g$CO_{2\text{-eq}}$/MJ of diluent when algal biomass is used. For pyrolysis, microalgae conversion incorporates two main processes, both of which are energy intensive: microalgae drying and heat requirement in the pyrolysis reactor using natural gas. Together these have a direct environmental impact and make up 64.7% of global GHG emissions. The hydrotreating plant contributes 35.3%, more than HTL does, due to the requirement for a two-step hydrotreating process in pyrolysis. If char is used instead of natural gas for heat supply from

pyrolysis, the GHG emissions are reduced to 51.3 $gCO_{2\text{-}eq}$/MJ of diluent. HTL offers better environmental performance than pyrolysis, mainly due to the requirement for dry biomass and the excessive energy demand in the pyrolysis reactor.

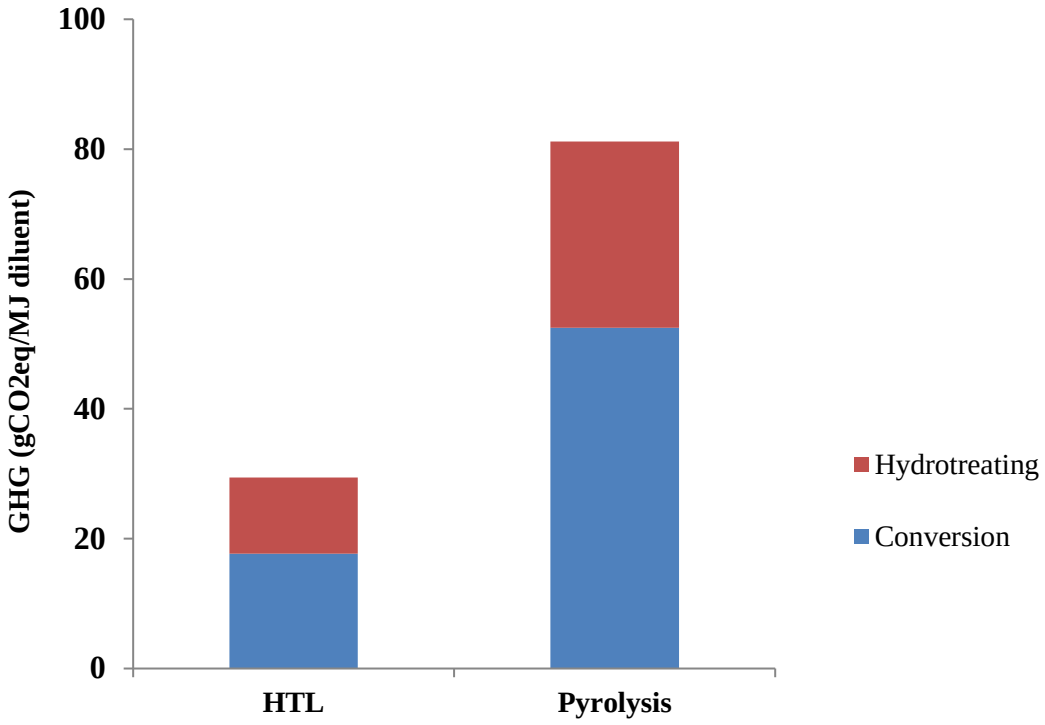

Figure 55: Breakdown of GHG emissions for HTL and pyrolysis for diluent production

For hydrogen production, the SCWG pathway results in lower GHG emissions than TG, as shown in Figure 56. Hydrogen production through SCWG emits GHGs of 28.5 g $CO_{2\text{-}eq}$/MJ of hydrogen. SCWG uses high moisture containing biomass such as microalgae, thereby reducing energy and corresponding emissions pertaining to microalgal drying. Microalgae conversion through the TG pathway has higher GHG emissions (173.8 $gCO_{2\text{-}eq}$/MJ) as it involves the drying process, which is energy extensive. The use of hydrogen for drying in thermal gasification reduces the GHG emissions to 133.2 $gCO_{2\text{-}eq}$/MJ.

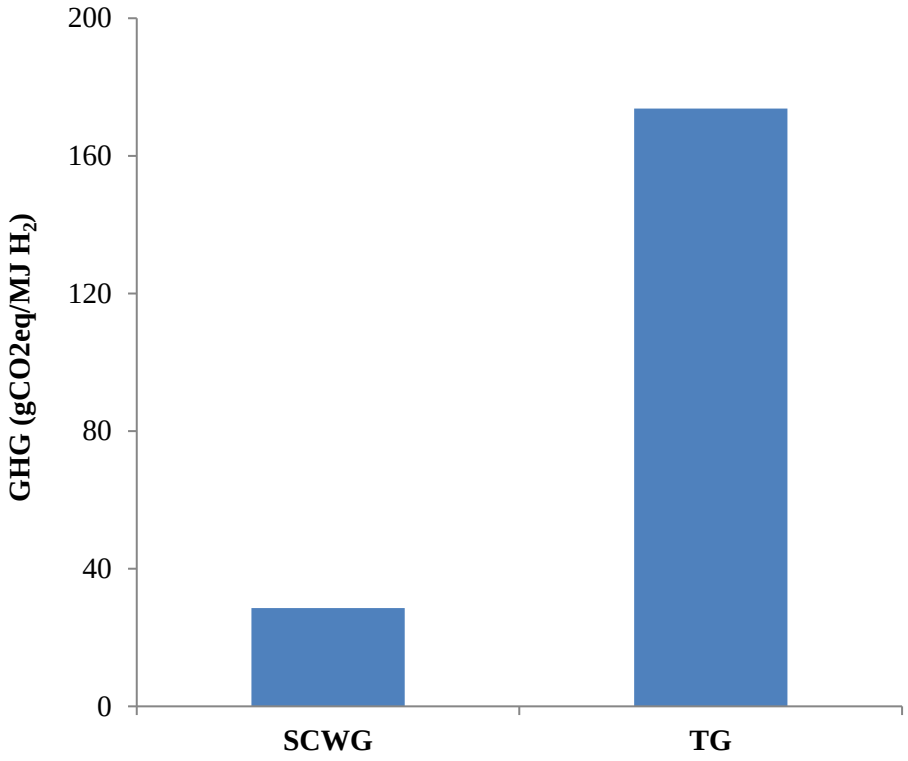

Figure 56: GHG emissions from SCWG and TG for hydrogen production

9.2.3 Combined LCA

The state-of-the-art development of thermochemical technologies for microalgae to desired products requires an evaluation with respect to the global warming potentials of these technologies. LCA allows us to compare various sub-processes in an entire process to understand and quantify GHG emissions. The combined results for algal thermochemical conversion systems including growth, cultivation, and conversion systems for diluent and hydrogen production are summarized in Table 49. In general, the global warming potential values for algal-based fuel systems report a wide range from -75 to 534 g $CO_{2\text{-eq}}$/MJ [841]. In this study, a negative 5.9-11.5 g $CO_{2\text{-eq}}$/MJ of GHG emissions was estimated in the HTL process. From the information provided, we note that HTL conversion to diluent emissions represent slightly less than half (43% PBR and 47% OPR) the combined emissions. Juneja et al. conducted a life cycle analysis of renewable diesel production with the help of microalgae grown on wastewater and estimated total GHG emissions of -110 g $CO_{2\text{-eq}}$/MJ of renewable diesel [648]. Bennion et al. conducted a life cycle analysis of microalgae for thermochemical pathways and reported GHG emissions for the HTL pathway at -11.4 g $CO_{2\text{-eq}}$/MJ [661]. At a productivity of 25 g afdw/m^2/day with a biocrude yield of 38% (afdw), a GWP of -44 g $CO_{2\text{-eq}}$/MJ was reported by Frank et al., signifying a net negative GWP resulting from the carbon credit due to CO_2 uptake during algal growth [830].

Very few studies have evaluated microalgae as a biomass for pyrolysis. In this study, pyrolysis GHG emissions of 10.2-45.65 g $CO_{2\text{-eq}}$/MJ were estimated. In pyrolysis, the combined emissions for conversion to diluent are 68% (PBR) and 71% (OPR). With respect to GWP, producing diluent

through HTL offers significant benefits compared to pyrolysis as the former avoids the energy penalty and GHG emissions associated with drying. The requirement of a dry biomass together with energy demands in the pyrolysis reactor makes it challenging to obtain an environmentally favorable algal-based product. In addition, microalgae drying and reactor heating have a direct environmental impact in pyrolysis. Bennion et al. studied the energy requirements for the pyrolysis of microalgae and found GHG emissions of 166-210 g $CO_{2\text{-eq}}$/MJ [661]. Grierson et al. performed an environmental assessment of a microalgal pyrolysis system and found GHG emissions of 290.24 g $CO_{2\text{-eq}}$/MJ [828]. The key factor influencing the outcome of life cycle analysis is the energy recovery in the form of desired product [842]. Hence, any amelioration in process technologies ranging from algal productivity to conversion methods has a positive impact on life cycle analysis.

On the other hand, GWP elucidates the net positive gaseous emissions resulting from the production of hydrogen during SCWG and TG. In this study, a negative 7.0-12.56 g $CO_{2\text{-eq}}$/MJ of GHG emissions was estimated in SCWG. The heat supply to SCWG was the main contributor to GHG emissions during hydrogen production. When we consider conversion to hydrogen, the SCWG pathway represents 43% (PBR) and 47% (OPR) of the combined emissions, thus essentially the same as the HTL pathway leading to diluent. Galera et al. conducted an LCA analysis of hydrogen and electricity production via supercritical water reforming of glycerol and attributed 19.14 g $CO_{2\text{-eq}}$/MJ (2.68 $gCO_{2\text{-eq}}$ H_2/g) production for sub-processes involving supercritical water reforming including water-gas shift and pressure swing absorption (PSA) systems [843]. Gasafi et al. studied the environmental impacts of SCWG using sewage sludge at approximately 5 $gCO_{2\text{-eq}}$/MJ (0.7 $gCO_{2\text{-eq}}$ H_2/g) [844]. Little information exists on thermal gasification performance in terms of life cycle analysis of algae. In this study, GHG emissions for the algal thermal gasification pathway range from 92.1-138.3 $gCO_{2\text{-eq}}$/MJ. TG conversion to hydrogen production represents 82% (PBR) and 84% (OPR) of the combined emissions. The higher GHG emissions associated with the thermal gasification pathway are due to the drying step for high-moisture containing algae.

Table 49: LCA of thermochemical technologies for diluent and hydrogen production (gCO_2eq/MJ)

Cultivation	**PBR**		**OPR**		**PBR**		**OPR**	
Process								
Hydro Thermal Process	**HTL**	**Pyrolysis**	**HTL**	**Pyrolysis**	**SCWG**	**TG**	**SCWG**	**TG**
Production of diluent (Base case)	-5.90	45.65	-11.5	40.05				
Production of diluent (Scenario)	-5.90	15.8	-11.5	10.2				
Production of hydrogen (Base case)					-7.0	138.3	-12.56	132.68
Production of hydrogen (Scenario)					-7.0	97.7	-12.56	92.1

9.2.4 Net energy ratio

In addition to a life cycle analysis, the thermochemical pathways for diluent and hydrogen production were quantified on the basis of net energy ratio. The net energy ratio (NER) is the relationship between energy produced and energy consumed. It is an indicator of the effectiveness of the energetics of the system. Hence, an NER of greater than one is desirable. In this study, an NER of 1.26 was obtained for large-scale hydrothermal liquefaction. This value is in accordance with others reported previously [234, 661, 830, 845, 846]. Frank et al. performed an NER analysis of HTL and obtained an NER of 1.0 for upgrading to produce stabilized biocrude [830, 846]. Another study on non-catalytic and catalytic processes for the conversion of agricultural waste via hydrothermal liquefaction showed NERs of 0.86-1.20 [234]. Another study involving algae cultivation with wastewater treatment, conversion, and upgrading, assuming mid-range productivity and yield, resulted in an NER of 1.23 [845]. The differences in NERs from HTL conversion pathways are due to differences in product yields, recovery, and heating values. In this study, an NER of 0.59 was obtained for pyrolysis. This is in accordance with the values reported in the literature. An NER of 0.44 was reported for an industrial-scale system model for a pyrolysis plant facility [661]. That study found that HTL is more favorable than pyrolysis because pyrolysis requires additional drying using thermal methods, unlike wet algal HTL. Vardon et al. studied the energetics of the thermochemical conversion of raw and defatted algal feedstock through hydrothermal liquefaction and pyrolysis and concluded that HTL is more favorable than pyrolysis due to the need to volatize water in the latter approach [646]. Similarly, Tzanetis et al. found HTL to be more energy efficient than pyrolysis [847]. Further research and development to improve process efficiency would help increase diluent yield, thereby improving the NER of the HTL pathway. For hydrogen production, an NER of 1.15 was obtained for the supercritical water gasification and thermal gasification pathways. Brandenberger et al. [580] also studied synthetic natural gas from microalgae via SCWG and found that such ratios are dependent on microalgae yield and energy input requirements with respect to cultivation and processing, respectively.

9.3 Sensitivity analysis

A sensitivity assessment was conducted to understand input parameters that influence the life cycle GHG emission results. To understand the sensitivity of the environmental impacts associated with key factors involved in the production of algae biomass, the factors were altered by 10%. The results clarify environmental impact differences between OPR and PBR technologies.

Figure 57 provides the key GHG emissions associated with OPR systems. Apart from the fertilizer nutrient inputs, these factors all consume electricity where the greatest sensitivity, 2.3%, would be related to the amount of electricity required by a shift of 10% in the volume of media needing to be processed (dewatered) via centrifugation. This would be followed by the requirement for pumping (2.2%) the additional (reduction) media to be processed, which in a similar manner impacts power used for filtration of the media (0.95%) and the paddlewheels (0.3%) required to keep the media in motion. A 10% shift in the amount of NH_3 and DAP commercial fertilizer used in cultivation results in changes of 2% and 0.5% in the respective environmental impacts. Other environmental impacts related to water use, lighting, and sparging have limited impact (0.1%).

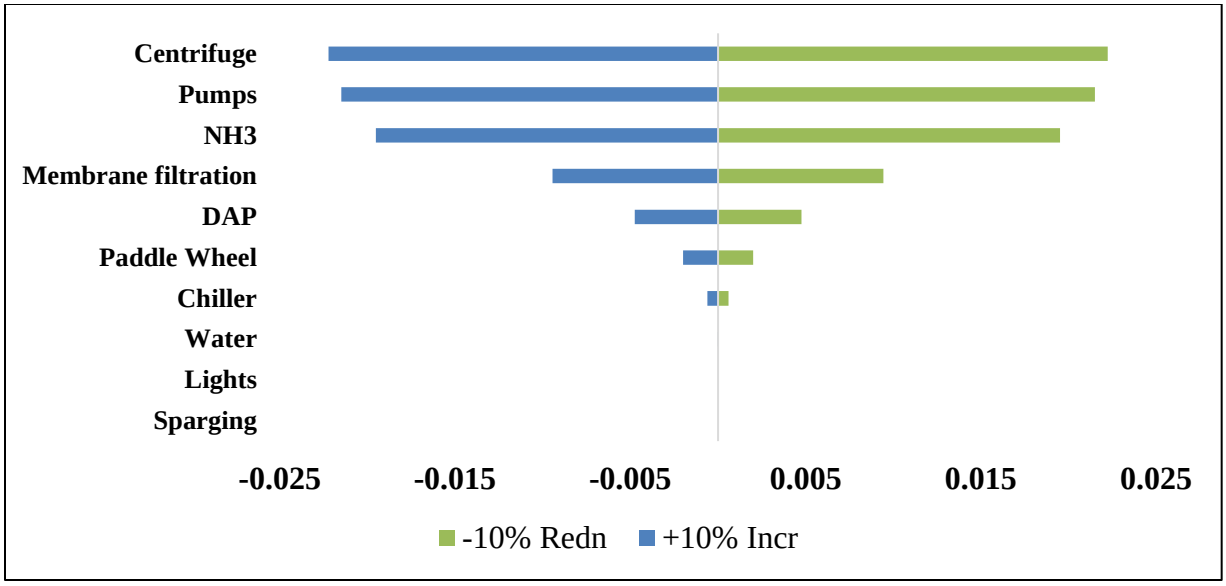

Figure 57: Key factor environmental impact sensitivity for OPR algae cultivation systems /kg $CO_{2\text{-eq}}$/kg biomass produced

The key environmental impacts associated with PBR systems are shown in Figure 58. In this scenario, although environmental factors are primarily related to electrical energy used, the most significant sensitivity is due to the PBR lighting systems at close to 5.5% for a 10% shift in the amount of energy required for this factor. Altering the amount of fertilizers used by 10% would again shift environmental impacts by 2% for NH_3 and 0.5% for DAP. Sparging impacts would increase due to higher pressures and volumes of air/CO_2 that would be required for the respective technology's application at ~0.7%. However, since much lower quantities of media need to be processed with PBRs, impacts would be lower than those experienced by OPR systems, ~0.1% and 0.2% for centrifugation and membrane filtration, respectively. Environmental impacts related to 10% shifts in chilling, water use, and pumping are below 0.1%, and there is no requirement for the use of a paddlewheel.

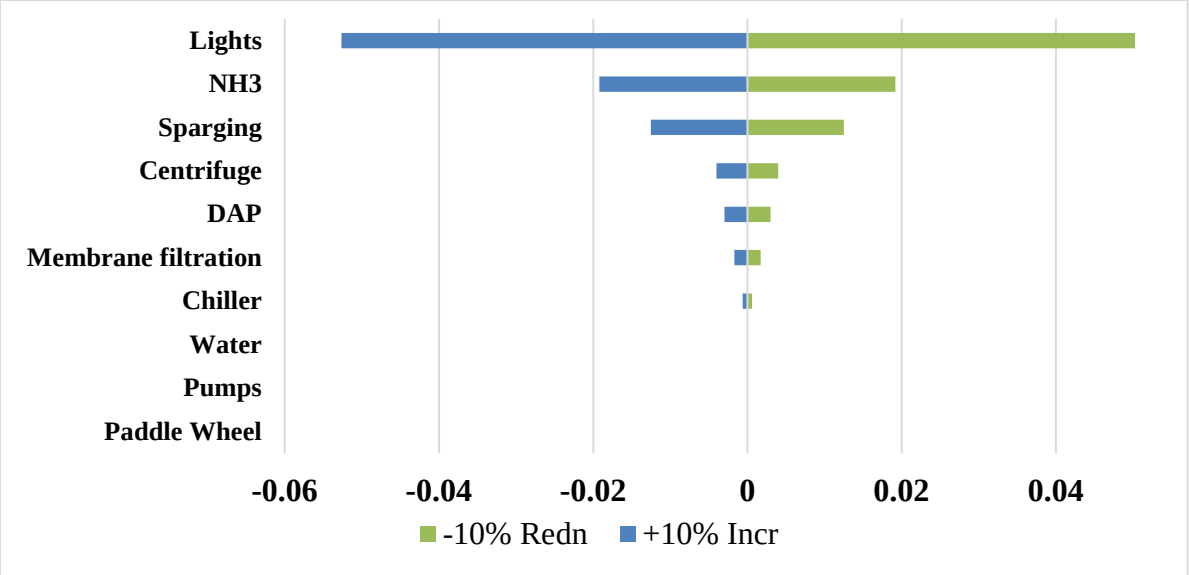

Figure 58: Key factor environmental impact sensitivity for PBR algae cultivation systems /kg $CO_{2\text{-}eq}$/kg biomass produced

What we note from the above is that where changes in key cultivation factors can be seen to have measurable environmental impacts, the key factors with greatest sensitivity to changes differ depending on whether we are considering OPR or PBR systems. In the former case, centrifugation and pumping are the primary factors. In the latter, the lighting system has slightly greater environmental impacts than the centrifugation and pumping environmental impacts of the OPR system.

9.4 Improvement measures and comparison with other known systems

Based on environmental indicators, a number of steps may be incorporated to ameliorate the environmental performance metrics. Improved energy integration through optimized energy demand for diluent and hydrogen production, the use of renewable electricity, and adopting efficient algal cultivation systems would considerably improve process performance. The development of advanced catalysts in terms of selectivity and ability to withstand high temperatures would improve the energetics and reduce the environmental impact on the system [843]. For gasification systems, the gasifier could be optimized to produce more hydrogen and less methane. Power recovery methods from turbines and the use of heat exchangers to transfer waste heat from one operation to another would also save energy, thereby reducing environmental impacts. Using autothermal processes and combusting a portion of the produced gas for the required heat production in the reactor would reduce heat loss during heat transfer, a method employed in supercritical water oxidation [844]. More refined sensitivity analysis would lead to better understanding of process sensitivity to variations in operating parameters and identify opportunities for additional energy savings.

Figure 59 shows the GHG emissions from several thermochemical technologies used in the production of fuels and chemicals. The methods and results from various studies are difficult to

compare given differences in system boundaries, assumptions, and criteria, and thus lead to different environmental outcomes. The consideration of a process or unit with respect to a particular technology may change with different performance metrics and data standards. Nevertheless, such analysis and comparison is helpful in gaining insights into the current state of a technology in relation to other known technologies. The widely adopted conventional method of hydrogen production through gasification using fossil fuels including coal and steam methane reforming results in high GHG emissions, with coal gasification and natural gas thermolysis approaching 29.33 g $CO_{2\text{-eq}}$ H_2/g [848] and 37.11 g $CO_{2\text{-eq}}$ H_2/g [849], respectively. Biochemical hydrogen production based on photosynthetic routes helps mitigate environmental impacts. The case of hydrogen production via dark fermentation results in a 5.5 g $CO_{2\text{-eq}}$ H_2/g GWP [850], but this technology is still at a nascent stage of development. Similarly, gasification technologies using renewable biomass have considerably lower GHG emissions (e.g., 5.40 g $CO_{2\text{-eq}}$ H_2/g) [851]. Compared to these known carbon footprints, the SCWG of algal biomass offers a considerably better environmental profile with respect to global warming potential and thus has the potential to be a promising energy resource.

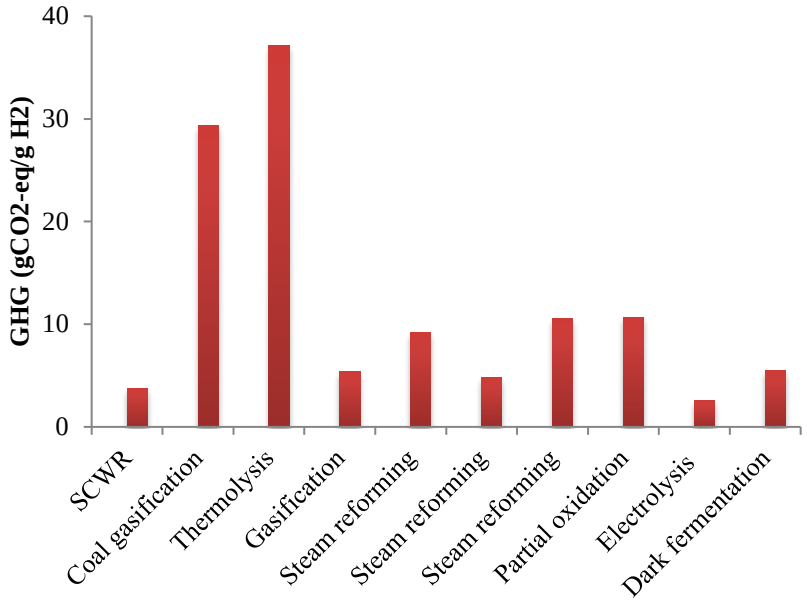

Figure 59: Life cycle analysis results of key technologies for hydrogen production [843]

9.5 Conclusion

This research study conducted a comparative LCA on microalgae feedstock cultivated in both open raceway pond and photobioreator systems in Canada. The biomass feedstock was subsequently processed via thermochemical conversion to the end products diluent and hydrogen. Of the thermochemical conversion pathways considered in our study, SCWG offers the best performance in terms of GHG emissions in the production of hydrogen, followed by TG. For diluent production we studied two thermochemical pathways, HTL and pyrolysis. There are environmental benefits associated only with HTL processing, which can use wet biomass feedstock, thereby avoiding

energy and consequently GHG emissions associated with drying the biomass feedstock. These results will help make better informed investment decisions related to these processes.

10 Key Observations

- This work has demonstrated the successful development of a data-intensive model whose results show good correlation with a data set from the NREL ATP3 testbed in Mesa, AZ. The key parameters in developing the SATOPR model are media temperature and solar light intensity. Given the global reach of satellites, using this data source to predict open raceway pond (OPR) system performance both in Canada and the rest of the globe makes the model both unique and beneficial for comparative analyses of OPR system performance.
- We have also demonstrated how the model provides additional supportive analytic capabilities useful in techno-economic analyses (TEAs) and life cycle assessments (LCAs). A key weakness in the current analysis is access to timely experimental yield data (i.e., 15-minute incremental results that could be matched with other model parameter results that are provided at these same intervals). This would enable better analysis and assist in refining capabilities in the SATOPR model. It is anticipated that the ultimate value of the model will be revealed as results from the model are correlated with experimental field data from multiple sites using identical species and operating protocols.
- The techno-economic analysis of the cost of producing algae biomass in Canada shows that the minimum biomass selling price for a tonne of algae biomass from OPR and photobioreactor (PBR) cultivation systems in Fort Saskatchewan, AB, would be $1,288/tonne, and $550/tonne, respectively. This analysis shows that in Canada a PBR cultivation system has the potential to produce algae biomass at a significantly lower MBSP than an OPR system at the same location. In fact, it is projected that the PBR MBSP could rival that of OPR systems located in even the most favorable climatic locations. Environmental and operating parameters have been identified and show potential for continuing to improve MBSP and are recommended for further study.
- The cost results show that the cost of diluent production from HTL is around 1.60 $/L for a plant capacity of 2000 tonnes day^{-1}. The fixed capital investment at this capacity is 503 M$. On the other hand, the cost of diluent production from pyrolysis is 1.69 $/L for a plant capacity of 2000 tonnes day^{-1}, while the fixed capital investment at this capacity for pyrolysis is lower than that of HTL (around 385 M$). The sensitivity analysis shows that diluent cost is highly sensitive to diluent yield, algal biomass cost, and the internal rate of return (IRR). The plant capacity versus price profile shows that the optimum capacity can exceed 6000 tonnes day^{-1} of algal biomass; however, availability of algal biomass at this capacity is a challenge. Therefore, the price of diluent at this capacity (i.e., 6000 tonnes day^{-1}) is 1.55 $/kg and 1.63 $/kg, respectively, for HTL and pyrolysis process. On a commercial scale the size of the plan will be smaller to reduce the risk.
- A techno-economic assessment of hydrothermal gasification and thermal gasification showed that a 2000 dry tonnes/day plant required fixed capital investments of 277.7 M $ and 196.62 M $ with hydrogen product values of 4.59 ± 0.10 $/kg and 5.66 ± 0.10 $/kg, respectively. In Western Canada, most hydrogen is obtained from natural gas at a cost of 0.78 $/kg. The thermochemical plant using 2000 dry tonnes/day algae as a feedstock is not economical. The technoeconomic analysis suggested that the feasibility of the technology depends heavily on the cost of algal biomass and the yield obtained.
- The GHG emissions for the four pathways studied arise from the conversion process only. An HTL pathway contributes GHG emissions of 29.6 $gCO_{2\text{-}eq}$/MJ based on inputs from process

modeling developed for the HTL pathway in this study. The production of diluent from HTL has advantages with respect to the use of high moisture containing microalgae; drying is not needed, and thus energy and corresponding GHG emissions pertaining to microalgae drying are eliminated. The algae-based pyrolysis pathway in this study has GHG emissions of 81.1 $gCO_{2\text{-}eq}$/MJ of diluent based on process modeling inputs. Microalgae conversion incorporates two main processes in pyrolysis, microalgae drying and natural gas heating in the pyrolysis reactor; both are energy intensive and have direct environmental impacts.

- Hydrogen production in the supercritical water gasification (SCWG) pathway emits GHGs of 28.5 $gCO_{2\text{-}eq}$/MJ of hydrogen, based on inputs from the process modeling developed, whereas the algae-based thermal gasification pathway contributes GHG emissions of 173.8 $gCO_{2\text{-}eq}$/MJ of hydrogen based on process modeling inputs. The GHG emission results showed that HTL performed better than pyrolysis for diluent production, while HTG had better environmental metrics than thermal gasification for hydrogen production from biomass. The production of diluent from HTL has advantages with respect to the use of high moisture containing microalgae, thereby reducing energy and corresponding emissions from microalgal drying.
- The results for the life cycle water footprint show that there is high fresh water requirement for algae production and a need to recycle harvested water or use alternative water sources. To produce 1 kg of algae through ponds, 1564 L of water is required. When photobioreactors (PBRs) are used, only 372 L water is required; however, PBRs require about 30 times more energy than ponds. From a final product perspective, the gasification of algae biomass is the thermochemical conversion method that requires the most water per MJ produced (mainly due to its low hydrogen yield), followed by pyrolysis and HTL. HTG has the lowest water footprint, mainly because the large amount of electricity generated as part of the process compensates for the electricity used by the system. The performance for all pathways can be improved through recycling channels. Supercritical water gasification offers the best performance in terms of GHG emissions in the production of hydrogen compared to thermal gasification (92.1-138.3 g $CO_{2\text{-}eq}$/MJ). With respect to GHG emissions for diluent production, there are environmental benefits associated with HTL, which avoids the energy and consequently GHG emissions associated with drying the biomass feedstock in pyrolysis (10.2-45.65 g $CO_{2\text{-}eq}$/MJ).

These results will prove useful in making better informed investment decisions related to these processes.

11 Recommendations

11.1 Recommendations for future algae cultivation studies

Although there has been significant interest in assessing the potential of microalgae to produce bio-feedstocks in Canada since the 1950's, given the chemical composition of microalgae including significant amounts of lipids, proteins and carbohydrates, research to date has not succeeded in addressing important factors that remain as impediments to the mass implementation of cultivation of algae. To address these shortcomings, the following recommendations are offered.

11.1.1 Focus on utilizing PBR systems for cultivating algae in Canada integrated with waste heat produced from industrial sector

Given the information supported by this research, it becomes extraordinarily evident that Canada will not be able to compete in cultivating algae autotrophically utilizing OPR systems with other regions of the world that have warmer climates located in regions with access to better year-round sunlight. The geography places significant climatic challenges on attempting this form of cultivation both from an environmental impact perspective as well as an economic perspective. In Canada we need to focus research and development activities around PBR algae cultivation systems where there is seen to be greater potential to breaking through with both positive environmental impacts as well as achieving economic sustainability long term in conjuction with the utilization of waste heat from the industrial facilities.

11.1.2 Conduct research in Canada that leads to achieving consistent yield equivalents at 5,000 g/m^2/d (20 gL/d) for PBR systems

Consistent with the findings of this research improving yield is the factor that has the greatest sensitivity to impacting the MBSP. Restating what has already been presented: At Mesa AZ increasing productivity in the OPR by 60% from 25 g/m^2/d to 40 g/m^2/d would result in a $127 /tonne (23%) reduction in MBSP. The impact of the same OPR in Canada would be much greater because of the scaling factor. A cost reduction of over $384/tonne (17%) would result from a 60% productivity increase. For the PBR technology, a 60% yield increase from 1250 g/m^2/d to 2000 g/m^2/d (8 g/L/d) would result in (21%) $123/tonne price reduction. As in many areas of life, the challenge of achieving success has often less to do with actual failure, as it has to do with low aim – not setting your objective high enough. It is proposed that algae cultivation research in Canada establish setting an objective to attain consistent yields of 5,000 g/m^2/d (20 gL/d) utilizing PBR technologies. This should be achieved using any algae species that demonstrates meeting specific compositional objectives. The achievement of this single objective would establish Canada's position as the global leader in algae cultivation technology and open the door to multiple bio-refinery scenarios to be established within this country. Once the attainment of achieving the improvement of algae yields has been accomplished, there is need to move through a series of scaling operations to determine where the limits of scale-up are. It is anticipated that it will be possible to achieve certain economies of scale that will enable higher profitability, thereby improving techno-economics performance and as well as maintaining minimum benchmark LCA performance.

11.1.3 Conduct research leading to improving the efficiency of dewatering and harvesting algae and isolating active compounds from the biomass

Given that one of the highest energy utilization processes used in the algae cultivation process is related to harvesting, dewatering and drying, research and development activities must be employed to conduct these operations more efficiently and effectively.

11.1.4 Establishing microalgae cultivation bio-refinery platforms

As already indicated above, utilization of an algae species that has not only high lipid concentration but also has within its makeup a relatively high concentration of other active compounds that have much greater value than diluent or hydrogen, albeit in a market size that may be more limited than diluent and hydrogen, should be pursued as part of a bio-refinery production platform to achieve higher profitability. Research into both potential bio-actives within algae and identifying species where the bio-actives are found to be synthesized in higher concentrations is recommended.

11.2 Recommendations for future algae conversion studies

While the work performed in this research study is itself comprehensive, further improvements and suggestions in the present modeling study can be made. The author recommends the following future studies.

11.2.1 Solvents for gas purification in gasification

In the current modeling study, Selexol solvent was used for gas purification in gasification. However, incorporating other solvents such as amine and alcohol-based ones such as methanol, methyl-diethyl-amine (MDEA), etc., will improve the scope. The use of such solvents will assist in understanding the economic and environmental feasibility of using them for H_2 production from biomass.

11.2.2 Reaction kinetics

Hydrothermal liquefaction occurs at high pressure and temperature, which leads to higher operating and capital costs. The understanding of reaction kinetics and products obtained from biomass fractions like carbohydrates, proteins, and lipids will help optimize reactor design and thus reduce costs associated with the process. In other words, comprehending the stability and quality of oil will help identify primary reactions and upgrading needs.

11.2.3 Stability of bio-crude/bio-oil

Little is known on the stability of oil obtained from HTL. A future study on its stability will help in an analysis when bio-crude is used offsite (when the hydrotreating plant is not co-located with the HTL facility).

11.2.4 Experimental studies

Studies using different strains of microalgae are required to comprehend the impact of cellular compositional structure on product yields. Compared to other pathways such as biodiesel

production, HTL does not entail high lipid algal biomass. As HTL can work on whole biomass, robust and fast cultivation of strains seem more appropriate and can improve the economics of the process. Testing other algal strains will also help establish baseline yields of products, which will also assist in developing commercial applications. Moreover, novel algal strains can be considered for improved cultivation systems that enhance productivity.

12 Challenges

The major challenge faced during the course of this research was obtaining accurate and reliable data. The Aspen model requires a lot of input data. Examples of data required on the conversion side include bio-oil composition, yield, reaction composition, and catalyst stability. Validation of the results is a key component of this research, and reliable data is needed to do this.

The production of bio-oil and hydrogen, especially via the hydrothermal process, has not yet been fully commercialized, and obtaining data from the few companies conducting this research is difficult.

13 List of Publications from this Research

This research work generated 11 research papers, four of which have been published in high impact journals. The rest have been submitted or are about to be submitted for publication. The results generated from this work have also been presented at 12 conferences and academic and industrial workshops. The list of papers is given below.

1. Refereed Journal Articles, Published, Submitted and Prepared.

1. Edson, N., Jr., Kumar, M., Pankratz, S., Oyedun, A.O., Kumar, A. “Development of life cycle water footprints for the production of fuels and chemicals from algae biomass,” Water Research, Volume 140, Pages 311-322.
2. Kumar, M., Oyedun, A.O., Kumar, A. (2018) “A review on the current status of various hydrothermal technologies on biomass feedstock,” Renewable and Sustainable Energy Reviews, Volume 81, Part 2, Pages 1742-1770.
3. Pankratz, S., Oyedun, A.O., Zhang, X., Kumar, A. (2017) “Algae production platforms for Canada's northern climate,” Renewable and Sustainable Energy Reviews, Volume 80, Pages 109-120.
4. Kumar, M., Oyedun, A.O., Kumar, A. (2017) “Hydrothermal liquefaction of biomass for the production of diluents for bitumen transport,” Biofuels, Bioproducts & Biorefining, Volume 11 (5), Pages 811-829.
5. Pankratz, S., Oyedun, A.O., Kumar, A., “Development of analytical model to predict microalgae growth in open pond raceway systems based on local solar irradiance” Algal Research Journal, accepted, January 2018.
6. Kumar, M., Oyedun, A.O., Kumar, A. “Development of a process model and parameter study for the hydrothermal gasification of algal biomass” (Submitted to Enegy and Fuels, January, 2019).
7. Pankratz, S., Oyedun, A.O., Kumar, A., “Techno-economic analysis (TEA) of algae biomass production from landfill CHP flue gas and utilizing agricultural waste water” (Submitted to Biofuels, Bioproducts & Biorefining, October, 2018).
8. Kumar, M., Oyedun, A.O., Kumar, A. “A comparative analysis for production of diluents from different thermochemical conversions of algae” (Submitted to Waste and Biomass Valorization, December, 2018).
9. Kumar, M., Oyedun, A.O., Kumar, A. “A comparative analysis of hydrogen production from the thermochemical conversions of algal biomass” (Submitted to International Journal of Hydrogen Energy, October, 2018).
10. Pankratz, S., Kumar, M., Oyedun, A.O., Gemechu, E., Kumar, A. “Life cycle assessment of algae-based diluent and hydrogen production in colder climate”. To be submitted to the Journal of Cleaner Production.
11. Edson, N. J., Oyedun, A.O., Kumar, A. “A review of the life cycle analysis of thermochemical conversion of algae”. To be submitted to Renewable and Sustainable Energy Reviews.

2. Conferences Presentations and Posters.

1. Kumar M, Oyedun AO, Kumar A. Techno-economic and life cycle analyses of the production of hydrogen and diluents from algae biomass for oil sands use, NSERC/Cenovus/Alberta Innovates Industrial Research Chair in Energy and Environmental Systems Engineering Workshop, July 30, 2018, Ottawa, ON.
2. Pankratz S, Kumar M, Oyedun AO, Gemechu E, Kumar A. Life cycle assessment of algae-based diluent production in colder climate, abstract presented at the 8th International Conference on Algal Biomass, Biofuels and Bioproducts, June 11-13, 2018, Seattle, USA.
3. Kumar M, Javed K, Oyedun AO, Vaezi M, Kumar A. Can we marry pipeline transportation with hydrothermal processing? 26th European Biomass Conference & Exhibition (EUBCE 2018), May 14-18, 2018, Copenhagen, Denmark.
4. Pankratz S, Oyedun AO, Kumar A. Techno-economic analysis of algae cultivation, presented at the SPARK 2017 Conference Nov. 6-8 2017, Edmonton, AB.
5. Kumar M, Oyedun AO, Kumar A. Techno-economic and life cycle analyses of the production of hydrogen and diluents from algae biomass for oil sands use, presented at the SPARK 2017 Conference Nov. 6-8 2017, Edmonton, AB.
6. Nogueira E Jr, Oyedun AO, Kumar A. Water footprint of diluent and hydrogen production via thermochemical conversion of algae, presented at the CSBE/SCGAB Annual General Meeting and Technical Conference, Aug. 6-10, 2017, Winnipeg, MB.
7. Kumar M, Oyedun AO, Kumar A. Techno-economic analysis of the production of hydrogen from hydrothermal gasification of algal biomass, presented at the ASABE 2017 Annual International Meeting, July 16-19, 2017, Spokane, Washington.
8. Pankratz S, Oyedun AO, Kumar A. Modeling algae in a Canadian context – ponds and photobioreactors, presented at the ABO – Algae Biomass Organization Summit, Oct 23-26, 2016, Phoenix, AZ.
9. Kumar M, Oyedun AO, Kumar A. Hydrothermal liquefaction of biomass to biofuels: A techno-economic analysis, presented at the ASABE 2016 Annual International Meeting, July 17-20, 2016, Orlando, Florida.
10. Kumar M, Vaezi M, Oyedun AO, Kumar A. Review of hydro-thermal processing technologies, presented at the CSBE/SCGAB Technical Conference and AGM 2015, Innovation in Water, Energy and Biosystems (iWEB) Positioning the Globe for 2050, July 5-8, 2015, Edmonton, AB.
11. Pankratz S, Oyedun A, Zhang X, Kumar A. Algae production platforms for Canada's northern climate, presented at the CSBE/SCGAB Technical Conference and AGM 2015, Innovation in Water, Energy and Biosystems (iWEB) Positioning the Globe for 2050, July 5-8, 2015, Edmonton, AB.
12. Pankratz S, Zhang X, Kumar A. A review of algae production and harvesting technologies for Canada, presented at the Algae Biomass Summit, September 29-October 2, 2014, San Diego, California, USA.

References

1. Myers, R., MacLeod, J., Ghosh, M., and Chakrabarty, T. (2000). Exxon Research and Engineering Co. Producing Pipelinable Bitumen. Available from: https://patents-google-com.login.ezproxy.library.ualberta.ca/patent/US6096192A/en [Accessed: January 28, 2019]
2. Ordorica-Garcia, G., Croiset, E., Douglas, P., Elkamel, A., and Gupta, M. (2007). Modeling the energy demands and greenhouse gas emissions of the Canadian oil sands industry. Energy & Fuels 21(4), 2098-2111.
3. Demirbaş, A. (2001). Biomass resource facilities and biomass conversion processing for fuels and chemicals. Energy Conversion and Management 42(11), 1357-1378.
4. Naik, S., Goud, V. V., Rout, P. K., and Dalai, A. K. (2010). Production of first and second generation biofuels: a comprehensive review. Renewable and Sustainable Energy Reviews 14(2), 578-597.
5. Sims, R., Taylor, M., Saddler, J., and Mabee, W. (2008). From 1st-to 2nd-generation biofuel technologies: an overview of current industry and RD&D activities. International Energy Agency, 16-20.
6. John, R.P., Anisha, G., Nampoothiri, K.., and Pandey, A. (2011). Micro and macroalgal biomass: a renewable source for bioethanol. Bioresource Technology 102(1), 186-193.
7. Wijffels, R.H. and Barbosa, M.J. (2010). An outlook on microalgal biofuels. Science 329(5993), 796-799.
8. Chisti, Y. (2007). Biodiesel from microalgae. Biotechnology Advances 25(3), 294-306.
9. Brennan, L. and Owende, P. (2010). Biofuels from microalgae—A review of technologies for production, processing, and extractions of biofuels and co-products. Renewable and Sustainable Energy Reviews 14(2), 557-577.
10. Sheehan, J., Dunahay, T., Benemann, J., and Roessler, P. (1998). A Look Back At The U.S Department of Energy's Aquatic Species Program: Biodiesel From Algae. Available from: https://s3.amazonaws.com/academia.edu.documents/31018751/Biodiesel_from_algae_-_USDOD_report.pdf?AWSAccessKeyId=AKIAIWOWYYGZ2Y53UL3A&Expires=1548712544&Signature=pBjLE1vVJMX%2FbMvwBWJWzbd2O0E%3D&response-content-disposition=inline%3B%20filename%3DA_look_back_at_the_US_department_of_ener.pdf [Accessed: January 28, 2019]
11. Weissman, J.C. and Goebel, R.P. (1997). Design and Analysis of Microalgal Open Pond Systems for the Purpose of Producing Fuels. Solar Energy Research Inst., Golden, CO (USA). Available from: https://www.osti.gov/biblio/6546458.
12. Schenk, P.M., Thomas-Hall, S.R., Stephens, E., Marx, U.C., Mussgnug, J.H., Posten, C., Kruse, O., and Hankamer, B. (2008). Second generation biofuels: high-efficiency microalgae for biodiesel production. Bioenergy Research 1(1), 20-43.
13. Tsukahara, K. and Sawayama, S. (2005). Liquid fuel production using microalgae. Journal of the Japan Petroleum Institute 48(5), 251-259.
14. Subhadra, B. and Grinson, G. (2011). Algal biorefinery-based industry: an approach to address fuel and food insecurity for a carbon-smart world. Journal Science Food Agriculture 91(1), 2-13.
15. Kiran, B., Kumar, R., and Deshmukh, D. (2014). Perspectives of microalgal biofuels as a renewable source of energy. Energy Conversion and Management 88, 1228-1244.
16. Rhodes, C.J. (2009). Oil from algae: salvation from peak oil? Science Progress 92(1), 39-90.

17. Parmar, A., Singh, N.K., Pandey, A., Gnansounou, E., and Madamwar, D. (2011). Cyanobacteria and microalgae: A positive prospect for biofuels. Bioresource Technology 102(22), 10163-10172.
18. Melis, A. (2012). Photosynthesis-to-fuels: From sunlight to hydrogen, isoprene, and botryococcene production. Energy and Environmental Science 5(2), 5531-5539.
19. Becker, E.W. (2007). Micro-algae as a source of protein. Biotechnology Advances 25(2), 207-210.
20. Stane, A., Jorgensen, S., Lindeboom, N., and Nickerson, M. (2014). Microalgae: Canada's Next Blooming Industry: Canadian Food Insights. Available from: https://canadianfoodbusiness.com/2014/10/26/microalgae-canadas-next-blooming-industry. [Accessed: Jan 28, 2019].
21. Graziani, G., Schiavo, S., Nicolai, M. A., Buono, S., Fogliano, V., Pinto, G., and Pollio, A. (2013). Microalgae as human food: Chemical and nutritional characteristics of the thermo-acidophilic microalga Galdieria sulphuraria. Food and Function 4(1), 144-152.
22. Gressel, J. (2013). Transgenic marine microalgae: A value-enhanced fishmeal and fish oil replacement, in Handbook of Microalgal Culture: Applied Phycology and Biotechnology, John Wiley and Sons. pp. 653-670.
23. Marques, A.E., Miranda, J.R., Batista, A.P., and Gouveia, L. (2013). Microalgae biotechnological applications: Nutrition, health and environment, in Microalgae: Biotechnology, Microbiology and Energy, Nova Science Publishers, Inc. pp. 1-60.
24. Chauton, M.S., Reitan, K.I., Norsker, N.H., Tveterås, R., and Kleivdal, H.T. (2015). A techno-economic analysis of industrial production of marine microalgae as a source of EPA and DHA-rich raw material for aquafeed: Research challenges and possibilities. Aquaculture 436, 95-103.
25. Duerr, E.O., Molnar, A., and Sato, V. (1998). Cultured microalgae as aquaculture feeds. Journal of Marine Biotechnology 6(2), 65-70.
26. Renuka, N., Sood, A., Ratha, S.K., Prasanna, R., and Ahluwalia, A.S. (2013). Nutrient sequestration, biomass production by microalgae and phytoremediation of sewage water. International Journal of Phytoremediation 15(8), 789-800.
27. Bhatt, N.C., Panwar, A., Bisht, T.S., and Tamta, S. (2014). Coupling of algal biofuel production with wastewater. Scientific World Journal 2014.
28. Kothari, R., Prasad, R., Kumar, V., and Singh, D.P. (2013). Production of biodiesel from microalgae Chlamydomonas polypyrenoideum grown on dairy industry wastewater. Bioresource Technology 144, 499-503.
29. Koreiviene, J., Valčiukas, R., Karosiene, J., and Baltrenas, P. (2014). Testing of Chlorella/Scenedesmus microalgae consortia for remediation of wastewater, CO_2 mitigation and algae biomass feasibility for lipid production. Journal of Environmental Engineering and Landscape Management 22(2), 105-114.
30. Van Den Hende, S., Carré, E., Cocaud, E., Beelen, V., Boon, N., and Vervaeren, H. (2014). Treatment of industrial wastewaters by microalgal bacterial flocs in sequencing batch reactors. Bioresource Technology 161, 245-254.
31. Maity, J.P., Bundschuh, J., Chen, C.Y., and Bhattacharya, P. (2014). Microalgae for third generation biofuel production, mitigation of greenhouse gas emissions and wastewater treatment: Present and future perspectives – A mini review. Energy. 78, 104-113.
32. Rinanti, A., Kardena, E., Astuti, D.I., and Dewi, K. (2014). Improvement of carbon dioxide removal through artificial light intensity and temperature by constructed green microalgae

consortium in a vertical bubble column photobioreactor. Malaysian Journal of Microbiology 10(1), 29-37.
33. Kumar, A., Ergas, S., Yuan, X., Sahu, A., Zhang, Q., Dewulf, J., Malcata, F. X., and van Langenhove, H. (2010). Enhanced CO_2 fixation and biofuel production via microalgae: Recent developments and future directions. Trends in Biotechnology 28(7), 371-380.
34. Guiry, M.D. (2012). How many species of algae are there? Journal of Phycology 48(5), 1057-1063.
35. Xu, Y. and Boeing, W.J. (2014). Modeling maximum lipid productivity of microalgae: Review and next step. Renewable and Sustainable Energy Reviews 32, 29-39.
36. Chiaramonti, D., Prussi, M., Buffi, M., Rizzo, A.M., and Pari, L. (2017). Review and experimental study on pyrolysis and hydrothermal liquefaction of microalgae for biofuel production. Applied Energy 185, 963-972.
37. Mostafa, S.S.M. (2012). Microalgal Biotechnology: Prospects and Applications. In Plant Science, edited by N.K. Dahl, pp. 275-314, Open Source, DOI: 10.5772/53694.
38. Chisti, Y. (2013). Constraints to commercialization of algal fuels. Journal of Biotechnology 167(3), 201-214.
39. Acién, F.G., Fernández, J.M., Magán, J.J., and Molina, E. (2012). Production cost of a real microalgae production plant and strategies to reduce it. Biotechnology Advances 30(6), 1344-1353.
40. Norsker, N.-H., Barbosa, M.J., Vermuë, M.H., and Wijffels, R.H. (2011). Microalgal production — A close look at the economics. Biotechnology Advances 29(1), 24-27.
41. Chen, C.-Y., Yeh, K.-L., Aisyah, R., Lee, D.-J., and Chang, J.-S. (2011). Cultivation, photobioreactor design and harvesting of microalgae for biodiesel production: a critical review. Bioresource Technology 102(1), 71-81.
42. Abdelaziz, A.E., Leite, G.B., and Hallenbeck, P.C. (2013). Addressing the challenges for sustainable production of algal biofuels: II. Harvesting and conversion to biofuels. Environmental Technology 34(13-14), 1807-1836.
43. Slade, R. and Bauen, A. (2013). Micro-algae cultivation for biofuels: Cost, energy balance, environmental impacts and future prospects. Biomass and Bioenergy 53, 29-38.
44. Chen, G., Zhao, L., and Qi, Y. (2015). Enhancing the productivity of microalgae cultivated in wastewater toward biofuel production: A critical review. Applied Energy 137, 282-291.
45. Zhu, L. (2015). Biorefinery as a promising approach to promote microalgae industry: An innovative framework. Renewable and Sustainable Energy Reviews 41, 1376-1384.
46. Lam, M.K. and Lee, K.T. (2013). Scale-up and commercialization of algal cultivation and biofuel production, in Biofuels from Algae, edited by A. Pandey, D-J. Lee, Y. Christi, and C.R. Soccol. Elsevier, pp. 261-286.
47. Sikes, K., Van Walwijk, M., and McGill, R. (2010). Algae as Feedstock for Biofuels: An Assessment of the State of Technology and Opportunities, International Energy Agency. Available from: https://www.ieabioenergy.com/publications/algae-as-a-feedstock-for-biofuels/.
48. Chojnacka, K. and Marquez-Rocha, F.-J. (2004). Kinetic and stoichiometric relationships of the energy and carbonmetabolism in the culture of microalgae. Biotechnology 3, 21-34.
49. Mata, T.M., Martins, A.A., and Caetano, N.S. (2010). Microalgae for biodiesel production and other applications: a review. Renewable and Sustainable Energy Reviews 14(1), 217-232.

50. Harun, R., Yip, J.W., Thiruvenkadam, S., Ghani, W.A., Cherrington, T., and Danquah, M.K. (2014). Algal biomass conversion to bioethanol – a step-by-step assessment. Biotechnology journal 9(1), 73-86.
51. Baicha, Z., Salar-García, M.J., Ortiz-Martínez, V.M., Hernández-Fernández, F.J., de los Ríos, A.P., Labjar, N., Lotfi, E., and Elmahi, M. (2016). A critical review on microalgae as an alternative source for bioenergy production: A promising low cost substrate for microbial fuel cells. Fuel Processing Technology 154, 104-116.
52. Liang, Y., Sarkany, N., and Cui, Y. (2009). Biomass and lipid productivities of Chlorella vulgaris under autotrophic, heterotrophic and mixotrophic growth conditions. Biotechnology letters 31(7), 1043-1049.
53. Perez-Garcia, O., Escalante, F.M., de-Bashan, L.E., and Bashan, Y. (2011). Heterotrophic cultures of microalgae: Metabolism and potential products. Water Research 45(1), 11-36.
54. Liu, J. (2016). Interspecific biodiversity enhances biomass and lipid productivity of microalgae as biofuel feedstock. Journal of Applied Phycology 28(1), 25-33.
55. Adesanya, V.O., Davey, M.P., Scott, S.A., and Smith, A.G. (2014). Kinetic modelling of growth and storage molecule production in microalgae under mixotrophic and autotrophic conditions. Bioresource Technology 157, 293-304.
56. O'leary, S., Hogan, E., McGinn, P., and Knickle, L. (2010). AAFC-NRCan-NRC National Bioproducts Program Algal Biofuels Initiative, Nova Scotia Energy Research and Development Forum Biosciences: Halifax. Available from: http://www.oera.ca/wp-content/uploads/2013/05/9.30-9.45-Marine-Renewable-Biofuels-Stephen-OLeary.pdf.
57. Armstong, S.M., Staples, L., Bauder, A.., and Craigie, J.S. (2012). Photobioreactor, National Resarch Council of Canada. Available from: https://www.nrc-cnrc.gc.ca/eng/solutions/facilities/alga_biofinery_pilot_plant.html.
58. Deane, A. (2011). An apparatus, method and system for algae growth. Available from: http://www.oilgae.com/blog/2007/02/apparatus-method-for-growing-algae-1968.html.
59. Gonzalez, J.A., Martin, S.C., and Kolesnik, M. (2011). Supplying bioreactor gaseous effluent to combustion process P.B. Inc. Available from: https://patents.google.com/patent/US20110283618A1/en.
60. Gonzalez, J.A., Martin, S. C., and Kolesnik, M. (2011). Process for growing biomass by modulating supply of gas to reaction zone.
61. Gonzalez, J.A., Martin, S.C., and Kolesnik, M. (2011). Producing biomass using pressurized exhaust gas, P.B. Inc.
62. Gonzalez, J.A., Martin, S.C., and Kolesnik, M. (2011). Recoverying make-up water during biomass production, P.B. Inc.
63. Gonzalez, J.A., Martin, S.C., and Kolesnik, M. (2011). Diluting exhaust gas being supplied to bioreactor.
64. Gonzalez, J.A., Martin, S.C., and Kolesnik, M. (2012). Supplying Treated exhaust gases for effecting growth of phototrophic biomass.
65. Gonzalez, J.A., Martin, S.C., and Kolesnik, M. (2012). Light energy supply for photobioreactor system.
66. Gonzalez, J.A., Martin, S.C., and Kolesnik, M. (2013). Producing biomass using pressurized exhaust gas, P.B. Inc.
67. Gonzalez, J.A., Martin, S.C., and Kolesnik, M. (2014). Process for managing photobioreactor exhaust.

68. Gonzalez, J.A., Martin, S.C., and Kolesnik, M. (2014). Recovering off-gas from photobioreactor, P.B. Inc..
69. Gonzalez, J.A., Martin, S.C., Kolesnik, M., Di Pietro, E., and Di Ietro, T. (2011). Biomass production, P.B. Inc.
70. Gonzalez, J.A., Martin, S.C., Kolesnik, M., Di Pietro, E., and Di Ietro, T. (2012). Biomass production.
71. Gonzalez, J.A., Martin, S.C., Kolesnik, M., Di Pietro, E., and Di Ietro, T. (2013). Biomass production: CA.
72. Gonzalez, J.A., Martin, S.C., Kolesnik, M., Di Pietro, E., and Di Ietro, T. (2014). Process of operating a plurality of photobioreactors, P.B. Inc..
73. Mottahedeh, S. (2014). Low-cost photobioreactor. Available from: https://patents.google.com/patent/US20140315290A1/en.
74. Roulston, R. (2014). Photobioreactor for liquid cultures. Available from: https://patents.google.com/patent/US9688950B2/en.
75. Smith, M.F. (2014). Biorefinery Control System, Components, I. Algae Aqua-Culture Technology. Available from: https://patents.google.com/patent/US20140030695A1/en.
76. Smith, M.F., Holecek, R.M., and Kelson, R.D. (2014). Biorefinery System Components, I. Algae Aqua-Culture Technology. Available from: https://patents.google.com/patent/US20140024528A1/en.
77. Smith, M.F. and Rockwell, J. M. J. (2012). Biorefinery System Components, I. Algae Aqua-Culture Technology. Available from: https://patents.google.com/patent/US20120208254A1/en.
78. Melcher, J. (2011). Wood Waste Utilization – Greenhouse Packs A Power Punch, in BioCycle, JG Press, Inc: Montana.
79. Gaiser, H. (2012). Green Power, Daily Inter Lake. Available from: https://www.dailyinterlake.com/archive/article-ab1dd3ee-e439-11e1-a6b7-001a4bcf887a.html.
80. Sieg, D. (2013). Algae Biorefineries and Micro-Farming. Available from: http://www.making-biodiesel-books.com/custom-2/Microfarming-Book-sample1.pdf.
81. Company Overview of Algae Tec Limited, Bloomberg Business. Available from: https://www.bloomberg.com/research/stocks/private/snapshot.asp?privcapId=281560074.
82. Energy From Algae. (2009) [20150216] (archived); Available from: http://www.nrc-cnrc.gc.ca/eng/achievements/highlights/2009/algae_biofuels.html.
83. Integrating the Brite Box Technology into a Shellfish Hatchery. 2010 [20150216]; Available from: http://www.dfo-mpo.gc.ca/aquaculture/sustainable-durable/rapports-reports/2008-G02-eng.htm.
84. Blanchard, B. (2004). Productivity of brite box systems.
85. Park, K.C., Whitney, C., McNichol, J. C., Dickinson, K. E., MacQuarrie, S., Skrupski, B. P., Zou, J., Wilson, K.E., O'Leary, S.J., and McGinn, P. J. (2012). Mixotrophic and photoautotrophic cultivation of 14 microalgae isolates from Saskatchewan, Canada: potential applications for wastewater remediation for biofuel production. Journal of Applied Phycology, 24 (3), 339–348.
86. Pond Biofuels Inc. patents. (2015) [20150424]; Available from: http://stks.freshpatents.com/Pond-Biofuels-Inc-nm1.php. Accessed: [May 10, 2015].
87. Dodge, D. and Kinney, D. Pond Biofuels: Their algae eats cement plant pollution for breakfast. 2014 [cited 2014 May 14, 2014]; Available from:

http://www.greenenergyfutures.ca/blog/pond-biofuels-their-algae-eats-cement-plant-pollution-breakfast.
88. Process news: Canada seeks profit from oil sands emissions. (2013). The Chemical Engineer (864), 20.
89. Javanmardian, M. and Palsson, B.O. (1991). High-density photoautotrophic algal cultures: Design, construction, and operation of a novel photobioreactor system. Biotechnology and Bioengineering 38(10), 1182-1189.
90. Gim, G.H., Kim, J.K., Kim, H.S., Kathiravan, M.N., Yang, H., Jeong, S.H., and Kim, S. W. (2014). Comparison of biomass production and total lipid content of freshwater green microalgae cultivated under various culture conditions. Bioprocess and Biosystems Engineering 37(2), 99-106.
91. Cifuentes, A.S., González, M.A., Vargas, S., Hoeneisen, M., and González, N. (2003). Optimization of biomass, total carotenoids and astaxanthin production in Haematococcus pluvialis Flotow strain Steptoe (Nevada, USA) under laboratory conditions. Biological Research 36(3-4), 343-357.
92. Galvão, R.M., Santana, T.S., Fontes, C.H.O., and Sales, E. A. (2013). Modeling of biomass production of Haematococcus pluvialis. Scientific Research Applied Mathematics (4), 50-56.
93. Gami, B., Patel, J.P., and Kothari, I.L. (2014). Cultivation of Chlorella protothecoides (ISIBES –101) under autotrophic and heterotrophic conditions for biofuel production. Journal of Algal Biomass 5(2), 20-29.
94. Hakalin, N.L.S., Paz, A.P., Aranda, D.A.G., and Morales, L.M.P. (2014). Enhancement of cell growth and lipid content of a freshwater microalga scenedesmus sp. by optimizing nitrogen, phosphorus and vitamin concentrations for biodiesel production. Natural Science 6(12), 1044-1054.
95. Poonkum, W., Powtongsook, S., and Pavasant, P. (2015). Astaxanthin induction in microalga H. pluvialis with flat panel airlift photobioreactors under indoor and outdoor conditions. Preparative Biochemistry and Biotechnology 45(1), 1-17.
96. Biofuels International. (2008). Algae Investments, in Biofuels International. Available from: https://pdfs.semanticscholar.org/948d/d1fdf080b9e10eb8fcaa70e879f0897e6bea.pdf.
97. Alic, J. (2013). Exxon's $100m Algae Investment Falls Flat, in OilPrice.com. Accessed [January 28, 2019].
98. Industry: Size, Growth Projections, Global Competition. (2015) [20150427]; Available from: http://allaboutalgae.com/faq-industry/. Accessed [Jan 28, 2019].
99. Gong, J. and You, F. (2014). Optimal design and synthesis of algal biorefinery processes for biological carbon sequestration and utilization with zero direct greenhouse gas emissions: MINLP model and global optimization algorithm. Industrial and Engineering Chemistry Research 53(4), 1563-1579.
100. Prieto, C.V.G., Ramos, F.D., Estrada, V., and Díaz, M.S. (2014). Optimal design of an integrated microalgae biorefinery for the production of biodiesel and PHBS, in Chemical Engineering Transactions, pp. 319-324.
101. Wahidin, S., Idris, A., and Shaleh, S.R.M. (2013). The influence of light intensity and photoperiod on the growth and lipid content of microalgae Nannochloropsis sp. Bioresource Technology 129, 7-11.

102. Krzemińska, I., Pawlik-Skowrońska, B., Trzcińska, M., and Tys, J. (2014). Influence of photoperiods on the growth rate and biomass productivity of green microalgae. Bioprocess and Biosystems Engineering 37(4), 735-741.
103. Gris, B., Morosinotto, T., Giacometti, G. M., Bertucco, A., and Sforza, E. (2014). Cultivation of Scenedesmus obliquus in photobioreactors: Effects of light intensities and light-dark cycles on growth, productivity, and biochemical composition. Applied Biochemistry and Biotechnology 172(5), 2377-2389.
104. Veal, M.W., Caffrey, K.R., Chinn, M.S., and Grunden, A.M. (2013). Algae for Biofuels – Economic and Environmental Costs, Southern Regional Aquaculture Center, p. 8. Available from: https://www.cabdirect.org/cabdirect/abstract/20143127963.
105. Nguyen, K.D. (2013). Astaxanthin: A comparative Case of Synthetic vs Natural Production., University of Tenessee: Tenessee Research and Creative Exchange (TRACE), p. 9.
106. Montingelli, M.E., Tedesco, S., and Olabi, A.G. (2015). Biogas production from algal biomass: A review. Renewable and Sustainable Energy Reviews 43, 961-972.
107. Abbas, S. (2015). Dynamical analysis of a model of harmful algae in flowing habitats with variable rates. Nonlinear Analysis: Real World Applications 22, 16-33.
108. Beer, L.L., Boyd, E.S., Peters, J.W., and Posewitz, M.C. (2009). Engineering algae for biohydrogen and biofuel production. Current Opinion Biotechnology 20(3), 264-71.
109. Melis, A. (2013). Carbon partitioning in photosynthesis. Current Opinion in Chemical Biology 17(3), 453-456.
110. Mettler, T., Mühlhaus, T., Hemme, D., Schöttler, M. A., Rupprecht, J., Idoine, A., Veyel, D., Pal, S.K., Yaneva-Roder, L., Winck, F.V., Sommer, F., Vosloh, D., Seiwert, B., Erban, A., Burgos, A., Arvidsson, S., Schönfelder, S., Arnold, A., Günther, M., Krause, U., Lohse, M., Kopka, J., Nikoloski, Z., Mueller-Roeber, B., Willmitzer, L., Bock, R., Schroda, M., and Stitt, M. (2014). Systems analysis of the response of photosynthesis, metabolism, and growth to an increase in irradiance in the photosynthetic model organism Chlamydomonas reinhardtii. Plant Cell 26(6), 2310-2350.
111. Long, S.P., Zhu, XG., Naidu, S.L., and Ort, D.R. (2006). Can improvement in photosynthesis increase crop yields? Plant, Cell and Environment 29(3), 315-330.
112. Zhu, X.G., Long, S.P., and Ort, D.R. (2008). What is the maximum efficiency with which photosynthesis can convert solar energy into biomass? Current Opinion in Biotechnology 19(2), 153-159.
113. Xu, J., Fan, X., Zhang, X., Xu, D., Mou, S., Cao, S., Zheng, Z., Miao, J., and Ye, N. (2012). Evidence of coexistence of C3 and C4 photosynthetic pathways in a green-tide-forming alga, ulva prolifera. PLoS ONE 7(5).
114. Tekin, K. and Karagöz, S. (2013). Non-catalytic and catalytic hydrothermal liquefaction of biomass. Research on Chemical Intermediates 39(2), 485-498.
115. McKendry, P. (2002). Energy production from biomass (part 1): overview of biomass. Bioresource technology 83(1), 37-46.
116. Tekin, K. and Karagöz, S. (2013). t-BuOK catalyzed bio-oil production from woody biomass under sub-critical water conditions. Environmental Chemistry Letters 11(1), 25-31.
117. Briens, C., Piskorz, J., and Berruti, F. (2008). Biomass valorization for fuel and chemicals production – A review. International Journal of Chemical Reactor Engineering 6(1), 1542-6580.

118. Savage, P.E., Levine, R.., and Huelsman, C.M. (2010). Hydrothermal processing of biomass. In Thermochemical Conversion of Biomass to Liquid Fuels and Chemicals, edited by M. Crocker. Cambridge: Royal Society of Chemistry, pp. 192-221.
119. Brunner, G. (2009). Near critical and supercritical water. Part I. Hydrolytic and hydrothermal processes. The Journal of Supercritical Fluids 47(3), 373-381.
120. Gao, X., Yu, Y., and Wu, H. (2013). Life cycle energy and carbon footprints of microalgal biodiesel production in western australia: A comparison of byproducts utilization strategies. ACS Sustainable Chemistry & Engineering 1(11), 1371-1380.
121. Yokoyama, S. and Matsumura, Y. (2008). The Asian biomass handbook: a guide for biomass production and utilization. The Japan Institute of Energy, 61-62.
122. Elliott, D.C. (2011). Hydrothermal Processing, in Thermochemical Processing of Biomass: Conversion into Fuels, Chemicals and Power, pp. 200-231.
123. Chiaramonti, D., Prussi, M., Buffi, M., Rizzo, A. M., and Pari, L. (2017). Review and experimental study on pyrolysis and hydrothermal liquefaction of microalgae for biofuel production. Applied Energy 185, Part 2, 963-972.
124. Zhang, L., Xu, C., and Champagne, P. (2010). Overview of recent advances in thermo-chemical conversion of biomass. Energy Conversion and Management 51(5), 969-982.
125. Karagöz, S., Bhaskar, T., Muto, A., Sakata, Y., and Uddin, M. A. (2003). Low-temperature hydrothermal treatment of biomass: effect of reaction parameters on products and boiling point distributions. Energy & Fuels 18(1), 234-241.
126. Kruse, A., Funke, A., and Titirici, M.-M. (2013). Hydrothermal conversion of biomass to fuels and energetic materials. Current Opinion in Chemical Biology 17(3), 515-521.
127. Toor, S.S., Rosendahl, L., and Rudolf, A. (2011). Hydrothermal liquefaction of biomass: a review of subcritical water technologies. Energy 36(5), 2328-2342.
128. Dimitriadis, A. and Bezergianni, S. (2017). Hydrothermal liquefaction of various biomass and waste feedstocks for biocrude production: A state of the art review. Renewable and Sustainable Energy Reviews 68, Part 1, 113-125.
129. Peterson, A.A., Vogel, F., Lachance, R.P., Fröling, M., Antal M.J., Jr., and Tester, J.W. (2008). Thermochemical biofuel production in hydrothermal media: a review of sub-and supercritical water technologies. Energy & Environmental Science 1(1), 32-65.
130. Luterbacher, J.S., Fröling, M., Vogel, F., Maréchal, F., and Tester, J.W. (2009). Hydrothermal gasification of waste biomass: Process design and life cycle asessment. Environmental Science & Technology 43(5), 1578-1583.
131. Steubing, B., Zah, R., and Ludwig, C. (2011). Heat, electricity, or transportation? The optimal use of residual and waste biomass in Europe from an environmental perspective. Environmental science & technology 46(1), 164-171.
132. Maddi, B., Panisko, E.A., Wietsma, T., Lemmon, T., Swita, M., Albrecht, K., and Howe, D. T. (2017). Quantitative Characterization of Aqueous Byproducts from Hydrothermal Liquefaction of Municipal Wastes, Food Industry Wastes, and Biomass Grown on Waste. ACS Sustainable Chemistry & Engineering.
133. Chen, Y., Ren, X., Wei, Q., and Guo, J. (2016). Hydrothermal liquefaction of Undaria pinnatifida residues to organic acids with recyclable trimethylamine. Bioresource Technology 221, 477-484.
134. Hadhoum, L., Balistrou, M., Burnens, G., Loubar, K., and Tazerout, M. (2016). Hydrothermal liquefaction of oil mill wastewater for bio-oil production in subcritical conditions. Bioresource Technology 218, 9-17.

135. Kumar, G., Shobana, S., Chen, W.-H., Bach, Q.-V., Kim, S.-H., Atabani, A., and Chang, J.-S. (2017). A review of thermochemical conversion of microalgal biomass for biofuels: chemistry and processes. Green Chemistry 19(1), 44-67.
136. Modell, M. (1985). Gasification and liquefaction of forest products in supercritical water, in Fundamentals of Thermochemical Biomass Conversion, Springer. pp. 95-119.
137. Elliott, D.C., Biller, P., Ross, A. B., Schmidt, A. J., and Jones, S. B. (2015). Hydrothermal liquefaction of biomass: Developments from batch to continuous process. Bioresource Technology 178, 147-156.
138. Matsumura, Y., Minowa, T., Potic, B., Kersten, S R., Prins, W., van Swaaij, W.P., van de Beld, B., Elliott, D.C., Neuenschwander, G.G., and Kruse, A. (2005). Biomass gasification in near-and super-critical water: status and prospects. Biomass and Bioenergy 29(4), 269-292.
139. Biller, P. and Ross, A.B. (2012). Hydrothermal processing of algal biomass for the production of biofuels and chemicals. Biofuels 3(5), 603-623.
140. Schaleger, L., Figueroa, C., and Davis, H. (1982). Direct liquefaction of biomass: results from operation of continuous bench-scale unit in liquefaction of water slurries of Douglas fir wood. in Biotechnology Bioengineering Symposium (United States). Lawrence Berkeley Lab., CA.
141. Thigpen, P. (1982). Final Report: An Investigation of Liquefaction of Wood at the Biomass Liquefaction Facility, Albany, Oregon, Battelle Pacific Northwest Laboratories, Department of Energy, Wheelabrator Cleanfuel Corporation. Technical Information Center, Office of Scientific and Technical Information, US Department of Energy.
142. Elliott, D.C. (1980). Process development for biomass liquefaction. Am. Chem. Soc., Div. Fuel Chem., Prepr.; (United States) 25(CONF-800814-P3). Available from: https://web.anl.gov/PCS/acsfuel/preprint%20archive/Files/25_4_SAN%20FRANCISCO_08-80_0257.pdf.
143. Goudnaan, F., Van de Beld, B., Boerefijn, F., Bos, G., Naber, J., Van der Wal, S., and Zeevalkink, J. (2008). Thermal efficiency of the HTU® process for biomass liquefaction. Progress in Thermochemical Biomass Conversion, 1312-1325.
144. Green Car Congress. NextFuels introduces hydrothermal process to produce biofuels from wet, unprocessed waste; solution for palm plantation residue (2017). Available from: http://www.greencarcongress.com/2013/08/20130819-next.html.
145. Nielsen, R.P., Olofsson, G., and Søgaard, E.G. (2012). CatLiq–High pressure and temperature catalytic conversion of biomass: The CatLiq technology in relation to other thermochemical conversion technologies. biomass and bioenergy 39, 399-402.
146. Steeper Energy. Available from: http://steeperenergy.com/.
147. Adams, T., Appel, B., Samson, P., and Roberts, M. (2004). Converting turkey offal into bio-derived hydrocarbon oil with the CWT thermal process. Presented at the Power-Gen Renewable Energy Conference.
148. Canadian firm acquires Carthage RES plant (2013).
149. Tran, K.-Q. (2016). Fast hydrothermal liquefaction for production of chemicals and biofuels from wet biomass – The need to develop a plug-flow reactor. Bioresource Technology 213, 327-332.
150. Matsumura, Y. (2015). Hydrothermal gasification of biomass. In Recent Advances in Thermo-Chemical Conversion of Biomass, 1st ed, edited by A. Pandey, T. Bhaskar, M. Stöcker, and R.K. Sukumaran. Elsevier: Boston, pp. 251-267.

151. Bermejo, M. and Cocero, M. (2006). Supercritical water oxidation: a technical review. AIChE Journal 52(11), 3933-3951.
152. Sealock, L.J., Jr., Elliott, D.C., Baker, E.G., and Butner, R.S. (1993). Chemical processing in high-pressure aqueous environments. 1. Historical perspective and continuing developments. Industrial & Engineering Chemistry Research 32(8), 1535-1541.
153. Elliott, D.C., Sealock, L.J., Jr., and Baker, E.G. (1993). Chemical processing in high-pressure aqueous environments. 2. Development of catalysts for gasification. Industrial & Engineering Chemistry Research 32(8), 1542-1548.
154. Xu, X., Matsumura, Y., Stenberg, J., and Antal, M.J. (1996). Carbon-catalyzed gasification of organic feedstocks in supercritical water. Industrial & Engineering Chemistry Research 35(8), 2522-2530.
155. Yu, D., Aihara, M., and Antal, M.J., Jr. (1993). Hydrogen production by steam reforming glucose in supercritical water. Energy & Fuels 7(5), 574-577.
156. Kruse, A., Meier, D., Rimbrecht, P., and Schacht, M. (2000). Gasification of pyrocatechol in supercritical water in the presence of potassium hydroxide. Industrial & Engineering Chemistry Research 39(12), 4842-4848.
157. Yoshida, T. and Matsumura, Y. (2001). Gasification of cellulose, xylan, and lignin mixtures in supercritical water. Industrial & Engineering Chemistry Research 40(23), 5469-5474.
158. Savage, P.E. (2009). A perspective on catalysis in sub-and supercritical water. The Journal of Supercritical Fluids 47(3), 407-414.
159. Onwudili, J.A. and Williams, P.T. (2011). Reaction of different carbonaceous materials in alkaline hydrothermal media for hydrogen gas production. Green Chemistry 13(10), 2837-2843.
160. Landais, P. (1991). Assessment of coal potential evolution by experimental simulation of natural coalification. Organic Geochemistry, 17(6), 705-710.
161. Bobleter, O. (1994). Hydrothermal degradation of polymers derived from plants. Progress in Polymer Science 19(5), 797-841.
162. Kambo, H.S. and Dutta, A. (2015). A comparative review of biochar and hydrochar in terms of production, physico-chemical properties and applications. Renewable and Sustainable Energy Reviews 45, 359-378.
163. Wörmeyer, K., Ingram, T., Saake, B., Brunner, G., and Smirnova, I. (2011). Comparison of different pretreatment methods for lignocellulosic materials. Part II: Influence of pretreatment on the properties of rye straw lignin. Bioresource Technology 102(5), 4157-4164.
164. Takata, E., Tsutsumi, K., Tsutsumi, Y., and Tabata, K. (2013). Production of monosaccharides from napier grass by hydrothermal process with phosphoric acid. Bioresource Technology 143, 53-58.
165. Tian, C., Liu, Z., Zhang, Y., Li, B., Cao, W., Lu, H., Duan, N., Zhang, L., and Zhang, T. (2015). Hydrothermal liquefaction of harvested high-ash low-lipid algal biomass from Dianchi Lake: Effects of operational parameters and relations of products. Bioresource Technology 184, 336-343.
166. Tekin, K., Karagöz, S., and Bektaş, S. (2014). A review of hydrothermal biomass processing. Renewable and Sustainable Energy Reviews 40, 673-687.
167. Mtui, G.Y. (2009). Recent advances in pretreatment of lignocellulosic wastes and production of value added products. African Journal of Biotechnology 8(8),1398-1415

168. Sánchez, C. (2009). Lignocellulosic residues: biodegradation and bioconversion by fungi. Biotechnology advances 27(2), 185-194.
169. Delmer, D.P. and Amor, Y. (1995). Cellulose biosynthesis. The Plant Cell 7(7), 987.
170. Rowell, R.M., Pettersen, R., Han, J. S., Rowell, J.S., and Tshabalala, M.A. (2005). Cell wall chemistry. Handbook of Wood Chemistry and Wood Composites, 35-74. DOI: https://doi.org/10.1201/b12487.
171. Sun, R. (2010). Cereal straw as a resource for sustainable biomaterials and biofuels: chemistry, extractives, lignins, hemicelluloses and cellulose. Elsevier.
172. Vassilev, S.V., Baxter, D., Andersen, L.K., Vassileva, C.G., and Morgan, T. J. (2012). An overview of the organic and inorganic phase composition of biomass. Fuel 94, 1-33.
173. Telmo, C. and Lousada, J. (2011). The explained variation by lignin and extractive contents on higher heating value of wood. Biomass and Bioenergy 35(5), 1663-1667.
174. Weingärtner, H. and Franck, E.U. (2005). Supercritical water as a solvent. Angewandte Chemie International Edition 44(18), 2672-2692.
175. Xu, X., De Almeida, C., and Antal, M. J. (1990). Mechanism and kinetics of the acid-catalyzed dehydration of ethanol in supercritical water. The Journal of Supercritical Fluids 3(4), 228-232.
176. Sasaki, M., Furukawa, M., Minami, K., Adschiri, T., and Arai, K. (2002). Kinetics and mechanism of cellobiose hydrolysis and retro-aldol condensation in subcritical and supercritical water. Industrial & Engineering Chemistry Research 41(26), 6642-6649.
177. Möller, M., Nilges, P., Harnisch, F., and Schröder, U. (2011). Subcritical water as reaction environment: fundamentals of hydrothermal biomass transformation. ChemSusChem 4(5), 566-579.
178. Broell, D., Kaul, C., Kraemer, A., Krammer, P., Richter, T., Jung, M., Vogel, H., and Zehner, P. (1999). Chemistry in supercritical water. Angewandte Chemie International Edition 38(20), 2998-3014.
179. Marshall, W.L. and Franck, E. (1981). Ion product of water substance, 0–1000° C, 1–10,000 bars new international formulation and its background. Journal of Physical and Chemical Reference Data 10(2), 295-304.
180. Kritzer, P. (2004). Corrosion in high-temperature and supercritical water and aqueous solutions: a review. The Journal of Supercritical Fluids 29(1), 1-29.
181. Ding, Z.Y., Frisch, M.A., Li, L., and Gloyna, E.F. (1996). Catalytic oxidation in supercritical water. Industrial & Engineering Chemistry Research 35(10), 3257-3279.
182. Henrikson, J.T., Chen, Z., and Savage, P.E. (2003). Inhibition and acceleration of phenol oxidation by supercritical water. Industrial & Engineering Chemistry Research 42(25), 6303-6309.
183. Penninger, J., Kersten, R., and Baur, H. (1999). Reactions of diphenylether in supercritical water—mechanism and kinetics. The Journal of Supercritical Fluids 16(2), 119-132.
184. Penninger, J., Kersten, R., and Baur, H. (2000). Hydrolysis of diphenylether in supercritical water: effects of dissolved NaCl. The Journal of Supercritical Fluids 17(3), 215-226.
185. Ogunsola, O.M. and Berkowitz, N. (1995). Removal of heterocyclic S and N from oil precursors by supercritical water. Fuel 74(10), 1485-1490.
186. Onwudili, J.A. and Williams, P.T. (2008). Hydrothermal gasification and oxidation as effective flameless conversion technologies for organic wastes. Journal of the Energy Institute 81(2), 102-109.

187. Kruse, A. (2008). Supercritical water gasification. Biofuels, Bioproducts and Biorefining 2(5), 415-437.
188. Kayserilioğlu, B.Ş., Bakir, U., Yilmaz, L., and Akkaş, N. (2003). Use of xylan, an agricultural by-product, in wheat gluten based biodegradable films: mechanical, solubility and water vapor transfer rate properties. Bioresource Technology 87(3), 239-246.
189. Vegas, R., Kabel, M., Schols, H.A., Alonso, J.L., and Parajó, J.C. (2008). Hydrothermal processing of rice husks: effects of severity on product distribution. Journal of Chemical Technology & Biotechnology 83(7), 965-972.
190. Nabarlatz, D., Farriol, X., and Montane, D. (2004). Kinetic modeling of the autohydrolysis of lignocellulosic biomass for the production of hemicellulose-derived oligosaccharides. Industrial & Engineering Chemistry Research 43(15), 4124-4131.
191. Carvalheiro, F., Esteves, M., Parajó, J., Pereira, H., and Gırio, F. (2004). Production of oligosaccharides by autohydrolysis of brewery's spent grain. Bioresource Technology 91(1), 93-100.
192. Kabel, M., Carvalheiro, F., Garrote, G., Avgerinos, E., Koukios, E., Parajó, J., Gırio, F., Schols, H., and Voragen, A. (2002). Hydrothermally treated xylan rich by-products yield different classes of xylo-oligosaccharides. Carbohydrate Polymers 50(1), 47-56.
193. Gullón, P., Pereiro, G., Alonso, J.L., and Parajó, J.C. (2009). Aqueous pretreatment of agricultural wastes: characterization of soluble reaction products. Bioresource Technology 100(23), 5840-5845.
194. Garrote, G., Domínguez, H., and Parajó, J. (2001). Manufacture of xylose-based fermentation media from corncobs by posthydrolysis of autohydrolysis liquors. Applied Biochemistry and Biotechnology 95(3), 195-207.
195. Rivas, B., Domınguez, J., Domınguez, H., and Parajó, J. (2002). Bioconversion of posthydrolysed autohydrolysis liquors: an alternative for xylitol production from corn cobs. Enzyme and Microbial Technology 31(4), 431-438.
196. Duarte, L.C., Carvalheiro, F., Lopes, S., Marques, S., Parajo, J.C., and Gírio, F.M. (2004). Comparison of two posthydrolysis processes of brewery's spent grain autohydrolysis liquor to produce a pentose-containing culture medium. In Proceedings of the Twenty-Fifth Symposium on Biotechnology for Fuels and Chemicals, May 4–7, 2003, Breckenridge, CO. Springer.
197. Vila, C., Campos, A.R., Cristovão, C., Cunha, A.., Santos, V., and Parajó, J. C. (2008). Sustainable biocomposites based on autohydrolysis of lignocellulosic substrates. Composites Science and Technology 68 (3–4), 944-952.
198. Michelin, M., Maria de Lourdes, T., Ruzene, D.S., Silva, D.P., Ruiz, H.A., Vicente, A.A., Jorge, J.A., Terenzi, H.F., and Teixeira, J.A. (2012). Production of xylanase and β-xylosidase from autohydrolysis liquor of corncob using two fungal strains. Bioprocess and Biosystems Engineering 35(7), 1185-1192.
199. Montané, D., Nabarlatz, D., Martorell, A., Torné-Fernández, V., and Fierro, V. (2006). Removal of lignin and associated impurities from xylo-oligosaccharides by activated carbon adsorption. Industrial & Engineering Chemistry Research 45(7), 2294-2302.
200. Vegas, R., Moure, A., Domínguez, H., Parajó, J.C., Álvarez, J.R., and Luque, S. (2006). Purification of oligosaccharides from rice husk autohydrolysis liquors by ultra-and nano-filtration. Desalination 199(1), 541-543.
201. Garrote, G. and Parajó, J. (2002). Non-isothermal autohydrolysis of Eucalyptus wood. Wood Science and Technology 36(2), 111-123.

202. Liu, C. and Wyman, C.E. (2004). Impact of fluid velocity on hot water only pretreatment of corn stover in a flowthrough reactor. in Proceedings of the Twenty-Fifth Symposium on Biotechnology for Fuels and Chemicals, May 4–7, 2003, Breckenridge, CO. Springer.
203. Makishima, S., Mizuno, M., Sato, N., Shinji, K., Suzuki, M., Nozaki, K., Takahashi, F., Kanda, T., and Amano, Y. (2009). Development of continuous flow type hydrothermal reactor for hemicellulose fraction recovery from corncob. Bioresource Technology 100(11), 2842-2848.
204. Buranov, A.U. and Mazza, G. (2008). Lignin in straw of herbaceous crops. Industrial crops and products 28(3), 237-259.
205. Pandey, M.P. and Kim, C.S. (2011). Lignin depolymerization and conversion: a review of thermochemical methods. Chemical Engineering & Technology 34(1), 29-41.
206. Kristensen, J.B., Thygesen, L.G., Felby, C., Jørgensen, H., and Elder, T. (2008). Cell-wall structural changes in wheat straw pretreated for bioethanol production. Biotechnology for Biofuels 1(5), 1-9.
207. Zhang, T., Wyman, C.E., Jakob, K., and Yang, B. (2012). Rapid selection and identification of Miscanthus genotypes with enhanced glucan and xylan yields from hydrothermal pretreatment followed by enzymatic hydrolysis. Biotechnology for Biofuels 5(1), 56.
208. Cannella, D., Hsieh, C.-W., Felby, C., and Jørgensen, H. (2012). Production and effect of aldonic acids during enzymatic hydrolysis of lignocellulose at high dry matter content. Biotechnology for Biofuels 5(1), 26.
209. Garrote, G., Dominguez, H., and Parajo, J. (1999). Hydrothermal processing of lignocellulosic materials. European Journal of Wood and Wood Products 57(3), 191-202.
210. Gullón, P., Conde, E., Moure, A., Domínguez, H., and Parajó, J.C. (2010). Selected process alternatives for biomass refining: a review. Open Agriculture Journal 4(2), 135-144.
211. Zhang, B., Huang, H.-J., and Ramaswamy, S. (2008). Reaction kinetics of the hydrothermal treatment of lignin. Applied Biochemistry and Biotechnology 147(1-3), 119-131.
212. Chi, C., Zhang, Z., Chang, H.-M., and Jameel, H. (2009). Determination of furfural and hydroxymethylfurfural formed from biomass under acidic conditions. Journal of Wood Chemistry and Technology 29(4), 265-276.
213. Schmidt, J.A. (2009). Electronic spectroscopy of lignins. In Lignin and Lignans: Advances in Chemistry, edited by C. Heitner, D.R. Dimmel, and J.A. Schmidt, pp. 49-102. CRC Press, Taylor and Francis Group.
214. Conde, E., Moure, A., Domínguez, H., and Parajó, J.C. (2011). Production of antioxidants by non-isothermal autohydrolysis of lignocellulosic wastes. LWT-Food Science and Technology 44(2), 436-442.
215. Garrote, G., Cruz, J., Moure, A., Domınguez, H., and Parajó, J. (2004). Antioxidant activity of byproducts from the hydrolytic processing of selected lignocellulosic materials. Trends in Food Science & Technology 15(3), 191-200.
216. Tsubaki, S., Sakamoto, M., and Azuma, J.-I. (2010). Microwave-assisted extraction of phenolic compounds from tea residues under autohydrolytic conditions. Food Chemistry 123(4), 1255-1258.
217. Ruiz, H.A., Rodríguez-Jasso, R.M., Fernandes, B.D., Vicente, A.A., and Teixeira, J.A. (2013). Hydrothermal processing, as an alternative for upgrading agriculture residues and marine biomass according to the biorefinery concept: A review. Renewable and Sustainable Energy Reviews 21, 35-51.

218. Savage, P.E., Levine, R.B., Huelsman, C.M. (2010). Hydrothermal processing of biomass. In Thermochemical Conversion of Biomass to Liquid Fuels and Chemicals, edited by M. Crocker. Cambridge: Royal Society of Chemistry.
219. Savage, P., Levine, R., and Huelsman, C. (2010). Thermochemical Conversion of Biomass to Liquid Fuels and Chemicals.
220. Tekin, K., Akalin, M. K., and Karagöz, S. (2016). The effects of water tolerant Lewis acids on the hydrothermal liquefaction of lignocellulosic biomass. Journal of the Energy Institute 89(4), 627-635.
221. Kumar, K., Ghosh, S., Angelidaki, I., Holdt, S. L., Karakashev, D.B., Morales, M.A., and Das, D. (2016). Recent developments on biofuels production from microalgae and macroalgae. Renewable and Sustainable Energy Reviews 65, 235-249.
222. Li, C., Aston, J.E., Lacey, J.A., Thompson, V.S., and Thompson, D.N. (2016). Impact of feedstock quality and variation on biochemical and thermochemical conversion. Renewable and Sustainable Energy Reviews 65, 525-536.
223. Arvindnarayan, S., Sivagnana Prabhu, K.K., Shobana, S., Kumar, G., and Dharmaraja, J. Upgrading of micro algal derived bio-fuels in thermochemical liquefaction path and its perspectives: A review. International Biodeterioration & Biodegradation. 119, 260-272.
224. Maurya, R., Paliwal, C., Ghosh, T., Pancha, I., Chokshi, K., Mitra, M., Ghosh, A., and Mishra, S. (2016). Applications of de-oiled microalgal biomass towards development of sustainable biorefinery. Bioresource Technology 214, 787-796.
225. López Barreiro, D., Gómez, B.R., Ronsse, F., Hornung, U., Kruse, A., and Prins, W. (2016). Heterogeneous catalytic upgrading of biocrude oil produced by hydrothermal liquefaction of microalgae: State of the art and own experiments. Fuel Processing Technology 148, 117-127.
226. Haarlemmer, G., Guizani, C., Anouti, S., Déniel, M., Roubaud, A., and Valin, S. (2016). Analysis and comparison of bio-oils obtained by hydrothermal liquefaction and fast pyrolysis of beech wood. Fuel 174, 180-188.
227. Patel, B., Guo, M., Shah, N., and Hellgardt, K. (2016). Environmental profile of algal hydrothermal liquefaction — A country specific case study. Algal Research 16, 127-140.
228. Saber, M., Nakhshiniev, B., and Yoshikawa, K. (2016). A review of production and upgrading of algal bio-oil. Renewable and Sustainable Energy Reviews 58, 918-930.
229. Pearce, M., Shemfe, M., and Sansom, C. (2016). Techno-economic analysis of solar integrated hydrothermal liquefaction of microalgae. Applied Energy 166, 19-26.
230. Albrecht, K.O., Zhu, Y., Schmidt, A.., Billing, J.M., Hart, T.R., Jones, S.B., Maupin, G., Hallen, R., Ahrens, T., and Anderson, D. (2016). Impact of heterotrophically stressed algae for biofuel production via hydrothermal liquefaction and catalytic hydrotreating in continuous-flow reactors. Algal Research 14, 17-27.
231. Déniel, M., Haarlemmer, G., Roubaud, A., Weiss-Hortala, E., and Fages, J. (2016). Energy valorisation of food processing residues and model compounds by hydrothermal liquefaction. Renewable and Sustainable Energy Reviews 54, 1632-1652.
232. Patel, B., Guo, M., Izadpanah, A., Shah, N., and Hellgardt, K. (2016). A review on hydrothermal pre-treatment technologies and environmental profiles of algal biomass processing. Bioresource Technology 199, 288-299.
233. Chaudry, S., Bahri, P. A., and Moheimani, N.R. (2015). Pathways of processing of wet microalgae for liquid fuel production: A critical review. Renewable and Sustainable Energy Reviews 52, 1240-1250.

234. Summers, H.M., Ledbetter, R.N., McCurdy, A.T., Morgan, M.R., Seefeldt, L.C., Jena, U., Hoekman, S.K., and Quinn, J.C. (2015). Techno-economic feasibility and life cycle assessment of dairy effluent to renewable diesel via hydrothermal liquefaction. Bioresource Technology 196, 431-440.
235. Huang, H.-J. and Yuan, X.-Z. (2015). Recent progress in the direct liquefaction of typical biomass. Progress in Energy and Combustion Science 49, 59-80.
236. Guo, Y., Yeh, T., Song, W., Xu, D., and Wang, S. (2015). A review of bio-oil production from hydrothermal liquefaction of algae. Renewable and Sustainable Energy Reviews 48, 776-790.
237. Gerber Van Doren, L., Posmanik, R., Bicalho, F.A., Tester, J.W., and Sills, D.L. (2017). Prospects for energy recovery during hydrothermal and biological processing of waste biomass. Bioresource Technology 225, 67-74.
238. López Barreiro, D., Prins, W., Ronsse, F., and Brilman, W. (2013). Hydrothermal liquefaction (HTL) of microalgae for biofuel production: State of the art review and future prospects. Biomass and Bioenergy 53, 113-127.
239. Chornet, E. and Overend, R. P. (1985). Biomass liquefaction: an overview, in Fundamentals of thermochemical biomass conversion, Springer. p. 967-1002.
240. Kumar, S. and Gupta, R. B. (2009). Biocrude production from switchgrass using subcritical water. Energy & Fuels 23(10), 5151-5159.
241. Patil, V., Tran, K.-Q., and Giselrød, H. R. (2008). Towards sustainable production of biofuels from microalgae. International journal of molecular sciences 9(7), 1188-1195.
242. Peterson, A. A., Vogel, F., Lachance, R. P., Froling, M., Antal, J. M. J., and Tester, J. W. (2008). Thermochemical biofuel production in hydrothermal media: A review of sub- and supercritical water technologies. Energy & Environmental Science 1(1), 32-65.
243. Savage, P. E. (2009). A perspective on catalysis in sub- and supercritical water. The Journal of Supercritical Fluids 47(3), 407-414.
244. Wahyudiono, Sasaki, M., and Goto, M. (2008). Recovery of phenolic compounds through the decomposition of lignin in near and supercritical water. Chemical Engineering and Processing: Process Intensification 47(9-10), 1609-1619.
245. He, W., Li, G., Kong, L., Wang, H., Huang, J., and Xu, J. (2008). Application of hydrothermal reaction in resource recovery of organic wastes. Resources, Conservation and Recycling 52(5), 691-699.
246. Molten, P., Demmitt, T., Donovan, J., and Miller, R. (1983). Mechanism of conversion of cellulose wastes to liquid in alkaline solution. Energy from biomass and wastes III. Chicago, IL: Institute of Gas Technology 293. Available from: https://www.osti.gov/biblio/6498295.
247. Yang, W., Li, X., Li, Z., Tong, C., and Feng, L. (2015). Understanding low-lipid algae hydrothermal liquefaction characteristics and pathways through hydrothermal liquefaction of algal major components: Crude polysaccharides, crude proteins and their binary mixtures. Bioresource Technology 196, 99-108.
248. Oomori, T., Khajavi, S. H., Kimura, Y., Adachi, S., and Matsuno, R. (2004). Hydrolysis of disaccharides containing glucose residue in subcritical water. Biochemical Engineering Journal 18(2), 143-147.
249. Liu, H.-M., Li, M.-F., Yang, S., and Sun, R.-C. (2013). Understanding the mechanism of cypress liquefaction in hot-compressed water through characterization of solid residues. Energies 6(3), 1590-1603.

250. Yaylayan, V. and Kaminsky, E. (1998). Isolation and structural analysis of Maillard polymers: caramel and melanoidin formation in glycine/glucose model system. Food Chemistry 63(1), 25-31.
251. Peterson, A. A., Lachance, R. P., and Tester, J. W. (2010). Kinetic evidence of the Maillard reaction in hydrothermal biomass processing: glucose− glycine interactions in high-temperature, high-pressure water. Industrial & Engineering Chemistry Research 49(5), 2107-2117.
252. Xu, C. and Etcheverry, T. (2008). Hydro-liquefaction of woody biomass in sub-and super-critical ethanol with iron-based catalysts. Fuel 87(3), 335-345.
253. Karagöz, S., Bhaskar, T., Muto, A., and Sakata, Y. (2006). Hydrothermal upgrading of biomass: effect of K 2 CO 3 concentration and biomass/water ratio on products distribution. Bioresource technology 97(1), 90-98.
254. Xiu, S., Shahbazi, A., Shirley, V., and Cheng, D. (2010). Hydrothermal pyrolysis of swine manure to bio-oil: effects of operating parameters on products yield and characterization of bio-oil. Journal of Analytical and Applied Pyrolysis 88(1), 73-79.
255. Muppaneni, T., Reddy, H. K., Selvaratnam, T., Dandamudi, K. P. R., Dungan, B., Nirmalakhandan, N., Schaub, T., Omar Holguin, F., Voorhies, W., Lammers, P., and Deng, S. (2017). Hydrothermal liquefaction of Cyanidioschyzon merolae and the influence of catalysts on products. Bioresource Technology 223, 91-97.
256. Sudasinghe, N., Reddy, H., Csakan, N., Deng, S., Lammers, P., and Schaub, T. (2015). Temperature-dependent lipid conversion and nonlipid composition of microalgal hydrothermal liquefaction oils monitored by fourier transform ion cyclotron resonance mass spectrometry. BioEnergy Research 8(4), 1962-1972.
257. Durak, H. and Aysu, T. (2014). Effects of catalysts and solvents on liquefaction of Onopordum heteracanthum for production of bio-oils. Bioresource Technology 166, 309-317.
258. Chan, Y. H., Yusup, S., Quitain, A. T., Uemura, Y., and Sasaki, M. (2014). Bio-oil production from oil palm biomass via subcritical and supercritical hydrothermal liquefaction. The Journal of Supercritical Fluids 95, 407-412.
259. Chen, W.-T., Zhang, Y., Zhang, J., Yu, G., Schideman, L.C., Zhang, P., and Minarick, M. (2014). Hydrothermal liquefaction of mixed-culture algal biomass from wastewater treatment system into bio-crude oil. Bioresource Technology 152, 130-139.
260. Vo, T.K., Lee, O.K., Lee, E.Y., Kim, C.H., Seo, J.-W., Kim, J., and Kim, S.-S. (2016). Kinetics study of the hydrothermal liquefaction of the microalga Aurantiochytrium sp. KRS101. Chemical Engineering Journal 306, 763-771.
261. Huang, Y., Chen, Y., Xie, J., Liu, H., Yin, X., and Wu, C. (2016). Bio-oil production from hydrothermal liquefaction of high-protein high-ash microalgae including wild Cyanobacteria sp. and cultivated Bacillariophyta sp. Fuel 183, 9-19.
262. Reddy, H.K., Muppaneni, T., Ponnusamy, S., Sudasinghe, N., Pegallapati, A., Selvaratnam, T., Seger, M., Dungan, B., Nirmalakhandan, N., Schaub, T., Holguin, F. O., Lammers, P., Voorhies, W., and Deng, S. (2016). Temperature effect on hydrothermal liquefaction of Nannochloropsis gaditana and Chlorella sp. Applied Energy 165, 943-951.
263. Pedersen, T.H., Jasiūnas, L., Casamassima, L., Singh, S., Jensen, T., and Rosendahl, L.A. (2015). Synergetic hydrothermal co-liquefaction of crude glycerol and aspen wood. Energy Conversion and Management 106, 886-891.

264. López Barreiro, D., Beck, M., Hornung, U., Ronsse, F., Kruse, A., and Prins, W. (2015). Suitability of hydrothermal liquefaction as a conversion route to produce biofuels from macroalgae. Algal Research 11, 234-241.
265. Gao, Y., Liu, S., Du, J., Wang, Z., Wang, H., and Zhao, T. (2015). Conversion and extracting bio-oils from rod-shaped cornstalk by sub-critical water. Journal of Analytical and Applied Pyrolysis 115, 316-325.
266. Singh, R., Chaudhary, K., Biswas, B., Balagurumurthy, B., and Bhaskar, T. (2015). Hydrothermal liquefaction of rice straw: Effect of reaction environment. The Journal of Supercritical Fluids 104, 70-75.
267. Sangon, S., Ratanavaraha, S., Ngamprasertsith, S., and Prasassarakich, P. (2006). Coal liquefaction using supercritical toluene–tetralin mixture in a semi-continuous reactor. Fuel Processing Technology 87(3), 201-207.
268. Kabyemela, B.M., Adschiri, T., Malaluan, R.M., and Arai, K. (1997). Kinetics of glucose epimerization and decomposition in subcritical and supercritical water. Industrial & Engineering Chemistry Research 36(5), 1552-1558.
269. Kabyemela, B., Takigawa, M., Adschiri, T., Malaluan, R., and Arai, K. (1998). Mechanism and kinetics of cellobiose decomposition in sub-and supercritical water. Industrial & Engineering Chemistry Research 37(2), 357-361.
270. Chan, Y.H., Yusup, S., Quitain, A.T., Tan, R.R., Sasaki, M., Lam, H.L., and Uemura, Y. (2015). Effect of process parameters on hydrothermal liquefaction of oil palm biomass for bio-oil production and its life cycle assessment. Energy Conversion and Management 104, 180-188.
271. Zhang, B., von Keitz, M., and Valentas, K. (2009). Thermochemical liquefaction of high-diversity grassland perennials. Journal of Analytical and Applied Pyrolysis 84(1), 18-24.
272. Karagöz, S., Bhaskar, T., Muto, A., Sakata, Y., and Uddin, M. A. (2004). Low-temperature hydrothermal treatment of biomass: effect of reaction parameters on products and boiling point distributions. Energy & fuels 18(1), 234-241.
273. Boocock, D. and Sherman, K. (1985). Further aspects of powdered poplar wood liquefaction by aqueous pyrolysis. The Canadian Journal of Chemical Engineering 63(4), 627-633.
274. Yan, Y., Xu, J., Li, T., and Ren, Z. (1999). Liquefaction of sawdust for liquid fuel. Fuel processing technology 60(2), 135-143.
275. Meryemoğlu, B., Hasanoğlu, A., Irmak, S., and Erbatur, O. (2014). Biofuel production by liquefaction of kenaf (Hibiscus cannabinus L.) biomass. Bioresource Technology 151, 278-283.
276. Grigoras, I.F., Stroe, R.E., Sintamarean, I.M., and Rosendahl, L. A. Effect of biomass pretreatment on the product distribution and composition resulting from the hydrothermal liquefaction of short rotation coppice willow. Bioresource Technology.
277. Li, R., Xie, Y., Yang, T., Li, B., Zhang, Y., and Kai, X. (2016). Characteristics of the products of hydrothermal liquefaction combined with cellulosic bio-ethanol process. Energy 114, 862-867.
278. Hietala, D.C., Faeth, J.L., and Savage, P.E. (2016). A quantitative kinetic model for the fast and isothermal hydrothermal liquefaction of Nannochloropsis sp. Bioresource Technology 214, 102-111.
279. Yang, L., Nazari, L., Yuan, Z., Corscadden, K., Xu, C., and He, Q. (2016). Hydrothermal liquefaction of spent coffee grounds in water medium for bio-oil production. Biomass and Bioenergy 86, 191-198.

280. Xu, D. and Savage, P. E. (2015). Effect of reaction time and algae loading on water-soluble and insoluble biocrude fractions from hydrothermal liquefaction of algae. Algal Research 12, 60-67.
281. Biller, P., Sharma, B.K., Kunwar, B., and Ross, A.B. (2015). Hydroprocessing of bio-crude from continuous hydrothermal liquefaction of microalgae. Fuel 159, 197-205.
282. Guo, Y., Song, W., Lu, J., Ma, Q., Xu, D., and Wang, S. (2015). Hydrothermal liquefaction of Cyanophyta: Evaluation of potential bio-crude oil production and component analysis. Algal Research 11, 242-247.
283. Zheng, J.-L., Zhu, M.-Q., and Wu, H.-T. (2015). Alkaline hydrothermal liquefaction of swine carcasses to bio-oil. Waste Management 43, 230-238.
284. Gai, C., Li, Y., Peng, N., Fan, A., and Liu, Z. (2015). Co-liquefaction of microalgae and lignocellulosic biomass in subcritical water. Bioresource Technology 185, 240-245.
285. Akhtar, J. and Amin, N. A. S. (2011). A review on process conditions for optimum bio-oil yield in hydrothermal liquefaction of biomass. Renewable and Sustainable Energy Reviews 15(3), 1615-1624.
286. Abu El-Rub, Z., Bramer, E., and Brem, G. (2004). Review of catalysts for tar elimination in biomass gasification processes. Industrial & Engineering Chemistry Research 43(22), 6911-6919.
287. Zhou, D., Zhang, L., Zhang, S., Fu, H., and Chen, J. (2010). Hydrothermal liquefaction of macroalgae Enteromorpha prolifera to bio-oil. Energy & Fuels 24(7), 4054-4061.
288. Yin, S., Dolan, R., Harris, M., and Tan, Z. (2010). Subcritical hydrothermal liquefaction of cattle manure to bio-oil: Effects of conversion parameters on bio-oil yield and characterization of bio-oil. Bioresource Technology 101(10), 3657-3664.
289. Sugano, M., Takagi, H., Hirano, K., and Mashimo, K. (2008). Hydrothermal liquefaction of plantation biomass with two kinds of wastewater from paper industry. Journal of Materials Science 43(7), 2476-2486.
290. Kersten, S.R., Potic, B., Prins, W., and Van Swaaij, W.P. (2006). Gasification of model compounds and wood in hot compressed water. Industrial & engineering chemistry research 45(12), 4169-4177.
291. Xu, C. and Lancaster, J. (2008). Conversion of secondary pulp/paper sludge powder to liquid oil products for energy recovery by direct liquefaction in hot-compressed water. Water Research 42(6), 1571-1582.
292. Sasaki, M., Adschiri, T., and Arai, K. (2003). Production of cellulose II from native cellulose by near-and supercritical water solubilization. Journal of agricultural and food chemistry 51(18), 5376-5381.
293. Zhang, H.-F., Su, X.-L., Sun, D.-K., Zhang R., and Bi, J.-C (2007). Investigation on degradation of polyethylene to oil in a continuous supercritical water reactor. Journal of Fuel Chemistry and Technology 35(4), 487-491.
294. Zhong, C. and Wei, X. (2004). A comparative experimental study on the liquefaction of wood. Energy 29(11), 1731-1741.
295. Mazaheri, H., Lee, K.T., and Mohamed, A.R. (2013). Influence of temperature on liquid products yield of oil palm shell via subcritical water liquefaction in the presence of alkali catalyst. Fuel Processing Technology 110, 197-205.
296. Minowa, T., Zhen, F., and Ogi, T. (1998). Cellulose decomposition in hot-compressed water with alkali or nickel catalyst. The Journal of Supercritical Fluids 13(1), 253-259.

297. Mok, W.S., Antal, M.J., Jr., and Varhegyi, G. (1992). Productive and parasitic pathways in dilute acid-catalyzed hydrolysis of cellulose. Industrial & Engineering Chemistry Research 31(1), 94-100.
298. Song, C., Hu, H., Zhu, S., Wang, G., and Chen, G. (2004). Nonisothermal catalytic liquefaction of corn stalk in subcritical and supercritical water. Energy & fuels 18(1), 90-96.
299. Wang, Y., Wang, H., Lin, H., Zheng, Y., Zhao, J., Pelletier, A., and Li, K. (2013). Effects of solvents and catalysts in liquefaction of pinewood sawdust for the production of bio-oils. Biomass and Bioenergy 59, 158-167.
300. Watanabe, M., Aizawa, Y., Iida, T., Aida, T. M., Levy, C., Sue, K., and Inomata, H. (2005). Glucose reactions with acid and base catalysts in hot compressed water at 473K. Carbohydrate Research 340(12), 1925-1930.
301. Watanabe, M., Iida, T., Aizawa, Y., Ura, H., Inomata, H., and Arai, K. (2003). Conversions of some small organic compounds with metal oxides in supercritical water at 673 K. Green Chemistry 5(5), 539-544.
302. Yang, B.Y. and Montgomery, R. (1996). Alkaline degradation of glucose: effect of initial concentration of reactants. Carbohydrate Research 280(1), 27-45.
303. Zhu, Z., Toor, S.S., Rosendahl, L., and Chen, G. (2014). Analysis of product distribution and characteristics in hydrothermal liquefaction of barley straw in subcritical and supercritical water. Environmental Progress & Sustainable Energy 33(3), 737-743.
304. Zhu, Z., Toor, S.S., Rosendahl, L., Yu, D., and Chen, G. (2015). Influence of alkali catalyst on product yield and properties via hydrothermal liquefaction of barley straw. Energy 80, 284-292.
305. Arturi, K.R., Strandgaard, M., Nielsen, R.P., Søgaard, E.G., and Maschietti, M. (2017). Hydrothermal liquefaction of lignin in near-critical water in a new batch reactor: Influence of phenol and temperature. The Journal of Supercritical Fluids 123, 28-39.
306. Jindal, M.K. and Jha, M.K. (2016). Catalytic hydrothermal liquefaction of waste furniture sawdust to bio-oil. Indian Chemical Engineer 58(2), 157-171.
307. Bi, Z., Zhang, J., Peterson, E., Zhu, Z., Xia, C., Liang, Y., and Wiltowski, T. (2017). Biocrude from pretreated sorghum bagasse through catalytic hydrothermal liquefaction. Fuel 188, 112-120.
308. Wang, Y., Wang, H., Lin, H., Zheng, Y., Zhao, J., Pelletier, A., and Li, K. (2013). Effects of solvents and catalysts in liquefaction of pinewood sawdust for the production of bio-oils. Biomass and Bioenergy 59, 158-167.
309. Jena, U., Das, K.C., and Kastner, J.R. (2012). Comparison of the effects of Na2CO3, Ca3(PO4)2, and NiO catalysts on the thermochemical liquefaction of microalga Spirulina platensis. Applied Energy 98, 368-375.
310. Nazari, L., Yuan, Z., Souzanchi, S., Ray, M.B., and Xu, C. (2015). Hydrothermal liquefaction of woody biomass in hot-compressed water: Catalyst screening and comprehensive characterization of bio-crude oils. Fuel 162, 74-83.
311. Déniel, M., Haarlemmer, G., Roubaud, A., Weiss-Hortala, E., and Fages, J. (2016). Optimisation of bio-oil production by hydrothermal liquefaction of agro-industrial residues: Blackcurrant pomace (Ribes nigrum L.) as an example. Biomass and Bioenergy 95, 273-285.
312. Chang, C.-C., Chen, C.-P., Yang, C.-S., Chen, Y.-H., Huang, M., Chang, C.-Y., Shie, J.-L., Yuan, M.-H., Chen, Y.-H., Ho, C., Li, K., and Yang, M.-T. (2016). Conversion of waste bamboo chopsticks to bio-oil via catalytic hydrothermal liquefaction using K_2CO_3. Sustainable Environment Research 26(6), 262-267.

313. Cao, L., Zhang, C., Hao, S., Luo, G., Zhang, S., and Chen, J. (2016). Effect of glycerol as co-solvent on yields of bio-oil from rice straw through hydrothermal liquefaction. Bioresource Technology 220, 471-478.
314. Biller, P., Madsen, R.B., Klemmer, M., Becker, J., Iversen, B.B., and Glasius, M. (2016). Effect of hydrothermal liquefaction aqueous phase recycling on bio-crude yields and composition. Bioresource Technology 220, 190-199.
315. Qian, L., Wang, S., and Savage, P.E. Hydrothermal liquefaction of sewage sludge under isothermal and fast conditions. Bioresource Technology, 232, 27-34.
316. Shakya, R., Whelen, J., Adhikari, S., Mahadevan, R., and Neupane, S. (2015). Effect of temperature and Na_2CO_3 catalyst on hydrothermal liquefaction of algae. Algal Research 12, 80-90.
317. Demirbaş, A. (2000). Mechanisms of liquefaction and pyrolysis reactions of biomass. Energy Conversion and Management 41(6), 633-646.
318. Karagöz, S., Bhaskar, T., Muto, A., Sakata, Y., Oshiki, T., and Kishimoto, T. (2005). Low-temperature catalytic hydrothermal treatment of wood biomass: analysis of liquid products. Chemical Engineering Journal 108(1), 127-137.
319. Miyazawa, T. and Funazukuri, T. (2005). Polysaccharide Hydrolysis Accelerated by Adding Carbon Dioxide under Hydrothermal Conditions. Biotechnology Progress 21(6), 1782-1785.
320. Arturi, K.R., Kucheryavskiy, S., and Søgaard, E.G. (2016). Performance of hydrothermal liquefaction (HTL) of biomass by multivariate data analysis. Fuel Processing Technology 150, 94-103.
321. Durak, H. and Aysu, T. (2016). Structural analysis of bio-oils from subcritical and supercritical hydrothermal liquefaction of Datura stramonium L. The Journal of Supercritical Fluids 108, 123-135.
322. Christensen, P.R., Mørup, A.J., Mamakhel, A., Glasius, M., Becker, J., and Iversen, B.B. (2014). Effects of heterogeneous catalyst in hydrothermal liquefaction of dried distillers grains with solubles. Fuel 123, 158-166.
323. Hammerschmidt, A., Boukis, N., Hauer, E., Galla, U., Dinjus, E., Hitzmann, B., Larsen, T., and Nygaard, S. D. (2011). Catalytic conversion of waste biomass by hydrothermal treatment. Fuel 90(2), 555-562.
324. Watanabe, M., Iida, T., and Inomata, H. (2006). Decomposition of a long chain saturated fatty acid with some additives in hot compressed water. Energy Conversion and Management 47(18–19), 3344-3350.
325. Yim, S.C., Quitain, A.., Yusup, S., Sasaki, M., Uemura, Y., and Kida, T. (2017). Metal oxide-catalyzed hydrothermal liquefaction of Malaysian oil palm biomass to bio-oil under supercritical condition. The Journal of Supercritical Fluids 120, Part 2, 384-394.
326. Shi, W., Li, S., Jin, H., Zhao, Y., and Yu, W. (2013). The hydrothermal liquefaction of rice husk to bio-crude using metallic oxide catalysts. Energy Sources, Part A: Recovery, Utilization, and Environmental Effects 35(22), 2149-2155.
327. Long, J., Li, Y., Zhang, X., Tang, L., Song, C., and Wang, F. (2016). Comparative investigation on hydrothermal and alkali catalytic liquefaction of bagasse: Process efficiency and product properties. Fuel 186, 685-693.
328. Saber, M., Golzary, A., Hosseinpour, M., Takahashi, F., and Yoshikawa, K. (2016). Catalytic hydrothermal liquefaction of microalgae using nanocatalyst. Applied Energy 183, 566-576.

329. Zhou, C., Zhu, X., Qian, F., Shen, W., Xu, H., Zhang, S., and Chen, J. (2016). Catalytic hydrothermal liquefaction of rice straw in water/ethanol mixtures for high yields of monomeric phenols using reductive CuZnAl catalyst. Fuel Processing Technology 154, 1-6.
330. Duan, P. and Savage, P.E. (2010). Hydrothermal liquefaction of a microalga with heterogeneous catalysts. Industrial & Engineering Chemistry Research 50(1), 52-61.
331. Davari, M., Karimi, S., Tavasoli, A., and Karimi, A. (2014). Enhancement of activity, selectivity and stability of CNTs-supported cobalt catalyst in Fischer–Tropsch via CNTs functionalization. Applied Catalysis A General 485, 133-142.
332. Xu, T., Zhang, Q., Cen, J., Xiang, Y., and Li, X. (2015). Selectivity tailoring of Pd/CNTs in phenol hydrogenation by surface modification: Role of C O oxygen species. Applied Surface Science 324, 634-639.
333. Chen, Y., Mu, R., Yang, M., Fang, L., Wu, Y., Wu, K., Liu, Y., and Gong, J. (2017). Catalytic hydrothermal liquefaction for bio-oil production over CNTs supported metal catalysts. Chemical Engineering Science 161, 299-307.
334. Xu, C.C., Su, H., and Cang, D. (2008). Liquefaction of corn distillers dried grains with solubles (DDGS) in hot-compressed phenol. BioResources 3(2), 363-382.
335. Jakab, E., Liu, K., and Meuzelaar, H.L. (1997). Thermal decomposition of wood and cellulose in the presence of solvent vapors. Industrial & Engineering Chemistry Research 36(6), 2087-2095.
336. Liu, Z. and Zhang, F.-S. (2008). Effects of various solvents on the liquefaction of biomass to produce fuels and chemical feedstocks. Energy Conversion and Management 49(12), 3498-3504.
337. Mun, S.P. and El Barbary, M. H. (2004). Liquefaction of lignocellulosic biomass with dioxane/polar solvent mixtures in the presence of an acid catalyst. Journal of Industrial and Engineering Chemistry 10(3), 473-477.
338. Kržan, A., Kunaver, M., and Tišler, V. (2005). Wood liquefaction using dibasic organic acids and glycols. Acta Chimica Slovenica 52, 253-258.
339. Lee, J.H., Hwang, H., Moon, J., and Choi, J.W. (2016). Characterization of hydrothermal liquefaction products from coconut shell in the presence of selected transition metal chlorides. Journal of Analytical and Applied Pyrolysis 122, 415-421.
340. Cherad, R., Onwudili, J.A., Biller, P., Williams, P.T., and Ross, A.B. (2016). Hydrogen production from the catalytic supercritical water gasification of process water generated from hydrothermal liquefaction of microalgae. Fuel 166, 24-28.
341. Ortiz, F.G., Ollero, P., Serrera, A., and Galera, S. (2012). An energy and exergy analysis of the supercritical water reforming of glycerol for power production. International Journal of Hydrogen Energy 37(1), 209-226.
342. De Vlieger, D., Chakinala, A., Lefferts, L., Kersten, S., Seshan, K., and Brilman, D. (2012). Hydrogen from ethylene glycol by supercritical water reforming using noble and base metal catalysts. Applied catalysis B: Environmental 111, 536-544.
343. Ruppert, A.M., Weinberg, K., and Palkovits, R. (2012). Hydrogenolysis goes bio: from carbohydrates and sugar alcohols to platform chemicals. Angewandte Chemie International Edition 51(11), 2564-2601.
344. Azadi, P., Syed, K., and Farnood, R. (2009). Catalytic gasification of biomass model compound in near-critical water. Applied Catalysis A General 358(1), 65-72.
345. Knezevic, D. (2009). Hydrothermal conversion of biomass. University of Twente.

346. Knezevic, D., van Swaaij, W., and Kersten, S. (2009). Hydrothermal conversion of biomass. II. Conversion of wood, pyrolysis oil, and glucose in hot compressed water. Industrial & Engineering Chemistry Research 49(1), 104-112.
347. Vertes, A.A., Qureshi, N., Yukawa, H., and Blaschek, H. (2010). Biomass to biofuels: strategies for global industries. Wiley Online Library.
348. Sealock, L.J. and Elliott, D.C. (1991). Method for the catalytic conversion of lignocellulosic materials, Google Patents.
349. Elliott, D.C. and Sealock, J.L. (1998). Nickel/ruthenium catalyst and method for aqueous phase reactions, Pacific Northwest National Laboratory (PNNL), Richland, WA.
350. Elliott, D.C., Baker, E.G., Butner, R.., and Sealock, L. J. (1993). Bench-scale reactor tests of low temperature, catalytic gasification of wet industrial wastes. Journal of Solar Energy Engineering 115(1), 52-56.
351. Yoshida, Y., Dowaki, K., Matsumura, Y., Matsuhashi, R., Li, D., Ishitani, H., and Komiyama, H. (2003). Comprehensive comparison of efficiency and CO_2 emissions between biomass energy conversion technologies — position of supercritical water gasification in biomass technologies. Biomass and Bioenergy 25(3), 257-272.
352. Kruse, A. (2009). Hydrothermal biomass gasification. The Journal of Supercritical Fluids 47(3), 391-399.
353. Cantero, D.A., Bermejo, M.D., and Cocero, M.J. (2015). Reaction engineering for process intensification of supercritical water biomass refining. The Journal of Supercritical Fluids 96, 21-35.
354. Van Rossum, G., Potic, B., Kersten, S., and Van Swaaij, W. (2009). Catalytic gasification of dry and wet biomass. Catalysis Today 145(1), 10-18.
355. Williams, P.T. and Onwudili, J. (2005). Composition of products from the supercritical water gasification of glucose: a model biomass compound. Industrial & Engineering Chemistry Research 44(23), 8739-8749.
356. Bagnoud-Velásquez, M., Brandenberger, M., Vogel, F., and Ludwig, C. (2014). Continuous catalytic hydrothermal gasification of algal biomass and case study on toxicity of aluminum as a step toward effluents recycling. Catalysis Today 223, 35-43.
357. Hasler, P. and Nussbaumer, T. (1999). Gas cleaning for IC engine applications from fixed bed biomass gasification. Biomass and Bioenergy 16(6), 385-395.
358. Kirkels, A.F. and Verbong, G.P. (2011). Biomass gasification: Still promising? A 30-year global overview. Renewable and Sustainable Energy Reviews 15(1), 471-481.
359. Güngören Madenoğlu, T., Sağlam, M., Yüksel, M., and Ballice, L. (2016). Hydrothermal gasification of biomass model compounds (cellulose and lignin alkali) and model mixtures. The Journal of Supercritical Fluids 115, 79-85.
360. Klingler, D. and Vogel, H. (2010). Influence of process parameters on the hydrothermal decomposition and oxidation of glucose in sub-and supercritical water. The Journal of Supercritical Fluids 55(1), 259-270.
361. Watanabe, M., Aizawa, Y., Iida, T., Levy, C., Aida, T. M., and Inomata, H. (2005). Glucose reactions within the heating period and the effect of heating rate on the reactions in hot compressed water. Carbohydrate Research 340(12), 1931-1939.
362. Lundquist, K. (1976). Low-molecular weight lignin hydrolysis products. Applied Polymer Symposium. Available from: https://gup.ub.gu.se/publication/130663?lang=sv.
363. Saisu, M., Sato, T., Watanabe, M., Adschiri, T., and Arai, K. (2003). Conversion of lignin with supercritical water− phenol mixtures. Energy & Fuels 17(4), 922-928.

364. Bühler, W., Dinjus, E., Ederer, H., Kruse, A., and Mas, C. (2002). Ionic reactions and pyrolysis of glycerol as competing reaction pathways in near-and supercritical water. The Journal of Supercritical Fluids 22(1), 37-53.
365. Lee, I.-G., Kim, M.-S., and Ihm, S.-K. (2002). Gasification of glucose in supercritical water. Industrial & Engineering Chemistry Research 41(5), 1182-1188.
366. Guo, Y., Wang, S., Gong, Y., Xu, D., Tang, X., and Ma, H. (2010). Partial oxidation of municipal sludge with activited carbon catalyst in supercritical water. Journal of Hazardous Materials 180(1), 137-144.
367. Sinağ, A., Kruse, A., and Rathert, J. (2004). Influence of the heating rate and the type of catalyst on the formation of key intermediates and on the generation of gases during hydropyrolysis of glucose in supercritical water in a batch reactor. Industrial & Engineering Chemistry Research 43(2), 502-508.
368. Guo, L., Lu, Y., Zhang, X., Ji, C., Guan, Y., and Pei, A. (2007). Hydrogen production by biomass gasification in supercritical water: a systematic experimental and analytical study. Catalysis Today 129(3), 275-286.
369. Lu, Y., Guo, L., Zhang, X., and Yan, Q. (2007). Thermodynamic modeling and analysis of biomass gasification for hydrogen production in supercritical water. Chemical Engineering Journal 131(1), 233-244.
370. Lu, Y., Guo, L., Ji, C., Zhang, X., Hao, X., and Yan, Q. (2006). Hydrogen production by biomass gasification in supercritical water: a parametric study. International Journal of Hydrogen Energy 31(7), 822-831.
371. Kabyemela, B.M., Adschiri, T., Malaluan, R.M., and Arai, K. (1999). Glucose and fructose decomposition in subcritical and supercritical water: Detailed reaction pathway, mechanisms, and kinetics. Industrial & Engineering Chemistry Research 38(8), 2888-2895.
372. Susanti, R.F., Dianningrum, L.W., Yum, T., Kim, Y., Lee, B. G., and Kim, J. (2012). High-yield hydrogen production from glucose by supercritical water gasification without added catalyst. International Journal of Hydrogen Energy 37(16), 11677-11690.
373. Matsumura, Y., Yanachi, S., and Yoshida, T. (2006). Glucose Decomposition kinetics in water at 25 MPa in the temperature range of 448-673 K. Industrial & Engineering Chemistry Research 45(6), 1875-1879.
374. Safari, F., Salimi, M., Tavasoli, A., and Ataei, A. (2016). Non-catalytic conversion of wheat straw, walnut shell and almond shell into hydrogen rich gas in supercritical water media. Chinese Journal of Chemical Engineering 24(8), 1097-1103.
375. Nanda, S., Isen, J., Dalai, A.K., and Kozinski, J.A. (2016). Gasification of fruit wastes and agro-food residues in supercritical water. Energy Conversion and Management 110, 296-306.
376. Üremek Cengiz, N., Eren, S., Sağlam, M., Yüksel, M., and Ballice, L. (2016). Influence of temperature and pressure on hydrogen and methane production in the hydrothermal gasification of wood residues. The Journal of Supercritical Fluids 107, 243-249.
377. Graz, Y., Bostyn, S., Richard, T., Bocanegra, P. E., de Bilbao, E., Poirier, J., and Gokalp, I. (2016). Hydrothermal conversion of Ulva macro algae in supercritical water. The Journal of Supercritical Fluids 107, 182-188.
378. Alshammari, Y.M. and Hellgardt, K. (2016). Sub and supercritical water reforming of n-hexadecane in a tubular flow reactor. The Journal of Supercritical Fluids 107, 723-732.

379. Seif, S., Tavakoli, O., Fatemi, S., and Bahmanyar, H. (2015). Subcritical water gasification of beet-based distillery wastewater for hydrogen production. The Journal of Supercritical Fluids 104, 212-220.
380. Su, Y., Zhu, W., Gong, M., Zhou, H., Fan, Y., and Amuzu-Sefordzi, B. (2015). Interaction between sewage sludge components lignin (phenol) and proteins (alanine) in supercritical water gasification. International Journal of Hydrogen Energy 40(30), 9125-9136.
381. Deniz, I., Vardar-Sukan, F., Yüksel, M., Saglam, M., Ballice, L., and Yesil-Celiktas, O. (2015). Hydrogen production from marine biomass by hydrothermal gasification. Energy Conversion and Management 96, 124-130.
382. Yanik, J., Ebale, S., Kruse, A., Saglam, M., and Yüksel, M. (2008). Biomass gasification in supercritical water: II. Effect of catalyst. International Journal of Hydrogen Energy 33(17), 4520-4526.
383. Watanabe, M., Osada, M., Inomata, H., Arai, K., and Kruse, A. (2003). Acidity and basicity of metal oxide catalysts for formaldehyde reaction in supercritical water at 673 K. Applied Catalysis A General 245(2), 333-341.
384. Jarana, M.G., Sánchez-Oneto, J., Portela, J. R., Sanz, E.N., and de la Ossa, E.M. (2008). Supercritical water gasification of industrial organic wastes. The Journal of Supercritical Fluids 46(3), 329-334.
385. Watanabe, M., Inomata, H., Osada, M., Sato, T., Adschiri, T., and Arai, K. (2003). Catalytic effects of NaOH and ZrO_2 for partial oxidative gasification of n-hexadecane and lignin in supercritical water. Fuel 82(5), 545-552.
386. Nanda, S., Dalai, A K., and Kozinski, J.A. (2016). Supercritical water gasification of timothy grass as an energy crop in the presence of alkali carbonate and hydroxide catalysts. Biomass and Bioenergy 95, 378-387.
387. Gökkaya, D.S., Saglam, M., Yuksel, M., and Ballice, L. (2016). Hydrothermal gasification of xylose: Effects of reaction temperature, pressure, and $K2CO_3$ as a catalyst on product distribution. Biomass and Bioenergy 91, 26-36.
388. Kang, K., Azargohar, R., Dalai, A.K., and Wang, H. (2016). Hydrogen production from lignin, cellulose and waste biomass via supercritical water gasification: Catalyst activity and process optimization study. Energy Conversion and Management 117, 528-537.
389. Nanda, S., Dalai, A.K., Gökalp, I., and Kozinski, J. A. (2016). Valorization of horse manure through catalytic supercritical water gasification. Waste Management 52, 147-158.
390. Louw, J., Schwarz, C. E., and Burger, A.J. (2016). Catalytic supercritical water gasification of primary paper sludge using a homogeneous and heterogeneous catalyst: Experimental vs thermodynamic equilibrium results. Bioresource Technology 201, 111-120.
391. Güngören Madenoğlu, T., Üremek Cengiz, N., Sağlam, M., Yüksel, M., and Ballice, L. (2016). Catalytic gasification of mannose for hydrogen production in near- and super-critical water. The Journal of Supercritical Fluids 107, 153-162.
392. Ferreira-Pinto, L., Feirhrmann, A.C., Corazza, M.L., Fernandes-Machado, N.R.C., dos Reis Coimbra, J.., Saldaña, M.D.A., and Cardozo-Filho, L. (2015). Hydrogen production and TOC reduction from gasification of lactose by supercritical water. International Journal of Hydrogen Energy 40(36), 12162-12168.
393. Selvi Gökkaya, D., Saglam, M., Yüksel, M., and Ballice, L. (2015). Supercritical water gasification of phenol as a model for plant biomass. International Journal of Hydrogen Energy 40(34), 11133-11139.

394. Akgül, G., Madenoğlu, T.G., Cengiz, N.Ü., Gökkaya, D., Sağlam, M., and Yüksel, M. (2014). Hydrothermal gasification of Rosa Damascena residues: Gaseous and aqueous yields. The Journal of Supercritical Fluids 85, 135-142.
395. Güngören Madenoğlu, T., Boukis, N., Sağlam, M., and Yüksel, M. (2011). Supercritical water gasification of real biomass feedstocks in continuous flow system. International Journal of Hydrogen Energy 36(22), 14408-14415.
396. Schmieder, H., Abeln, J., Boukis, N., Dinjus, E., Kruse, A., Kluth, M., Petrich, G., Sadri, E., and Schacht, M. (2000). Hydrothermal gasification of biomass and organic wastes. The Journal of Supercritical Fluids 17(2), 145-153.
397. Gong, M., Nanda, S., Romero, M.J., Zhu, W., and Kozinski, J.A. (2017). Subcritical and supercritical water gasification of humic acid as a model compound of humic substances in sewage sludge. The Journal of Supercritical Fluids 119, 130-138.
398. Louw, J., Schwarz, C.E., and Burger, A.J. (2016). Supercritical water gasification of Eucalyptus grandis and related pyrolysis char: Effect of feedstock composition. Bioresource Technology 216, 1030-1039.
399. Sinağ, A., Kruse, A., and Schwarzkopf, V. (2003). Key compounds of the hydropyrolysis of glucose in supercritical water in the presence of K_2CO_3. Industrial & Engineering Chemistry Research 42(15), 3516-3521.
400. Guo, Y., Wang, S.Z., Xu, D.H., Gong, Y.M., Ma, H.H., and Tang, X.Y. (2010). Review of catalytic supercritical water gasification for hydrogen production from biomass. Renewable and Sustainable Energy Reviews 14(1), 334-343.
401. Ding, N., Azargohar, R., Dalai, A.K., and Kozinski, J.A. (2014). Catalytic gasification of glucose to H_2 in supercritical water. Fuel Processing Technology 127, 33-40.
402. Gong, M., Zhu, W., Zhang, H.W., Ma, Q., Su, Y., and Fan, Y.J. (2014). Influence of NaOH and Ni catalysts on hydrogen production from the supercritical water gasification of dewatered sewage sludge. International Journal of Hydrogen Energy 39(35), 19947-19954.
403. Guo, Y., Wang, S., Wang, Y., Zhang, J., Xu, D., and Gong, Y. (2012). Gasification of two and three-components mixture in supercritical water: Influence of NaOH and initial reactants of acetic acid and phenol. International Journal of Hydrogen Energy 37(3), 2278-2286.
404. Lin, S.-Y., Suzuki, Y., Hatano, H., and Harada, M. (2001). Hydrogen production from hydrocarbon by integration of water-carbon reaction and carbon dioxide removal (HyPr-RING method). Energy & Fuels 15(2), 339-343.
405. Muangrat, R., Onwudili, J.A., and Williams, P.T. (2010). Alkali-promoted hydrothermal gasification of biomass food processing waste: A parametric study. International Journal of Hydrogen Energy 35(14), 7405-7415.
406. Onwudili, J.A. and Williams, P.T. (2009). Role of sodium hydroxide in the production of hydrogen gas from the hydrothermal gasification of biomass. International Journal of Hydrogen Energy 34(14), 5645-5656.
407. Watanabe, M., Inomata, H., Osada, M., Sato, T., Adschiri, T., and Arai, K. (2003). Catalytic effects of NaOH and ZrO_2 for partial oxidative gasification of n-hexadecane and lignin in supercritical water. Fuel 82(5), 545-552.
408. Sınağ, A., Kruse, A., and Rathert, J. (2004). Influence of the heating rate and the type of catalyst on the formation of key intermediates and on the generation of gases during hydropyrolysis of glucose in supercritical water in a batch reactor. Industrial & Engineering Chemistry Research 43(2), 502-508.

409. Lu, Y.J., Jin, H., Guo, L.J., Zhang, X.M., Cao, C.Q., and Guo, X. (2008). Hydrogen production by biomass gasification in supercritical water with a fluidized bed reactor. International Journal of Hydrogen Energy 33(21), 6066-6075.
410. Güngören Madenoğlu, T., Yıldırır, E., Sağlam, M., Yüksel, M., and Ballice, L. (2014). Improvement in hydrogen production from hard-shell nut residues by catalytic hydrothermal gasification. The Journal of Supercritical Fluids 95, 339-347.
411. Antal, M.J.,Jr., Allen, S.G., Schulman, D., Xu, X., and Divilio, R.J. (2000). Biomass gasification in supercritical water. Industrial & Engineering Chemistry Research 39(11), 4040-4053.
412. Xu, X. and Antal, M.J. (1998). Gasification of sewage sludge and other biomass for hydrogen production in supercritical water. Environmental Progress 17(4), 215-220.
413. Cao, W., Cao, C., Guo, L., Jin, H., Dargusch, M., Bernhardt, D., and Yao, X. (2016). Hydrogen production from supercritical water gasification of chicken manure. International Journal of Hydrogen Energy 41(48), 22722-22731.
414. Matsumura, Y., Xu, X., and Antal, M. (1997). Gasification characteristics of an activated carbon in supercritical water. Carbon 35(6), 819-824.
415. Elliott, D.C., Phelps, M.R., Sealock, L. J., and Baker, E G. (1994). Chemical processing in high-pressure aqueous environments. 4. Continuous-flow reactor process development experiments for organics destruction. Industrial & Engineering Chemistry Research 33(3), 566-574.
416. Minowa, T. and Ogi, T. (1998). Hydrogen production from cellulose using a reduced nickel catalyst. Catalysis Today 45(1), 411-416.
417. Resende, F.L. and Savage, P.E. (2010). Effect of metals on supercritical water gasification of cellulose and lignin. Industrial & Engineering Chemistry Research 49(6), 2694-2700.
418. Yin, J., Cheng, Z., Guo, L., Li, S., and Jin, H. Products distribution and influence of nickel catalyst on glucose hydrothermal decomposition. International Journal of Hydrogen Energy, 42(7), 4642-4650.
419. Nanda, S., Reddy, S.N., Dalai, A.K., and Kozinski, J.A. (2016). Subcritical and supercritical water gasification of lignocellulosic biomass impregnated with nickel nanocatalyst for hydrogen production. International Journal of Hydrogen Energy 41(9), 4907-4921.
420. Byrd, A.J., Pant, K.K., and Gupta, R.B. (2008). Hydrogen production from glycerol by reforming in supercritical water over Ru/Al2O3 catalyst. Fuel 87(13-14), 2956-2960.
421. Wang, H.-M., Miao, R.-R., Yang, Y., Qiao, Y.-H., Zhang, Q.-f., Li, C.-S., and Huang, J.-P. (2015). Study on the catalytic gasification of alkali lignin over Ru/C nanotubes in supercritical water. Journal of Fuel Chemistry and Technology 43(10), 1195-1201.
422. Huo, Z.-B., Liu, J.-K., Yao, G.-D., Zeng, X., Luo, J., and Jin, F.-M. (2015). Efficient hydrothermal conversion of cellulose into methane over porous Ni catalyst. Applied Catalysis A General 490, 36-41.
423. Azadi, P., Afif, E., Azadi, F., and Farnood, R. (2012). Screening of nickel catalysts for selective hydrogen production using supercritical water gasification of glucose. Green Chemistry 14(6), 1766-1777.
424. de Vlieger, D.J.M., Mojet, B.L., Lefferts, L., and Seshan, K. (2012). Aqueous phase reforming of ethylene glycol – Role of intermediates in catalyst performance. Journal of Catalysis 292, 239-245.

425. Pairojpiriyakul, T., Croiset, E., Kiatkittipong, K., Kiatkittipong, W., Arpornwichanop, A., and Assabumrungrat, S. (2014). Catalytic reforming of glycerol in supercritical water with nickel-based catalysts. International Journal of Hydrogen Energy 39(27), 14739-14750.
426. Rashidi, M. and Tavasoli, A. (2015). Hydrogen rich gas production via supercritical water gasification of sugarcane bagasse using unpromoted and copper promoted Ni/CNT nanocatalysts. The Journal of Supercritical Fluids 98, 111-118.
427. Yan, B., Wu, J., Xie, C., He, F., and Wei, C. (2009). Supercritical water gasification with Ni/ZrO2 catalyst for hydrogen production from model wastewater of polyethylene glycol. The Journal of Supercritical Fluids 50(2), 155-161.
428. Zhang, L., Champagne, P., and Xu, C. (2011). Supercritical water gasification of an aqueous by-product from biomass hydrothermal liquefaction with novel Ru modified Ni catalysts. Bioresource Technology 102(17), 8279-8287.
429. Huang, J., Lian, X., Wang, L., Zhu, C., Jin, H., and Wang, R. Hydrogen production from glucose by supercritical water gasification with Ni/Zr(Ce,Y)O2-δ catalysts. International Journal of Hydrogen Energy,42(7), 4613-4625.
430. Elliott, D.C., Neuenschwander, G.G., Phelps, M.R., Hart, T.R., Zacher, A.H., and Silva, L.J. (1999). Chemical processing in high-pressure aqueous environments. 6. Demonstration of catalytic gasification for chemical manufacturing wastewater cleanup in industrial plants. Industrial & Engineering Chemistry Research 38(3), 879-883.
431. Elliott, D.C. (2008). Catalytic hydrothermal gasification of biomass. Biofuels, Bioproducts and Biorefining 2(3), 254-265.
432. Waldner, M.H. and Vogel, F. (2005). Renewable production of methane from woody biomass by catalytic hydrothermal gasification. Industrial & Engineering Chemistry Research 44(13), 4543-4551.
433. Elliott, D.C., Hart, T.R., and Neuenschwander, G.G. (2006). Chemical processing in high-pressure aqueous environments. 8. Improved catalysts for hydrothermal gasification. Industrial & Engineering Chemistry Research 45(11), 3776-3781.
434. Lu, Y., Li, S., and Guo, L. (2013). Hydrogen production by supercritical water gasification of glucose with Ni/CeO2/Al2O3: Effect of Ce loading. Fuel 103, 193-199.
435. Furusawa, T., Sato, T., Saito, M., Ishiyama, Y., Sato, M., Itoh, N., and Suzuki, N. (2007). The evaluation of the stability of Ni/MgO catalysts for the gasification of lignin in supercritical water. Applied Catalysis A General 327(2), 300-310.
436. Furusawa, T., Sato, T., Sugito, H., Miura, Y., Ishiyama, Y., Sato, M., Itoh, N., and Suzuki, N. (2007). Hydrogen production from the gasification of lignin with nickel catalysts in supercritical water. International Journal of Hydrogen Energy 32(6), 699-704.
437. DiLeo, G.J., Neff, M.E., and Savage, P.E. (2007). Gasification of guaiacol and phenol in supercritical water. Energy & Fuels 21(4), 2340-2345.
438. Osada, M., Sato, O., Arai, K., and Shirai, M. (2006). Stability of supported ruthenium catalysts for lignin gasification in supercritical water. Energy & Fuels 20(6), 2337-2343.
439. Byrd, A.J., Pant, K., and Gupta, R.B. (2007). Hydrogen production from glucose using Ru/Al2O3 catalyst in supercritical water. Industrial & Engineering Chemistry Research 46(11), 3574-3579.
440. Sato, T., Osada, M., Watanabe, M., Shirai, M., and Arai, K. (2003). Gasification of alkylphenols with supported noble metal catalysts in supercritical water. Industrial & Engineering Chemistry Research 42(19), 4277-4282.

441. Osada, M., Sato, T., Watanabe, M., Adschiri, T., and Arai, K. (2004). Low-temperature catalytic gasification of lignin and cellulose with a ruthenium catalyst in supercritical water. Energy & Fuels 18(2), 327-333.
442. Elliott, D.C., Neuenschwander, G.G., Hart, T.R., Butner, R.S., Zacher, A.H., Engelhard, M.H., Young, J.S., and McCready, D.E. (2004). Chemical processing in high-pressure aqueous environments. 7. Process development for catalytic gasification of wet biomass feedstocks. Industrial & Engineering Chemistry Research 43(9), 1999-2004.
443. Onwudili, J.A. (2016). Supercritical water gasification of RDF and its components over RuO2/γ-Al2O3 catalyst: New insights into RuO_2 catalytic reaction mechanisms. Fuel 181, 157-169.
444. Onwudili, J.A. and Williams, P.T. (2016). Catalytic supercritical water gasification of plastics with supported RuO2: A potential solution to hydrocarbons–water pollution problem. Process Safety and Environmental Protection 102, 140-149.
445. Byrd, A.J., Pant, K., and Gupta, R.B. (2008). Hydrogen production from glycerol by reforming in supercritical water over Ru/Al 2 O 3 catalyst. Fuel 87(13), 2956-2960.
446. Hao, X., Guo, L., Zhang, X., and Guan, Y. (2005). Hydrogen production from catalytic gasification of cellulose in supercritical water. Chemical Engineering Journal 110(1), 57-65.
447. Onwudili, J.A. and Williams, P.T. (2013). Hydrogen and methane selectivity during alkaline supercritical water gasification of biomass with ruthenium-alumina catalyst. Applied Catalysis B: Environmental 132–133, 70-79.
448. Zhang, L., Champagne, P., and Xu, C. (2011). Screening of supported transition metal catalysts for hydrogen production from glucose via catalytic supercritical water gasification. International Journal of Hydrogen Energy 36(16), 9591-9601.
449. Zöhrer, H. and Vogel, F. (2013). Hydrothermal catalytic gasification of fermentation residues from a biogas plant. Biomass and Bioenergy 53, 138-148.
450. Lee, I.-G. (2011). Effect of metal addition to Ni/activated charcoal catalyst on gasification of glucose in supercritical water. International Journal of Hydrogen Energy 36(15), 8869-8877.
451. Elif, D. and Nezihe, A. (2016). Hydrogen production by supercritical water gasification of fruit pulp in the presence of Ru/C. International Journal of Hydrogen Energy 41(19), 8073-8083.
452. Norouzi, O., Safari, F., Jafarian, S., Tavasoli, A., and Karimi, A. Hydrothermal gasification performance of Enteromorpha intestinalis as an algal biomass for hydrogen-rich gas production using Ru promoted Fe–Ni/γ-Al2O3 nanocatalysts. Energy Conversion and Management. Add vol, pg #s
453. Zhu, C., Guo, L., Jin, H., Huang, J., Li, S., and Lian, X. (2016). Effects of reaction time and catalyst on gasification of glucose in supercritical water: Detailed reaction pathway and mechanisms. International Journal of Hydrogen Energy 41(16), 6630-6639.
454. Behnia, I., Yuan, Z., Charpentier, P., and Xu, C. (2016). Production of methane and hydrogen via supercritical water gasification of renewable glucose at a relatively low temperature: Effects of metal catalysts and supports. Fuel Processing Technology 143, 27-34.
455. Tiong, L., Komiyama, M., Uemura, Y., and Nguyen, T. T. (2016). Catalytic supercritical water gasification of microalgae: Comparison of Chlorella vulgaris and Scenedesmus quadricauda. The Journal of Supercritical Fluids 107, 408-413.

456. Lee, I.-G., Nowacka, A., Yuan, C.-H., Park, S.-J., and Yang, J.-B. (2015). Hydrogen production by supercritical water gasification of valine over Ni/activated charcoal catalyst modified with Y, Pt, and Pd. International Journal of Hydrogen Energy 40(36), 12078-12087.
457. Ishihara, A., Imai, T., Hashimoto, T., and Nasu, H. (2015). Hydrothermal gasification of phenol water on novel carbon-supported Ni catalysts prepared by the sol–gel method using tartaric acid and alminum tri-sec-butoxide. Fuel Processing Technology 136, 34-40.
458. Osada, M., Hiyoshi, N., Sato, O., Arai, K., and Shirai, M. (2007). Effect of sulfur on catalytic gasification of lignin in supercritical water. Energy & Fuels 21(3), 1400-1405.
459. Osada, M., Hiyoshi, N., Sato, O., Arai, K., and Shirai, M. (2007). Reaction pathway for catalytic gasification of lignin in presence of sulfur in supercritical water. Energy & Fuels 21(4), 1854-1858.
460. Peng, G., Ludwig, C., and Vogel, F. (2017). Catalytic supercritical water gasification: Interaction of sulfur with ZnO and the ruthenium catalyst. Applied Catalysis B: Environmental 202, 262-268.
461. Cortright, R., Davda, R., and Dumesic, J.A. (2002). Hydrogen from catalytic reforming of biomass-derived hydrocarbons in liquid water. Nature 418(6901), 964-967.
462. Watanabe, M., Inomata, H., and Arai, K. (2002). Catalytic hydrogen generation from biomass (glucose and cellulose) with ZrO 2 in supercritical water. Biomass and Bioenergy 22(5), 405-410.
463. Yamamura, T., Mori, T., Park, K.C., Fujii, Y., and Tomiyasu, H. (2009). Ruthenium(IV) dioxide-catalyzed reductive gasification of intractable biomass including cellulose, heterocyclic compounds, and sludge in supercritical water. The Journal of Supercritical Fluids 51(1), 43-49.
464. Seif, S., Fatemi, S., Tavakoli, O., and Bahmanyar, H. (2016). Hydrogen production through hydrothermal gasification of industrial wastewaters using transition metal oxide catalysts. The Journal of Supercritical Fluids 114, 32-45.
465. Tavasoli, A., Barati, M., and Karimi, A. (2016). Sugarcane bagasse supercritical water gasification in presence of potassium promoted copper nano-catalysts supported on γ-Al2O3. International Journal of Hydrogen Energy 41(1), 174-180.
466. Boucard, H., Watanabe, M., Takami, S., Weiss-Hortala, E., Barna, R., and Adschiri, T. (2015). Beneficial use of CeO_2 nanocatalyst for black liquor conversion under sub and supercritical conditions. The Journal of Supercritical Fluids 105, 66-76.
467. Tavasoli, A., Barati, M., and Karimi, A. (2015). Conversion of sugarcane bagasse to gaseous and liquid fuels in near-critical water media using $K2O$ promoted Cu/γ-$Al2O_3$–MgO nanocatalysts. Biomass and Bioenergy 80, 63-72.
468. Gadhe, J.B. and Gupta, R.B. (2005). Hydrogen production by methanol reforming in supercritical water: suppression of methane formation. Industrial & Engineering Chemistry Research 44(13), 4577-4585.
469. Boukis, N., Diem, V., Habicht, W., and Dinjus, E. (2003). Methanol reforming in supercritical water. Industrial & Engineering Chemistry Research 42(4), 728-735.
470. Yu, D., Aihara, M., and Antal, M. J. (1993). Hydrogen production by steam reforming glucose in supercritical water. Energy & Fuels 7(5), 574-577.
471. Jin, H., Zhao, X., Su, X., Zhu, C., Cao, C., and Guo, L. Supercritical water synthesis of bimetallic catalyst and its application in hydrogen production by furfural gasification in supercritical water. International Journal of Hydrogen Energy, 42 (8), 4943-4950.

472. Tushar, M., Dutta, A., and Xu, C.C. (2016). Catalytic supercritical gasification of biocrude from hydrothermal liquefaction of cattle manure. Applied Catalysis B Environmental 189, 119-132.
473. Falco, C., Baccile, N., and Titirici, M.-M. (2011). Morphological and structural differences between glucose, cellulose and lignocellulosic biomass derived hydrothermal carbons. Green Chemistry 13(11), 3273-3281.
474. Funke, A. and Ziegler, F. (2010). Hydrothermal carbonization of biomass: a summary and discussion of chemical mechanisms for process engineering. Biofuels, Bioproducts and Biorefining 4(2), 160-177.
475. Mumme, J., Eckervogt, L., Pielert, J., Diakité, M., Rupp, F., and Kern, J. (2011). Hydrothermal carbonization of anaerobically digested maize silage. Bioresource Technology 102(19), 9255-9260.
476. Jain, A., Balasubramanian, R., and Srinivasan, M.P. (2016). Hydrothermal conversion of biomass waste to activated carbon with high porosity: A review. Chemical Engineering Journal 283, 789-805.
477. Dinjus, E., Kruse, A., and Troeger, N. (2011). Hydrothermal carbonization–1. Influence of lignin in lignocelluloses. Chemical Engineering & Technology 34(12), 2037-2043.
478. Chen, W.-H., Ye, S.-C., and Sheen, H.-K. (2012). Hydrothermal carbonization of sugarcane bagasse via wet torrefaction in association with microwave heating. Bioresource technology 118, 195-203.
479. Heilmann, S.M., Jader, L.R., Sadowsky, M J., Schendel, F.J., von Keitz, MG., and Valentas, K.J. (2011). Hydrothermal carbonization of distiller's grains. Biomass and Bioenergy 35(7), 2526-2533.
480. Hoekman, S.K., Broch, A., and Robbins, C. (2011). Hydrothermal carbonization (HTC) of lignocellulosic biomass. Energy & Fuels 25(4), 1802-1810.
481. Xiao, L.-P., Shi, Z.-J., Xu, F., and Sun, R.-C. (2012). Hydrothermal carbonization of lignocellulosic biomass. Bioresource Technology 118, 619-623.
482. Berge, N.D., Ro, K.S., Mao, J., Flora, J.R., Chappell, M.A., and Bae, S. (2011). Hydrothermal carbonization of municipal waste streams. Environmental Science & Technology 45(13), 5696-5703.
483. Ramke, H., Blöhse, D., and Lehmann, H. (2012). Hydrothermal carbonization of organic municipal solid waste - Scientific and technical principles. Müll und Abfall 9, 476-483.
484. Stemann, J. and Ziegler, F. (2011). Hydrothermal carbonisation (HTC): recycling of process water. In Proceedings of 19th European Biomass Conference, Berlin. DOI: http://www.etaflorence.it/proceedings/?detail=6648.
485. Erlach, B. and Tsatsaronis, G. (2010). Upgrading of biomass by hydrothermal carbonisation: analysis of an industrial-scale plant design. Presented at the 23rd International Conference on Efficiency, Cost, Optimization, Simulation and Environmental Impact of Energy Systems. Lausanne, Switzerland.
486. Erlach, B., Harder, B., and Tsatsaronis, G. (2012). Combined hydrothermal carbonization and gasification of biomass with carbon capture. Energy 45(1), 329-338.
487. Stemann, J. and Ziegler, F. (2011). Assessment of the energetic efficiency of a continuously operating plant for hydrothermal carbonisation of biomass. Presented at the World Renewable Energy Congress.
488. Funke, A. and Ziegler, F. (2011). Heat of reaction measurements for hydrothermal carbonization of biomass. Bioresource technology 102(16), 7595-7598.

489. Wei, L., Sevilla, M., Fuertes, A.B., Mokaya, R., and Yushin, G. (2011). Hydrothermal Carbonization of Abundant Renewable Natural Organic Chemicals for High-Performance Supercapacitor Electrodes. Advanced Energy Materials 1(3), 356-361.
490. Tang, K., Fu, L., White, R. J., Yu, L., Titirici, M. M., Antonietti, M., and Maier, J. (2012). Hollow carbon nanospheres with superior rate capability for sodium-based batteries. Advanced Energy Materials 2(7), 873-877.
491. Tang, K., White, R. J., Mu, X., Titirici, M. M., van Aken, P. A., and Maier, J. (2012). Hollow carbon nanospheres with a high rate capability for lithium-based batteries. ChemSusChem 5(2), 400-403.
492. Tusi, M.M., Brandalise, M., Polanco, N.S. O., Correa, O. V., Silva, A.C., Villalba, J.C., Anaissi, F.J., Neto, A.O., and Spinacé, E.V. (2013). Ni/carbon hybrid prepared by hydrothermal carbonization and thermal treatment as support for ptru nanoparticles for direct methanol fuel cell. Journal of Materials Science & Technology 29(8), 747-751.
493. Wang, Z.-B., Li, C.-Z., Gu, D.-M., and Yin, G.-P. (2013). Carbon riveted PtRu/C catalyst from glucose in-situ carbonization through hydrothermal method for direct methanol fuel cell. Journal of Power Sources 238, 283-289.
494. Kim, D., Lee, K., and Park, K.Y. (2014). Hydrothermal carbonization of anaerobically digested sludge for solid fuel production and energy recovery. Fuel 130, 120-125.
495. He, C., Giannis, A., and Wang, J.-Y. (2013). Conversion of sewage sludge to clean solid fuel using hydrothermal carbonization: Hydrochar fuel characteristics and combustion behavior. Applied Energy 111, 257-266.
496. Kang, S., Li, X., Fan, J., and Chang, J. (2012). Solid fuel production by hydrothermal carbonization of black liquor. Bioresource Technology 110, 715-718.
497. Fang, G., Kaneko, S., Liu, W., Xia, B., Sun, H., Zhang, R., Zheng, J., and Li, D. (2013). Facile synthesis of nitrogen-doped carbon coated $CoSnO_3$ via hydrothermal carbonization of carboxylated chitosan as anode materials for lithium-ion batteries. Applied Surface Science 283, 963-967.
498. Sevilla, M., Gu, W., Falco, C., Titirici, M. M., Fuertes, A. B., and Yushin, G. (2014). Hydrothermal synthesis of microalgae-derived microporous carbons for electrochemical capacitors. Journal of Power Sources 267, 26-32.
499. Kurniawan, A., Effendi, C., Ong, L. K., Kurniawan, F., Lin, C. X., Angkawijaya, A. E., Ju, Y.-H., Ismadji, S., and Zhao, X. S. (2013). Preparation of nanoporous carbon microspheres by subcritical water carbonization and electrocapacitive study. Electrochimica Acta 111, 99-107.
500. Jiang, W., Jia, X., Luo, Z., and Wu, X. (2014). Supercapacitor performance of spherical nanoporous carbon obtained by a CaCO3-assisted template carbonization method from polytetrafluoroethene waste and the electrochemical enhancement by the nitridation of CO(NH2)2. Electrochimica Acta 147, 183-191.
501. Tooming, T., Thomberg, T., Kurig, H., Jänes, A., and Lust, E. (2015). High power density supercapacitors based on the carbon dioxide activated d-glucose derived carbon electrodes and 1-ethyl-3-methylimidazolium tetrafluoroborate ionic liquid. Journal of Power Sources 280, 667-677.
502. Zheng, C., Zhou, X., Cao, H., Wang, G., and Liu, Z. (2014). Synthesis of porous graphene/activated carbon composite with high packing density and large specific surface area for supercapacitor electrode material. Journal of Power Sources 258, 290-296.

503. Unur, E., Brutti, S., Panero, S., and Scrosati, B. (2013). Nanoporous carbons from hydrothermally treated biomass as anode materials for lithium ion batteries. Microporous and Mesoporous Materials 174, 25-33.
504. Álvarez-Murillo, A., Sabio, E., Ledesma, B., Román, S., and González-García, C. M. (2016). Generation of biofuel from hydrothermal carbonization of cellulose. Kinetics modelling. Energy 94, 600-608.
505. Patil, S.K. and Lund, C.R. (2011). Formation and growth of humins via aldol addition and condensation during acid-catalyzed conversion of 5-hydroxymethylfurfural. Energy & Fuels 25(10), 4745-4755.
506. Rosatella, A.A., Simeonov, S.P., Frade, R.F., and Afonso, C.A. (2011). 5-Hydroxymethylfurfural (HMF) as a building block platform: Biological properties, synthesis and synthetic applications. Green Chemistry 13(4), 754-793.
507. Titirici, M.-M., White, R. J., Falco, C., and Sevilla, M. (2012). Black perspectives for a green future: hydrothermal carbons for environment protection and energy storage. Energy & Environmental Science 5(5), 6796-6822.
508. Falco, C., Perez Caballero, F., Babonneau, F., Gervais, C., Laurent, G., Titirici, M.-M., and Baccile, N. (2011). Hydrothermal carbon from biomass: structural differences between hydrothermal and pyrolyzed carbons via 13C solid state NMR. Langmuir 27(23), 14460-14471.
509. Kambo, H.S. and Dutta, A. (2015). Comparative evaluation of torrefaction and hydrothermal carbonization of lignocellulosic biomass for the production of solid biofuel. Energy Conversion and Management 105, 746-755.
510. Sevilla, M. and Fuertes, A.B. (2009). Chemical and structural properties of carbonaceous products obtained by hydrothermal carbonization of saccharides. Chemistry–A European Journal 15(16), 4195-4203.
511. Antal, M.J., Jr., Mok, W.S.L., and Richards, G.N. (1990). Mechanism of formation of 5-(hydroxymethyl)-2-furaldehyde from d-fructose and sucrose. Carbohydrate Research 199(1), 91-109.
512. Sinag, A., Kruse, A., and Schwarzkopf, V. (2003). Formation and degradation pathways of intermediate products formed during the hydropyrolysis of glucose as a model substance for wet biomass in a tubular reactor. Engineering in Life Sciences 3(12), 469-473.
513. Salak Asghari, F. and Yoshida, H. (2006). Acid-catalyzed production of 5-hydroxymethyl furfural from D-fructose in subcritical water. Industrial & Engineering Chemistry Research 45(7), 2163-2173.
514. Sun, X. and Li, Y. (2004). Colloidal carbon spheres and their core/shell structures with noble-metal nanoparticles. Angewandte Chemie 116(5), 607-611.
515. Kambo, H.S. and Dutta, A. (2014). Strength, storage, and combustion characteristics of densified lignocellulosic biomass produced via torrefaction and hydrothermal carbonization. Applied Energy 135, 182-191.
516. Hoekman, S.K., Broch, A., Warren, A., Felix, L., and Irvin, J. (2014). Laboratory pelletization of hydrochar from woody biomass. Biofuels 5(6), 651-666.
517. Gil, M.V., Oulego, P., Casal, M.D., Pevida, C., Pis, J. ., and Rubiera, F. (2010). Mechanical durability and combustion characteristics of pellets from biomass blends. Bioresource Technology 101(22), 8859-8867.

518. Reza, M.T., Lynam, J.G., Vasquez, V.R., and Coronella, C.J. (2012). Pelletization of biochar from hydrothermally carbonized wood. Environmental Progress & Sustainable Energy 31(2), 225-234.
519. Liu, Z., Guo, Y., Balasubramanian, R., and Hoekman, S.K. (2016). Mechanical stability and combustion characteristics of hydrochar/lignite blend pellets. Fuel 164, 59-65.
520. Oliver-Villanueva, J.-V., Enrique, G.-A., and Patricia, G.-G. (2016). Analysis of durability and dimensional stability of hydrothermal carbonized wooden pellets. Wood Research 61(2), 321-330.
521. Wirth, B. and Mumme, J. (2014). Anaerobic digestion of waste water from hydrothermal carbonization of corn silage. Applied Bioenergy 1(1).
522. Erdogan, E., Atila, B., Mumme, J., Reza, M. T., Toptas, A., Elibol, M., and Yanik, J. (2015). Characterization of products from hydrothermal carbonization of orange pomace including anaerobic digestibility of process liquor. Bioresource Technology 196, 35-42.
523. Wirth, B., Reza, T., and Mumme, J. (2015). Influence of digestion temperature and organic loading rate on the continuous anaerobic treatment of process liquor from hydrothermal carbonization of sewage sludge. Bioresource Technology 198, 215-222.
524. Wirth, B. and Reza, M. T. (2016). Continuous anaerobic degradation of liquid condensate from steam-derived hydrothermal carbonization of sewage sludge. ACS Sustainable Chemistry & Engineering 4(3), 1673-1678.
525. Poerschmann, J., Weiner, B., Wedwitschka, H., Baskyr, I., Koehler, R., and Kopinke, F.-D. (2014). Characterization of biocoals and dissolved organic matter phases obtained upon hydrothermal carbonization of brewer's spent grain. Bioresource technology 164, 162-169.
526. Oliveira, I., Blöhse, D., and Ramke, H.-G. (2013). Hydrothermal carbonization of agricultural residues. Bioresource Technology 142, 138-146.
527. Uddin, M.H., Reza, M.T., Lynam, J.G., and Coronella, C.J. (2014). Effects of water recycling in hydrothermal carbonization of loblolly pine. Environmental Progress & Sustainable Energy 33(4), 1309-1315.
528. Stemann, J., Putschew, A., and Ziegler, F. (2013). Hydrothermal carbonization: process water characterization and effects of water recirculation. Bioresource Technology 143, 139-146.
529. Weiner, B., Poerschmann, J., Wedwitschka, H., Koehler, R., and Kopinke, F.-D. (2014). Influence of process water reuse on the hydrothermal carbonization of paper. ACS Sustainable Chemistry & Engineering 2(9), 2165-2171.
530. Kabadayi Catalkopru, A., Kantarli, I.C., and Yanik, J. (2017). Effects of spent liquor recirculation in hydrothermal carbonization. Bioresource Technology 226, 89-93.
531. Shen, Y., Yu, S., Ge, S., Chen, X., Ge, X., and Chen, M. (2017). Hydrothermal carbonization of medical wastes and lignocellulosic biomass for solid fuel production from lab-scale to pilot-scale. Energy 118, 312-323.
532. Tremel, A., Stemann, J., Herrmann, M., Erlach, B., and Spliethoff, H. (2012). Entrained flow gasification of biocoal from hydrothermal carbonization. Fuel 102, 396-403.
533. Gao, P., Zhou, Y., Meng, F., Zhang, Y., Liu, Z., Zhang, W., and Xue, G. (2016). Preparation and characterization of hydrochar from waste eucalyptus bark by hydrothermal carbonization. Energy 97, 238-245.
534. Álvarez-Murillo, A., Sabio, E., Ledesma, B., Román, S., and González-García, C. (2016). Generation of biofuel from hydrothermal carbonization of cellulose. Kinetics modelling. Energy 94, 600-608.

535. Nakason, K., Panyapinyopol, B., Kanokkantapong, V., Viriya-empikul, N., Kraithong, W., and Pavasant, P. Characteristics of hydrochar and liquid fraction from hydrothermal carbonization of cassava rhizome. Journal of the Energy Institute, 91(2), 184-193.
536. Tekin, K., Karagöz, S., and Bektaş, S. (2014). A review of hydrothermal biomass processing. Renewable and sustainable Energy Reviews 40, 673-687.
537. Hoekman, S.K., Broch, A., Felix, L., and Farthing, W. (2017). Hydrothermal carbonization (HTC) of loblolly pine using a continuous, reactive twin-screw extruder. Energy Conversion and Management 134, 247-259.
538. Reza, M.T., Yang, X., Coronella, C.J., Lin, H., Hathwaik, U., Shintani, D., Neupane, B.P., and Miller, G.C. (2015). Hydrothermal carbonization (HTC) and pelletization of two arid land plants bagasse for energy densification. ACS Sustainable Chemistry & Engineering 4(3), 1106-1114.
539. Liu, Z., Quek, A., and Balasubramanian, R. (2014). Preparation and characterization of fuel pellets from woody biomass, agro-residues and their corresponding hydrochars. Applied Energy 113, 1315-1322.
540. Yang, W., Wang, H., Zhang, M., Zhu, J., Zhou, J., and Wu, S. (2016). Fuel properties and combustion kinetics of hydrochar prepared by hydrothermal carbonization of bamboo. Bioresource Technology 205, 199-204.
541. Elaigwu, S.E. and Greenway, G.M. (2016). Microwave-assisted hydrothermal carbonization of rapeseed husk: A strategy for improving its solid fuel properties. Fuel Processing Technology 149, 305-312.
542. Fu, Y., Ye, J., Chang, J., Lou, H., and Zheng, X. (2016). Solid fuel production by hydrothermal carbonization of water-like phase of bio-oil. Fuel 180, 591-596.
543. Koottatep, T., Fakkaew, K., Tajai, N., Pradeep, S.V., and Polprasert, C. (2016). Sludge stabilization and energy recovery by hydrothermal carbonization process. Renewable Energy 99, 978-985.
544. Guo, S., Dong, X., Wu, T., Shi, F., and Zhu, C. (2015). Characteristic evolution of hydrochar from hydrothermal carbonization of corn stalk. Journal of Analytical and Applied Pyrolysis 116, 1-9.
545. Mäkelä, M., Benavente, V., and Fullana, A. (2015). Hydrothermal carbonization of lignocellulosic biomass: Effect of process conditions on hydrochar properties. Applied Energy 155, 576-584.
546. Kim, D., Lee, K., and Park, K.Y. (2016). Upgrading the characteristics of biochar from cellulose, lignin, and xylan for solid biofuel production from biomass by hydrothermal carbonization. Journal of Industrial and Engineering Chemistry 42, 95-100.
547. Hamelinck, C.N. and Faaij, A.P. (2002). Future prospects for production of methanol and hydrogen from biomass. Journal of Power Sources 111(1), 1-22.
548. Tijmensen, M.J., Faaij, A.P., Hamelinck, C.N., and van Hardeveld, M.R. (2002). Exploration of the possibilities for production of Fischer Tropsch liquids and power via biomass gasification. Biomass and Bioenergy 23(2), 129-152.
549. Phillips, S. (2007). Technoeconomic analysis of a lignocellulosic biomass indirect gasification process to make ethanol via mixed alcohols synthesis. Industrial & Engineering Chemistry Research 46(26), 8887-8897.
550. Sarkar, S. and Kumar, A. (2010). Biohydrogen production from forest and agricultural residues for upgrading of bitumen from oil sands. Energy 35(2), 582-591.

551. Patel, M., Zhang, X., and Kumar, A. (2016). Techno-economic and life cycle assessment on lignocellulosic biomass thermochemical conversion technologies: A review. Renewable and Sustainable Energy Reviews 53, 1486-1499.
552. Dutta, A., Talmadge, M., Hensley, J., Worley, M., Dudgeon, D., Barton, D., Groendijk, P., Ferrari, D., Stears, B., and Searcy, E. M. (2011). Process design and economics for conversion of lignocellulosic biomass to ethanol: Thermochemical pathway by indirect gasification and mixed alcohol synthesis. National Renewable Energy Laboratory (NREL), Golden, CO.
553. Mirkouei, A., Haapala, K. R., Sessions, J., and Murthy, G. S. (2017). A review and future directions in techno-economic modeling and optimization of upstream forest biomass to bio-oil supply chains. Renewable and Sustainable Energy Reviews 67, 15-35.
554. Zhao, X., Brown, T. R., and Tyner, W. E. (2015). Stochastic techno-economic evaluation of cellulosic biofuel pathways. Bioresource Technology 198, 755-763.
555. Thilakaratne, R., Wright, M.M., and Brown, R.C. (2014). A techno-economic analysis of microalgae remnant catalytic pyrolysis and upgrading to fuels. Fuel 128, 104-112.
556. Do, T.X., Lim, Y.-I., and Yeo, H. (2014). Techno-economic analysis of biooil production process from palm empty fruit bunches. Energy Conversion and Management 80, 525-534.
557. Brown, D., Rowe, A., and Wild, P. (2013). A techno-economic analysis of using mobile distributed pyrolysis facilities to deliver a forest residue resource. Bioresource Technology 150, 367-376.
558. Rogers, J. and Brammer, J. (2012). Estimation of the production cost of fast pyrolysis bio-oil. Biomass and Bioenergy 36, 208-217.
559. Ghezzaz, H. and Stuart, P. (2011). Biomass availability and process selection for an integrated forest biorefinery. Pulp & Paper Canada 112(3), 19-26.
560. Trippe, F., Fröhling, M., Schultmann, F., Stahl, R., and Henrich, E. (2010). Techno-economic analysis of fast pyrolysis as a process step within biomass-to-liquid fuel production. Waste and Biomass Valorization 1(4), 415-430.
561. Anex, R., Aden, A., Kazi, F.K., Fortman, J., Swanson, R.M., Wright, M., Satrio, J., Brown, R.C., Daugaard, D.E., Platon, A., Kothandaraman, G., Hsu, D.D., and Dutta. A. (2010). Techno-economic comparison of biomass-to-transportation fuels via pyrolysis, gasification, and biochemical pathways. Fuel 89, S29-S35.
562. Wright, M.M., Daugaard, D., Satrio, J. and Brown, R.C. (2010). Techno-economic analysis of biomass fast pyrolysis to transportation fuels. Fuel 89, S2-S10.
563. Oasmaa, A., Solantausta, Y., Arpiainen, V., Kuoppala, E., and Sipilä, K. (2009). Fast pyrolysis bio-oils from wood and agricultural residues. Energy & Fuels 24(2), 1380-1388.
564. Magalhães, A.I., Rodriguez, A.L., Putra, Z.A., and Thielemans, G. (2009). Techno-economic assessment of biomass pre-conversion processes as a part of biomass-to-liquids line-up. Biofuels, Bioproducts and Biorefining 3(6), 584-600.
565. Beckman, D., Elliott, D., Gevert, B., Hörnell, C., and Kjellström, B. (1990). Techno-economic assessment of selected biomass liquefaction processes. Available from: https://www.osti.gov/etdeweb/biblio/7795606.
566. Kerssen, M. and Berends, R. (2005). Life cycle analysis of the HTU process. Apeldoom, The Netherlands, Dutch Research Organization for Environment, Energy and Process Innovation. Available from: https://www.researchgate.net/publication/237363338.

567. Zhu, Y., Biddy, M J., Jones, S.B., Elliott, D.C., and Schmidt, A.J. (2014). Techno-economic analysis of liquid fuel production from woody biomass via hydrothermal liquefaction (HTL) and upgrading. Applied Energy 129, 384-394.
568. Kumar, M., Oyedun, A.O., and Kumar, A. Hydrothermal liquefaction of biomass for production of diluents for bitumen transport (submitted).
569. Matsumura, Y. (2002). Evaluation of supercritical water gasification and biomethanation for wet biomass utilization in Japan. Energy Conversion and Management 43(9), 1301-1310.
570. Gasafi, E., Reinecke, M.-Y., Kruse, A., and Schebek, L. (2008). Economic analysis of sewage sludge gasification in supercritical water for hydrogen production. Biomass and Bioenergy 32(12), 1085-1096.
571. Al-Mosuli, D., Barghi, S., Fang, Z., and Xu, C. C. (2014). Techno-economic Analysis of renewable hydrogen production via scwg of biomass using glucose as a model compound, in Near-critical and Supercritical Water and Their Applications for Biorefineries, edited by Z. Fang and C.C. Xu. Springer, pp. 445-471.
572. Zhu, Y., Albrecht, K. O., Elliott, D. C., Hallen, R. T., and Jones, S. B. (2013). Development of hydrothermal liquefaction and upgrading technologies for lipid-extracted algae conversion to liquid fuels. Algal Research 2(4), 455-464.
573. Faeth, J.L., Valdez, P.J., and Savage, P. E. (2013). Fast hydrothermal liquefaction of Nannochloropsis sp. to produce biocrude. Energy & Fuels 27(3), 1391-1398.
574. Elliott, D.C., Neuenschwander, G., and Hart, T.R. (2013). Combined hydrothermal liquefaction and catalytic hydrothermal gasification system and process for conversion of biomass feedstocks, Google Patents.
575. Jones, S., Zhu, Y., Anderson, D., Hallen, R., Elliott, D.C., Schmidt, A.., Albrecht, K., Hart, T., Butcher, M., and Drennan, C. (2014). Process design and economics for the conversion of algal biomass to hydrocarbons: whole algae hydrothermal liquefaction and upgrading. US Department of Energy Bioenergy Technologies Office.
576. Spath, P.L., Mann, M., and Amos, W. (2003). Update of hydrogen from biomass-determination of the delivered cost of hydrogen. Department of Energy and National Renewable Energy Laboratory, NREL/MP-510-33112. Available from: https://www-energy-gov.login.ezproxy.library.ualberta.ca/sites/prod/files/2014/03/f10/33112.pdf. Accessed: Januaray 28, 2019.
577. Balat, H. and Kırtay, E. (2010). Hydrogen from biomass – Present scenario and future prospects. International Journal of Hydrogen Energy 35(14), 7416-7426.
578. Kruse, A., Abeln, J., Dinjus, E., Kluth, M., Petrich, G., Schacht, M., Sadri, H., and Schmieder, H. (1999). Gasification of biomass and model compounds in hot compressed water. Presented at the International Meeting of the GVC-Fachausschuβ Hochdruckverfahrenstechnik, Karlsruhe, Germany. Accessed: May 2, 2016.
579. Amos, W. (1999). Assessment of supercritical water gasification: alternative designs. Golden, USA: National Renewable Energy Laboratory.
580. Brandenberger, M., Matzenberger, J., Vogel, F., and Ludwig, C. (2013). Producing synthetic natural gas from microalgae via supercritical water gasification: A techno-economic sensitivity analysis. Biomass and Bioenergy 51, 26-34.
581. Knorr, D., Lukas, J., Schoen, P. 2013. Production of Advanced Biofuels via Liquefaction – Hydrothermal Liquefaction Reactor Design: April 5, 2013. NREL/SR-5100-60462, National Renewable Energy Laboratory, Golden, Colorado, USA. Available from: https://www.nrel.gov/docs/fy14osti/60462.pdf.

582. NASA Prediction of Worldwide Energy Resource (POWER) Higher Resolution Daily Time Series by Location [cited April 6, 2018]. Available from: https://power-larc-nasa-gov.login.ezproxy.library.ualberta.ca/.
583. Béchet, Q., Shilton, A., and Guieysse, B. (2016). Maximizing productivity and reducing environmental impacts of full-scale algal production through optimization of open pond depth and hydraulic retention time. Environmental Science and Technology 50(7), 4102-4110.
584. Singh, S.P. and Singh, P. (2015). Effect of temperature and light on the growth of algae species: A review. Renewable and Sustainable Energy Reviews 50, 431-444.
585. Sandnes, J.M., Källqvist, T., Wenner, D., and Gislerød, R. (2005). Combined influence of light and temperature on growth rates of Nannochloropsis oceanica: Linking cellular responses to large-scale biomass production. Journal of Applied Phycology 17(6), 515-525.
586. Jayaraman, S.K. and Rhinehart, R.R. (2015). Modeling and optimization of algae growth. Industrial and Engineering Chemistry Research 54(33), 8063-8071.
587. Li, X. and Wang, H. (2010). A stoichiometrically derived algal growth model and its global analysis. Mathematical Biosciences and Engineering 7(4), 825-836.
588. Straub, Q. and Ordonez, J. (2011). A methodology for the determination of the light distribution profile of a micro-algal photobioreactor. Presented at the ASME 2011 5th International Conference on Energy Sustainability, ES 2011.
589. Huesemann, M.H., Van Wagenen, J., Miller, T., Chavis, A., Hobbs, S., and Crowe, B. (2013). A screening model to predict microalgae biomass growth in photobioreactors and raceway ponds. Biotechnology and Bioengineering 110(6), 1583-1594.
590. Park, S. and Li, Y. (2015). Integration of biological kinetics and computational fluid dynamics to model the growth of Nannochloropsis salina in an open channel raceway. Biotechnology and Bioengineering 112(5), 923-933.
591. Droop, M.R., Mickelson, M.., Scott, JM., and Turner, M. F. (1982). Light and nutrient status of algal cells. Journal of the Marine Biological Association UK 62(2), 403-434.
592. Jamu, D. and Piedrahita, R.H. (1997). Aquaculture pond modeling for the analysis of environmental impacts and integration with agriculture: relationship between carbon input and sediment quality in aquaculture ponds. Oregon State University: Corvallis, Oregon. p. 191, pp. 62-67.
593. James, S.C. and Boriah, V. (2010). Modeling algae growth in an open-channel raceway. Journal of Computational Biology 17(7), 895-906.
594. Rosso, L., Lobry, J.R., and Flandrois, J.P. (1993). An unexpected correlation between cardinal temperatures of microbial growth highlighted by a new model. Journal of Theoretical Biology 162(4), 447-463.
595. Béchet, Q., Shilton, A., and Guieysse, B. (2013). Modeling the effects of light and temperature on algae growth: State of the art and critical assessment for productivity prediction during outdoor cultivation. Biotechnology Advances 31(8), 1648-1663.
596. Chen, M., Fan, M., Liu, R., Wang, X., Yuan, X., and Zhu, H. (2015). The dynamics of temperature and light on the growth of phytoplankton. Journal of Theoretical Biology 385, 8-19.
597. Ras, M., Steyer, J.P., and Bernard, O. (2013). Temperature effect on microalgae: A crucial factor for outdoor production. Reviews in Environmental Science and Biotechnology 12(2), 153-164.

598. Weinberger, H. (1964). The physics of the solar pond. Solar Energy 8(2), 45-56.
599. Hull, J.R. (1980). Computer simulation of solar pond thermal behavior. Solar Energy 25(1), 33-40.
600. Dahmani, S., Zerrouki, D., Ramanna, L., Rawat, I., and Bux, F. (2016). Cultivation of Chlorella pyrenoidosa in outdoor open raceway pond using domestic wastewater as medium in arid desert region. Bioresource Technology 219, 749-752.
601. Monod, J. (1949). The growth of bacterial cultures. Annual Review of Microbiology 3(1), 371-394.
602. Knoshaug, E., Laurens, L., Kinchin, C., and Davis, R. (2016). Use of Cultivation Data from the Algae Testbed Public Private Partnership as Utilized in NREL's Algae State of Technology Assessments: United States. Available from: https://www.nrel.gov/docs/fy17osti/67289.pdf.
603. Harmon, V.L., T. A. D., McGowen, J. A. (2014). UFS Summer 2014 Experimental Protocol – Standard Operating Procedure. Algae Testbed Public Private Partnership (ATP3) consortium in conjunction with National Renewable Energy Laboratory (NREL) – US Department of Energy, National Renewable Energy Laboratory, Golden, Colorado. pp. 1-14.
604. Bennett, M.C., Turn, S.Q., and Chan, W. Y. (2014). A methodology to assess open pond, phototrophic, algae production potential: A Hawaii case study. Biomass and Bioenergy 66, 168-175.
605. Kumar, K., Mishra, S.K., Shrivastav, A., Park, M.S., and Yang, J.W. (2015). Recent trends in the mass cultivation of algae in raceway ponds. Renewable and Sustainable Energy Reviews 51, 875-885.
606. Harmon, V.L., T. A. D., John A. McGowen (2014). UFS Summer 2014 UFS-3 Experiement (Jun - Sept 2014) Algae Testbed Public Privat Partnership (ATP3) consortium in conjunction with National Renewable Energy Laboratory (NREL) – US Department of Energy, Editor, national Renewable Energy Laboratory (NREL): Golden, Colorado.
607. Pankratz, S., Oyedun, A. O., and Kumar, A. (2018). Development of an analytical model to predict microalgae yields in open pond raceway sytems based on local solar irradiance. Algae Research, in press.
608. Project Status – Alberta Industrial Heartland. (February 4, 2017 http://aih.staging.tritontech.ca/resources/project-status/) June 27, 2016 [cited 2017 February 4, 2017]; Available from: http://aih.staging.tritontech.ca/resources/project-status/.
609. Government of Alberta. Carbon levy and rebates. Putting a price on carbon is the most cost-effective way to reduce greenhouse gas emissions that cause climate change. [cited 2017 February 4, 2017]; Available from: https://www.alberta.ca/climate-carbon-pricing.aspx.
610. Fozer, D., Valentinyi, N., Racz, L., and Mizsey, P. (2016). Evaluation of microalgae-based biorefinery alternatives. Clean Technologies and Environmental Policy, 1-15.
611. Davis, R., Markham, J., Kinchin, C., Grundl, N., Tan, E. C. D., and Humbird, D. (2016). Process design and economics for the production of algal biomass: Algal biomass production in open pond systems and processing through dewatering for downstream conversion. National Renewable Energy Laboratory. https://www.nrel.gov/docs/fy16osti/64772.pdf. Accessed [August 10, 2017].
612. Davis, R., Kinchin, C., Markham, J., Tan, E., Laurens, L., Sexton, D., Knorr, D., Schoen, P., and Lukas, J. (2014). Process design and economics for the conversion of algal biomass to biofuels: Algal biomass fractionation to lipid and carbohydrate derived fuel products.

National Renewable Energy Laboratory. Available from: https://www.osti.gov/biblio/1159351. Accessed: October 7, 2018.
613. Apel, A.C., Pfaffinger, C.E., Basedahl, N., Mittwollen, N., Göbel, J., Sauter, J., Brück, T., and Weuster-Botz, D. (2017). Open thin-layer cascade reactors for saline microalgae production evaluated in a physically simulated Mediterranean summer climate. Algal Research 25, 381-390.
614. Jones, S.B., Zhu, Y., Anderson, D.B., Hallen, R.T., Elliott, D C., Schmidt, A.J., Albrecht, K.O., Hart, T.R., Butcher, M.., Drennan, C., Snowden-Swan, L.J., Davis, R., and Kinchin, C. (2014). Process Design and economics for the conversion of algal biomass to hydrocarbons: whole algae hydrothermal liquefaction and upgrading. Pacific Northwest National Laboratory. Available from: https://www.pnnl.gov/main/publications/external/technical_reports/PNNL-23227.pdf. Accessed: February 15, 2016.
615. ISL Engineering and Land Services (2007). Capital Region Integrated Growth Management Plan – Final Report on Core Infrastructure, Calgary AB, pp. 132-158.
616. EBA Engineering Consultants Ltd. (2013). Alberta Capital Region Integrated Waste Management Plan – Phase 1 Report – Integrated Waste Management Options, Edmonton AB, pp. 1-149.
617. Thorhild Project – Class II Landfill. October 5, 2018]; Available from: https://www.wmsolutions.com/pdf/factsheet/Thorhild-Fact-Sheet-June-20-2017.pdf.
618. Biller, P. and Ross, A. (2011). Potential yields and properties of oil from the hydrothermal liquefaction of microalgae with different biochemical content. Bioresource Technology 102(1), 215-225.
619. Delrue, F., Li-Beisson, Y., Setier, P.-A., Sahut, C., Roubaud, A., Froment, A.-K., and Peltier, G. (2013). Comparison of various microalgae liquid biofuel production pathways based on energetic, economic and environmental criteria. Bioresource Technology 136, 205-212.
620. Bridgwater, A.V. (2003). Renewable fuels and chemicals by thermal processing of biomass. Chemical Engineering Journal 91(2), 87-102.
621. Oasmaa, A., Källi, A., Lindfors, C., Elliott, D.C., Springer, D., Peacocke, C., and Chiaramonti, D. (2012). Guidelines for transportation, handling, and use of fast pyrolysis bio-oil. 1. Flammability and toxicity. Energy & Fuels 26(6), 3864-3873.
622. Miao, X. and Wu, Q. (2004). High yield bio-oil production from fast pyrolysis by metabolic controlling of Chlorella protothecoides. Journal of Biotechnology 110(1), 85-93.
623. Harman-Ware, A.E., Morgan, T., Wilson, M., Crocker, M., Zhang, J., Liu, K., Stork, J., and Debolt, S. (2013). Microalgae as a renewable fuel source: fast pyrolysis of Scenedesmus sp. Renewable Energy 60, 625-632.
624. Miao, X., Wu, Q., and Yang, C. (2004). Fast pyrolysis of microalgae to produce renewable fuels. Journal of analytical and applied pyrolysis 71(2), 855-863.
625. Gong, X., Zhang, B., Zhang, Y., Huang, Y., and Xu, M. (2013). Investigation on pyrolysis of low lipid microalgae Chlorella vulgaris and Dunaliella salina. Energy & Fuels 28(1), 95-103.
626. Belotti, G., de Caprariis, B., De Filippis, P., Scarsella, M., and Verdone, N. (2014). Effect of Chlorella vulgaris growing conditions on bio-oil production via fast pyrolysis. Biomass and Bioenergy 61, 187-195.
627. Hognon, C., Delrue, F., Texier, J., Grateau, M., Thiery, S., Miller, H., and Roubaud, A. (2015). Comparison of pyrolysis and hydrothermal liquefaction of Chlamydomonas

reinhardtii. Growth studies on the recovered hydrothermal aqueous phase. Biomass and Bioenergy 73, 23-31.
628. Elliott, D.C., Hart, T.R., Schmidt, A.J., Neuenschwander, G.G., Rotness, L.J., Olarte, M. V., Zacher, A.H., Albrecht, K.O., Hallen, R.T., and Holladay, J.E. (2013). Process development for hydrothermal liquefaction of algae feedstocks in a continuous-flow reactor. Algal Research 2(4), 445-454.
629. Pavlovič, I., Knez, Z.E., and Škerget, M. (2013). Hydrothermal reactions of agricultural and food processing wastes in sub-and supercritical water: a review of fundamentals, mechanisms, and state of research. Journal of Agricultural and Food Chemistry 61(34), 8003-8025.
630. Kumar, M., Oyedun, A.O., and Kumar, A. (2018). A review on the current status of various hydrothermal technologies on biomass feedstock. Renewable and Sustainable Energy Reviews 81(Part 2), 1742-1770.
631. Yang, Y., Gilbert, A., and Xu, C.C. (2009). Production of bio-crude from forestry waste by hydro-liquefaction in sub-/super-critical methanol. AIChE Journal 55(3), 807-819.
632. Minowa, T., Yokoyama, S.-Y., Kishimoto, M., and Okakura, T. (1995). Oil production from algal cells of Dunaliella tertiolecta by direct thermochemical liquefaction. Fuel 74(12), 1735-1738.
633. Dote, Y., Sawayama, S., Inoue, S., Minowa, T., and Yokoyama, S.-Y. (1994). Recovery of liquid fuel from hydrocarbon-rich microalgae by thermochemical liquefaction. Fuel 73(12), 1855-1857.
634. Jazrawi, C., Biller, P., He, Y., Montoya, A., Ross, A. B., Maschmeyer, T., and Haynes, B.S. (2015). Two-stage hydrothermal liquefaction of a high-protein microalga. Algal Research 8, 15-22.
635. Roussis, S.G., Cranford, R., and Sytkovetskiy, N. (2012). Thermal treatment of crude algae oils prepared under hydrothermal extraction conditions. Energy & Fuels 26(8), 5294-5299.
636. Costanzo, W., Jena, U., Hilten, R., Das, K., and Kastner, J.R. (2015). Low temperature hydrothermal pretreatment of algae to reduce nitrogen heteroatoms and generate nutrient recycle streams. Algal Research 12, 377-387.
637. Kumar, M., Oyedun, A.O., and Kumar, A. (2017). Hydrothermal liquefaction of biomass for the production of diluents for bitumen transport. Biofuels, Bioproducts and Biorefining, 11:811–829.
638. Jones, S., Zhu, Y., Anderson, D., Hallen, R. T., Elliott, D. C., Schmidt, A., Albrecht, K., Hart, T., Butcher, M., and Drennan, C. (2014). Process design and economics for the conversion of algal biomass to hydrocarbons: whole algae hydrothermal liquefaction and upgrading. Pacific Northwest National Laboratory.
639. Davis, R., Markham, J., Kinchin, C., Grundl, N., Tan, E. C., and Humbird, D. (2016). Process design and economics for the production of algal biomass: Algal biomass production in open pond systems and processing through dewatering for downstream conversion, National Renewable Energy Laboratory, Golden, CO.
640. Tews, I.J., Zhu, Y., Drennan C., Elliott, D.C., Snowden-Swan L.J., Onarheim, K., Solantausta, Y. and Beckman D. (2014). Biomass direct liquefaction options: technoeconomic and life cycle assessment. Available from: https://www.osti.gov/biblio/1184983. Accessed: April 13, 2016.

641. Jazrawi, C., Biller, P., Ross, A. B., Montoya, A., Maschmeyer, T., and Haynes, B.S. (2013). Pilot plant testing of continuous hydrothermal liquefaction of microalgae. Algal Research 2(3), 268-277.
642. Jena, U., Das, K., and Kastner, J. (2011). Effect of operating conditions of thermochemical liquefaction on biocrude production from Spirulina platensis. Bioresource technology 102(10), 6221-6229.
643. Berglin, E.J., Enderlin, C.W., and Schmidt, A. J. (2012). Review and assessment of commercial vendors/options for feeding and pumping biomass slurries for hydrothermal liquefaction, Pacific Northwest National Laboratory. Available from: https://www.pnnl.gov/main/publications/external/technical_reports/PNNL-21981.pdf. Accessed: August 5, 2017.
644. Tang, X., Zhang, C., Li, Z., and Yang, X. (2016). Element and chemical compounds transfer in bio-crude from hydrothermal liquefaction of microalgae. Bioresource Technology 202, 8-14.
645. Mohan, D., Pittman, C.U., and Steele, P.H. (2006). Pyrolysis of wood/biomass for bio-oil: a critical review. Energy & Fuels 20(3), 848-889.
646. Vardon, D.R., Sharma, B.K., Blazina, G V., Rajagopalan, K., and Strathmann, T. J. (2012). Thermochemical conversion of raw and defatted algal biomass via hydrothermal liquefaction and slow pyrolysis. Bioresource Technology 109, 178-187.
647. Brown, T.M., Duan, P., and Savage, P.E. (2010). Hydrothermal liquefaction and gasification of Nannochloropsis sp. Energy & Fuels 24(6), 3639-3646.
648. Juneja, A. and Murthy, G. S. (2017). Evaluating the potential of renewable diesel production from algae cultured on wastewater: techno-economic analysis and life cycle assessment. AIMS Energy 5(2), 239-257.
649. Ou, L., Thilakaratne, R., Brown, R.C., and Wright, M.M. (2015). Techno-economic analysis of transportation fuels from defatted microalgae via hydrothermal liquefaction and hydroprocessing. Biomass and Bioenergy 72, 45-54.
650. Wright, M.M., Daugaard, D.E., Satrio, J.A., and Brown, R.C. (2010). Techno-economic analysis of biomass fast pyrolysis to transportation fuels. Fuel 89, Supplement 1, S2-S10.
651. Wang, X., Sheng, L., and Yang, X. (2017). Pyrolysis characteristics and pathways of protein, lipid and carbohydrate isolated from microalgae Nannochloropsis sp. Bioresource Technology, 229,119-125.
652. Jones, S., Meyer, P., Snowden-Swan, L.J., Padmaperuma, A., Tan, E., Dutta, A., Jacobson, J., and Cafferty, K. (2013). Process design and economics for the conversion of lignocellulosic biomass to hydrocarbon fuels: Fast pyrolysis and hydrotreating bio-oil pathway. Prepared for the U.S. Department of Energy Bioenergy Technologies Office, Pacific Northwest National Laboratory. Available from: https://www.osti.gov/biblio/1115839. Accessed: March 18, 2017.
653. Sardella Palma, R., Schweitzer, J., Wu, H., Lopez-Garcia, C., and Morbidelli, M. (2010). Stationary thermal stability analysis of a gas oil hydrotreating reactor. Industrial & Engineering Chemistry Research 49 (21), 10581-10587.
654. Jones, S.B., Valkenburt, C., Walton, C.W., Elliott, D.C., Holladay, J.E., Stevens, D.J., Kinchin, C., and Czernik, S. (2009). Production of gasoline and diesel from biomass via fast pyrolysis, hydrotreating and hydrocracking: a design case. Pacific Northwest National Laboratory. Available from: https://www.osti.gov/biblio/950728. Accessed: July 13, 2017.

655. Peters, M.S. and Timmerhaus, K.D. (1968). Plant design and economics for chemical engineers. Vol. 4: McGraw-Hill New York.
656. Shahrukh, H., Oyedun, A.O., Kumar, A., Ghiasi, B., Kumar, L., and Sokhansanj, S. (2016). Techno-economic assessment of pellets produced from steam pretreated biomass feedstock. Biomass and Bioenergy 87, 131-143.
657. Agbor, E., Oyedun, A.O., Zhang, X., and Kumar, A. (2016). Integrated techno-economic and environmental assessments of sixty scenarios for co-firing biomass with coal and natural gas. Applied Energy 169, 433-449.
658. Dave, A., Huang, Y., Rezvani, S., McIlveen-Wright, D., Novaes, M., and Hewitt, N. (2013). Techno-economic assessment of biofuel development by anaerobic digestion of European marine cold-water seaweeds. Bioresource Technology 135, 120-127.
659. Fasahati, P. and Liu, J. (2014). Techno-economic analysis of production and recovery of volatile fatty acids from brown algae using membrane distillation. In Computer Aided Chemical Engineering, edited by M.R. Eden, J.D. Siirola, and G.P. Towler. Elsevier, pp. 303-308.
660. Shabangu, S., Woolf, D., Fisher, E.M., Angenent, L.T., and Lehmann, J. (2014). Techno-economic assessment of biomass slow pyrolysis into different biochar and methanol concepts. Fuel 117, 742-748.
661. Bennion, E.P., Ginosar, D.M., Moses, J., Agblevor, F., and Quinn, J.C. (2015). Lifecycle assessment of microalgae to biofuel: comparison of thermochemical processing pathways. Applied Energy 154, 1062-1071.
662. Alabi, A., Tampier, M., and Bibeau, E. (2009). Microalgae Technologies and process for Biofuels. Bioenergy production in British Columbia. Available from: http://www.etipbioenergy.eu/databases/reports/69-microalgae-technologies-processes-for-biofuels-bioenergy-production-in-british-columbia-current-technology-barriers-to-implementation.
663. Zhu, Y., Tjokro Rahardjo, S.A., Valkenburg, C., Snowden-Swan, L., Jones, S., and Machinal, M. (2011). Techno-economic analysis for the thermochemical conversion of biomass to liquid fuels. Richland, Washington: Pacific Northwest National Laboratory. Available from: https://www.osti.gov/biblio/1128665.
664. Jones, S. B., Valkenburg, C., Walton, C.W., Elliott, D.C., Holladay, J.E., Stevens, D J., Kinchin, C., and Czernik, S. (2009). Production of gasoline and diesel from biomass via fast pyrolysis, hydrotreating and hydrocracking: a design case. Pacific Northwest National Laboratory.
665. Lundquist, T.J., Woertz, I.C., Quinn, N., and Benemann, J.R. (2010). A realistic technology and engineering assessment of algae biofuel production. Energy Biosciences Institute. Available from: https://digitalcommons.calpoly.edu/cenv_fac/188/.
666. Orfield, N.D., Fang, A.J., Valdez, P.J., Nelson, M.C., Savage, P.E., Lin, X.N., and Keoleian, G.A. (2014). Life cycle design of an algal biorefinery featuring hydrothermal liquefaction: effect of reaction conditions and an alternative pathway including microbial regrowth. ACS Sustainable Chemistry & Engineering 2(4), 867-874.
667. Hoffman, J. (2016). Techno-economic assessment of micro-algae production systems. Available from: https://digitalcommons.usu.edu/gradreports/789/.
668. Anex, R. P., Aden, A., Kazi, F. K., Fortman, J., Swanson, R. M., Wright, M. M., Satrio, J. A., Brown, R. C., Daugaard, D. E., Platon, A., Kothandaraman, G., Hsu, D. D., and Dutta,

A. (2010). Techno-economic comparison of biomass-to-transportation fuels via pyrolysis, gasification, and biochemical pathways. Fuel 89, S29-S35.
669. Brown, T.R., Thilakaratne, R., Brown, R.C., and Hu, G. (2013). Techno-economic analysis of biomass to transportation fuels and electricity via fast pyrolysis and hydroprocessing. Fuel 106, 463-469.
670. Thilakaratne, R., Brown, T., Li, Y., Hu, G., and Brown, R. (2014). Mild catalytic pyrolysis of biomass for production of transportation fuels: a techno-economic analysis. Green Chemistry 16(2), 627-636.
671. Li, B. (2015). Techno-economic and uncertainty analysis of fast pyrolysis and gasification for biofuel production, Iowa State University. Available from: https://lib.dr.iastate.edu/cgi/viewcontent.cgi?article=5939&context=etd.
672. De Jong, S., Hoefnagels, R., Faaij, A., Slade, R., Mawhood, R., and Junginger, M. (2015). The feasibility of short-term production strategies for renewable jet fuels–a comprehensive techno-economic comparison. Biofuels, Bioproducts and Biorefining 9(6), 778-800.
673. Al-Mayyahi, M.A., Hoadley, A.F.A., Smith, N.E., and Rangaiah, GP. (2011). Investigating the trade-off between operating revenue and CO2 emissions from crude oil distillation using a blend of two crudes. Fuel 90(12), 3577-3585.
674. Lerkkasemsan, N. and Achenie, L.E. (2013). Life cycle costs and life cycle assessment for the harvesting, conversion, and the use of switchgrass to produce electricity. International Journal of Chemical Engineering 2013. DOI: http://dx.doi.org/10.1155/2013/492058.
675. Brownbridge, G., Azadi, P., Smallbone, A., Bhave, A., Taylor, B., and Kraft, M. (2014). The future viability of algae-derived biodiesel under economic and technical uncertainties. Bioresource Technology 151, 166-173.
676. Sarkar, S. and Kumar, A. (2007). A review of techno-economics of bio-hydrogen production technologies. Presented at the 2007 American Society of Agricultural and Biological Engineers meeting.
677. Braimakis, K., Atsonios, K., Panopoulos, K. D., Karellas, S., and Kakaras, E. (2014). Economic evaluation of decentralized pyrolysis for the production of bio-oil as an energy carrier for improved logistics towards a large centralized gasification plant. Renewable and Sustainable Energy Reviews 35, 57-72.
678. Brown, T.R., Wright, M.M., and Brown, R.C. (2011). Estimating profitability of two biochar production scenarios: slow pyrolysis vs fast pyrolysis. Biofuels, Bioproducts and Biorefining 5(1), 54-68.
679. Ringer, M., Putsche, V., and Scahill, J. (2006). Large-scale pyrolysis oil production: a technology assessment and economic analysis, National Renewable Energy Laboratory. Available from: https://www.osti.gov/biblio/894989.
680. Elliott, D.C. (2007). Historical developments in hydroprocessing bio-oils. Energy & Fuels 21(3), 1792-1815.
681. Stevens, C. (2011). Thermochemical processing of biomass: conversion into fuels, chemicals and power. John Wiley & Sons.
682. Bridgwater, A.V. (2012). Review of fast pyrolysis of biomass and product upgrading. Biomass and Bioenergy 38, 68-94.
683. Barelli, L., Bidini, G., Gallorini, F., and Servili, S. (2008). Hydrogen production through sorption-enhanced steam methane reforming and membrane technology: a review. Energy 33(4), 554-570.

684. Sucipta, M., Kimijima, S., and Suzuki, K. (2007). Performance analysis of the SOFC–MGT hybrid system with gasified biomass fuel. Journal of Power Sources 174(1), 124-135.
685. Weerachanchai, P., Horio, M., and Tangsathitkulchai, C. (2009). Effects of gasifying conditions and bed materials on fluidized bed steam gasification of wood biomass. Bioresource Technology 100(3), 1419-1427.
686. Mermoud, F., Salvador, S., Van de Steene, L., and Golfier, F. (2006). Influence of the pyrolysis heating rate on the steam gasification rate of large wood char particles. Fuel 85(10-11), 1473-1482.
687. Tanaka, Y., Yamaguchi, T., Yamasaki, K., Ueno, A., and Kotera, Y. (1984). Catalyst for steam gasification of wood to methanol synthesis gas. Industrial & Engineering Chemistry product research and development 23(2), 225-229.
688. Baker, E.G., Mudge, L.K., and Mitchell, D.H. (1984). Oxygen/steam gasification of wood in a fixed-bed gasifier. Industrial & Engineering Chemistry Process Design and Development 23(4), 725-728.
689. Aziz, M., Oda, T., and Kashiwagi, T. (2014). Integration of energy-efficient drying in microalgae utilization based on enhanced process integration. Energy 70, 307-316.
690. Aziz, M. (2016). Integrated hydrogen production and power generation from microalgae. International Journal of Hydrogen Energy 41(1), 104-112.
691. Craig, K.R. and Mann, M.K. (1996). Cost and performance analysis of biomass-based integrated gasification combined-cycle (BIGCC) power systems, National Renewable Energy Lab. Available from: https://www.osti.gov/biblio/419974.
692. Leckner, B., Szentannai, P., and Winter, F. (2011). Scale-up of fluidized-bed combustion–A review. Fuel 90(10), 2951-2964.
693. Arena, U. (2012). Process and technological aspects of municipal solid waste gasification. A review. Waste management 32(4), 625-639.
694. Devi, L., Ptasinski, K.J., and Janssen, F. J. J. G. (2003). A review of the primary measures for tar elimination in biomass gasification processes. Biomass and Bioenergy 24(2), 125-140.
695. Hirano, A., Hon-Nami, K., Kunito, S., Hada, M., and Ogushi, Y. (1998). Temperature effect on continuous gasification of microalgal biomass: theoretical yield of methanol production and its energy balance. Catalysis Today 45(1-4), 399-404.
696. Raheem, A., Dupont, V., Channa, A. Q., Zhao, X., Vuppaladadiyam, A.K., Taufiq-Yap, Y.-H., Zhao, M., and Harun, R. (2017). Parametric Characterization of Air Gasification of Chlorella vulgaris Biomass. Energy & Fuels 31(3), 2959-2969.
697. Akiya, N. and Savage, P.E. (2002). Roles of water for chemical reactions in high-temperature water. Chemical reviews 102(8), 2725-2750.
698. Savage, P.E. (1999). Organic chemical reactions in supercritical water. Chemical reviews 99(2), 603-622.
699. Amos W. Assessment of supercritical water gasification: alternative designs. National Renewable Energy Laboratory (1999).
700. Aspen Plus. User Guide. Version 84. Aspen Technology Inc., Burlington, MA (2014).
701. Moazami, N., Ashori, A., Ranjbar, R., Tangestani, M., Eghtesadi, R., and Nejad, A. S. (2012). Large-scale biodiesel production using microalgae biomass of Nannochloropsis. Biomass and Bioenergy 39, 449-453.

702. Nogueira, E., Jr.. Kumar, M., Pankratz, S., Oyedun, A. O., and Kumar, A. (2018). Development of life cycle water footprints for the production of fuels and chemicals from algae biomass. Water Research 140, 311-322.
703. Aziz, M., Oda, T., and Kashiwagi, T. (2014). Advanced energy harvesting from macroalgae—innovative integration of drying, gasification and combined cycle. Energies 7(12), 8217-8235.
704. Kumar, M., Oyedun, A. O., and Kumar, A. Development of a process model and parameter study for the hydrothermal gasification of algal biomass (submitted).
705. Kumar, A., Cameron, J.B., and Flynn, P.C. (2003). Biomass power cost and optimum plant size in western Canada. Biomass and Bioenergy 24(6), 445-464.
706. Wei, L., Pordesimo, L.O., Herndon, C., and Batchelor, W.D. (2008). Cost analysis of micro-scale biomass gasification facilities through mathematical modeling. Presented at the 2008 meeting of the American Society of Agricultural and Biological Engineers.
707. Akbari, M., Oyedun, A.O., and Kumar, A. (2018). Ammonia production from black liquor gasification and co-gasification with pulp and waste sludges: A techno-economic assessment. Energy 151, 133-143.
708. Gassner, M. and Maréchal, F. (2012). Thermo-economic optimisation of the polygeneration of synthetic natural gas (SNG), power and heat from lignocellulosic biomass by gasification and methanation. Energy & Environmental Science 5(2), 5768-5789.
709. Kumar, M., Oyedun, A.O., and Kumar, A. (2017). Hydrothermal liquefaction of biomass for the production of diluents for bitumen transport. Biofuels, Bioproducts and Biorefining 11(5), 811-829.
710. Oyedun, A.O., Kumar, A., Oestreich, D., Arnold, U., and Sauer, J. (2018). The development of the production cost of oxymethylene ethers as diesel additives from biomass. Biofuels, Bioproducts and Biorefining 12(4), 694-710.
711. Davis, R., Fishman, D., Frank, E.D., Wigmosta, M.S., Aden, A., Coleman, A.M., Pienkos, P.T., Skaggs, R.J., Venteris, E.R., and Wang, M.Q. (2012). Renewable diesel from algal lipids: an integrated baseline for cost, emissions, and resource potential from a harmonized model, National Renewable Energy Laboratory. Available from: https://www.osti.gov/biblio/1044475.
712. Zhang, Y., Brown, T.R., Hu, G., and Brown, R.C. (2013). Comparative techno-economic analysis of biohydrogen production via bio-oil gasification and bio-oil reforming. Biomass and Bioenergy 51, 99-108.
713. Singh, N.R., Mallapragada, D.S., Agrawal, R., and Tyner, W.E. (2012). Economic analysis of novel synergistic biofuel (H 2 Bioil) processes. Biomass Conversion and Biorefinery 2(2), 141-148.
714. Berstad, D., Roussanaly, S., Skaugen, G., Anantharaman, R., Nekså, P., and Jordal, K. (2014). Energy and cost evaluation of a low-temperature CO2 capture unit for IGCC plants. Energy Procedia 63, 2031-2036.
715. Lina, C.-Y., Lib, Y.-H., and Leec, C.-Y. Cost estimation of hydrogen generation from palm oil waste via supercritical water gasification. Available from: http://59.125.238.48/zaplab/upload/results/2017031217584440.pdf.
716. Lu, Y., Zhao, L., and Guo, L. (2011). Technical and economic evaluation of solar hydrogen production by supercritical water gasification of biomass in China. International Journal of Hydrogen Energy 36(22), 14349-14359.

717. Spath, P., Aden, A., Eggeman, T., Ringer, M., Wallace, B., and Jechura, J. (2005). Biomass to hydrogen production detailed design and economics utilizing the Battelle Columbus laboratory indirectly-heated gasifier, National Renewable Energy Lab. Available from: http://neotericsint.com/pubs/BCL%20Gasifier.pdf.
718. Clarens, A.F., Resurreccion, E.P., White, M.A., and Colosi, L M. (2010). Environmental life cycle comparison of algae to other bioenergy feedstocks. Environmental Science and Technology 44(5), 1813-1819.
719. van Beilen, J.B. (2010). Why microalgal biofuels won't save the internal combustion machine. Biofuels, Bioproducts and Biorefining 4(1), 41-52.
720. Williams, P.J.l.B. and Laurens, L.M. (2010). Microalgae as biodiesel & biomass feedstocks: review & analysis of the biochemistry, energetics & economics. Energy & Environmental Science 3(5), 554-590.
721. Hallale, N., Moore, I., Vauk, D., and Robinson, P.R. (2017). Hydrogen Network Optimization, in Springer Handbook of Petroleum Technology, Springer. p. 817-831.
722. Dodds, P.E. and McDowall, W. (2012). The future of the natural gas pipeline system in the UK. Presented at the International Energy Workshop, Cape Town.
723. Elliott, D.C. (2016). Review of recent reports on process technology for thermochemical conversion of whole algae to liquid fuels. Algal Research 13, 255-263.
724. Sheehan, J., Dunahay, T., Benemann, J., and Roessler, P. (1998). Look back at the US department of energy's aquatic species program: biodiesel from algae; close-out report, National Renewable Energy Lab.
725. Manganaro, J.L., Lawal, A., and Goodall, B. (2015). Techno-economics of microalgae production and conversion to refinery-ready oil with co-product credits. Biofuels, Bioproducts and Biorefining 9(6), 760-777.
726. Murakami, M. and Ikenouchi, M. (1997). The biological CO_2 fixation and utilization project by rite (2)—Screening and breeding of microalgae with high capability in fixing CO_2—. Energy Conversion and Management 38, S493-S497.
727. Hunt, A.J., Sin, E.H., Marriott, R., and Clark, J.H. (2010). Generation, capture, and utilization of industrial carbon dioxide. ChemSusChem: Chemistry & Sustainability Energy & Materials 3(3), 306-322.
728. Murray, B. and Rivers, N. (2015). British Columbia’s revenue-neutral carbon tax: A review of the latest “grand experiment” in environmental policy. Energy Policy 86, 674-683.
729. Pankratz, S., Oyedun, A. O., Zhang, X., and Kumar, A. (2017). Algae production platforms for Canada's northern climate. Renewable and Sustainable Energy Reviews 80, 109-120.
730. Antal, M.J., Jr., Allen, S.G., Schulman, D., Xu, X., and Divilio, R. J. (2000). Biomass gasification in supercritical water. Industrial & Engineering Chemistry Research 39(11), 4040-4053.
731. Benemann, J.R. (1997). CO_2 mitigation with microalgae systems. Energy Conversion and Management 38, S475-S479.
732. Matsumoto, H., Shioji, N., Hamasaki, A., Ikuta, Y., Fukuda, Y., Sato, M., Endo, N., and Tsukamoto, T. (1995). Carbon dioxide fixation by microalgae photosynthesis using actual flue gas discharged from a boiler. Applied Biochemistry and Biotechnology 51(1), 681-692.
733. Vunjak-Novakovic, G., Kim, Y., Wu, X., Berzin, I., and Merchuk, J.C. (2005). Air-lift bioreactors for algal growth on flue gas: mathematical modeling and pilot-plant studies. Industrial and Engineering Chemistry Research 44(16), 6154-6163.

734. Benarji, N., Balaji, C., and Venkateshan, S. (2008). Optimum design of cross-flow shell and tube heat exchangers with low fin tubes. Heat Transfer Engineering 29(10), 864-872.
735. Goldsberry, F.L. (1984). Variable pressure power cycle and control system, Google Patents.
736. Grima, E.M., Belarbi, E.-H., Fernández, F.A., Medina, A.R., and Chisti, Y. (2003). Recovery of microalgal biomass and metabolites: process options and economics. Biotechnology Advances 20(7-8), 491-515.
737. International Organization for Standardization, ISO 14010:2006 Environmental management – life cyle assessment – principles and framework (2006). Available from: https://www.iso.org/standard/37456.html.
738. Aspen Plus (2009). Aspen Technology, Inc., version 11. Available from: https://www.aspentech.com/.
739. Moazami, N., Ashori, A., Ranjbar, R., Tangestani, M., Eghtesadi, R., and Nejad, A.S. (2012). Large-scale biodiesel production using microalgae biomass of Nannochloropsis. Biomass and Bioenergy 39(Supplement C), 449-453.
740. Berndes, G. (2002). Bioenergy and water—the implications of large-scale bioenergy production for water use and supply. Global Environmental Change 12(4), 253-271.
741. Singh, R.N. and Sharma, S. (2012). Development of suitable photobioreactor for algae production – A review. Renewable and Sustainable Energy Reviews 16(4), 2347-2353.
742. Singh, S. and Kumar, A. (2011). Development of water requirement factors for biomass conversion pathway. Bioresource Technology 102(2), 1316-1328.
743. Chiaramonti, D., Prussi, M., Casini, D., Tredici, M. R., Rodolfi, L., Bassi, N., Zittelli, G. C., and Bondioli, P. (2013). Review of energy balance in raceway ponds for microalgae cultivation: Re-thinking a traditional system is possible. Applied Energy 102, 101-111.
744. Lee, Y.-K. (2001). Microalgal mass culture systems and methods: Their limitation and potential. Journal of Applied Phycology 13(4), 307-315.
745. Moheimani, N.R. and Borowitzka, M.A. (2006). The long-term culture of the coccolithophore Pleurochrysis carterae (Haptophyta) in outdoor raceway ponds. Journal of Applied Phycology 18(6), 703-712.
746. Borowitzka, M.A. (1999). Commercial production of microalgae: ponds, tanks, tubes and fermenters. Journal of Biotechnology 70(1), 313-321.
747. Mbogga, M.S., Hamann, A., and Wang, T. (2009). Historical and projected climate data for natural resource management in western Canada. Agricultural and Forest Meteorology 149(5), 881-890.
748. Hage, K.D. (1978). Natural and enhanced evaporation from Lake Wabamun, Alberta. Canadian Water Resources Journal/Revue canadienne des ressources hydriques 3(3), 49-61.
749. Rodolfi, L., Chini Zittelli, G., Bassi, N., Padovani, G., Biondi, N., Bonini, G., and Tredici, M. R. (2009). Microalgae for oil: Strain selection, induction of lipid synthesis and outdoor mass cultivation in a low-cost photobioreactor. Biotechnology and Bioengineering 102(1), 100-112.
750. Li, X., Xu, H., and Wu, Q. (2007). Large-scale biodiesel production from microalga Chlorella protothecoides through heterotrophic cultivation in bioreactors. Biotechnology and Bioengineering 98(4), 764-771.
751. Watanabe, Y. and Hall, D.O. (1996). Photosynthetic CO 2 conversion technologies using a photobioreactor incorporating microalgae-energy and material balances. Energy conversion and management 37(6), 1321-1326.
752. Demirbas, A. (2008). Biodiesel: A Realistic Fuel Alternative for Diesel Engines. Springer.

753. Bridgwater, A., Meier, D., and Radlein, D. (1999). An overview of fast pyrolysis of biomass. Organic Geochemistry 30(12), 1479-1493.
754. Kumar, M., Oyedun, A.O., and Kumar, A. (2018). A comparative analysis of the production of diluents from the thermochemical conversion of algae (submitted).
755. Toor, S.., Rosendahl, L.A., Hoffmann, J., Pedersen, T.H., Nielsen, R.P., and Søgaard, E.G. (2014). Hydrothermal liquefaction of biomass. In Application of Hydrothermal Reactions to Biomass Conversion, edited by F. Jin. Springer: Berlin, Heidelberg, pp. 189-217.
756. Tews, I. J., Zhu, Y., Drennan, C., Elliott, D. C., Snowden-Swan, L. J., Onarheim, K., Solantausta, Y., and Beckman, D. (2014). Biomass Direct Liquefaction Options. TechnoEconomic and Life Cycle Assessment, Pacific Northwest National Laboratory.
757. Jones, S., Zhu, Y., Anderson, D., Hallen, R. T., Elliott, D. C., Schmidt, A., Albrecht, K., Hart, T., Butcher, M., and Drennan, C. (2014). Process design and economics for the conversion of algal biomass to hydrocarbons: whole algae hydrothermal liquefaction and upgrading. Pacific Northwest National Laboratory, pp. 1-69.
758. Statistics Canada (2014). Electric power generation by class of electricity producer. Retrieved June 10, 2017, from http://www5.statcan.gc.ca/cansim/a26?lang=eng&retrLang=eng&id=1270007&paSer=&pattern=&stByVal=1&p1=1&p2=35&tabMode=dataTable&csid=.
759. Environment Canada. Water withdrawal and consumption by sector data. Retrieved June 10, 2017, from https://www.ec.gc.ca/indicateurs-indicators/default.asp?lang=en&n=5736C951-1. 2013 [cited 2017 June 10]; Available from: https://www.ec.gc.ca/indicateurs-indicators/default.asp?lang=en&n=5736C951-1.
760. Wong, A., Zhang, H., and Kumar, A. (2016). Life cycle water footprint of hydrogenation-derived renewable diesel production from lignocellulosic biomass. Water Research 102(Supplement C), 330-345.
761. Singh, S., Kumar, A., and Jain, S. (2014). Impact of biofuel production on water demand in Alberta. Canadian Biosystems Engineering 56, 8.11-8.21.
762. Hsu, D.D. (2012). Life cycle assessment of gasoline and diesel produced via fast pyrolysis and hydroprocessing. Biomass and Bioenergy 45, 41-47.
763. Patel, M. and Kumar, A. (2016). Production of renewable diesel through the hydroprocessing of lignocellulosic biomass-derived bio-oil: A review. Renewable and Sustainable Energy Reviews 58(Supplement C), 1293-1307.
764. Baker, E.G. and Elliott, D.C. (1986). Catalytic hydrotreating of biomass-derived oils. Conference: 193. National meeting of the American Chemical Society, Denver, CO, USA, 5 Apr 1987; Other Information: Portions of this document are illegible in microfiche products. Pacific Northwest Lab. Available from: http://web.anl.gov/PCS/acsfuel/preprint%20archive/Files/32_2_Denver_04-87_0257.pdf.
765. Zhu, Y., Tjokro Rahardjo, S.A., Valkenburt, C., Snowden-Swan, L.J., Jones, S B., and Machinal, M.A. (2011). Techno-economic analysis for the thermochemical conversion of biomass to liquid fuels, Pacific Northwest National Laboratory. Available from: https://www.osti.gov/biblio/1128665.
766. Davis, R., Aden, A., and Pienkos, P.T. (2011). Techno-economic analysis of autotrophic microalgae for fuel production. Applied Energy 88(10), 3524-3531.
767. Turn, S., Kinoshita, C., Zhang, Z., Ishimura, D., and Zhou, J. (1998). An experimental investigation of hydrogen production from biomass gasification. International Journal of Hydrogen Energy 23(8), 641-648.

768. Rapagnà, S., Jand, N., and Foscolo, P. U. (1998). Catalytic gasification of biomass to produce hydrogen rich gas. International Journal of Hydrogen Energy 23(7), 551-557.
769. Verma, A., Olateju, B., Kumar, A., and Gupta, R. (2015). Development of a process simulation model for energy analysis of hydrogen production from underground coal gasification (UCG). International Journal of Hydrogen Energy 40(34), 10705-10719.
770. Fang, Z. and Xu, C.C. (2014). Near-critical and supercritical water and their applications for biorefineries. Springer, 441-475.
771. Yang, J., Xu, M., Zhang, X., Hu, Q., Sommerfeld, M., and Chen, Y. (2011). Life-cycle analysis on biodiesel production from microalgae: water footprint and nutrients balance. Bioresource Technology 102(1), 159-165.
772. Weissman, J.C., Tillett, D.M., and Goebel, R. (1989). Design and operation of an outdoor microalgae test facility, Microbial Products, Inc., Vacaville, CA (USA).
773. Vose, D., Koupeev, T., Van Hauwermeiren, M., Smet, W., and van den Bossche, S. (2007). Help File for ModelRisk Version 5 Vose Software.
774. Habibi, R. (2017). Applications of Vose ModelRisk Software in Simulated Data. Asian Journal of Economics, Business and Accounting 2(1), 1-10.
775. Alberta Energy (2013). Facts and statistics. Last modified. Available from: http://www.energy.gov.ab.ca/Pages/default.aspx. Accessed: May 10, 2017.
76. Spampinato, G., Massimo, D.E., Musarella, C.M., De Paola, P., Malerba, A., and Musolino, M. (2019). Carbon sequestration by cork oak forests and raw material to built up post carbon city, in Smart Innovation, Systems and Technologies, pp. 663-671.
777. Bernstein, L., Lee, A., and Crookshank, S. (2006). Carbon dioxide capture and storage: A status report. Climate Policy 6(2), 241-246.
778. Watson, R.T.., Zinyowera, M.C., and Moss, R.H. (1996). Technologies, Policies and Measures for Mitigating Climate Change, Intergovernmental Panel on Climate Change.
779. Rizzo, A.M., Prussi, M., Bettucci, L., Libelli, I.M., and Chiaramonti, D. (2013). Characterization of microalga Chlorella as a fuel and its thermogravimetric behavior. Applied Energy 102, 24-31.
780. Nimana, B., Canter, C., and Kumar, A. (2015). Energy consumption and greenhouse gas emissions in upgrading and refining of Canada's oil sands products. Energy 83 (Supplement C), 65-79.
781. Parker, G.B. and Dahowski, R.T. (2008). The elephant in the room: Dealing with carbon emissions from synthetic transportation fuels production? Strategic Planning for Energy and the Environment 28(1), 12-33.
782. Verma, R., Kumar, R., Mehan, L., and Srivastava, A. (2018). Modified conventional bioreactor for microalgae cultivation. Journal of Bioscience and Bioengineering 125(2), 224-230.
783. Daniel Jamu, R. H. P. (1997). Aquaculture pond modeling for the analysis of environmental impacts and integration with agriculture: relationship between carbon input and sediment quality in aquaculture ponds. Oregon State University: Corvallis, Oregon. p. 191, pp. 62-67.
784. Choquette-Levy, N., MacLean, H.L., and Bergerson, J.A. (2013). Should Alberta upgrade oil sands bitumen? An integrated life cycle framework to evaluate energy systems investment tradeoffs. Energy Policy 61, 78-87.
785. Rao, F. and Liu, Q. (2013). Froth treatment in Athabasca oil sands bitumen recovery process: A review. Energy & Fuels 27(12), 7199-7207.

786. Miadonye, A., Doyle, N., Britten, A., Latour, N., and Puttagunta, V. (2001). Modelling viscosity and mass fraction of bitumen-diluent mixtures. Journal of Canadian Petroleum Technology 40(07).
787. Tipman, R.N. and Long, Y.-C. (1999). Solvent process for bitumen separation from oil sands froth, Google Patents.
788. Pollard, A.J., Banasiak, D.S., Ellens, C.J., and Brown, J.N. (2015). Methods, apparatus, and systems for incorporating bio-derived materials into oil sands processing, Google Patents.
789. Tessel, D. (2015). Systems and methods for using gas to liquids (gtl) technology, Google Patents.
790. Ellens, C., Brown, J., Pollard, A., and Banasiak, D. (2012). Methods, apparatus, and systems for incorporating bio-derived materials into oil sands processing, Google Patents.
791. Liu, X., Saydah, B., Eranki, P., Colosi, L. M., Greg Mitchell, B., Rhodes, J., and Clarens, A. F. (2013). Pilot-scale data provide enhanced estimates of the life cycle energy and emissions profile of algae biofuels produced via hydrothermal liquefaction. Bioresource Technology 148, 163-171.
792. Corbetta, M., Frassoldati, A., Bennadji, H., Smith, K., Serapiglia, M.J., Gauthier, G., Melkior, T., Ranzi, E., and Fisher, E.M. (2014). Pyrolysis of centimeter-scale woody biomass particles: Kinetic modeling and experimental validation. Energy & Fuels 28(6), 3884-3898.
793. Septien, S., Valin, S., Dupont, C., Peyrot, M., and Salvador, S. (2012). Effect of particle size and temperature on woody biomass fast pyrolysis at high temperature (1000–1400 C). Fuel 97, 202-210.
794. Wannapeera, J., Fungtammasan, B., and Worasuwannarak, N. (2011). Effects of temperature and holding time during torrefaction on the pyrolysis behaviors of woody biomass. Journal of Analytical and Applied Pyrolysis 92(1), 99-105.
795. Gao, L., Sun, J., Xu, W., and Xiao, G. (2017). Catalytic pyrolysis of natural algae over Mg-Al layered double oxides/ZSM-5 (MgAl-LDO/ZSM-5) for producing bio-oil with low nitrogen content. Bioresource Technology 225, 293-298.
796. Aboulkas, A., Hammani, H., El Achaby, M., Bilal, E., and Barakat, A. (2017). Valorization of algal waste via pyrolysis in a fixed-bed reactor: Production and characterization of bio-oil and bio-char. Bioresource Technology 243, 400-408.
797. Ramachandran, R. and Menon, R.K. (1998). An overview of industrial uses of hydrogen. International Journal of Hydrogen Energy 23(7), 593-598.
798. Kumar, M., Oyedun, A. O., and Kumar, A. (2017). A review on the current status of various hydrothermal technologies on biomass feedstock. Renewable and Sustainable Energy Reviews, 81(2), 1742-1770. .
799. Onwudili, J.A., Lea-Langton, A.R., Ross, A.B., and Williams, P.T. (2013). Catalytic hydrothermal gasification of algae for hydrogen production: composition of reaction products and potential for nutrient recycling. Bioresource Technology 127, 72-80.
800. Guan, Q., Wei, C., and Savage, P.E. (2012). Hydrothermal gasification of Nannochloropsis sp. with Ru/C. Energy & Fuels 26(7), 4575-4582.
801. Onwudili, J.A., Lea-Langton, A.., Ross, A.B., and Williams, P.T. (2013). Catalytic hydrothermal gasification of algae for hydrogen production: Composition of reaction products and potential for nutrient recycling. Bioresource Technology 127(Supplement C), 72-80.
802. Duman, G., Uddin, M.A., and Yanik, J. (2014). Hydrogen production from algal biomass via steam gasification. Bioresource Technology 166 (Supplement C), 24-30.

803. Kaewpanha, M., Guan, G., Hao, X., Wang, Z., Kasai, Y., Kusakabe, K., and Abudula, A. (2014). Steam co-gasification of brown seaweed and land-based biomass. Fuel Processing Technology 120 (Supplement C), 106-112.
804. Sanchez-Silva, L., López-González, D., Garcia-Minguillan, A.M., and Valverde, J. L. (2013). Pyrolysis, combustion and gasification characteristics of Nannochloropsis gaditana microalgae. Bioresource Technology 130(Supplement C), 321-331.
805. Díaz-Rey, M.R., Cortés-Reyes, M., Herrera, C., Larrubia, M.A., Amadeo, N., Laborde, M., and Alemany, L.J. (2015). Hydrogen-rich gas production from algae-biomass by low temperature catalytic gasification. Catalysis Today 257(Part 2), 177-184.
806. Handler, R.M., Canter, C.E., Kalnes, T N., Lupton, F.S., Kholiqov, O., Shonnard, DR., and Blowers, P. (2012). Evaluation of environmental impacts from microalgae cultivation in open-air raceway ponds: Analysis of the prior literature and investigation of wide variance in predicted impacts. Algal Research 1(1), 83-92.
807. Demirbas, A. and Demirbas, M. F. (2010). Algae energy: Algae as a new source of biodiesel, in Green Energy and Technology. p. 139.
808. Odjadjare, E.C., Mutanda, T., and Olaniran, A.O. (2017). Potential biotechnological application of microalgae: a critical review. Critical Reviews in Biotechnology 37(1), 37-52.
809. Leite, G.., Abdelaziz, A.E.M., and Hallenbeck, P. C. (2013). Algal biofuels: Challenges and opportunities. Bioresource Technology 145, 134-141.
810. Sharp, C.E., Urschel, S., Dong, X., Brady, A., Slater, G.F., and Strous, M. (2017). Robust, high-productivity phototrophic carbon capture at high pH and alkalinity using natural microbial communities. Biotechnology for Biofuels 10(1).
811. Klassen, V., Blifernez-Klassen, O., Hoekzema, Y., Mussgnug, J.H., and Kruse, O. (2015). A novel one-stage cultivation/fermentation strategy for improved biogas production with microalgal biomass. Journal of Biotechnology 215, 44-51.
812. Matsudo, M.C., Sousa, T.F., Pérez-Mora, L.S., Bezerra, R.P., Sato, S., and Carvalho, J.C.M. (2017). Ethanol as complementary carbon source in Scenedesmus obliquus cultivation. Journal of Chemical Technology and Biotechnology 92 (4), 781-786.
813. International Organization for Standardization (2006). ISO 14040: Environmental management–life cycle assessment–principles and framework. London: British Standards Institution.
814. International Organization for Standardization. (2006). 14044: 2006, Life cycle assessment: Requirement and guidelines. Environmental Management (ISO) 2006b.
815. Clarens, A. and Colosi, L. (2013). Life cycle assessment of algae-to-energy systems. In Advanced Biofuels and Bioproducts, edited by J.W. Lee. Springer New York, pp. 759-778.
816. Clarens, A.F., Resurreccion, E.P., White, M.A., and Colosi, L.M. (2010). Response to comment on "environmental life cycle comparison of algae to other bioenergy feedstocks". Environmental Science and Technology 44(9), 3643.
817. Jorquera, O., Kiperstok, A., Sales, E.A., Embiruçu, M., and Ghirardi, M.L. (2010). Comparative energy life-cycle analyses of microalgal biomass production in open ponds and photobioreactors. Bioresource Technology 101(4), 1406-1413.
818. Sander, K. and Murthy, G.S. (2010). Life cycle analysis of algae biodiesel. International Journal of Life Cycle Assessment 15(7), 704-714.
819. Batan, L., Quinn, J., Willson, B., and Bradley, T. (2010). Net energy and greenhouse gas emission evaluation of biodiesel derived from microalgae. Environmental Science & Technology 44(20), 7975-7980.

820. Brentner, L.B., Eckelman, M.J., and Zimmerman, J.B. (2011). Combinatorial life cycle assessment to inform process design of industrial production of algal biodiesel. Environmental Science & Technology 45(16), 7060-7067.
821. Campbell, P.K., Beer, T., and Batten, D. (2011). Life cycle assessment of biodiesel production from microalgae in ponds. Bioresource Technology 102(1), 50-56.
822. Passell, H., Dhaliwal, H., Reno, M., Wu, B., Amotz, A.B., Ivry, E., Gay, M., Czartoski, T., Laurin, L., and Ayer, N. (2013). Algae biodiesel life cycle assessment using current commercial data. Journal of Environmental Management 129, 103-111.
823. Shirvani, T., Yan, X., Inderwildi, O.R., Edwards, P.P., and King, D.A. (2011). Life cycle energy and greenhouse gas analysis for algae-derived biodiesel. Energy & Environmental Science 4(10), 3773-3778.
824. Vasudevan, V., Stratton, R.W., Pearlson, M.N., Jersey, G.R., Beyene, A.G., Weissman, J.C., Rubino, M., and Hileman, J.I. (2012). Environmental performance of algal biofuel technology options. Environmental Science and Technology 46(4), 2451-2459.
825. Azadi, P., Brownbridge, G., Mosbach, S., Smallbone, A., Bhave, A., Inderwildi, O., and Kraft, M. (2014). The carbon footprint and non-renewable energy demand of algae-derived biodiesel. Applied Energy 113, 1632-1644.
826. Baliga, R. and Powers, S.E. (2010). Sustainable algae biodiesel production in cold climates. International Journal of Chemical Engineering 2010.
827. de Boer, K., Moheimani, N.R., Borowitzka, M.., and Bahri, P. A. (2012). Extraction and conversion pathways for microalgae to biodiesel: a review focused on energy consumption. Journal of Applied Phycology 24(6), 1681-1698.
828. Grierson, S., Strezov, V., and Bengtsson, J. (2013). Life cycle assessment of a microalgae biomass cultivation, bio-oil extraction and pyrolysis processing regime. Algal Research 2 (3), 299-311.
829. Liu, X., Saydah, B., Eranki, P., Colosi, L. M., Mitchell, B. G., Rhodes, J., and Clarens, A. F. (2013). Pilot-scale data provide enhanced estimates of the life cycle energy and emissions profile of algae biofuels produced via hydrothermal liquefaction. Bioresource Technology 148, 163-171.
830. Frank, E.D., Elgowainy, A., Han, J., and Wang, Z. (2013). Life cycle comparison of hydrothermal liquefaction and lipid extraction pathways to renewable diesel from algae. Mitigation and Adaptation Strategies for Global Change 18(1), 137-158.
831. International Organization for Standardization (2016). ISO 14040:2006(en) Environmental management – Life cycle assessment – Principles and framework.
832. Murphy, D.J., Moeller, D. (2016). Comparing apples to apples: Why the net energy analysis community needs to adopt the life-cycle analysis framework. Energies 9, 15.
833. Miao, X. and Wu, Q. (2006). Biodiesel production from heterotrophic microalgal oil. Bioresource Technology 97(6), 841-846.
834. Olivares, J.A. (2014). National Alliance for Advanced Biofuels and Bioproducts (NAABB)-Synopsys, U.S. Department of Energy, Office of Biomass Programs (Bioenergy Technologies Office, BETO), pp. 1-28.
835. Pankratz, S., Oyedun, A.O., Kumar, A. (2017). The development of analytical model to predict microalgae growth in open pond raceway systems based on local solar irradiance (submitted).
836. Mroz, B. Hy-Tek Bio. LLC. 2016 February 20, 2017 February 20, 2017]; Available from: http://www.hytekbio.com/home.html.

837. Davis, R., Kinchin, C., Markham, J., Tan, E., Laurens, L., Sexton, D., Knorr, D., Schoen, P., and Lukas, J. (2014). Process Design and Economics for the Conversion of Algal Biomass to Biofuels: Algal Biomass Fractionation to Lipid- and Carbohydrate-Derived Fuel Products. Same as 612
838. Davis, M., Ahiduzzaman, M., and Kumar, A. (2018). How will Canada's greenhouse gas emissions change by 2050? A disaggregated analysis of past and future greenhouse gas emissions using bottom-up energy modelling and Sankey diagrams. Applied Energy 220, 754-786.
839. Van Kooten, G.C. and Hauer, G. (2001). Global climate change: Canadian policy and the role of terrestrial ecosystems. Canadian Public Policy 27(3), 267-278.
840. Wong, A., Zhang, H., and Kumar, A. (2016). Life cycle assessment of renewable diesel production from lignocellulosic biomass. The International Journal of Life Cycle Assessment 21(10), 1404-1424.
841. Quinn, J.C. and Davis, R. (2015). The potentials and challenges of algae based biofuels: A review of the techno-economic, life cycle, and resource assessment modeling. Bioresource Technology 184, 444-452.
842. Nie, Y. and Bi, X. (2018). Life-cycle assessment of transportation biofuels from hydrothermal liquefaction of forest residues in British Columbia. Biotechnology for Biofuels 11(1), 23.
843. Galera, S. and Gutiérrez Ortiz, F.J. (2015). Life cycle assessment of hydrogen and power production by supercritical water reforming of glycerol. Energy Conversion and Management 96, 637-645.
844. Gasafi, E., Meyer, L., and Schebek, L. (2003). Using life-cycle assessment in process design. Journal of Industrial Ecology 7(3-4), 75-91.
845. Barlow, J. (2016). Engineering System Modeling for Sustainability Assessment, Colorado State University, Fort Collins, Colorado. Available from: https://mountainscholar.org/handle/10217/178875.
846. Bennion, E.P. (2014). Life cycle Assessment of Microalgae to Biofuel: Thermochemical Processing through Hydrothermal Liquefaction or Pyrolysis, Utah State University.
847. Tzanetis, K.F., Posada, J.A., and Ramirez, A. (2017). Analysis of biomass hydrothermal liquefaction and biocrude-oil upgrading for renewable jet fuel production: The impact of reaction conditions on production costs and GHG emissions performance. Renewable Energy 113, 1388-1398.
848. Kothari, R., Buddhi, D., and Sawhney, R. (2008). Comparison of environmental and economic aspects of various hydrogen production methods. Renewable and Sustainable Energy Reviews 12(2), 553-563.
849. Naterer, G., Suppiah, S., Stolberg, L., Lewis, M., Ferrandon, M., Wang, Z., Dincer, I., Gabriel, K., Rosen, M., and Secnik, E. (2011). Clean hydrogen production with the Cu–Cl cycle–progress of international consortium, II: simulations, thermochemical data and materials. International Journal of Hydrogen Energy 36(24), 15486-15501.
850. Manish, S. and Banerjee, R. (2008). Comparison of biohydrogen production processes. International Journal of Hydrogen Energy 33(1), 279-286.
851. Kalinci, Y., Hepbasli, A., and Dincer, I. (2012). Life cycle assessment of hydrogen production from biomass gasification systems. International Journal of Hydrogen Energy 37(19), 14026-14039.